ISSN 0970 - 3268

Journal of The Indian Association of Sedimentologists

VOLUME 34 NUMBERS 1 & 2 JAN - DEC. 2017

INDIAN ASSOCIATION OF SEDIMENTOLOGISTS

Journal of the Indian Association of Sedimentologists

VOLUME 34 **NUMBERS 1 & 2** **JAN- DEC. 2017**

The Indian Association of Sedimentologists

All subscription/orders of the Journal should be sent to
Prof. D. Rajasekhara Reddy, Chief Editor - Journal of IAS,
49-53-8/1, Sneha Apartments, Balaji Hills, Visakhapatnam - 530 013.
E-mail: drsreddy8@gmail.com

Annual Subscription:
Rs. 1,000.00 (In India) $ 120.00 (Abroad)

Published by the Indian Association of Sedimentologists.

Head Quarters: Department of Geology, Aligarh Muslim University, ALIGARH – 202 002.

Printed at Ramakrishna Printers, D. No. 49-24-5, Sankaramattam Road, Madhuranagar, Visakhapatnam – 530 016.

JOURNAL OF THE INDIAN ASSOCIATION OF SEDIMENTOLOGISTS

VOLUME 34 **NUMBERS 1 & 2** **JAN. - DEC. 2017**

CONTENTS

Jour. Indian Association of Sedimentologists, Vol. 34, Nos. 1 & 2. (2017), pp. 1-7

Source Rock Characterization, Diagenesis and Depositional Environment of the Upper Disang Formation from Gelmoul Area of Manipur, NE India

Y. Raghumani Singh[1*], B.P. Singh[2] and S. Ranjeeta Devi[1]
[1]Department of Earth Sciences, Manipur University, Imphal-795003, India
[2] CAS in Geology, Banaras Hindu University, Varanasi-221 005, India
E-mail: yengmani@gmail.com

Abstract: This paper reports, for the first time, the mineralogical composition of the Upper Disang Formation from Gelmoul area of Manipur, NE India, based on XRD results. The results suggest that these sediments were mainly derived from phyllite, chlorite schist, mica schist and gneissic source rock with a lesser contribution from mafic and ultramafic rocks. Diagenetically, the sediments attained phyllomorphic stage, which is most advanced geochemical stage of diagenesis. The present study also suggests an oxidising environment in shallow marine basin during the deposition of Upper Disang Formation of Gelmoul area of Manipur, NE India. Probably, the sediments were deposited in fault controlled continental margin basin environment, which is consistent with the previous view of rifting and crustal stretching during the formation of Indo-Myanmar basin on continental margin of the Myanmar landmass.

Keywords: Diagenesis, Source rock, Depositional environment, Disang, Indo-Myanmar Ranges

INTRODUCTION

Disang Group occupies a vast area of Manipur and constitutes the principal flysch sediments of the region. It also has large regional development and extent in parts of Arunachal Pradesh, Nagaland, small portion of North Cachar Hills and continues up to the Indo-Myanmar Range (IMR, Fig. 1)**.** IMR was formed due to the subduction of Indian plate beneath the Myanmar plate and is regarded as an arc-trench filled deposit. The Group is divided into Lower Disang and Upper Disang formations based on the shale and sand ratio (Sinha and Chatterjee, 1982). Lower Disang is monotonously argillaceous while, the Upper part is less argillaceous. Middle-Late Eocene age has been assigned for the Upper Disang Formation of Gelmoul area of Southern Manipur, NE India (Singh et al., 2013; Singh et al., 2016). The area under study has well-developed exposures of the Upper Disang Formation that is, however, least studied. The aim of the present study is to infer the source rocks, diagenesis and depositional environment of the Upper Disang Formation occurring in the Gelmoul area of Manipur, NE India based on mineral composition, clay minerals present and primary sedimentary structures from the study area (Fig. 2a-h). The study of source rock and diagenesis of sedimentary rocks of NE India bears significance in recent years as it is considered as a resource of oil and natural gas (Singh et al., 2015). However, there is no published work on the source rock characterization, diagenesis and depositional environment from Southern Manipur, NE India.

GEOLOGICAL AND TECTONIC SETTING

The IMR comprises of the Naga-Patkai Hills, Manipur Hills, Mizo-Chin Hills and Arakan Yoma Hills. Manipur Hills of the IMR represents an accretionary prism that evolved due to subduction of the Indian plate below the Myanmar plate (Gansser, 1980; Soibam, 1998). The Metamorphic Belt, in the easternmost part of the state, which is thought to be part of the continental crust of the Myanmar plate, overthrust the ophiolite Melange Belt towards west, that again, thrust over the sediments of Disang and Barail. Again, in turn, the latter overthrust the sediments of the Surma and Tipam groups towards west. Thus, a series of easterly dipping imbricate thrust system involves here. Disang Group is a group of monotonous sequence of dark grey to black splintery shales and has intercalations of siltstones and fine- to medium-grained sandstones of light to brownish gray, occasionally giving rise to rhythmite character. The thickness of Upper Disang in Manipur is about 2 km (Rajkumar and Klein, 2014).

METHODOLOGY

The sedimentary structures were identified in the field. Shale and fine-grained sandstone (Fig. 2. a-h) were collected from the Upper Disang Formation that outcrop around Gelmoul area, Southern Manipur (Fig. 1, GPS 24°20'40.4"N: 93°39'39.6"E). To determine bulk mineral composition, X-ray powder diffraction (XRD) analyses of six representative samples (G1, G5, G20, G22, GT13,

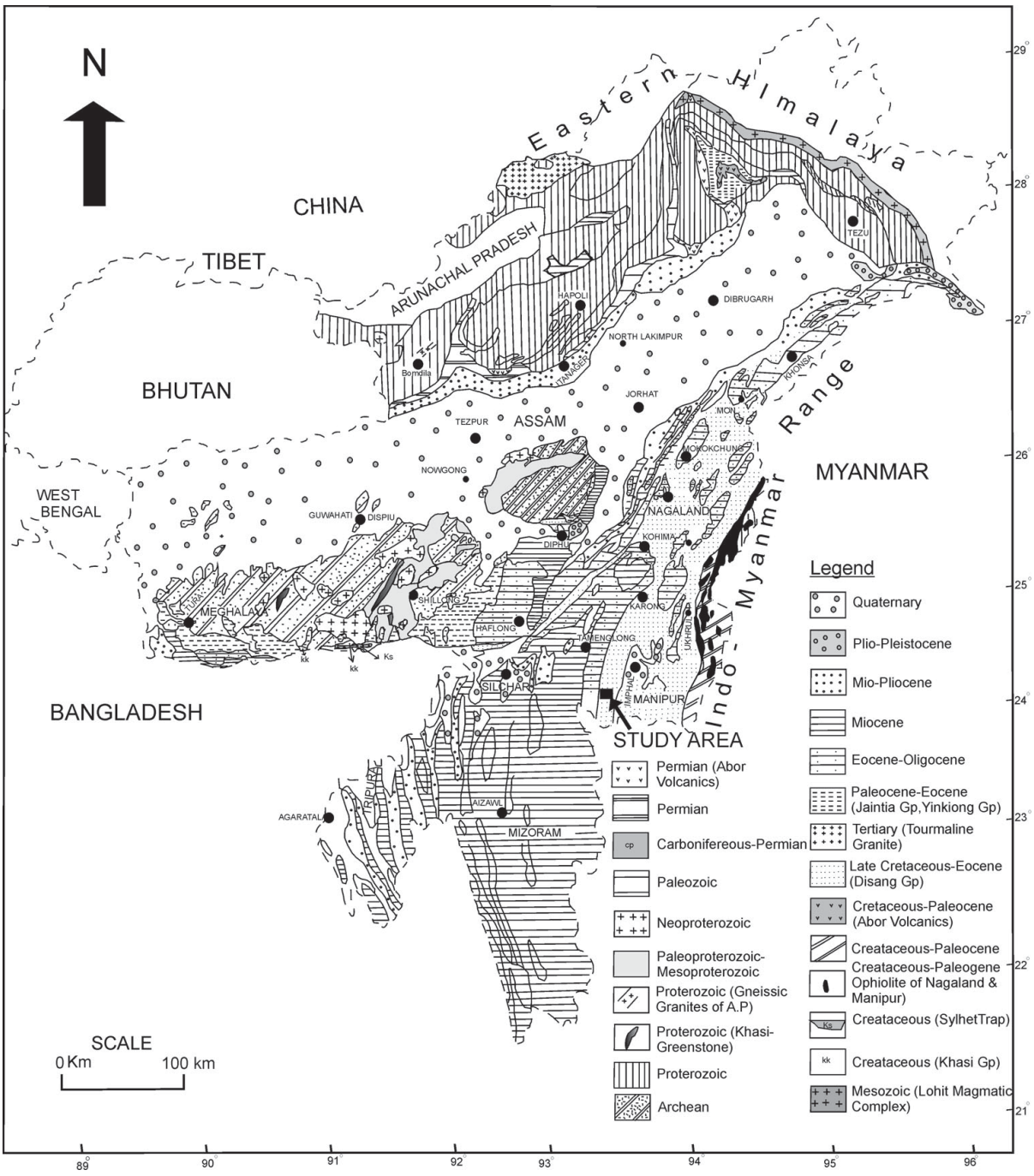

Fig. 1. Geological map of north east showing distribution of Disang Group (after Government of India, 1998).

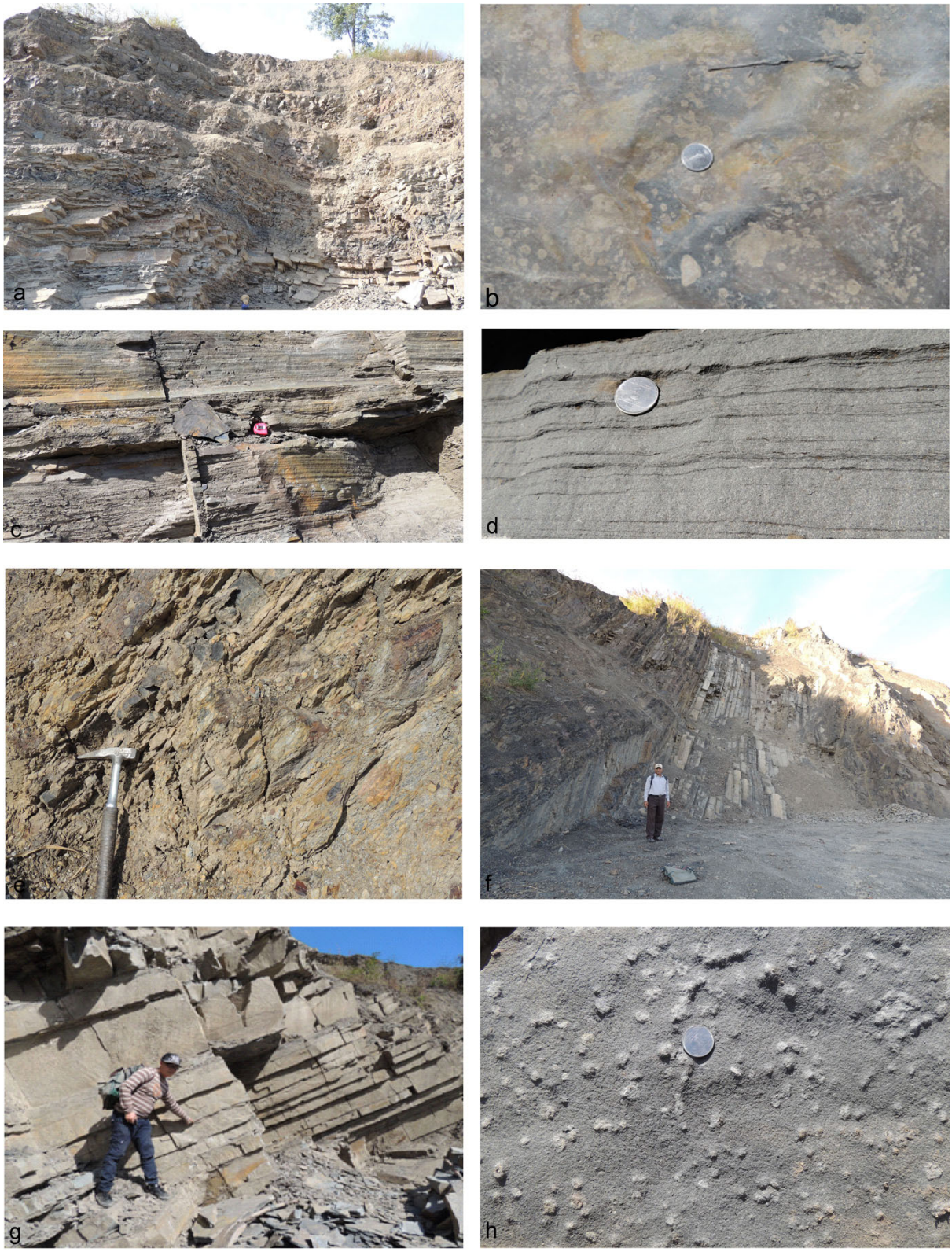

Fig. 2. Field photographs showing (a) exposures of the sandstone-shale alteration, (b) cuspate ripple mark with sinusoidal crest, (c) thick-thin lamina couplets (tidal bundles) within the sandstone (d) Mud flasers within the sandstone, (e) shale showing variegated colour may be due to paleweathering, (f) rhythmic alteration of sandstone and shale in the upper part of the succession, (g) planar-bedded sandstone and (h) Bioturbation/ carbonate accumulation on the surface of a sandstone bed in the Upper part of the Formation in the Gelmoul area, Southern Manipur.

GT20) were carried out at the Wadia Institute of Himalayan Geology (WIHG), Dehradun. XRD analysis was carried out on a PANalytical, X'pert PRO X-ray Diffractometer at room temperature, using a rotating Cu target with a voltage 45 kV and a current of 40mA. The scan range (2è) was 2–60^{O} with a step size of 0.0080^{O}. The mineral identification was carried out comparing the measured data to a reference database, viz., Inorganic Crystal Structure Database (ICSD) in PANalytical X'Pert High Score (Plus) v3.X database.

RESULTS AND DISCUSSION

The sedimentary succession of the Upper Disang Formation is comprised of sandstone- shale alternation (Fig. 2a). The sandstones are planar-bedded with 10 cm to 30 cm thick individual beds. Some of the beds are wavy in character. The upper surfaces of the sandstone possess ripple marks with sinusoidal and linguoid crests (Fig. 2b). The sandstones also contain tidal bundles in the form of thick and thin lamina couplets (Fig. 2c) and mud flasers (Fig. 2d). The shales are mainly laminated with paper thin laminae. Some of the shales show paleoweathering effect with variegated colour (Fig. 2e). In the upper part, the sandstone-shale alternation gives appearance of a rhythmite (Fig. 2f). In the upper part too the sandstones are chiefly planar-bedded (Fig. 2g). Some of the sandstones in the upper part are bioturbated (Fig. 2h).

The XRD data is being presented in Fig. 3. The X-ray diffractograms of representative samples show that quartz forms the dominant mineral in these sedimentary rocks of the Upper Disang Formation. Also, the peaks of quartz are sharp suggesting that this mineral occurs in detrital form. Chlorite with more or less sharp peak also suggests that it occurs in a detrital form. Similar is the case with biotite. Other minerals identified are zeolite, franklinite, vermiculite, muscovite and anatase.

Zeolites are among the most common authigenic silicate minerals in sedimentary rocks. The vermiculite is an alteration product of biotite during surface weathering and soil formation. This may also form during burial diagenesis.

Franklinite, spinel group of mineral, is the dominant zinc mineral in the zinc deposits at Franklin and Sterling Hill, New Jersey. Previous studies suggest that franklin-type sedimentary exhalative (SEDEX) non-sulfide zinc mineralization could indicate the presence of a hot exhalative system operating in a shallow-water oxidised environment, rather than a warm one which would deposit zinc sulphides. The hydrothermal alteration for franklinite deposit of New Jersey may have occurred at about 150^{o}c by reaction with ^{18}O enriched water (Johnson et al., 1990).The minerals of SEDEX deposits are mostly deposited in a marine second-order basin with discharge of metal bearing brine into the seawater (Maclntyre, 1991). Thus, the presence of franklinite in the studied rocks suggests similar depositional environment condition.

Anatase, a polynomorph of TiO_2, is one of the common trace minerals in sedimentary rocks suggesting that anatase could have been derived from a detrital mafic mineral or ultramafic rock. The anatase also forms during the early diagenesis following the dissolution of Ti-bearing ultramafic rock fragments.

On the north-eastern side of the study area, based on isotopic data substantiated with petro-mineralogical-geochemical data and geological tectonic setting of MOC (Manipur Ophiolite Complex), Tiwari et al. (2011) suggest a hydrothermal influence in the diagenetic fluids which may have been generated by volcanism, dyke injection and attended events of ophiolitic affinity in the region and basement fault served as conduits for hydrothermal fluids, which shows some similarity with the result of this study. The previous data strongly suggest the presence of isotopically light meteoric water rather than only sea-water or the concentrated d^{18} O-rich sea water derived brines. However, in contrast, result of the present study indicates d^{18} O rich sea-water derived brines.

SOURCE ROCK CHARACTERISTICS

As the quartz forms the dominant mineral in these sedimentary rocks of the Upper Disang Formation and it occurs in detrital form, it must have been derived from any rock that contains appreciable proportion of this mineral. Thus, felsic rock must have supplied this mineral to the studied sedimentary rocks. Authigenic formation of chlorite in marine sediments requires specific conditions hence, most chlorites in deep-sea sediments are detrital (Windom, 1976). The detrital chlorite was derived from chlorite schists and phyllites (e. g. Singh et al., 2000). The biotite is found both in a wide variety of igneous and metamorphic rocks. It is an essential constituent of many metamorphic schists and gneisses. The detrital biotite was probably derived from the mica schists and gneisses occurring in the nearby metamorphic complex of IMR. The presence of anatase in the Disang sedimentary rocks suggests that either it was supplied from a mafic and an ultramafic rock or it was formed as a result of alteration of rock fragments during diagenesis. Provenance study of the Upper Disang Formation from Nagaland also suggests that sediments were derived from granite/granite gneiss with some contribution from basic and ultrabasic sources (Imchen et al., 2014). Geochemical characteristics of Disang shale from Arunachal Pradesh also suggest the predominant derivation of the sediments from felsic volcanic rocks and /or granitic source rock (Gogoi and Sarmah, 2013).

DIAGENESIS

The known occurrences of sedimentary zeolite show that most of these minerals are formed during diagenesis of sedimentary rocks. Although it is suggested that the zeolite crystallizes in shallow marine

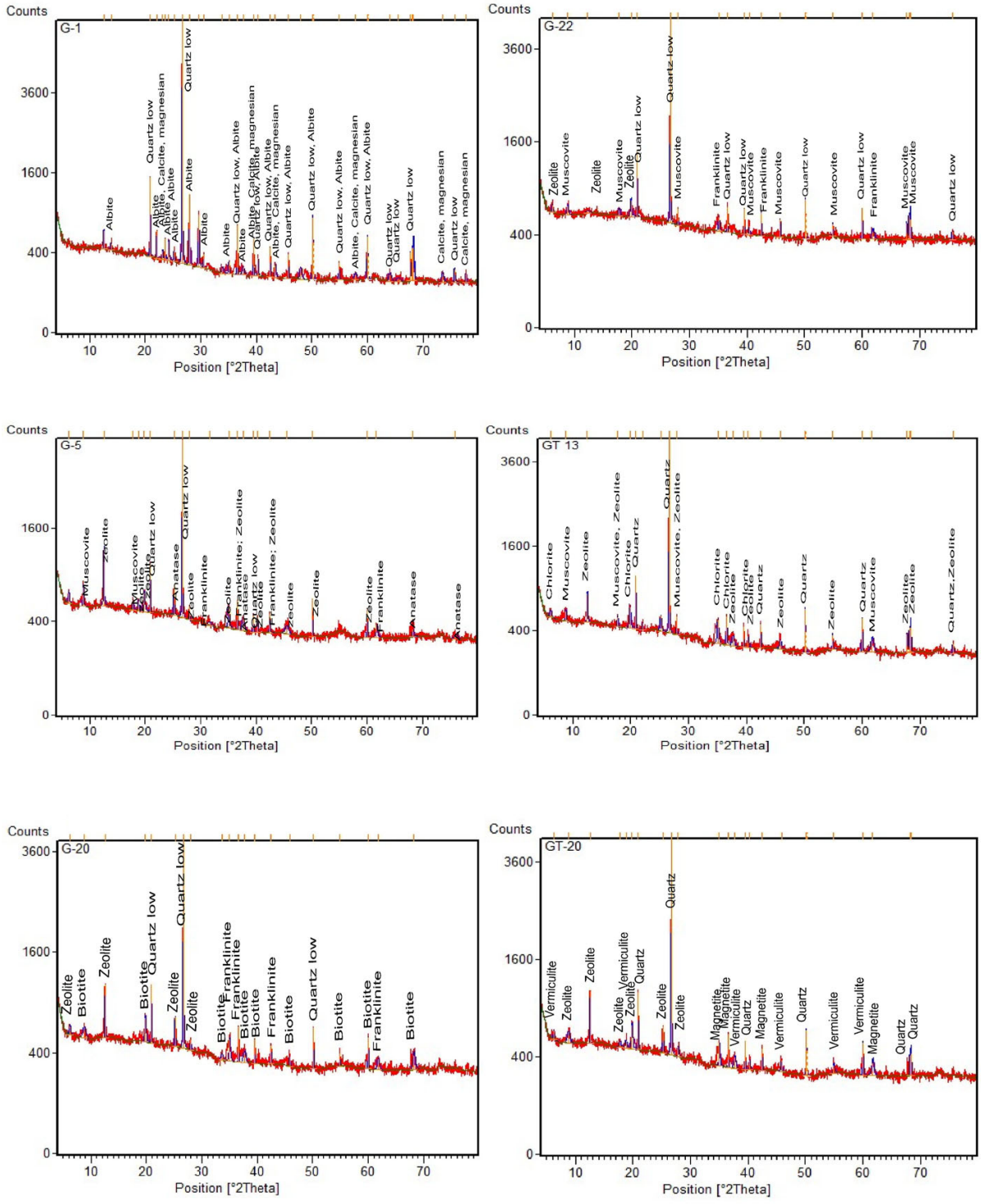

Fig. 3. X-ray Difractograms of the Upper Disang sedimentary rocks (Sample G-1, fine-grained sandstone; G-5, silty shale, G-20, shale; G-22, shale; GT-13, shale; GT-22, shale).

basins, it is thought to be a diagenetic product, thus, is a promising indicator of post-depositional diagenetic conditions. The vermiculite may also form during burial diagenesis. The anatase is also an indicator of the early diagenesis following the dissolution of Ti-bearing ultramafic rock fragments.

The feldspar, whether albite or K-feldspar are the most frequently found diagenetic mineral and predate any tectonic deformation (Pettijonh et al., 1972). They represent the general operation of diagenetic process in which other authigenic minerals are formed, however, some are related to hydrothermal activity. The geologic conditions that seem to be necessary are moderately elevated temperature and source of silica. However, with greater burial depth and increasing temperature, carbonate minerals such as calcite are more likely to precipitate.

It is inferred that diagenetically, the Gelmoul shales and sandstones attained the phyllomorphic stage as evidenced from the presence of albite in the lower most part of the sequence. Phyllomorphic stage is most advanced geochemical stage of diagenesis. Reactions categorized as phyllomorphic stage are favoured by increase in pressure and temperature or sediments have been subjected to strong pressure either in folded belt or along fault planes (Dapple, 1967). And these diagenetic modifications represented by the final phase (phyllomorphic stage) of diagenesis may also results from deep burial, increased geothermal gradient and pressure. The field study indicates that folds and fault in the area under investigation possibly favoured increase in pressure and temperature. The maximum depth of burial must have been 4-5 km and the sediments must have sustained a temperature range of 120-150º C.

DEPOSITIONAL ENVIRONMENT

Marine depositional environments are either shallow marine or deep marine depending upon the sedimentation above or below the fair-weather wave base. Some of the sedimentary structures are typical of a particular depositional environment. Particularly, the Flaser beddings occur in the tidally influenced environment (Reineck and Singh, 1980) and the tidal bundles are the most unequivocal evidence of the tidal influence (Visser, 1980). The sedimentary structures such as ripple marks, flaser bedding and tidal bundles in the Upper Disang Formation suggest shallow marine/ coastal depositional environment, above the wave base, influenced by waves and tides. Thus, based on these evidences, it is inferred that the sediments were deposited in shallow-marine environment during the Upper Disang Formation, which is consistent with result of Singh et al., (2013) that records a warm, shallow marine environment of deposition for the upper part of the Upper Disang Formation based on, foraminiferal lining and associated palynomorphs from this study area.

Johnson and Skinner (2003) states that franklinite mineral of Franklin forms from metaliferous brines that settled from the water column or they are formed diagenetically by reactions in shallow buried sequences and it would be pre-metamorphic. The occurrence of this mineral in the studied sedimentary rocks, however, may have been formed during diagenesis in a shallow marine basin. Moreover, the zeolite crystallization is also a promising indicator of post-depositional diagenetic conditions in shallow marine basins.

Major thrust fault may be reactivations of ancient continental margin rifts and this rifting results in the formation of restricted second and third order basin that are important for the localization of sedimentary mineral deposits today (Maclntyre, 1991). These deposits may be related to the rifting that initiated during Upper Crataceous in the Manipur region. Further, the tectonic activities that happened during the deposition of Upper Disang Formation of the study area reflect the orogenic activities of IMR. The result of this study is well consistent with the previous view that rifting and crustal stretching led to the formation of the Indo-Myanmar basin on the continental margin of the Myanmar landmass (Soibam, 2008). The stretching was possibly associated with formation of new oceanic crust, followed by the deposition of huge pile of Disang and Barail sediments. Previous works on diverse fauna and the stable isotope studies of carbonate rocks of ophiolitic melange zone in Manipur, to the north east of the study area, suggest the warm and humid paleoclimate conditions in shallow marine environment with the complex tectonics, paleoclimatic and paleoceanographic changes during Upper Cretaceous-Eocene (Tiwari et al., 2011), which also support the result of this study.

CONCLUSIONS

1. The sediments of the Upper Disang Formation of Gelmoul area, Manipur, NE India were derived from phyllite, chlorite schist, mica schist and gneisses with very less contribution from mafic and ultramafic rocks.

2. The sediments attained the phyllomorphic stage of diagenesis, the most advanced geochemical stage of diagenesis.

3. Sedimentatary structures and mineralogy suggest deposition in a shallow marine basin that developed as a fault controlled continental margin basin or a second order basin.

4. The sediments of the Disang and Barail groups were deposited as a result of rifting and crustal stretching in the Indo-Myanmar basin on continental margin of the Myanmar landmass.

Acknowledgments: Authors (YRS and BPS) are thankful to DST (Project No. SR/S4/ES-577/2011), New Delhi for financial assistance in form of a research project. YRS is also grateful to UGC, (F.No. 41-1024/2012 SR), New Delhi for financial assistance in form of Major Research Projects. The authors sincerely acknowledge Ksh Atamajit Singh, Mr. Venus Guruaribam and Miss Reshma Naorem (Research Scholars), Department of Earth Sciences, Manipur for their support during field work.

References

Dapples, E.C. (1967). Development in Sedimentology, Elsevier, 8, 91-121p.

Gansser, A. (1980). The significance of the Himalaya suture zone. *Tectonophysics*, 62, 37-52.

Gogoi, B.K. and Sarmah, R. K. (2013). Geochemical Characteristics of Shale of Disang Group, Tirap District, Arunachal Pradesh. International *Journal of Scientific and Technology research*, 2 (11), 186-192.

Government of India (1998). Published under the Direction of Director General, Geological Survey of India.

Imchen, W., Thong, G.T. and Pongen, T. (2014). Provenance, tectonic setting and age of the sediments of the Upper Disang Formation in the Phek District, Nagaland. *Journal of Asian Earth Science*, 88, 11–27.

Johnson, C.A., Rye, D.M. and Skinner, B.J. (1990). Petrology and stable isotope geochemistry of the metamorphosed zinc-iron-manganese deposit at Sterling Hill, New Jersey., *Economic Geology*, 85, 1133-1161.

Maclntrye, D.G.. (1991). Sedex - Sedimentary-exhalative Deposits, in Ore Deposits, Tectonics and Metallogeny in the Canadian Cordillera. McMillan, W.J., Coordinator, *B. C. Ministry of Energy, Mines and Petroleum Resources*, 25- 69.

Pettijohn, F. J., Potter , P. E. and Siever, R. (1972). Sand and sandstone. Springer-Verlag, New York, 618p .

Rajkumar, H. S. and Klein, H. (2014). First perissodactyl footprints from flysch deposits of the Barail Group (Lower Oligocene) of Manipur, India. *Journal Earth System Science*, 123, 413–420.

Reineck, H.E., Singh, I.B. (1980). Depositional sedimentary environment. Springer-Verlag, New York, 549 pp.

Singh, B. P., Andotra, D. S. and Kumar, R. (2000). Provenance of the lower Tertiary mudrocks in the Jammu Sub-Himalayan zone, Jammu and Kashmir state (India), NW Himalaya and its tectonic implications. *Geoscience Journal*, 4, 1-9.

Singh, B.P., Singh, Y.R., Andotra, D.S., Patra, A., Srivastava, V.K., Guruaribam, V.,Sijagurumayum, U. and Singh, G.P. (2016). Tectonically driven late Paleocene (57.9-54.7 Ma) transgression and climatically forced latest middle Eocene (41.3-38.0Ma) regression on the Indian subcontinent. *Journal Asian Earth Science*, 115, 124-132.

Singh, Y. R., Li, J, Singh, B. P., Guruaribam, V. (2013). Microforaminiferal linings from the upper part of the Upper Disang Formation at Gelmoul quarry, Churachandpur, Imphal valley and their bearing on palaeoenvironment. *Current Science*, 105, 1223-1226.

Singh, Y. R., Singh, B. P. and J. Li. (2015). Hydrocarbon potential of the Palaeogene Disang Group, Manipur region, India-A palynological approach. *In*: S. Mukherjee (ed.), Petroleum Geosciences: Indian Contexts. Springer. 191-204 p (DOI 10.1007/978-3-319-03119-4_8).

Sinha, N.K. and Chatterjee, B.P. (1982). Notes on the Disang Group in parts of Nagaland and fossil fauna. Records Geol Surv India, Part IV.

Soibam, I. (1998). On the Geology of Manipur. *In:* Souvenir, IX Manipur Science Congress (March, 25–27), 12–19.

Soibam, I. (2008). Geological and Tectonic setting of Manipur: Implications on the Tectonics of Indo-Myanmar Ranges. *In*: Souvenir, Indo-Myanmar Ranges in the Tectonic Framework of the Himalaya and Southeast Asia (November 27-29), 23-35.

Visser, M. J. (1980). Neap-spring cycles reflected in Holocene subtidal large scale bed-form deposits: a preliminary note. Geology, 8, 543-546.

Windom, H. L. (1976). Lithogenous material in marine sediments. *In:* J. P. Riley & R. Chester (eds.), Chemical oceanography). New York: Academic Press, 5, 103–135.

Jour. Indian Association of Sedimentologists, Vol. 34, Nos. 1 & 2. (2017), pp. 9-16

Geochemistry and the Factors Controlling on the Weathering and Erosion of the Barail Group of Rocks, NW Manipur, India

SALAM RANJEETA DEVI[1], M.E.A.MONDAL[2] AND JOHN S. ARMSTRONG-ALTRIN[3]
[1] Department of Earth Sciences, Manipur University, Imphal-795003
[2] Department of Geology, AMU, Aligarh-202002
[3] Instituto de Ciencias del Mar y Limnología, Universidad Nacional Autónoma de México, Unidad de Procesos Oceánicos y Costeros, Ciudad Universitaria, Ciudad de México 04510
E-mail: ranjeeta_27@rediffmail.com

Abstract: Geochemical study of the Barail sandstones and shales from NW Manipur are carried out to obtain information on the factors controlling the degree of weathering and rate of erosion as well as to evaluate recycling process upon source rock. Chemical Index of Alteration (CIA) and A-CN-K diagram indicate low to moderate chemical weathering in the source area. ICV (Index of compositional variability) value suggests predominant of compositionally mature recycle sediment and input of few first cycle sediment. The CIA-ICV diagram is useful to signify the mixing of first-cycle and recycles sediments and changes in weathering intensity as well as the variation in the composition of the source rock area during the deposition of the Barail Group. K_2O/Al_2O_3 ratio and Na_2O/Al_2O_3 vs. K_2O/Al_2O_3 diagram implies the existence of an illite rich fraction, suggesting physical erosion of metasedimentary rocks and weathering of K-feldspar from granite/ granite-gneissic parent rocks at high elevation under humid climate. This study records an uplift event producing more physical weathering, enhance by humid climate, and humid climate causes these weathering sediments to undergo more chemical weathering within the Barail Group. Our result suggests that it is not only the climate but also tectonic activities played a significant role in controlling weathering and erosion process in this area. The Oligocene Barail sedimentary deposit is an example of tectonically related deposit that is governed by the effect of low to moderate chemical weathering and recycling.

Keywords: Barail Group, Chemical index of alteration, Index of Compositional variability, weathering, Climate, Tectonic.

INTRODUCTION

With global tectonic movement during the Cenozoic, particularly, the uplift of the Himalayan-Tibetan plateau and its environment effect, the quantitative evaluation of the degree of chemical weathering and rate of erosion in continent and paleoclimate reconstruction is becoming of increased importance. Evaluating factors that control continental weathering and rate of erosion is crucial for understanding of earth science processes (Gaillardel et al., 1999; Cliff, 2006). On various geological timescales, tectonic driven mountain uplift, precipitation and climate variability have been considered as the primary factor controlling erosion, but their roles remain still debated (Molnar, 2004; Cliff et al., 2006). Such debate has further reinforced the need for a clear understanding of the factors that control weathering and erosion occurring in mountain belts (Gaillard et al., 1999).

The study area (Fig.1a&b.), bounded by the eastern Himalaya to the north and the Indo-Myanmar Ranges to the east is one area with weathering products particularly useful for evaluating the importance of climate or tectonic controlling on weathering and erosion. However, study on factor controlling the weathering and erosion base on geochemistry of sandstone and shale with petrographic information from this area have not, yet, been conducted, though the region is unique to study the tectonic- uplift-weathering and erosion process.

Many studies have proposed different chemical weathering indices based on sediment geochemical analysis (Nesbitt and Young, 1982; Harnois, 1988; Fedo et al. 1995; Ohta and Arai, 2007). Nesbitt and Young (1982) first proposed the chemical index of alteration (CIA) to calculate the degree of feldspar mineral weathering to clay and is the most accepted of the available weathering indices. CIA data can provide crucial insight into the changes in the relative contribution of chemical and physical weathering in the production of sedimentary detritus. Physical and chemical weathering can be reliably inferred if application of the CIA is combined with ICV and petrographic information. Thus, this study aims to evaluate the degree

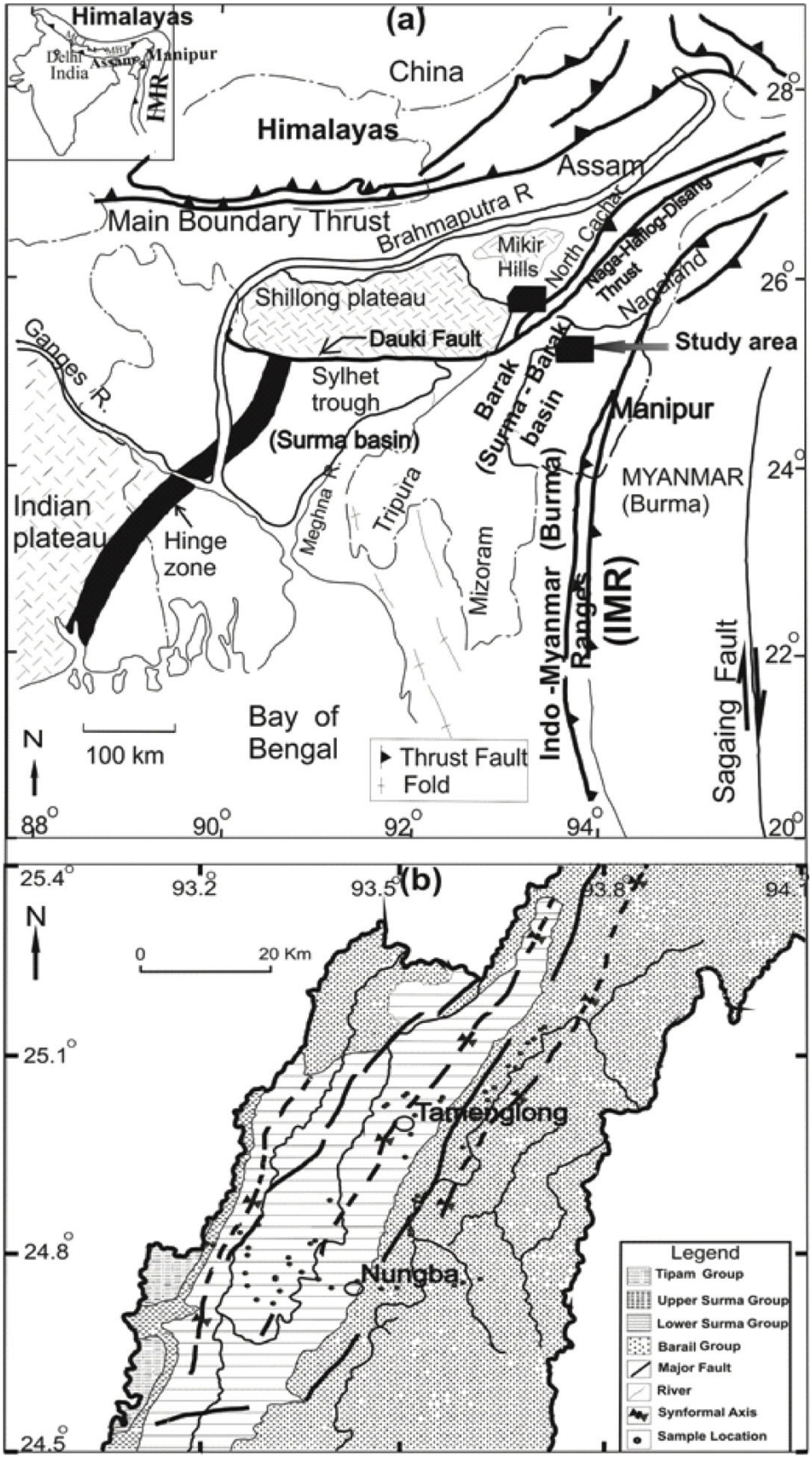

Fig.1 (a). Regional tectonic map of the study and adjoining area after Uddin and Lundberg, 1998). **(b)** Geological map of the study area (Chingkhei, 2002) important sample locations.

of weathering and erosion processes and the factors controlling the rate of weathering and erosion during deposition of Oligocene Barail Group of rock from the area that related to the uplift of two orogenic belts.

GEOLOGICAL SETUP AND SEDIMENTATION

The closing of the suture and collision of the Indian plate with Tibetan and Central Myanmar plate occurred during Middle Eocene and marks the initiation of the Himalaya Orogeny with many depositional basins. The flysch type sediment of the Disang Group, which represents the oldest Tertiary rock, was deposited in a shallow but rapidly sinking basin during the Eocene.

The movement related to second phase of the Himalayan Orogeny which was initiated in the Early Oligocene resulted in the deposition of the continental facies of the Barail Group, which terminated with the uplift in the late Oligocene. After a short break, sedimentation was resumed with a marine transgression during lower Miocene and the Surma Group was deposited (Gopendra Kumar, 1997). Johnson and Alam (1991) suggested that the Barail Group of the Oligocene age are fluvial but probably passed abruptly (to the southeast of Sylhet trough) into delta and prodelta deposition, a rapidly subsiding trough on the west flank of the Indo-Myanmar Ranges. With increasing subsidence rates during the Miocene the Surma Group was deposited during a prolong transgression that extended northward over at least part of the Shillong plateau (Banerji, 1984; Salt et al. 1986).

The Barail Group of alternating sandstone and shale (in varying proportion) is well exposed in North Cachar Hills of Assam, southwest of Kohima, Nagaland and western parts of Manipur. In Manipur, this Group consists dominantly of massive to thickly bedded sandstone with siltstone and minor dark grey to khaki green thinly bedded shale. The Barail Group has comparatively abundant carbonaceous matter. Plant fossils and leaf impressions are common at some area within the Barail Group (Table 1). The Barail of study area is unconformably overlies by the Surma Group and therefore, probably, represents the upper Barail.

METHODOLOGY

Fresh samples of the Barail sandstone and shale were collected from outcrop exposed in stream cuts, road cuts and small quarries from in and around Tamenglong, NW Manipur (Fig.1.b). About 500 counts per thin section were made using the Gazzi-Dickinson point counting method (Ingersoll et al. 1984).

Major element analysis were carried out on SIEMENS SRS 300 Sequential X-ray Spectromenter at Wadia Institute of Himalayan Geology with analytical accuracy of <5% and average precision better than 1.5% (Saini et al. 1998). Analytical accuracy of the major oxide data is <5% and average precision is always better than 1.5%. The trace elements and REE are determined by Inductively Couple Plasma Mass Spectrometry (ICP-MS Perkin Elmer Sciese ELAMDRA II) at National Geophysical Research Institute, Hyderabad, following procedure described by Balaram et al. (1996). The precisions achieved were <5% RSD with comparable levels of accuracy.

PETROGRAPHY

The Barail sandstones are rich in quartz followed by lithic fragments with less feldspar and mica. Quartz is the dominant fragment grain occurring as monocrystalline (most abundant) and polycrystalline grains. Polycrystalline quartz grains mostly consist of more than three crystals per grain and exhibit suture crystal boundaries with few elongate contacts. Both K-feldspar and plagioclase are present but plagioclase dominates in most samples. Very few plagioclase grains of sub-angular larger than the quartz grain are present. Next in abundance to quartz is the lithic fragments dominated by sedimentary (shale chert and quartz rich siltstone) and metasedimentary rock fragments (slate, phyllite, quartzite, quartz-mica lithic fragments). Both muscovite and biotite with negligible volcanic igneous rock fragments are also present. The Barail sandstones have quartzolithic and quartzose composition, diagnostic of a quartzose recycled orogen province (Dickinson, 1985) and thus, indicating that the sands were derived from a quartzose orogen province.

GEOCHEMISTRY

The SiO_2 concentration of the Barail sandstones varies from 75.85 to 84.29 and shales varies from 63.75 to 76.19 (Table 2).

Major element chemistry is perhaps most useful to determine the extent of weathering of the source terrain

Table 1. Lithostratigraphy of the Barail Group from the study area (Assam and Manipur).

Group	Age	Formation and lithology	
		Assam *(*after *Sen et al., 2012)*	Manipur (after *Soibam, 1998*)
Barail	Late Eocene to Oligocene	Grey, medium to fine grain-ed, ferruginous, massive and bedded, occasionally lamina-ted sandstone with siltstone and shale layers.	Massive to thickly bedded sandstones. Alterations of shale and sandstone with carbonaceous matters. Intercalations of bedded sandstones with shales.

Table 2. Major element (wt %) composition of the Barail sandstones and shales.

	Sandstone				Shale		
	BL-3	**BH-5**	**BH-7**	**DL-25**	**TP-1**	**KK-17**	**SPA-28**
SiO_2	75.85	79.88	76.78	84.29	63.75	68.75	76.19
TiO_2	0.52	0.56	0.69	0.44	0.75	0.78	0.64
Al_2O_3	11.46	8.86	11.84	6.92	14.84	14.28	11.24
Fe_2O_3	3.81	3.18	2.47	2.14	6.48	5.34	3.32
MnO	0.048	0.061	0.047	0.039	0.095	0.073	0.067
MgO	1.41	1.57	1.61	1.15	3.61	2.13	1.63
CaO	0.34	0.35	0.28	0.3	1.11	0.57	0.35
Na_2O	1.94	1.25	0.53	0.8	2.12	1.45	1.24
K_2O	3.81	1.83	2.49	1.33	1.9	2.68	2.33
P_2O_5	0.11	0.095	0.065	0.078	0.147	0.147	0.146
K_2O/Al_2O_3	0.33	0.21	0.21	0.19	0.13	0.19	0.21
CIA	59.09	65.47	74.39	67.70	66.24	69.31	68.38
ICV	1.04	0.99	0.69	0.90	1.08	0.91	0.85

CIA: Chemical index of alteration; ICV: Index of compositional variability

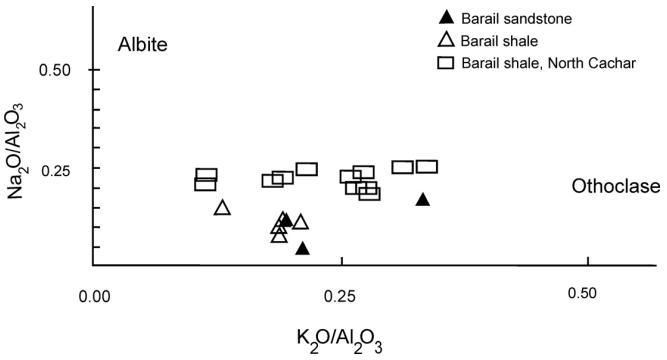

Fig.2. Na_2O/Al_2O_3 vs. K_2O/Al_2O_3 diagram (Deer et al. 1980).

and several chemical indices have been proposed to quantifying weathering effects. The most popular is the chemical index of alteration (CIA) defined as $[Al_2O_3/(Al_2O_3+CaO+K_2O+Na_2O)] \times 100$, where the oxides are expressed as molar proportions and CaO* is the amount of CaO incorporated in the silicic fraction of the rock. CIA values for the Barail sandstones range from 59.09 to 74.39 and those of the shales ranges from 66.24 to 69.31 indicating the moderate weathering of the source rock. The CIA value for average shale ranges from 70-75, which reflect the composition of muscovite, illite and smectite. K_2O/Al_2O_3 ratios of the Barail samples are around 0.2, typical of illite, which for K-Feldspar is around 0.4-0.45 (Cox et al. 1995) and in the Na_2O/Al_2O_3 vs. K_2O/Al_2O_3 diagram (Fig. 2). Deer et al. 1980) to differentiate two potassic mineral, the samples cluster near K_2O/Al_2O_3 value of 0.25 (illite) far from K-feldspar (0.53). The Barail shale samples from north Cachar, Assam (Sen et al. 1992) are also shown for comparison. These observations imply the existence of illite-rich fraction in the sediments.

The CIA indices reflect mostly the amount of feldspar relative to clay minerals. A-CN-K (Al_2O_3-CaO+Na_2O-K_2O) diagram (Fig. 3), which is more useful way of evaluating the chemical weathering trend, compared to CIA index (Nesbitt and Young, 1984), show that the bulk sample plot between 65 and 75% Al_2O_3 content representing a moderately weathered source and do not exhibit any evidence of K-metasomatism.

A better discrimination of parent rock types would include Fe and Mg. Cox et al. (1995) proposed a measure called the index of compositional variability (ICV):

$$(CaO+K_2O+Na_2O+Fe_2O_3(t)+MgO+MnO+TiO_2)/Al_2O_3,$$

where CaO includes all sources of Ca, oxides are in weight percent rather than moles, and the values decrease with increasing degree of weathering. A high ICV value suggests compositionally immature source rocks rich in non-clay silicate minerals whereas low values indicate compositional mature source rocks (Cox et al. 1995). However, ICV values less than one has also

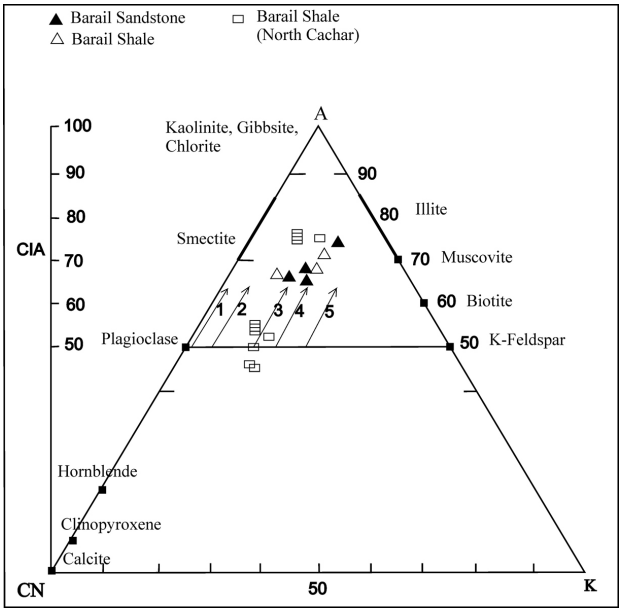

Fig.3. A-CN-K (Al_2O_3-CaO*+ Na_2O-K_2O) diagram (Nesbitt and Young, 1984) for the Barail sandstones and shales. The samples of the Barail shales (North Cachar, Sen et al. 2012) are also shown. Numbers 1-5 denote trends of initial weathering profiles of various rock types: 1, gabbro; 2, tonalite: 3, diorite; 4, granodiorite; 5, granite.

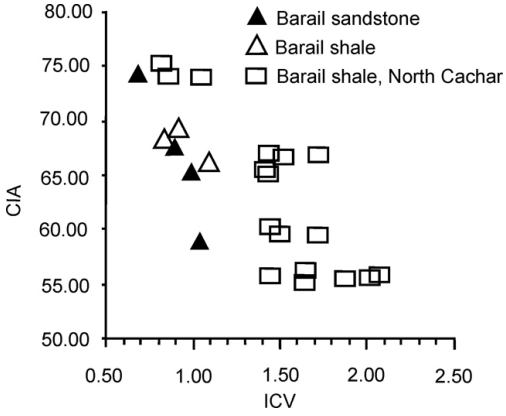

Fig. 4. ICV vs. CIA diagram showing relation between degree of weathering and source rock composition.

been found in some intensely weathered first cycle sediments (Barshad, 1966). The ICV values of the Barail sandstones and shales range from 0.69 to 1.04 and from 0.85 to 1.08 respectively.

Fig. 4. shows that the CIA increases with decreasing ICV value. This observation is well shown with more Barail shale samples (Table 3) from nearby area, North Cachar Hills, Assam (Sen et al. 1992). The vertical changes may reflect mixing of first-cycle and recycled sediments and changes in weathering intensity within the Barail Group. An interesting view of relation between CIA and ICV shows, probably, variation in the composition of the source rock area. Average basalt and average granite have strongly contrasting ICV values of 2.20 and 0.95 respectively (Li, 2000). Another important result is that sediments were derived from a gradually chemically less-weathered source terrain, reflecting increased erosion rates likely due to increasing tectonic activity.

WEATHERING AND RECYCLING

Low CIA and high ICV shows very little evidence of weathering and it is likely that the parent terrain contains mostly juvenile igneous rocks. If CIA is higher and ICV low, then the cause could be either high weathering of the source or recycling of previously weathered material. However, sandstone with abundant sedimentary rock fragments, have high CIA value, an indication that high CIA value were produced by recycling of older sediments rather than intense weathering of igneous rock. However, the Barail

Table. 3. CIA and ICV values of the Barail shale (Sen et al. 1992).

	SS1	SS2	SS3	SS4	SS5	SS6	SS7	SS8	SS9	SS10	SS11	SS12	SS13	SS14	SS15	SS16
CIA	75.1	55.86	59.45	55.36	73.81	59.67	55.7	65.41	55.48	66.95	74.18	66.76	55.38	66.7	55.92	60.12
ICV	0.82	1.47	1.72	1.90	1.06	1.50	2.09	1.43	1.66	1.46	0.86	1.54	2.03	1.73	1.66	1.46

CIA, Chemical index of alteration; ICV, Index of compositional variability

sandstones and shales have moderate CIA and low ICV indicating moderate chemical weathering and compositionally recycled sediments with input of some first cycle sediments during deposition. The sandstones have abundance of metasedimentary and sedimentary lithic fragments but the Barail sandstone and the shale does not show intense weathering, so, the sediments are dominantly product of the metasedimentary and sedimentary rocks which are not intensively weathered.

A combination of chemical and physical weathering affects exposed rocks to variable degree (Bland and Rolls, 1998). Progressive chemical weathering of labile minerals like feldspar lead to the loss of Ca^{2}+, K+ and Na+ and transformation to minerals more stable under surface conditions (Fedo et al. 1995). Ultimately, it results in the formations of shale rich in clay minerals like illite (minimial weathering) and kaolinite (maximum leaching in the humid tropics) and Fe-oxyhydrates like goethite. Physical weathering, in turn, leads to the degradation of rocks to smaller grain sizes and degrades a source rock into a clay-sized deposit, then, it should essentially preserve the mineralogical and geochemical composition of the original rock (Nesbitt and Young, 1982, 1996).

In general, hydrolytic weathering causes a progressive transformation of affected components into clay mineral (illite), ultimately kaolinite. Illite is considered as a primary mineral, which reflects weak hydrolytic processes in continental weathering and increased direct rock erosion under cold and arid climatic conditions. Or illite could have been derived from physical erosion of metamorphic and granitic parent rocks, mainly located at high elevation. Or it may have been formed by weathering of nonlayer silicate, such as feldspar from granites under moderate hydrolysis conditions, and by degradation of micas. In our study, it is suggested that illite could have been derived from physical erosion of metasedimentary rocks and from the decomposition of k-feldspar (from granite/ granite gneissic parent rocks) with degradation of mica from high elevation of dominantly the eastern Himalaya during moderate weathering under humid climatic condition of the Oligocene.

CLIMATE VERSUS TECTONIC CONTROL ON WEATHERING AND EROSION

Climate is an important factor that controls the geochemical environment of weathering processes and also has strong influence upon the characteristic of the weathering product (Nesbitt et al. 1980, Mc Lennan, 1993). The degree of weathering increases with high mean annual temperature and precipitation. The rapid erosion of mountain ranges in late Cenozoic times relate to climate changes.

The Oligocene sedimentary basin of Assam in the Indian subcontinent was situated at a low palaeolatitude, i.e., 10^{o}–15^{o}N (Molnar and Stock, 2010) and a monsoonal climate prevailed during the late Oligocene (Srivastava et al., 2012). Bases on rich morphological diversity of fossil leaves, Guleria et.al. (2005) suggested warm humid tropical climate during the deposition of late Eocene to early Oligocene sediments of the Imphal valley and its adjoining areas of Manipur and the presence of palm leaf also indicate humid climate at the time of deposition of the Barail Group of Manipur (Chandra et al., 2012). This warm humid tropical climate that prevailed during Oligocene in NE Indian subcontinent can produce high intensity of chemical weathering in this area. But on the basis of our result, the Barail sandstones and shales show no intense chemical weathering and no strong influence of climate on chemical weathering, however, might enhance the physical erosion. Therefore, beside the climate, other factors may also control the chemical weathering and erosion of this area.

Tectonic processes with the initiation of uplift of the eastern Himalaya and the Indo-Myanmar (Burma) Ranges can increase the rate of erosion. The high rate of physical weathering caused by tectonic activities can produced the lithic fragments and primary minerals like plagioclase, k-feldspar and illite. The tectonic uplift can increase the slope of the eastern Himalaya and the Indo-Myanmar Ranges. The increasing slope is most strongly associated with mechanical and chemical denudation rates (Summerfield and Hulton, 1994). Therefore, abundant lithic fragments and few primary minerals or first cycle sediments indicate more physical erosion than intense chemical weathering. These lithic fragments and primary minerals are transported very rapidly without intense chemical alteration. Therefore, sediments very sensitive to chemical weathering such as lithic fragments, which are more easily destroyed by chemical weathering than are the feldspar under normal weathering condition (Young et al., 1975) and fresh plagioclase are present in the Barail sandstone. However, intense rate of erosion cannot be assumed due to lack of coarse detritus and abundant fresh, unaltered mineral. Thus, the study provide an important clue that although, tectonic processes exerted the dominant control on the rate of erosion for the Barail sandstone and shale but tectonic uplift was only at initial stage and may not be very strong to cause intense rate of weathering and erosion during the Oligocene. Rea (1992)

also suggest that the Himalaya-Tibetan uplift was only about half of its present elevation even during late Miocene (between ~10-8 Ma). Moreover, the study also records an increasing rate of chemical weathering which, in turn, reflects that an uplift event produced more physical weathering sediments and humid climate, causes these weathering sediments to undergo more chemical weathering within the Barail Group. However, the humid climate, most likely, has had more impact on physical than chemical weathering.

CONCLUSIONS

Sedimentation of the Oligocene Barail sandstones and shales is controlled mostly by tectonics with chemical weathering and recycle process playing important role during their deposition. The CIA value and A-CN-K diagram indicate that the source terrain was affected by low to moderate weathering. ICV values of the Barail sandstones and shales suggest compositionally mature and were likely dominated by recycled sediments with few first cycle sediments. The CIA-ICV diagram also reflects mixing of first-cycle and recycled sources and indicates increasing weathering. This diagram is also a useful tool to show variation in the composition of the source rock for this study area. K_2O/Al_2O_3 ratio and Na_2O/Al_2O_3 vs. K_2O/Al_2O_3 diagram indicates illite rich in the samples, suggesting physical erosion of metasedimentary rocks and decomposition of k-feldspar from granite/ granite-gneissic parent rocks and degradation of muscovite from high elevation during low to moderate weathering under humid climate. The humid climate may have had more effect on physical weathering than the chemical weathering. Our result suggest that the sediments were derived from low to moderately weathered source terrain reflecting increasing erosion likely due to increasing tectonics of the eastern Himalaya and the Indo-Myanmar Ranges.

Acknowedgements: Our sincere thanks to the Chairman, Department of Geology, A.M.U., Aligarh for providing facilities to carry out this work. The first author also thanks to Head of Department, Department of Earth Sciences, Manipur University for the permission to publish this paper. We are also thankful to B.R. Arora, the Director, Wadia Institute of Himalayan Geology, Dehra Dun and Dr. V. Balaram, Geochemistry Division, National Geophysical Research Institute, Hyderabad for their help during chemical analysis.

References

Alam, M. (1989). Geology and depositional history of Cenozoic sediments of the Bengal Basin of Bangladesh. Palaeogeo. Palaeoclimat. Palaeoeco., 69, 125-139.

Balaram, V., Ramesh, S.L. and Anjaiah, K.V. (1996). New trace and REE data in thirteen GSF reference samples by ICP-MS. Geostandards Newsletter, 20, 71-78.

Bland, W. and Rolls, D. (1998). Weathering. An introduction to the scientific principles. Arnold Publishers, London, pp. 271.

Chingkhei, R., (2002). Application of GIS Tecniques in evaluation and monitoring of vegetation in Barak basin. Unpublised Ph.D. Manipur University, Manipur, India.

Cox R, Lowe, D.R, and Cullers, R.L. (1995). The influence of sediment recycling and basement composition of evolution of mudrock chemistry in the southwestern United States. Geochim Cosmochim Acta , 59, 2919–2940.

Dickinson, W.R., (1985). Interpreting provenance relations from detrital modes of sandstone. *In:* Zuffa, G.G. (Ed.), Reading provenance from arenites: Dordrecht, The Netherlands, Riedel, pp. 333-361.

Fedo, C.M., Nesbitt, H.W. and Young, G.M., (1995). Unravelling the effects of potassium metasomatism in sedimentary rocks and paleosols, with implications for weathering conditions and provenance. Geology, 23, 921-924.

Gopendra Kumar, (1997). Geology of Arunachal Pradesh, Geological Society of India, Bangalore, 217p.

Harnois, L., (1988). The CIW index: A new chemical index of weathering. Sediment Geol., v. 55, pp. 319–322.

Johnson, S.Y. and Nur Alam, A.M., (1991). Sedimentation and tectonics of the Sylhet trough, Bangladesh. Geol. Soc. Amer. Bull., 103, 1513-1527.

LI Y-H (2000). A compendium of Geochemistry. Princeton University Press, Princeton, NJ, 475 p

McLennan, S. M., (1993). Weathering and global denudation, Jour. Geol., 101, 295–303.

McLennan, S.M., Taylor, S.R., McCulloch, M.T., and Maynard, J.B., (1990). Geochemical and Nd-Sr isotopic composition of deep sea turbidites: crustal evolution and plate tectonic associations. Geochem. Cosmochim. Acta, 54, 2015-2050.

Molnar, P. and Stock, J. M., (2010). Slowing of India's convergence with Eurasia since 20 Ma and its implications for Tibetan mantle dynamics; *Tectonics* 28 TC3001.

Nesbitt, H.W. and Young, G.M., (1982). Early Proterozoic climates and plate motions inferred from major element chemistry of lutites. Nature, 299, 715-717.

Nesbitt, H. W., G. Mackovics, and R. C. Price., (1980). Chemical processes affecting alkalis and alkaline Earth during continental weathering, Geochim. Cosmochim. Acta, 44, 1659–1666.

Nesbitt, H.W. and Young, G.M., (1996). Effects of chemical weathering and sorting on the petrogenesis of siliciclastic sediments, with implications for provenance studied. Jour. Geology, 104, 525-542.

Ohta, T and Arai, H., (2007). Statistical empirical index of chemical weathering in igneous rocks: A new tool for evaluating the degree of weathering. Chemical Geology, 240, 280–297

Rea, D.K., (1992). Delivery of Himalayan sediment to the northern Indian Ocean and its relation to global climate, sea level, uplift, and seawater strontium. *In*: Duncan, R.A., Rea, D.K., Kidd, R.B., von Rad, U., and Weissel, J.K. (Eds.), Synthesis of Results from Scientific Drilling in the Indian Ocean. Amer. Geophys. Union, Washington, D.C. Geophysical Monograph, 70, 387- 402.

Sen, S., Das, P.K., Bhagaboty, B. and Singha, L.J.C., (2012). Geochemistry of Shales of Barail group occurring in and around Mandardisa, North Cachar Hills, Assam; India: Its Implications. International Journal of Chemistry and Applications. 4, 25-37.

Soibam, I., (1998). On the Geology of Manipur. *In:* Souvenir, IX Manipur Science Congress (March, 25–27) 12–19.

Srivastava, G., Spicer, R. A., Spicer, T. E. V., Yang, J., Kumar, M., Mehrotra, R. C. and Mehrotra, N. C., (2012). Megaflora and Palaeoclimate of a Late Oligocene Tropical Delta, Makum Coalfield, Assam: Evidence for the Early Development of the South Asia Monsoon; Palaeogeogr. Palaeoclimatol. Palaeoecol, 342–343, 130–142.

Summerfield, M. A. and Hulton, N. J., (1994). Natural controls of fluvial denudation rates in major world drainage basins. Jour. Geophys. Res., 99, 871- 883.

Uddin, A. and Lungberg, N., (1998). Cenozoic history of the Himalayan-Bengal System. Sand composition in the Bengal basin, Bangladesh. Geol. Soc. Amer. Bull., 110, 497.

Young, S.W., Basu, A., Mack, G., Darnell, N. and Suttner, L.J., (1975). Use of size-composition trends in Holocene soil and fluvial sand for paleoclimate interpretations. Pro. IX Intnl. Cong. Sed. Theme 1, Nice, France.

Jour. Indian Association of Sedimentologists, Vol. 34, Nos. 1 & 2. (2017), pp. 17-28

Petrofacies and Tectono Provenance of the Sandstones of Jara Dome, Kachchh, Gujarat

SHAISTA KHAN*[1], M. ADNAN QUASIM*[1], A. H. M. AHMAD[1] AND M. M. ALAM[2]
[1] Department of Geology, Aligarh Muslim University, Aligarh - 202002 (U.P.)
[2] Department of Civil Engineering, Z.H. College of Engineering, Aligarh Muslim University, Aligarh - 202002
E-mail: shaista.khans03@gmail.com, adnanquasim@gmail.com

Abstract: The Ridge and Athleta Sandstone members of Jara Dome have been analyzed for their petrofacies, provenance and tectonic setting. Various factors responsible for modification of the original detrital composition of the sandstones have been critically examined. In addition, heavy minerals have also been studied to strengthen the interpretation of the provenance. These sandstones were derived from a mixed provenance including granites, granite-gneisses, low and high-grade metamorphic and some basic rocks of the Aravalli Range and Nagarparkar Massif. The petrofacies analysis reveals that these sandstones belong to the continental block, recycled orogen and rifted continental margin tectonic regime. The first cycle and recycled detritus was further intensely modified as a result of weathering under warm humid climate and transport before burial, thereby providing mineralogical maturity to the sandstones of the Jara Dome.

Keywords: Petrofacies, Tectono-provenance, Ridge and Athleta Sandstone, Jara Dome, Kachchh, Gujarat.

INTRODUCTION

The goal of provenance studies is to deduce the characteristic of sediment source areas. Petrographic analysis is a standard method for studying provenance (Dickinson and Suczek, 1979; Ingersoll and Suczek, 1979). During the last two decades, several authors (Schwab, 1975; Dickinson and Suczek, 1979; Dickinson et al., 1993; Valloni, 1985) have demonstrated a close correlation between composition of terriginous sediments/ sedimentary rocks and plate tectonic settings. The relative proportions of detrital framework grains plotted on triangular diagrams are believed to discriminate among variety of plate tectonic settings (Ingersoll, 1983; Lash, 1986; Jett and Helier, 1988; Akhtar and Ahmad, 1991; Ahmad and Bhat, 2006; Quasim and Ahmad, 2015). However, the correlation between tectonic setting and sandstone petrofacies may not always be valid due to modification of its composition by recycling, transport and post-depositional processes. The most notable modifying agents are intense chemical weathering under tropical humid climate and low relief (Suttner et al., 1981; Basu, 1985; Grantham and Velbel, 1988; Girty, 1991), differential abrasion during predepositional and pre-burial transport (Lucchi, 1985; Espejo and Gamundi, 1994) and diagenesis (McBride, 1985). Sediment recycling (Cox and Lowe, 1995), mixing of detritus derived from two sources, temporal change in tectonic style (Mack, 1984) and long sediment transport across the 'mother' plate to tectonically alien basins also hinder the identification of 'generic' tectonic setting and provenance. This paper attempts to study petrofacies, provenance and tectonic setting of the sandstones of Jara Dome. The petrofacies of this basin is interpreted in the light of known geotectonic of the Aravalli craton, keeping in view the various modifying factors that control and influence the original detrital composition.

TECTONIC SETTING

The Jurassic sediments of Kachchh represent a thick pile of rocks ranging in age from Bajocian to Tithonian (Singh et al., 1982), which rest unconformably on the Precambrian basement (Table 1). The basin developed primarily due to rifting of Africa and India in the Late Triassic time during the fragmentation of the Gondwana Superplate (Biswas, 1987). The total thickness of Mesozoic sediments in Kachchh ranges from 1525 to 3050 m (Biswas and Deshpande, 1983). The sequences were developed due to repeated marine incursions during the Middle Jurassic to Lower Cretaceous period followed by major tectonic movements and Deccan Trap volcanism in the Late Cretaceous time. The basin is bordered by the subsurface Nagarparkar massif in the north, Radhanpur-Barmer Arch in the east and Kathiawar uplift to the south (Biswas, 1982). The Mesozoic sediments are exposed in the Kachchh Mainland, Patcham, Khadir, Bela, Wagad, Chorad Islands in the "Great Runn of Kachchh" (Fig. 1). These sediments are dominantly represented by siliciclastics. Fursich et al. (1991) interpreted these siliciclastics representing a wide range of depositional settings including coastal and estuarine environments; subtidal bar-storm influenced shallow shelf and mid-shelf

Table 1. Lithostratigraphic framework of the Jurassic and Lower Cretaceous Rocks of Kachchh Mainland (Fürsich et al., 2001).

Age	Kachchh Mainland	
Albian-Aptian	Umia Formation	Bhuj Member
		Ukra Member
Neocomian		Ghuneri Member
Tithonian		Umia Member
Tithonian-Kimmeridgion	Katrol Formation	
Late Early Oxfordian		Dhosa Oolite Member
Early Oxfordian	Chari Formation	Dhosa Sandstone Member
		Gypsiferous Shale Member
		Athleta Sandstone Member
Callovian		Ridge Sandstone Member
		Shelly Shale/Keera Golden Oolite Member
Bathonian	Patcham Formation	Sponge Limestone Member
		Purple Sst./Echinodermal Packstone Member
		Jumara Coralline Limestone Member
Bajocian-Bathonian	Jhurio Formation	Goradongar Yellow Flagstone Member
		Jhura Golden Oolite Member
		Canyon Lst./Badi Golden Oolite Member
		Badi White Limestone Member

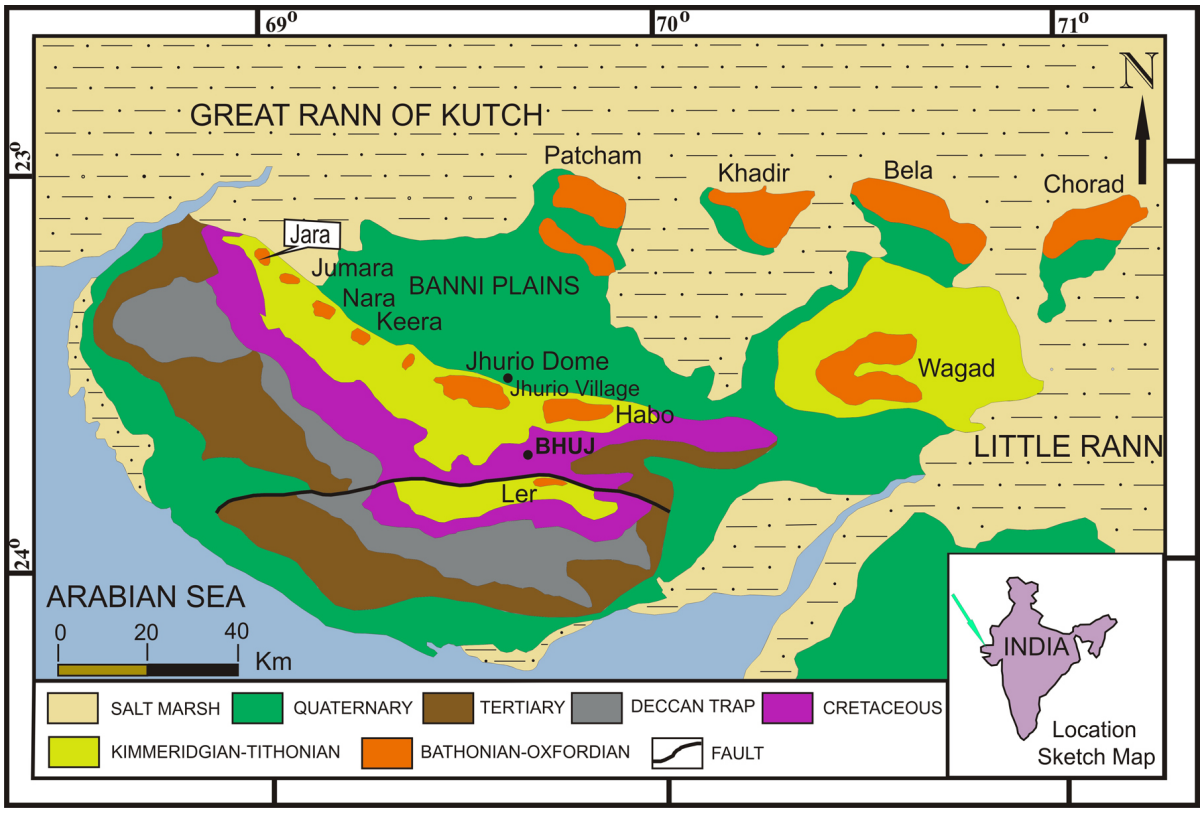

Fig. 1. Geological map of Kachchh Basin (after Biswas, 1977) showing the study area Jara Dome.

environments below storm wave base and sediment starved offshore settings.

The study area is the important part of the Kachchh Basin situated on the western margin of Indian Peninsula. The major part of the region is a desert which is either alluvial or partly fluvio-marine or windblown with saline wastes in Rann of Kachchh. Jara dome situated in the western part of the Mainland Kachchh comprises of Jumara, Jhuran and Bhuj formations. The Jhuran and Bhuj formations form the outer semicircular girdle of the Jara dome. Rudramata Shale Member and Upper Member of the Jhuran formation are exposed around Jara Dome and Lakhapat village which is situated on the outer periphery of the Jhuran-Bhuj girdle. In Jara Dome area in northwestern Mainland, the Formation is predominantly arenaceous. It is a quaquaversal dome, dipping away in all direction from the centre. It is 3km in diameter, bounded by the Northern latitudes of 23°43' to 23°45' and the East longitudes of 68°57' to 69°00'. The Jara Dome is represented by sandstone, shale and limestone. Here the Formation has two distinct parts, the upper part is composed mainly of sandstone beds and the lower is composed of alternating beds of sandstone and shales. There are good exposures of Middle to Late Jurassic rocks along various nalas and road cuttings.

METHODOLOGY

In the present study the detrital minerals of Ridge and Athleta Sandstone members were studied for the purpose of interpreting their provenance and plate tectonic setting. Thirty five samples of medium sandstones from the Ridge and Athleta members were collected from Jara for petrological analysis (Fig. 2). Sandstone samples were cut into standard petrographic thin sections, which were etched and stained for calcium and potassium feldspar and pore space. Framework grains varying from 200 to 250 per thin section were counted. For petrofacies analysis, counts for operational categories i.e. Qm, Qp, Qt, F, P, K, Lv, Ls, Lt and L as defined by Dickinson (1985) were performed and recalculated to 100 percent. The heavy mineral identification was undertaken following Krumbien and Pettijohn (1938); Milner (1962).The interbasinal grains are ignored (Zuffa, 1980). The percentages of heavy minerals are ignored because their different response to hydrodynamic conditions and geochemical influences, make varied volumetric distribution. Extrabasinal carbonate grains or detrital limeclast (Lc) are not recalculated with other lithic fragments because of their vastly different geochemical response during weathering and diagenesis as well as the case of confusion with

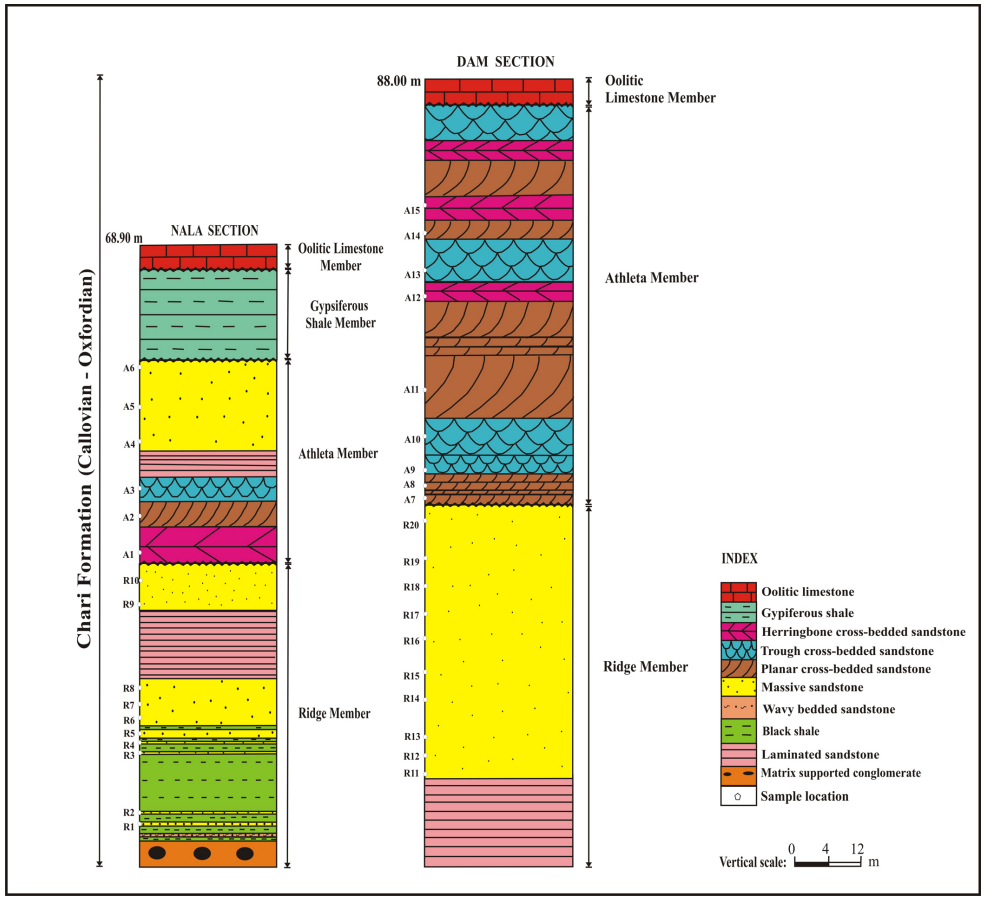

Fig. 2. Lithostratigraphic columns show various lithofacies of Jara Dome of the Kachchh basin.

intrabasinal carbonates grain (intraclast, bioclast, oolite and peloids).

DETRITAL MINERAL COMPOSITION

The detrital content comprises quartz, feldspar, mica, chert, rock fragments and minor constituent of heavy minerals. Although igneous quartz is the predominant mineral in the Jara Dome Sandstone, other varieties of quartz such as recrystallized and stretched metamorphic quartz are also common. The feldspar is mainly potassic variety comprising orthoclase and microcline. The small amount of plagioclase grains is also present. Rock fragments include chert, phyllite, schists and siltstones (Plate-1A-F). As per Folk's (1980) classification, the sandstones of the Jara Dome are mainly quartzarenites followed by subarkose. The average composition of detrital minerals of Ridge Sandstone represented by 86.85% quartz; 8.63% feldspar; 2.65% mica; 0.59% chert; 0.89% rock fragments and 0.31% heavy minerals. Athleta Sandstone consists of 86.59% quartz, 9.37% feldspar, 2.34% mica, 0.69% chert, 0.74% rock fragments and 0.26% heavy minerals (Table 2).

FACTORS CONTROLLING DETRITAL MINERALOGY

Palaeoclimate, distance of transport, source rock composition and diagenesis are the most important factors controlling the composition at the time of deposition. These factors were studied in detail in order to analyze their effect on detrital composition.

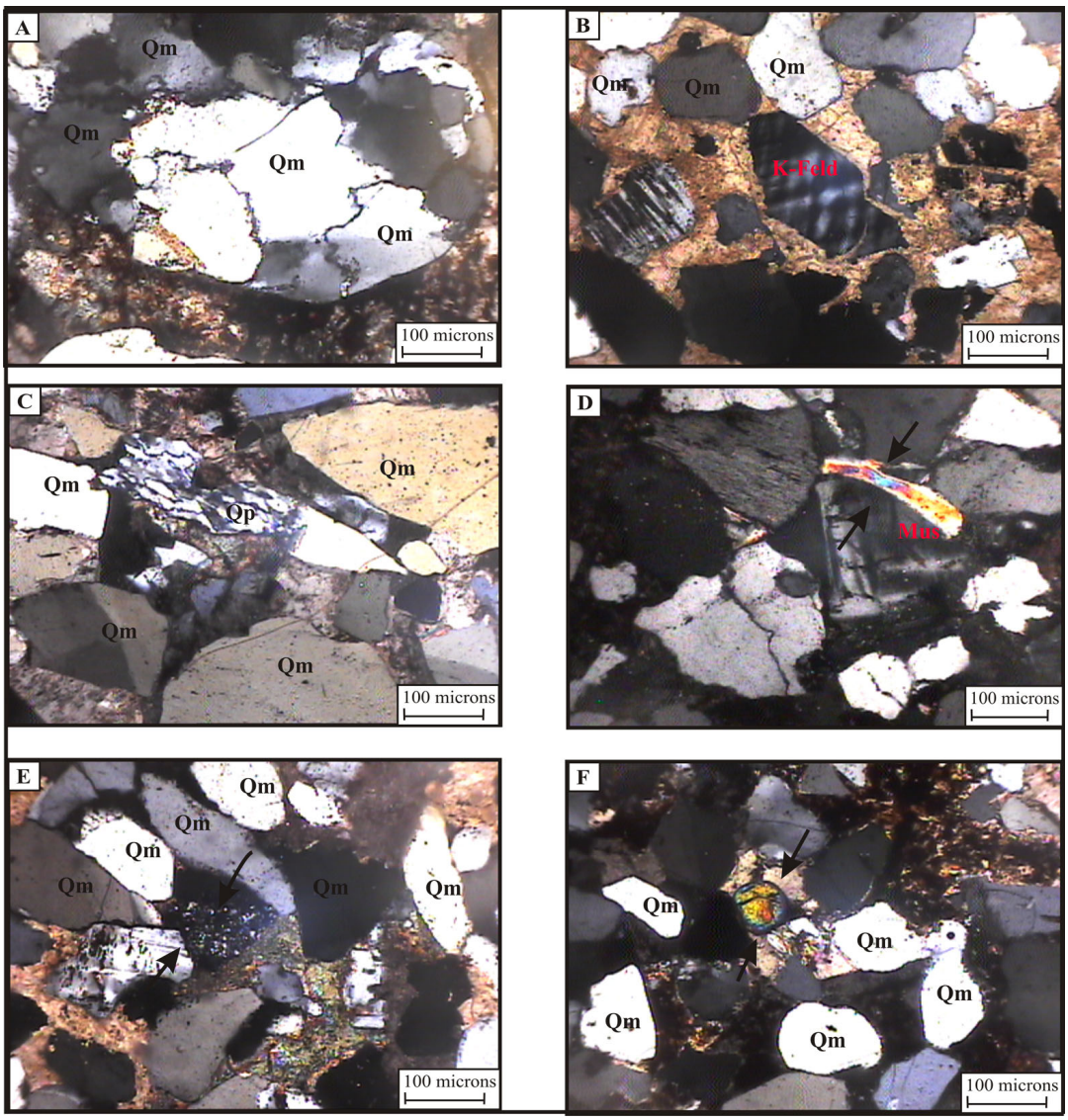

Plate. 1. Photomicrographs showing **(A)** Quartz grains are commonly monocrstalline, with straight to undulose extinction **(B)** fresh feldspar grain **(C)** Polycrystalline quartz of medium size, indicating derivation from metamorphic sources **(D)** Bended muscovite flakes between rigid detrital grains **(E)** sedimentary lithic fragment (chert) **(F)** rounded zircon grain.

Table 2. Percentages of Detrital minerals in the sandstones of Jara Dome, Kachchh, Gujarat.

S. No.	Monocrystalline Quartz	Polycrystalline Quartz		Feldspar		Mica		Chert	Rock Fragments	Heavies
	Common Quartz	Recrystallized Metamorphic Quartz	Stretched Metamorphic Quartz	Plagioclase	Microcline	Muscovite	Biotite			
Athleta Sandstone Member										
A1	84.02	0.33	1.2	0	8.65	2	0	1	1.01	0.56
A2	82.44	1	0.77	0.56	10	4.11	0.01	1.09	0.11	0.65
A3	72.11	3.5	3	1.23	11.56	3.23	0	1.34	1.45	0.9
A4	73.05	4	0.89	2	14.5	5	0	1	0.11	0.11
A5	86.33	1.25	1.45	1	5.11	1.22	0.4	0.23	2	0
A6	87.23	3.5	0.55	1.56	4.97	2	0	0.54	0.56	0
A7	81.34	2.1	0.12	1.5	9.56	1.45	0.11	1.45	1.11	0.1
A8	75.65	5	2	1.11	10	2.46	0	0.33	0	0
A9	76.45	4.23	1.22	1.78	11.24	2.1	0.1	0	1.54	0
A10	85.35	2.56	0.3	0.56	4.87	3.09	0	0.65	0	0.57
A11	85.45	1.45	1.45	0	7.49	1.07	0.23	0	0.45	0
A12	81.66	4.22	1.66	1.22	6.2	1.55	0	0.76	0.89	0.32
A13	84.5	3.87	0.54	0.32	8	1.43	0	0	1.08	0.12
A14	83.45	3.02	0.78	0.21	8.89	2	0.7	0.87	0	0
A15	79.45	6.7	2.1	0.11	6.56	1.01	0	1.23	0.86	0.67
Avg.	81.38	3.11	1.2	0.87	8.5	2.24	0.1	0.69	0.74	0.26
Ridge Sandstone Member										
R1	88.67	3.09	0.06	0	3.45	1.78	0.01	0.81	0.62	0.67
R2	80	2	1.13	1.45	9.68	1.67	0	1.04	0	0
R3	72.23	2.56	4.87	1.01	11	4.45	0.03	2	0.04	0.87
R4	75.98	3.98	0.64	0	13.23	4.32	0	0.37	1.09	0.32
R5	85.56	2.06	1.45	0.65	5.34	2.67	1.45	0.56	0	0
R6	83.66	1.34	1.32	0.82	7.03	2	0	1.24	0.86	0
R7	85	0.06	0.04	0.05	9	5.01	0	0	0	0.09
R8	74.03	2.43	3	1.22	11.04	4.09	0	1.03	1.54	0.9
R9	75.35	3.21	0.11	1.13	14.65	3.98	0	1.88	0	0
R10	86.16	2.14	1.56	0.45	4.85	2	0	0.06	2	0.02
R11	86.5	1.3	1.61	0.5	4.77	2.23	0	0	2.1	0.78
R12	78.09	4.39	0	1.14	10.45	1.54	0.01	0.45	1.5	0.69
R13	85.45	3.06	0.05	0.56	7.47	1.12	0	0	1.67	0.01
R14	83.11	4.56	0	0	5.56	3.56	0.34	0	0.5	0
R15	81	6.98	2.3	0.02	5.67	1.04	0	0.87	0.78	0.56
R16	76.17	6.55	1.12	1.67	10.63	2.87	0.78	0	0.23	0
R17	80	3.02	1.73	1.89	7.34	1.66	0	0.77	2	0.54
R18	86.56	4.12	1.78	0	3.09	1.59	0	0.01	1.98	0
R19	79.09	5.03	1.34	1.32	8.67	1.04	0	0	1	0.67
R20	84.66	6	0	0.72	5.09	1.09	0.82	0.87	0	0.22
Avg.	81.36	3.39	1.2	0.73	7.9	2.48	0.17	0.59	0.89	0.31

Paleoclimate

Bivariant log/log plot of the ratio of polycrystalline quartz to feldspar plus rock fragments (Suttner and Dutta, 1986) has been used for interpreting the palaeoclimate of Ridge and Athleta sandstones. The mean value of the ratio were plotted (Fig. 3) and these indicate humid climate for the area .The precipitation of large amount of carbonate during Jurassic is also supportive of the fact that the area was witnessing warm climate similar to found in tropics. A combination of low relief, hot humid climate and ample vegetation can produce quartz rich detritus (Franzinelli and Potter, 1983). Low relief provides prolonged residence time of sediments, thereby increasing the detritus of chemical weathering and thus the sediments rich in the stable quartz. Thus, climate might have been an important factor in the production of compositionally mature quartz rich sandstones. However, climate alone cannot produce quartz rich sands.

Source Rock Composition

The suite of heavy minerals present in the studied sandstones including biotite, tourmaline and zircon indicate an acid igneous source for these sandstones. The dominant alkali feldspar encountered in this study is microcline, which indicates a granite and pegmatite source. On the other hand the suite of heavy minerals including garnet, staurolite reflects a metamorphic

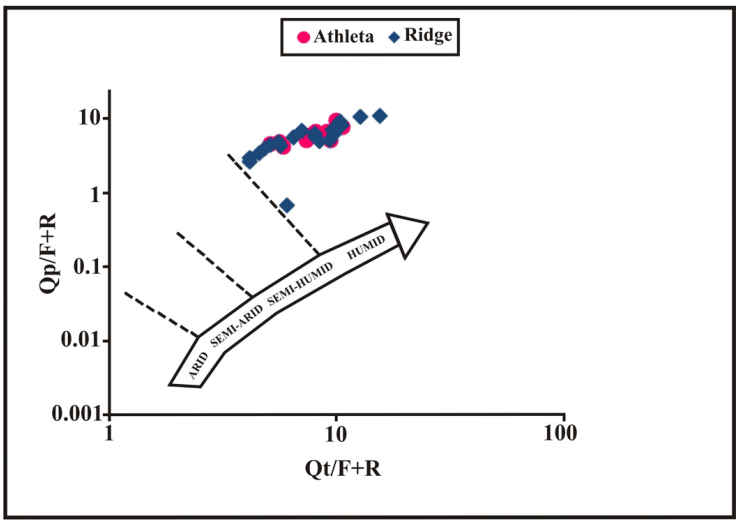

Fig. 3. Bivariant log/log plot for Jara Dome sandstones, Kachchh Basin, according to Suttner and Dutta (1986).

source. However, the occurrence of various shades of garnet indicates different source rocks from acid igneous to metamorphic rocks. The suite of heavy minerals, including rounded grains of tourmaline, rutile and zircon is indicative of the reworked source for these sandstones. These heavy mineral suites in the Ridge and Athleta sandstones reflect their source in a mixed provenance, such as believed to represent the eroded and weathered parts of the present day Aravalli Range situated east and northeast of the basin and Nagarparkar massif situated to the north and northwest (Dubey and Chatterjee, 1997).

Distance of Transport

The detrital grains of the Ridge and Athleta sandstones are in sand size range and derived from Aravalli Range that suggests transportation for a distance of few hundred kilometers. The studied sandstones show small amount of feldspar and one possible reason for this deficiency may be the transportation of sediments by high gradient streams and rapid destruction of feldspar by abrasion. Since deposition of Ridge and Athleta sandstones took place in a tectonically active rift, presence of high gradient stream is quite likely within the basin. However this premise does not stand to scrutiny because rock fragments which could have been destroyed more easily are common within studied sandstones. Therefore, some factor other than transportation was responsible for paucity of feldspar in both the studied sandstones. Feldspar is removed to large extent in humid climatic condition by chemical weathering.

Diagenetic Modification

The diagenetic modifications in the Ridge and Athleta sandstones include loss of detrital framework grains by dissolution, alteration of grains by replacements or by recrystallization and the loss of identity of certain ductile grains. The process of replacement is effective in modifying the detrital composition of sandstones. The replacements of quartz by carbonate and iron oxide cement in the studied sandstones suggest modification of the composition of the sandstones. The study of grain contacts of the sandstones indicates that the sandstones were subjected to compaction during burial and their original texture and fabric was slightly modified by the processes of compaction.

TECTONO-PROVENANCE

The plots of Jara Dome Sandstones on Qt-F-L and Qm-F-Lt diagram suggest that the detritus of the sandstones were derived from the granite-gneisses exhumed in the craton interior and low to high grade metamorphic supracrustal forming recycled orogen shedding quartzose debris of the continental affinity into the basin (Fig. 4A & B). It has been mentioned that provenance of Jara Dome sandstone is believed to be weathered parts of the present day Aravalli Range situated northeast, east and southeast of the basin and Nagarparkar massif situated north and northwest of the basin. This is indicated by sand dispersal pattern studied by various workers (Balagopal and Srivastava, 1975; Dubey and Chatterjee, 1997; Ahmad et al., 2008). The two source areas are represented by Precambrian metasediments and granite-gneiss of Aravalli Supergroup. The Qp-Lv-Ls plots reveal the source in rifted continental margin (Fig. 4C). In the Qm-P-K diagram, the data lie in the continental block provenance reflecting maturity of the sediments and stability of the source area (Fig. 4D) This may have stemmed from very long period of tectonic quiescence and mature geomorphology of the area.

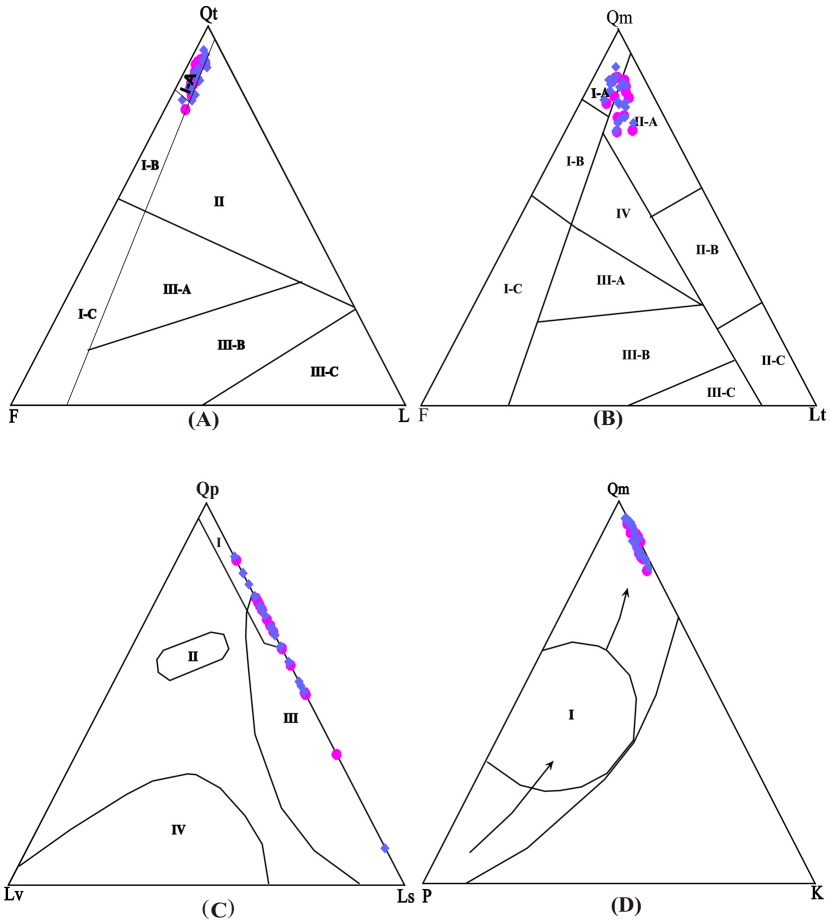

Fig. 4 A-D. Plots of the sandstone of Jara Dome, Kachchh, according to Dickinson (1985).

The Ridge and Athleta sandstones are generally sub-mature, moderately sorted and not well rounded. This indicates that the studied sandstones were largely deposited in environments, protected from persistence wave and current action. The wave and currents had sufficient strength to winnow away the mud, but were not strong enough to bring about sorting and rounding of the detrital grains. The detritus was also enriched in quartz by destruction of labile grains during long residence time at the sediment water interface.

The relative abundance of monocrysalline quartz to that of polycrystalline quartz appears to reflect the maturity of the sediment, because polycrystalline quartz is eliminated by recycling and disintegrates in the zone of weathering as does strained quartz (Basu, 1985). The sandstones have generally a considerably high percentage of monocrystalline quartz (Ridge Sandstone, 81.36%; Athleta Sandstone, 81.38%) as compared to polycrystalline quartz (Ridge Sandstone, 4.59%; Athleta Sandstone, 4.31%), which indicates removal of polycrystalline quartz by weathering and recycling (Table 3). The low percentages of polycrystalline quartz may also be ascribed to fine size of grains. Abundance of feldspar also serves as a guide to determine the maturity index since much of the feldspar is destroyed by weathering, where relief is low and rainfall is high. The very small percentage of feldspar in general, in the sandstone suggests that they are lost in soil profile or by abrasion during transit or lost by solution during diagenesis. However, even limited occurrence of weathered and fresh feldspars together indicates their derivation from two different sources.

The unconformity separating the Precambrian basement rocks and the overlying Jurassic sandstones represent a very long interval of time during which long continued weathering, especially under humid tropical climate and persistent tectonic stability should have destroyed all labile constituents including feldspar in the soil profile and may have produced compositionally mature and texturally sub-mature sediments. In some thin sections of very fine grained sandstones, markedly high percentages of feldspar are present. It is quite likely that the abundance of feldspar in the fine grained sediments came in contact with circulating of meteoric or subsurface water resulting into dissolution. In many thin sections of the sandstones, dissolution of feldspar is noted, sometimes yielding oversized pores. It appears therefore, that diagenetic processes have altered the depositional composition of the sandstones which contained a higher proportion of feldspars at the time of deposition.

Table 3. Percentages of framework modes of the sandstones of Jara Dome, Kachchh, Gujarat (Based on classification of Dickinson, 1985).

S.No.	Qt	F	L	Qm	F	Lt	Qp	Lv	Ls	Qm	P	K
Athleta Sandstone Member												
A1	87.00	9.23	3.23	84.56	9.23	5.78	50.13	0.00	49.65	90.00	0.46	9.13
A2	85.23	10.00	4.32	83.05	10.00	6.55	34.09	0.00	66.01	89.13	0.02	10.68
A3	81.14	13.09	5.00	72.41	13.01	14.12	71.68	0.01	28.00	84.56	1.56	13.57
A4	78.00	16.54	5.33	73.09	16.82	10.00	49.89	0.00	50.03	81.10	2.03	16.04
A5	89.87	5.72	4.04	87.00	5.46	7.34	57.14	0.00	42.43	93.67	0.45	5.46
A6	91.56	5.97	2.62	87.23	5.90	6.76	66.11	0.00	33.81	93.65	1.00	5.00
A7	85.07	11.45	3.21	81.50	11.50	6.58	61.57	0.02	38.12	87.90	1.47	10.42
A8	84.67	11.21	3.90	76.03	11.23	12.02	73.56	0.00	26.08	87.07	1.86	11.87
A9	83.00	12.60	3.70	76.63	12.67	10.16	74.87	0.00	25.11	85.56	1.82	12.76
A10	89.87	5.36	4.23	86.00	5.13	8.61	49.57	0.00	50.07	93.54	0.70	5.09
A11	90.00	8.00	1.98	86.12	8.00	5.34	67.70	0.00	32.12	91.24	0.45	8.31
A12	88.76	7.87	3.08	81.39	7.68	10.00	72.82	0.01	27.00	91.20	1.34	7.00
A13	88.34	8.53	3.10	84.16	8.32	6.38	69.00	0.00	30.47	90.81	0.11	8.48
A14	88.06	9.22	2.76	84.00	9.24	6.02	61.67	0.00	38.00	89.71	0.00	9.34
A15	90.00	6.90	2.14	80.24	6.67	13.00	84.80	0.00	15.10	92.00	0.43	7.48
Avg.	86.70	9.44	3.50	81.56	9.39	8.57	62.97	0.00	36.80	89.40	.91	9.37
Ridge Sandstone Member												
R1	93.45	4.04	1.99	89.79	4.10	5.78	66.67	0.00	33.12	95.13	0.49	3.89
R2	85.00	11.45	3.60	80.33	11.24	8.00	65.13	0.00	34.67	87.22	1.67	10.69
R3	82.26	12.46	4.67	72.59	12.61	14.25	67.25	0.00	32.56	85.09	1.03	13.65
R4	80.24	13.59	5.79	75.79	13.06	10.04	52.00	0.01	47.87	84.39	0.99	14.59
R5	90.00	5.34	4.34	85.36	5.19	8.69	50.25	0.00	49.34	93.88	0.03	6.56
R6	89.02	7.67	3.42	84.95	7.87	7.56	65.05	0.00	34.56	91.49	0.26	7.67
R7	85.45	9.09	5.03	85.00	9.12	5.86	9.56	0.00	90.19	90.05	0.00	9.89
R8	81.67	12.03	5.88	74.65	12.03	12.68	62.12	0.01	37.67	85.69	1.40	12.87
R9	80.00	16.00	3.24	75.00	16.09	8.75	58.00	0.00	41.87	82.14	1.34	16.02
R10	90.09	5.34	4.09	86.93	5.29	8.09	67.18	0.00	32.49	94.00	0.13	5.23
R11	90.25	5.14	4.14	87.12	5.40	7.16	58.19	0.00	41.60	94.06	0.46	5.68
R12	84.25	12.00	3.23	79.22	12.02	8.69	75.18	0.02	24.67	86.67	1.37	11.67
R13	88.73	8.03	3.00	85.65	8.10	6.12	70.02	0.00	29.57	91.13	0.36	7.89
R14	89.00	5.47	5.16	83.68	5.87	10.37	53.00	0.00	46.89	93.56	0.08	6.28
R15	91.00	5.76	3.06	81.00	5.56	13.10	81.49	0.00	18.45	93.24	0.00	6.35
R16	83.80	12.81	3.65	76.59	12.45	11.34	72.73	0.00	27.01	85.80	2.03	12.19
R17	86.46	9.20	4.20	80.57	9.13	9.89	75.45	0.00	24.54	89.49	1.87	8.57
R18	92.42	4.13	3.16	86.34	4.09	9.17	78.35	0.00	21.35	95.18	0.88	3.79
R19	87.15	9.68	2.72	80.09	9.96	10.01	86.09	0.00	14.09	89.00	1.45	9.74
R20	91.34	5.02	3.63	85.53	5.11	9.41	71.68	0.00	28.12	94.12	0.01	5.77
Avg.	87.07	8.71	3.90	81.80	8.71	9.24	64.26	0.00	35.53	90.08	0.79	8.94

Qt= Total quartz, F= Total feldspar, L= Total lithic fragments, Qm= Monocrystalline quartz, Lt= Total lithic grains, Qp= Polycrystalline quartz, Lv= Volcanic lithic grains, Ls= Sedimentary lithic grains, Qm= Monocrystalline quartz, P= Plagioclase, K= Orthoclase and microcline

The location of the study area lies within a humid tropical belt during the deposition of Kachchh Basin sediments (Bhalla, 1983; Chandler et al., 1992). Thus the evolution of Kachchh petrofacies was controlled by the prevailing warm and wet climate during Jurassic. This would have had resulted in the removal of metastable and unstable grain modes during the weathering process that will enrich quartz and quartzose mode thereby shifting the petrofacies plots towards continental block provenance field. Therefore, the continental block provenance that provided detritus to the study area during the deposition of the Ridge and Athleta sandstones was deeply weathered.

The detrital grains of Ridge and Athleta sandstones are the sand size range and in all probably they have undergone transportation for a distance of few hundred km from Aravalli range and this may add to more changes in detritus composition which has already been subjected to intense weathering at the source area. Bivariant plots against Mz versus Qm/Qp, Qm/F and Qm/L overall shows weak to moderate relationship both in Ridge and Athleta sandstones (Fig. 5a & b)**.** In Athleta

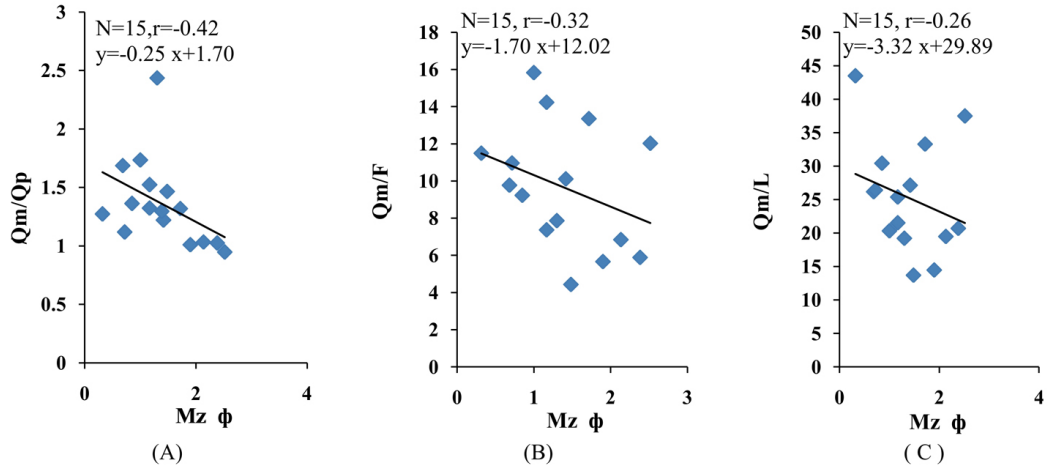

Fig. 5a. Bivariant plot and correlation coefficient of grain size ratios of Qm/Qp (A); Qm/F (B); and Qm/L of Athleta Sandstone. Equation is in form of y= mx+c.

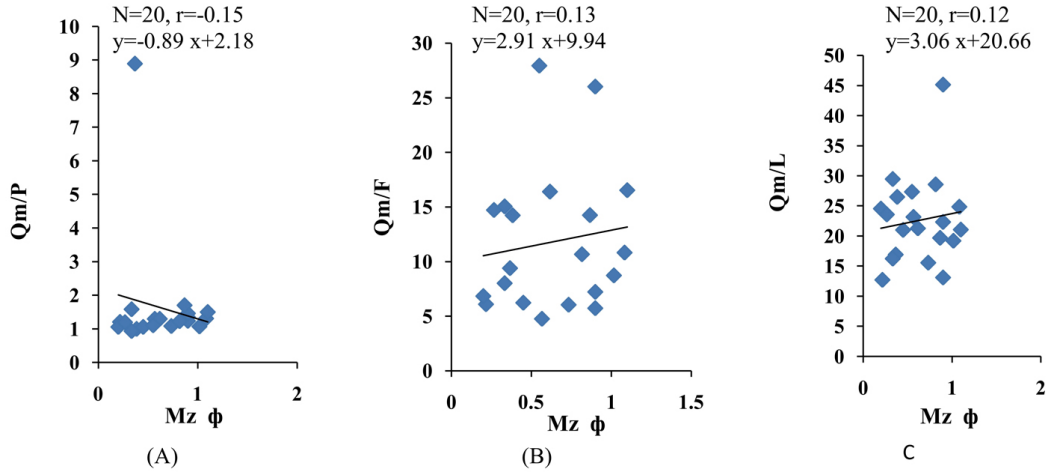

Fig. 5b. Bbivariant plot and correlation coefficient of grain size ratios of Qm/Qp (A); Qm/F (B); and Qm/L of Ridge Sandstone. Equation is in form of y= mx+c.

sandstone Mz versus Qm/Q show moderate inverse relationship suggest a slight increase in Qm at the expense of Qp and L with increasing grain size, probably as a result of intense chemical weathering during transport and deposition. The Qm/F ratio show moderate inverse relationship with grain size. It has been established that the average composition of sediment changes through time (Cox and Lowe, 1995). The tectonic style of Aravalli-Delhi folded belt makes it a collage of recycled orogen and basement uplift provenance. It is expected that sandstone detrital modes derived from them would plot in a recycled orogen provenance. False signature of continental block provenance may be result of several factors which have modified the original composition of the detritus in one way or the other. These factors include paleoclimate, distance of transport and diagenesis. Diagenetic process is in the form of grain dissolution and chemical compaction. Some of the samples show pervasive development of calcite and iron oxide cements resulting in destruction of the framework by erosion of detrital modes. In a few cases complete digestion of the feldspar grains has been observed in this study. This may have had modified the petrofacies in terms of quartz and quartzose material may have caused a shift towards continental block provenance.

According to Cannon et al., (1981) and Tankard et al., (1982) the beginning of plate separation in other parts of Gondwanaland during Jurassic and Early Cretaceous was marked by the formation of pericratonic rift basins which were similar to the pericratonic rifts (Kachchh and Saurashtra) may represent parts of an elongated extensional trough where up or down rifting during Jurassic-Cretaceous time brought about basin formation and sedimentation, first in northern part (Jurassic of Kachchh) and later in southern parts (Early Cretaceous

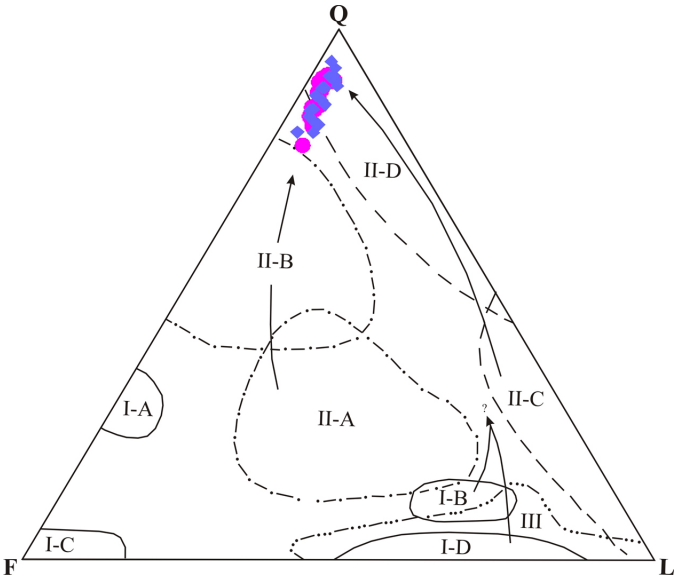

Fig. 6. Postulated idealized evolution model of Jara sandstones with emphasis on source rocks and climate. Expected petrofacies composition from ideal provenances with different climate and their relationship with primary source rocks by Alam (2002). The model modified after Cox and Lowe (1995), fields- IA, IB, IC, ID are of granite, rhyolite, gabbro and andesite- basalt respectively after McBirny (1984), IIA, IIB, IIC and IID are first cycle Holocene fluvial sands from granite (arid climate), granite (humid climate), metamorphic (arid climate) and metamorphic (humid climate) respectively after Suttner et al. (1981). III represents sediments from magmatic arcs after Marsaglia and Ingersoll (1993).

of Saurashtra) (Casshyap and Aslam, 1992). Kachchh Basin formed due to rifting during Late Triassic due to break up of Gondwanaland and is bounded by Nagarparkar fault in the north, Radhanpur Barmer Arch in the east and Kathiawar uplift in the south. The rift is styled by three main uplifts along three master faults with intervening half-grabens. The rift expanded from north to south by successive reactivation of primordial faults of Mid-Proterozoic Delhi fold belts. The rift evolution and syn-rift sedimentation continued till Early Cretaceous as Indian plate drifted northward along an anticlockwise path. The rifting was aborted by trailing age uplift during late Cretaceous pre-collision stage of the Indian plate. During post collision compressive regime of the Indian plate, the Kachchh rift Basin became a shear zone with convergent strike slip movements along sub-parallel rift faults.

It is now a well established fact that the Jurassic sedimentary rocks of Kachchh were deposited in faulted-troughs (Biswas, 1982). The study of Jurassic sediments of Kachchh Basin, especially their facies, helped in constructing their tectonic-sedimentary model (Fursich et al., 1991; Ahmad et al., 2008). The development and infilling of the Jurassic rift was concomitant with the pericratonic rifting and opening of the Arabian Sea in the west. Fault bounded basement uplifts along incipient rift belts within continental blocks shed arkosic sands mainly into adjacent linear troughs (Dickinson, 1985; Dickinson and Suczek, 1979). These authors have demonstrated that in such a tectonic setting, a spectrum of lithic poor quartzose-feldspathic sands forms a roughly linear array on Qt-F-L and Qm-F-Lt plots linking these arkosic sands with the craton derived quartzose sands that plot near the Qt and Qm poles. However Qm-F-Lt plot of Ridge and Athleta sandstones shows that points are fall in continental block and recycled orogen provenance fields. The basement uplifts may shed sands having affinity with detritus derived from recycled orogens provided erosion has been insufficient to remove cover rocks from basement (Mack, 1984). This may explain the false signatures of recycled orogen provenance in the case of the Ridge and Athleta sandstones.

Therefore from the foregoing discussion, the evolutionary trends of the Ridge and Athleta petrofacies are modeled which suggest two different evolutionary lineages (Fig. 6). An incipient rift developed during Late Triassic–Early Jurassic time within the Precambrian granite-gneiss and schist which formed the basement. The present petrofacies evolved through mixing of detritus from granite-gneiss basement uplift on the one hand, and from metasedimentary rocks of a recycled orogen on the other. The sediment composition was extensively modified during weathering under warm, humid climate at the source area and by weathering during transport and sedimentation. Thus quartz rich detritus were shed into the Kachchh rift. The relief of the provenance was low and erosion processes were not strong enough to remove the cover rocks from the basement.

CONCLUSIONS

1. The present petrofacies evolved through mixing of detritus from granite-gneisses basement uplift on the on hand and from metasedimentary rocks of a recycled orogen on the other. The sediment composition was extensively modified during weathering under warm, humid climate at the source area and by weathering during transport and sedimentation.

2. Plotting the data on the tectonic provenance discrimination diagrams (Qt-F-L, Qm-F-Lt, Qp-Lv-Ls and Qm-P-K) indicates sources in the continental block and recycled orogen provenance. In addition to this, the plot of the data on the Qp-Lv-Ls diagram indicates sediment contribution from uplifted rift margins.

3. The mineralogical composition of these sandstones reflects their sources in the mixed provenance that includes plutonic basement, sedimentary and metasedimentary rocks. The provenance is believed to represent the eroded and weathered parts of the present day Aravalli Range situated east and northeast of the basin and Nagarparkar Massif situated to the north and northwest. The maturity of the studied petrifacies is mainly due to recycling of the sediments which were sourced from the thick supracrustals typically of quiescent, shield areas adjacent to passive margin Kachchh Basin.

Acknowledgements: The authors gratefully thank the Chairman, Department of geology, Aligarh Muslim University, Aligarh for providing the necessary research facilities. We also gratefully acknowledge the critical and constructive suggestions offered by two anonymous referees, which improved the original manuscript.

References

Ahmad, A.H.M. and Bhat, G.M. (2006). Petrofacies, provenance and diagenesis of the Dhosa Sandstone Member (Chari Formation) at Ler, Kachchh sub-basin, Western India. Jour. Asian Ear. Science, 27, 857-872.

Ahmad, A.H.M., Khan, A.F. and Saikia, C. (2008). Palaeoenvironment and diagenesis of Middle Jurassic Athleta Sandstones, Jhurio Dome, Kachchh, Gujarat. Jour. Geol. Soc. India, 71, 73-78.

Akhtar, K. and Ahmad, A.H.M. (1991**).** Single-cycle cratonic quartzarenites produced by tropical weathering: the Nimar Sandstone (Lower Cretaceous), Narmada basin, India. Sed. Geol., 71, 23-32.

Alam, M.M. (2002). Generic provenance, tectonics and petrofacies evolution of sandstones, Jaisalmer Formation (Middle Jurassic), Rajasthan. Jour. Geol. Soc. India, 59, 47–58.

Balagopal, A.T. and Srivastava, V. K. (1975). A study of the paleocurrent and the provenances of the Jurassic rocks of Central Kutch, Gujarat state. Ind. Jour. Earth Science, 2, 62-76.

Basu, A. (1985). Influence of climate and relief on composition of sand release at source areas. In: Provenance of Arenites (Eds.G.G. Zuffa), Reidel, Dordrecht-Boston-Lancaster, 1-18.

Bhalla, (1983). India, In: The Phanerozoic Geology of the world II; The Mesozoic, B. Mallade, (Eds. M and Nairn, A.E.M.). Elsevier Publ; Amsterdam, 305-352.

Biswas, S. K. (1982). Rift Basins in western margin of India and their hydrocarbon prospects with special reference of Kutch Basin. Bull. Am. Assoc. Petrol. Geologists, 65**,** 1497-1515.

Biswas, S. K. (1987). Regional tectonic framework, structure and evolution of the western marginal Basins of India. Tectonophy., 135**,** 307-327.

Biswas, S.K. and Deshpandey, S.W. (1983). Geology and hydrocarbon prospects of Kutch, Saurastra and Narmada Basins. Petrol. Asia. Jour., 111-126.

Cannon, R.J., Simiyu Siambi, W.M.N. and Karanja, F.M. (1981**).** The Proto-Indian Ocean and probably Paleozoic/ Mesozoic tri-radial rift system in East Africa. Earth Planet. Sci. Letter, 52, 419-426.

Casshyap, S.M. and Aslam, M. (1992). Deltaic and shoreline sedimentation in Saurashtra basin, Western Indian: an example of infilling in an early Cretaceous failed rift. Jour. Sed. Petrology, 62, 972-991.

Chandler, M.A., Rind, D. and Ruedy, R. (1992). Pangean climate during early Jurassic GCMS simulations and sedimentary record of Paleoclimate. Bull. Geol. Soc. America, 104, 543-559.

Cox, R. and Lowe, D.R. (1995). A conceptual review of regional scale controls on the compositions of clastic sediments and the co-evolution of continental blocks and their sedimentary cover. Jour. Sed. Research, 65, 1-12.

Dickinson, W.R. (1985). Interpreting relations from detrital modes of sandstone. In: Provenance of Arenites. (Eds.G.G. Zuffa), Reidel, Dordrecht-Boston-Lancaster, 333-361.

Dickinson, W.R., Beard, L.S., Brakenridge, G.R., Erjavec, J.L., Ferguson, R.C., Inman, K.F., Knepp, R.A., Lindberg, F.A. and Ryberg, P.T, (1983). Provenance of North American Phanerozoic sandstones in relation to tectonic setting. Geol. Soc. Am. Bulletin, 94, 222-235.

Dickinson,W.R. and Suczek, C.A. (1979). Plate-tectonics and sandstones composition. Am. Assoc. Petrol. Geol. Bulletin, 63, 2164-2182.

Dubey, N. and Chatterjee, B.K. (1997). Sandstones of Mesozoic Kachchh Basins: Their provenance and basinal evolution. Ind. Jour. Petrol. Geology, 6, 55-58.

Espejo, I.S. and Gamundi, O.R.L. (1994). Source versus depositional controls on sandstone composition in a foreland basin: The Imperila formation (Mid-Carboniferous-Lower Permian), San Rafael Basin, Western Argentina. Jour. Sed. Research, 64, 8- 16.

Folk, R. L. (1980). Petrology of Sedimentary Rocks. Hemphill, Austin, Texas, 182.

Franzinelli, E. and Potter, P.E. (1983). Petrology, chemistry and texture of modern river sands, Amazon River system. Jour. Geol., 91, 23- 39.

Fursich, F.T., Oschmann, W., Jaitely, A.K. and Singh, I.B. (1991). Faunal response to transgressive and regressive cycles–examples from Jurassic of Western India. Palaeogeog. Palaeoclimat. Palaeoecology, 85, 149-159.

Fursich, F.T., Pandey, D.K., Callomon, J.H., Jaitely, A.K. and Singh, L.B. (2001). Marker beds in the Jurassic of the Kachchh basin, western India: their depositional environment and sequence stratigraphic significance. J. Palaeont. Soc. India, 46, 173-198.

Girty, G.H. (1991). A note on the composition of plutoniclastic sand produced in different climatic belts, (short notes). Jour. Sed. Petrology, 61, 428 - 433.

Grantham, J.H. and Velbel, M.A. (1988). The influence of climate and topography on rock-fragments abundance in modern fluvial sands of the southern Blue Ridge Mountains, North Carolina. Jour. Sed. Petrology, 5, 219-227.

Ingersoll, R.V. (1983). Petrofacies and Provenance of Late Mesozoic forearc basin, Northern and Central California. Bull.Am.Assoc. Petrol.Geol, 67, 1125-1142.

Ingersoll, R.V. and Suczek, C.A. (1979). Petrology and provenance of Neogene sand from Nicobar and Bengal Fans, DSDP sites 211 and 218. Jour. Sed. Petrology, 49, 1217 - 1218.

Jett, G.A. and Helier, P.L. (1988). Tectonic significance of polymodal compositions in mélange sandstones, Western mélange belt. North Cascade range, Washington. J. Sed. Petrol, 58, 52-61.

Krumbein, W.C and Pettijohn, F.J. (1938). Manual of the Sedimentary Petrology, Appleton Centaury, 549.

Lash, G.G. (1986). Anatomy of early Paleozoic subduction complex in the Central Appalachian Orogen. Sediment. Geol., 51, 75-96.

Lucchi, F.R. (1985). Influence of transport processes and Basin geometry on sandstone composition. In: Provenance of Arenites. (Eds. Zuffa, G.G.), D. Reidel, Dordrecht, 19- 45.

Mack, G.H. (1984). Exception to the relationship between plate tectonics and sandstone composition. Jour. Sed. Petrology, 54, 212 - 220.

Marsaglia, K.M. and Ingersoll, R.V. (1992). Compositional trends in arc–related, deep–marine sand and sandstone: a reassessment of magmatic–arc provenance. Geol. Soc. America Bulletin, 104, 1637–1649.

McBirney, A.R. (1983). Igneous Petrology, San Francisco, Freeman, Cooper, 504.

McBride, E.F. (1985). Diagenetic processes that effects provenance determination in sandstone. In: Provenance of Arenites. (Eds.G.G. Zuffa), Reidel, Dordrecht-Boston-Lancaster, 95-114.

Milner, H. B. (1962). Sedimentary Petrography Part II. George Allen and Unwin Ltd.London; 715.

Quasim, M.A. and Ahmad, A.H.M. (2015). Petrofacies and tectonic setup of Kaimur Group of rocks, Son Valley, India. The Palaeobotanist, 64(1), 1–11.

Schwab, F. L. (1975). Framework mineralogy and chemical composition of continental margin- type sandstone. Geology, 34, 331-340.

Singh, C.S.P., Jaitley, A.K. and Pandey, D.K. (1982). First report of some Bajocian Bathonian (Middle Jurassic) ammonoides and the age of the oldest sediments from Kachchh. Newsletters on stratigraphy, Western India. Jour. Geol. Soc. India, 34, 152-160.

Suttner, L.J., Basu, A. and Mack, L.M. (1981). Climate and the origin of quartzarenites. Jour. Sed. Petrology, 51, 1235-1246.

Suttner L.J. and Dutta P.K. (1986). Alluvial sandstones composition and paleoclimate, I. framework mineralogy. Jour. Sed. Petrology, 56, 329 – 345.

Tankard, A.J., Jackson, M.P., Erikson, K.A., Hobday, D.K., Hunter, D.R. and Minter, W.E.L. (1982). Crustal evolution of South Africa. New York. Springer-Verlag, 523.

Valloni, R. (1985). Reading provenance from modern marine sands. In: Provenance of Arenites. (Eds. G.G. Zuffa), Reidel, Dordrecht, 309 - 332.

Zuffa, G.G. (1980). Hybrid arenites: their composition and classification. Jour. Sed. Petrology, 50, 21-30.

Jour. Indian Association of Sedimentologists, Vol. 34, Nos. 1 & 2. (2017), pp. 29-37

Petrography, Provenance and Paleoclimate of Talchir Formation in and Around Nazarpur Village, Pench Valley, Satpura Gondwana Basin, Central India

MERADUL ISLAM* AND ABDULLAH KHAN
Department of Geology, Aligarh Muslim University, Aligarh
*Email: merad.amu17@gmail.com

Abstract: The Talchir Formation of Permo-Carboniferous is the lowermost lithostratigraphic unit of the Satpura Gondwana basin. The formation unconformably overlies the Precambrian basement. Twenty-five representative sandstones sample of Talchir Formation were analyzed for their petrographic attributes. The studies reveal that the sandstones are arkose, sub-arkose, lithic-arkose, medium to coarse grained, sub-angular to sub-rounded, poorly to well sorted and immature to sub-mature. The presence of varieties of quartz, feldspar, rock fragments, mica and heavy minerals suite in these sandstones attributes their derivation from igneous, metamorphic and mixed provenance. The Qt-F-L, Qm-F-Lt ternary diagrams suggest that these sandstones derived from craton interior, continental block provenance with basement uplift. Plot of quartz: (feldspar+ rock fragments) in the climate discrimination diagram suggests the prevalence of semi humid climate during the sedimentation of sandstones of Talchir Formation in this part of Satpura Gondwana basin.

Key words: Talchir Formation, Nazarpur, Petrography, Provenance, Paleoclimate, Satpura Gondwana basin.

INTRODUCTION

Gondwana rocks of the Peninsular India considered from Late Carboniferous to early Cretaceous (Robinson,1967; Pascoe,1959; Veevers and Tewari,1995). The sediments are distributed in a well defined linear basins, including the well-known east-west trending Koel-Damodar Basin, southeast-northwest trending Son-Mahanadi Basin and Pranhita-Godavari Basin and east-west trending Satpura Basin (Fig. 1a). The Satpura Basin is the westernmost Peninsular Gondwana basin. The Permo-Carboniferous Talchir Formation is the lowermost lithostratigraphic unit of the Indian Gondwana succession and unconformably overlies the Precambrian basement (Fig. 1b).

In Peninsular India, the Talchir Formation marks the initiation of sedimentation during the Permo-Carboniferous after a long hiatus since Proterozoic. Most of sedimentological work has been carried out by various workers mainly on the Lower Gondwana rocks (Shukla and Rai, 1971; Qidwai,1972; Casshyap and Qidwai,1974; Chakraborty et al., 2003; Ghosh, 2003; Ghosh et al., 2004; Chakraborty and Sarkar, 2005; Chakraborty and Ghosh, 2005; Ghosh, 2006; Chakraborty and Ghosh, 2008; Sarkar et al., 2009; Ghosh et al., 2012). However, there is no serious attempts has been on petrographic investigation particulary of Talchir Formation of this part of study area. Hence, in the present works an attempt has been made to study petrography of sandstone in order to deduce the provenance and paleoclimate.

GEOLOGICAL SETTING

The Gondwana basins of Peninsular India embodies Precambrian terrain of intracratonic nature. The Satpura Gondwana Basin of central India is rhomb-shaped and elongate in an ENE–WSW direction (200 km long, 60 km wide). The regional strike of the basin-fill strata is NE-SW, and the regional dip (~5^{O}) northerly. The Satpura Gondwana succession classified into seven major lithostratigraphy unit that forms oldest to youngest are the Talchir, Barakar, Motur, Bijori, Pachmarhi, Denwa and Bagra Formations (Fig. 2).

The Talchir Formation represented the uniform lithological associations in all the basins, which include diamictites, similar fossil assemblage, and diagnostic glacial depositional feature (Veevers and Tewari, 1995). During the Permo-Carboniferous similar lithology and Chron reported in Africa, Australia, South America, Antarctica and India that constituted the supercontinent Gondwanaland (Hobday,1987; Veevers, 2004). It believed that continental glaciations were responsible for the deposition of Talchir and a similar litho succession of the Gondwanaland assembly (Crowell and Frakes 1975; Veevers and Powell 1987; Crowell 1995; Gonzalez-Bonorino and Eyles 1995; Eyles et al., 1998, 2002, 2003). The lithology of Talchir Formation is olive green shale,

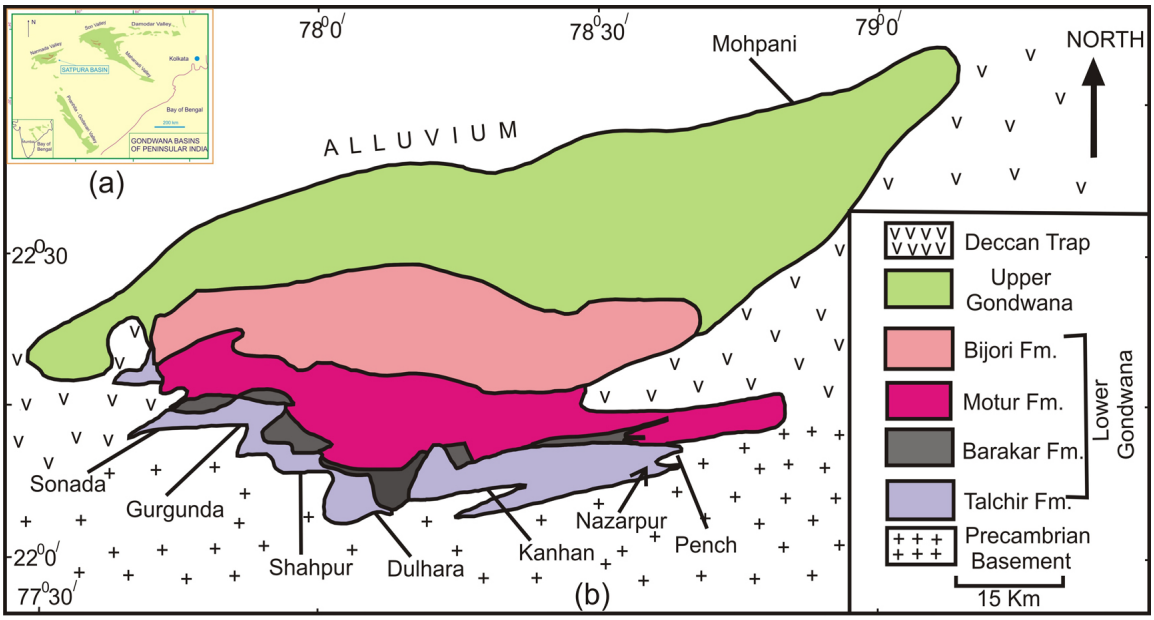

Fig. 1a. Map showing outcrops of the Gondwana Basins in the Peninsular India. **b.** Geological Map showing Lower Gondwana Formations of Satpura basin.

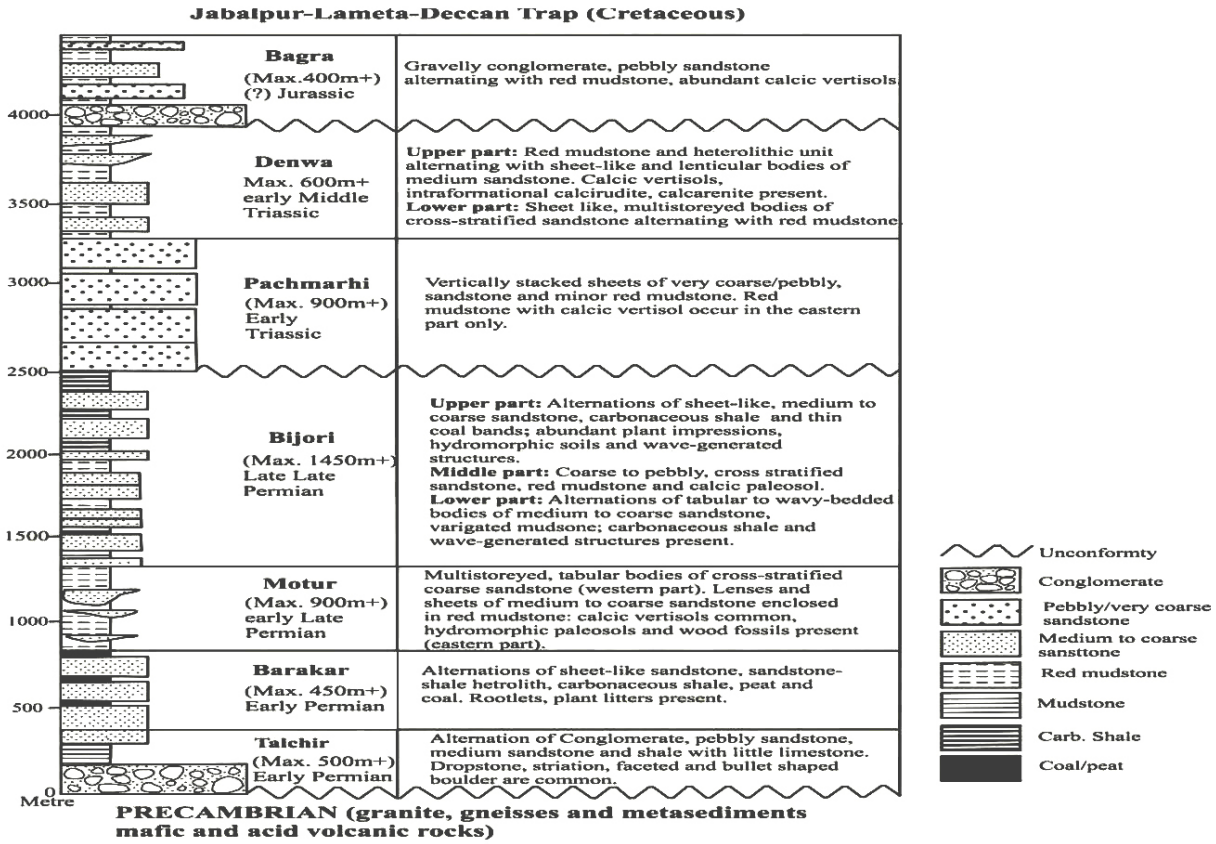

Fig. 2. Generalised lithostratigraphy of the Gondwana succession, Satpura Gondwana basin (after Ghosh et al., 2012).

conglomerate, sandstone, siltstone, mudstone with typical glaciogenic tillite at the base of succession.

METHODOLOGY

Twenty-five representative samples thin sections investigated for petrography. Thin sections stained with sodium cobaltinitrite solution for K-feldspar identification (Carver, 1971). 300-350 grains were counted using the Gazzi-Dickinson point counting method (Ingersoll et. al., 1984). The size data was grouped into the half-phi class interval. Cumulative frequency curves of grain size data plotted on log probability paper. The grain diameters in phi units represented by $\phi 5$, $\phi 16$, $\phi 25$, $\phi 50$, $\phi 75$, $\phi 84$, and $\phi 95$ percentiles accounted from the size frequency curves. In the present study Powers (1953) roundness, the scale is used. Mean roundness calculated by conventional statistical method (Powers,1953). Definitions of raw and recalculated parameters used in the analysis are presented in Table1. Sandstone provenance is classified according to the Dickinson (1985) scheme and detrital modes were recalculated to 100% as the sum of Qt, Qm, F, L and Lt. The counted grains were recalculated into percentage as summarised in Table 2.

Sandstone Petrography and Texture

The framework grains of the Talchir sandstones of Nazarpur area comprises of quartz, which occurs as detrital, recrystallized and stretched metamorphic quartz. The monocrystalline quartz has straight to slightly undulatory extinction, medium to coarse grained, sub-rounded orthoclase, microcline and plagioclase feldspar, lithic fragments and mica. The K-feldspar is abundant than the plagioclase feldspar. Heavy minerals; garnet, zircon, tourmaline, rutile, biotite, staurolite and opaque and the rock fragments; granite, gneiss, mafic, schist, chert, siltstone, sandstone, shale, phyllite and carbonates are accounted in the sandstone. These sandstones classified as arkose, sub-arkose and lithic arkose (Folk, 1980) (Fig. 3).

Provenance and Paleoclimate

The Qt-F-L relationship of Talchir sandstone infers the continental block provenance (Fig. 4) with a source primarily in the craton interior orogeny provenance with basement upliftment (Dickinson, 1988). The Qt-F-L emphasises the factors controlled by provenance, relief, weathering and transport mechanism and maturity. Continental block provenance comprises felsic-intermediate-mafic igneous, metamorphic and sedimentary to volcano-sedimentary rocks. The Qm-F-Lt relationship emphasises the source rock as craton interior of the continental block provenance and craton interior in particular (Fig. 5). The mineral composition of sandstone (Qt/(F+R) against Qp /(F+R), Fig. 6) infers that the semi-humid to humid paleoclimate for the early Permian Talchir Formation.

Table1. Key for petrographic and other parameters used in this study (after Folk, 1980; Dickinson and Suezek, 1979; Suttner and Dutta, 1986).

QFR
Q= Total quartz grains (Qm+Qp), where: Qm= Monocrystalline quartz Qp= Polycrystalline quartz F=Total feldspar (P+K), where: P=Plagioclase K=K-feldspar R= Total rock fragments including chert
QtFL
Qt= Total quartz grains (Qm+Qp) where: Qm= Monocrystalline quartz Qp= Polycrystalline quartz including chert F= Total feldspar L= Total lithic fragments
QmFLt
Qm= Monocrystalline quartz F= Total feldspar Lt= Total lithic fragments+ polycrystalline quartz
Qp/(F+R) and Qt/(F+R)
Qt= Total quartz (Qm+Qp) where: Qm= Monocrystalline quartz Qp= Polycrystalline quartz F= Total feldspar R= Total rock fragments

Table 2. Recalculated sandstone composition of the Talchir Sandstones of the Nazarpur area, Satpura Gondwana basin, Madhya Pradesh.

Sp.	**QFR**			**QtFL**			**QmFLt**				
No.	Q	F	R	Qt	F	L	Qm	F	Lt	Qp/F+R	Qt/F+R
NZS1	83.86	14.70	1.44	84.73	14.70	0.58	79.83	14.70	5.48	0.30	1.19
NZS2	78.48	18.23	3.29	79.75	18.23	2.03	76.20	18.23	5.57	0.16	0.99
NZS3	81.85	17.83	0.32	81.85	17.83	0.32	81.21	17.83	0.96	0.04	1.02
NZS4	77.87	18.42	3.72	80.13	18.42	1.45	75.12	18.42	6.46	0.23	1.02
NZS5	81.51	14.35	4.14	81.51	14.35	4.14	78.55	14.35	7.10	0.16	0.90
NZS6	75.28	17.98	6.74	78.65	17.98	3.37	73.31	17.98	8.71	0.22	0.88
NZS7	82.87	15.17	1.97	82.87	15.17	1.97	77.81	15.17	7.02	0.30	1.15
NZS8	84.97	13.61	1.42	85.92	13.61	0.47	82.01	13.61	4.38	0.26	1.14
NZS9	84.69	12.35	2.96	85.68	12.35	1.98	81.73	12.35	5.93	0.26	1.01
NZS10	87.58	9.80	2.61	87.58	9.80	2.61	86.60	9.80	3.59	0.08	0.85
NZS11	90.27	6.22	3.51	90.27	6.22	3.51	87.84	6.22	5.95	0.25	0.80
NZS12	85.87	11.88	2.24	87.00	11.88	1.12	84.08	11.88	4.04	0.21	1.01
NZS13	92.11	7.02	0.88	92.98	7.02	0.00	91.23	7.02	1.75	0.22	1.09
NZS14	90.87	7.64	1.49	90.87	7.64	1.49	88.54	7.64	3.82	0.26	1.05
NZS15	90.83	7.03	2.14	91.44	7.03	1.53	90.21	7.03	2.75	0.13	0.87
NZS16	93.04	6.33	0.63	93.04	6.33	0.63	90.19	6.33	3.48	0.41	1.28
NZS17	91.43	7.79	0.78	91.43	7.79	0.78	89.09	7.79	3.12	0.27	1.16
NZS18	70.27	25.80	3.93	71.50	25.80	2.70	69.29	25.80	4.91	0.07	0.93
NZS19	82.13	14.61	3.26	83.03	14.61	2.36	80.00	14.61	5.39	0.17	0.96
NZS20	83.73	13.27	3.00	84.20	13.27	2.53	82.78	13.27	3.95	0.09	0.89
NZS21	90.88	7.77	1.34	90.88	7.77	1.34	89.28	7.77	2.95	0.18	1.00
NZS22	94.71	3.80	1.49	94.71	3.80	1.49	93.39	3.80	2.81	0.25	0.90
NZS23	92.19	6.56	1.25	92.81	6.56	0.63	91.56	6.56	1.88	0.16	0.97
NZS24	87.82	7.47	4.72	89.39	7.47	3.14	86.25	7.47	6.29	0.26	0.77
NZS25	87.86	7.65	4.49	88.92	7.65	3.43	85.75	7.65	6.60	0.26	0.79

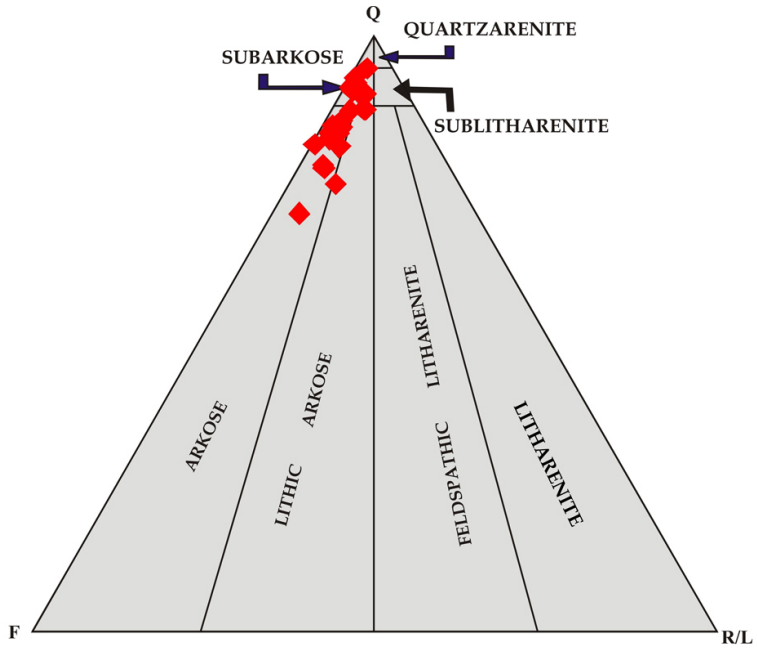

Fig. 3. Classification of Talchir Sandstone, Nazarpur area (after Folk, 1980).

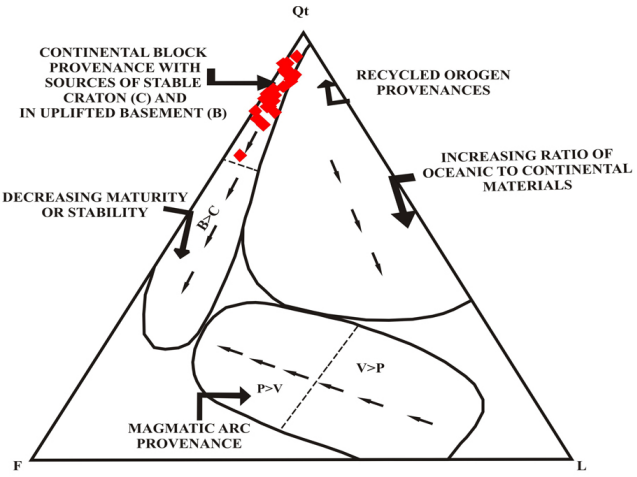

Fig. 4. Qt-F-L triangular diagram of Talchir Sandstones, Nazarpur area (after Dickinson, 1985).

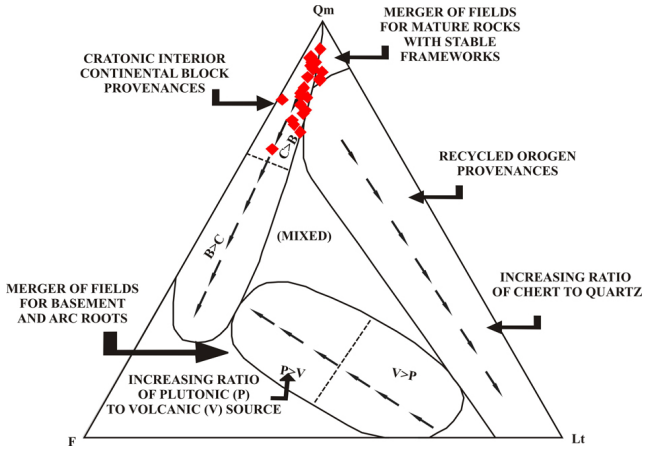

Fig. 5. Qm-F-Lt triangular diagram of Talchir Sandstone, Nazarpur area (after Dickinson, 1985).

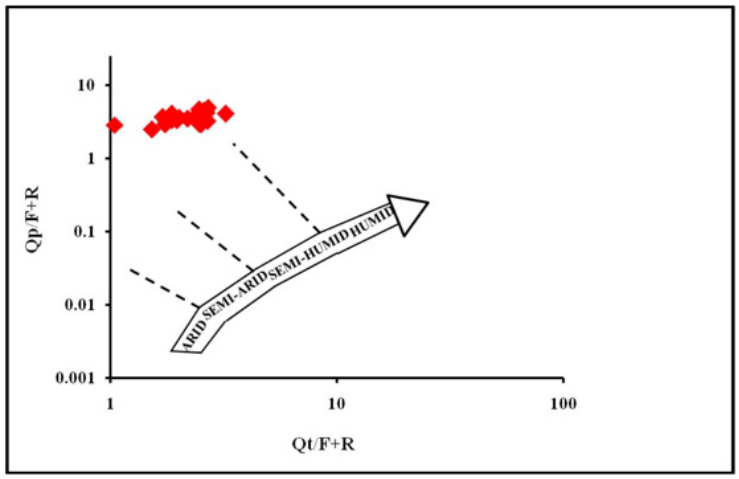

Fig. 6. Bivariant log-log plot of Qt/(F+R) and Qp/(F+R) ratios of Talchir Sandstones (after Suttner and Dutta, 1986).

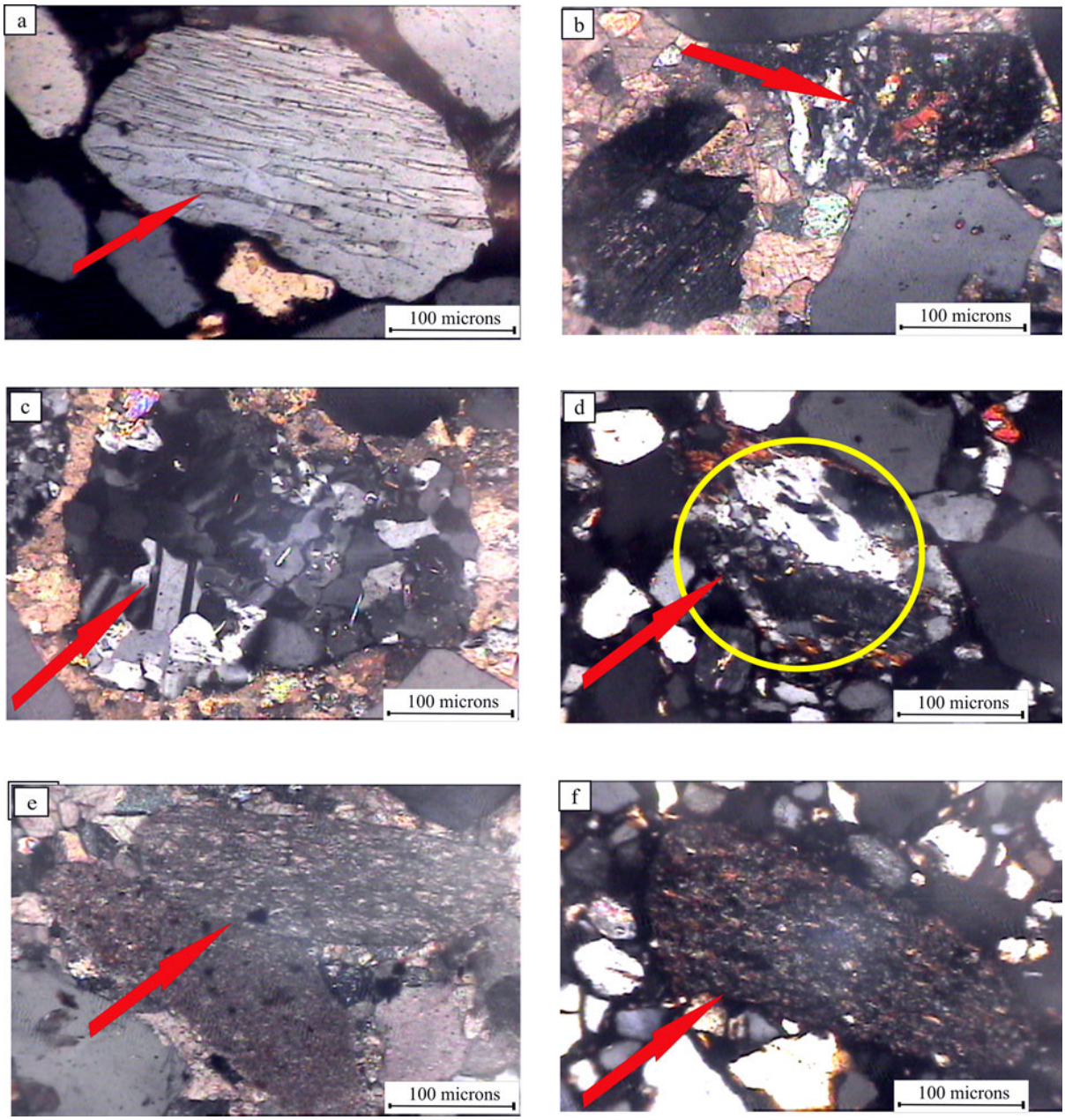

Plate 1. Photomicrographs of Talchir Formation of Nazarpur area, Chindwara district, Madhya Pradesh, arrows showing (a) Perthite grain; (b) Mafic rock fragment; (c) Granite fragment; (d) Low-grade gneiss fragment; (e) Carbonate grain; (f) Phyllite fragment.

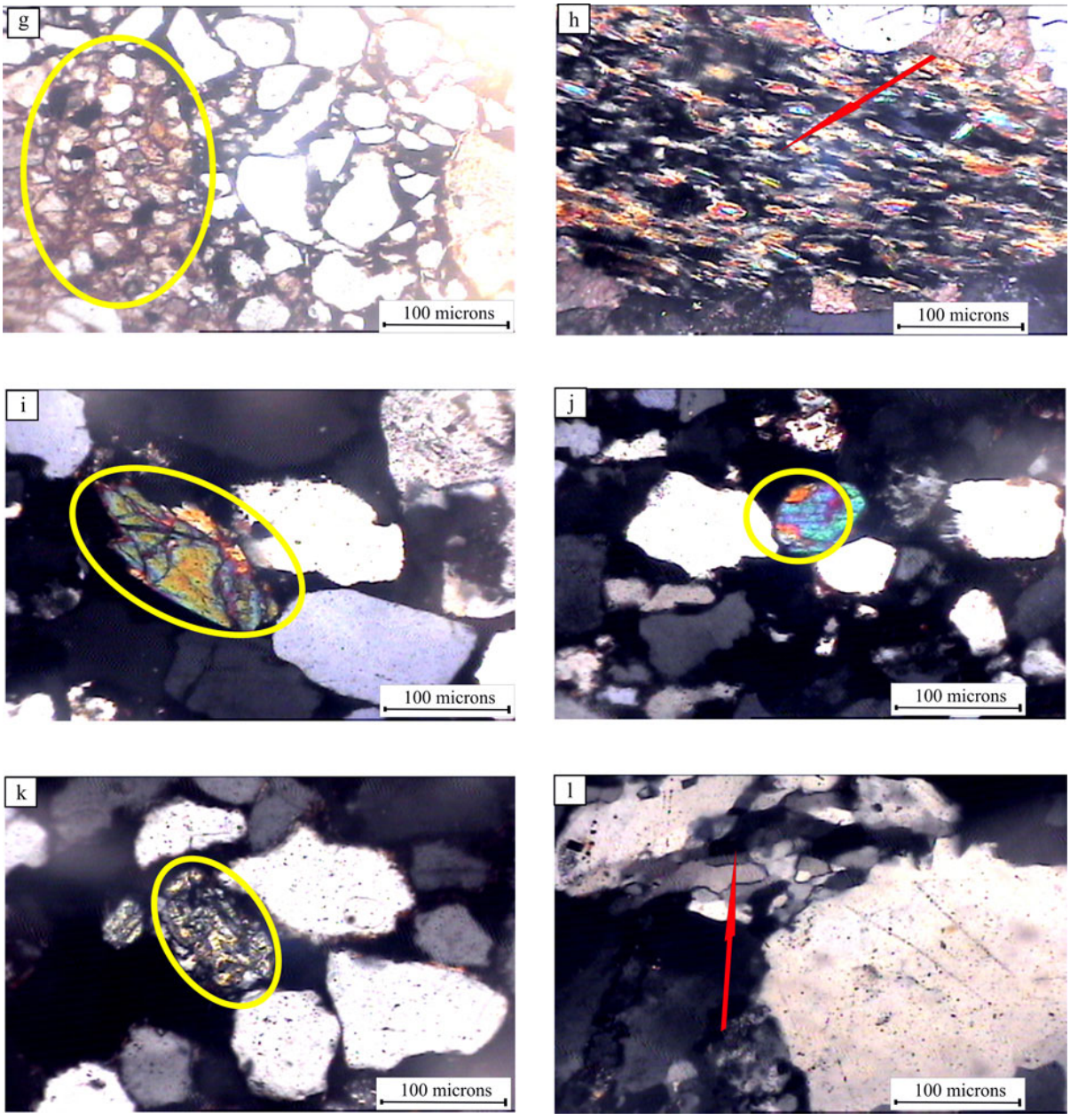

Plate 2. Photomicrographs of Talchir Formation of Nazarpur area, Chindwara district, Madhya Pradesh, arrows showing (g) Sandstone rock fragments (h) Low-grade schist rock fragments; (i) Tourmaline (j) Rounded zircon; (k) Staurolite; (l) Stretched metamorphic quartz.

RESULTS AND DISCUSSION

The modal analysis of sandstones (Table 2), on ternary diagram, indicates that the sediments of Talchir Formation of Nazarpur area derived from continental block provenances (Fig.4). Within these major provenances, sediments derived from craton interior of continental block and basement uplift region. These samples are medium to coarse grained, poorly sorted to well sorting with variation in grain size attributes to non-uniform current strength during the deposition. The quartz grains ranges from sub-angular to subrounded in shape, the angularity of indicating that these are the first cycle erosion sediments, a short distance of transportation whereas sub-rounded to rounded grains are of second cycle erosion and transported for longer distance. Overall, the sandstones are mainly comprise of arkose, subarkose, litharkose and mineralogically immature to submature in nature.

The petrography and heavy mineral analysis of the Talchir sandstone indicate multiple rock sources, which are not reflected in the triangular plots. The apparent reason for this could be diagenetic alteration and weathering of unstable framework grains and consequent increase in the proportion of quartz grains. The dominance of monocrystalline quartz indicates that the granitic provenance for these sediments (Basu, et al., 1975). The presence of alkali feldspars indicates their source as metamorphic and plutonic rocks (Trevena and Nash, 1981), perthite grains, rock fragment of granite (Plate 1a&1c), green coloured tourmaline (Plate 2i) are direct evidence of granitic source. The mafic rock fragment (Plate. 1b) infers the mafic source rock for these sandstones. Rock fragments of phyllite, granitic gneiss (Plate 1e & 1f) and schist (Plate 2h) attribute metamorphic source rock. Rounded zircon (Plate 2j) and the presence of carbonate rock fragments (Plate 1e) (Plate 2g) indicate a sedimentary source. The presence of staurolite and stretched metamorphic quartz (Plate 2k & 2l) indicate a metamorphic source. The heavy mineral suites and the rock fragments support their source in the mixed provenance.

CONCLUSIONS

Based on the petrography of the Talchir sandstone of Nazarpur area, Chindwara district, Madhya Pradesh the following conclusions are drawn:

- Qt-F-L and Qm-F-Lt relationship suggest that sediment supply is from the continental block provenance.
- The sandstones are medium to coarse grained, poorly to well sorted, subangular to subrounded in nature and mineralogical immature to sub-mature. Based on these characteristics the sandstone classified as arkose, sub-arkose and lithic arkose type.
- The heavy minerals suites indicate the multiple sources including plutonic basement to metasedimentary rocks, which represents granites, gneiss, low to high-grade metamorphic rocks and mafic igneous rocks provenance for these sandstones.
- The Talchir sandstone deposited in a semi-humid climatic condition.

***Acknowledgements*:** We thank Prof. L.A.K. Rao, Chairman and Prof. A.H.M. Ahmad, In-charge of the sedimentary Laboratory, Department of Geology, A.M.U., Aligarh for providing necessary facilities to carry out the research work. The comments and suggestions of the anonymous reviewer helped in improving the quality of the paper.

References

Basu, A., Young, S. W., Suttner, L. J., James, W. C., and Mack, G. H. (1975). Re-evaluation of the use of undulatory extinction and polycrystallinity in detrital quartz for provenance interpretation: Jour. Sed. Petrology., 45: 873-882.

Carver, R.E. (1971). Procedures in Sedimentary Petrology. Wiley-inter-science (a division of John Wiley & Sons Inc.), NY., 653p.

Casshyap, S.M. and Qidwai, H.A. (1974). Glacial sedimentation of late Palaeozoic Talchir diamictite, Pench Valley coalfield, central India. Geological Society of American Bulletin., 85: 749–760.

Chakraborty, C., Ghosh, S.K. and Chakraborty, T. (2003a). Depositional record of tidal flat sedimentation in the Permian coal measures of central India: Barakar Formation, Mohpani Coalfield, Satpura Gondwana basin. Gondwana Res., 6: 817-827.

Chakraborty, C. and Ghosh, S. (2005). Pull-apart origin of the Satpura Gondwana basin, central India.J. Earth Sys. Sci., 114(3): 259–273.

Chakraborty, C. and Ghosh, S.K. (2008). Pattern of sedimentation during the Late Paleozoic Gondwanaland glaciation: an example from the Talchir Formation, Satpura Gondwana basin, central India. J. Earth Syst. Sci., 117(4): 499–519.

Chakraborty, T. and Sarkar, S. (2005). Evidence of lacustrine sedimentation in the upper Permian Bijori formation, Satpura Gondwana basin: Palaeogeographical and tectonic implications. J. Earth Syst. Sci., 114 (3) : 303–323

Crowell, J.C. and Frakes, L. A. (1975). Late palaeozoic glaciations. In: Gondwana Geology, (ed.) Campbell, K.S.W., Australian National University Press, Canbera., 313-331.

Crowell, J.C. (1995). The ending of Late Paleozoic age during Permian period. In palaeogeography, paleoclimate and Stratigraphy (eds.) Scholle, P. A., Peryt, T.M. and Ulmer-Scholle D.S. Berlin: Springer –Verlag., 62-74.

Dickinson, W.R. (1985). Interpreting Provenance Relations from Detrital Modes of SandstFones.In: G. G. Zuffa, Ed., Provenance of Arenites, D. Reidel Publ. Co., New York., 333-361.

Dickinson, W.R. (1988). Provenance and Sediment Dispersal in Relation to Paleotectonics and Paleogeography of Sedimentary Basins. In: K. L Kleinspehn and C. Paola, Eds., New Perspectives in Basin Analysis, Springer, New York., 3-25.

Dickinson, W.R. and Suczek, C.A. (1979).Plate Tectonics and Sandstone Compositions. American Association of Petroleum Geological Bulletin., 63: 2164-2182.

Eyles, C.H., Eyles, N. and Gostin, V. A. (1998). Facies and allostrtigraphy of high latitude glacially influenced marine strata of early Permian southern Sydney Basin, Australia.Sedimentology., 45: 121-161.

Eyles, C.H., Mory, A. J. and Eyles, C. H. (2002). Carboniferous-Permian palynostratigraphy of West Australian Marine rift basin: resolving tectonic and eustatic controls during Gondwana glaciations.palaeogeography, Palaeoclimatology, and Paleoecology., 184:305-319

Eyles, C.H., Mory, A. J. and Eyles, N.(2003). Carboniferous-Permian facies and tectonostratigraphic successions of the glacially influenced and rifted Carnarvon Basin, Western Australia; Sedimentary Geology., 155: 63-86.

Folk, R. L. (1980). Petrology of Sedimentary Rocks, Hemphill, Austin, Textus., 182p.

Ghosh, S., Sarkar, P. and Ghosh, P., (2012). Petrography and major element geochemistry of the Permo-Triassic sandstones, central India: Implication for provenance in an intracratonic pull-apart basin. Jou. Asian Ear. Science., 43: 207-240.

Ghosh, S.K. (2003). First record of marine bivalves from the Talchir Formation of the Satpura Gondwana basin, India: palaeobiogeographic implications; Gondwana Res. Gondwana Newsletter Section., 6(2): 312–320.

Ghosh, S.K. (2006). Tectono-stratigraphic evolution of the lower Gondwana succession, Satpura basin, central India. PhD thesis, Jadavpur University.,104.

Ghosh, S. K., Chakraborty, C. and Chakraborty, T.(2004). Combined tide and wave influence on sedimentation of Lower Gondwana coal measures of central India: Barakar Formation (Permian), Satpura Basin; J. Geol. Soc. London., 161: 117–131.

Gonzalez-Bonarino, G., and Eyles, N., (1995). Inverse relationship between ice extent in the Late Paleozoic Glacial record of Gondwana. Geology.,23: 1015-1018.

Hobday, D. K. (1987). Gondwana coal basins of Australia and South Africa; Tectonic setting, depositional system and resources; In coal and coal-bearing strata: recent advances (ed.) A.C. Scott, Geological Society London Spec. Publication., 32: 219-233.

Ingersoll, R.V., Bullard, T.F., Ford, R.L., Grimm, J.P., Pickle, J.D. and Sares, S.W.(1984). "The Effect of Grain Size on Detrital Modes: A Test of the Gazzi-Dickinson Point Counting Method," Journal of Sedimentary Research., 54(1): 103-106.

Pascoe, E.H. (1959). A Manual of Geology of India and Burma. 3rd edition, Govt. of India publications, G.S.I., Calcutta., 2:485-1219.

Power, M. C. (1953) "A New Roundness Scale for Sedimentary Particles," Journal of Sedimentary Petrolium., 23: 117-119.

Qidwai, H.A.(1972). Lower Gondwana sedimentation in the Pench Valley coalfield MP. Unpublished PhD Thesis, Aligarh Muslim University, Aligarh., 311p.

Robinson, P. L. (1967). The Indian Gondwana Formations- A review; First Symposium on Gondwana Stratigraphy, Ar Del Plata, Argentina., 201-268.

Sarkar, S., Ghosh, S.K. and Chakraborty, C.(2009). Ichnology of a Late Palaeozoic ice-marginal shallow marine succession: Talchir Formation, Satpura Gondwana basin, central India. Jour. Palaeogeography, Palaeoclimatology, Palaeoecology; 283: 28–45.

Shukla, R.T and Rai, K.L. (1971). A study of sedimentary petrography of Lower Gondwana Sandstone in Kanhan Vally area with special reference to their heavy mineral assemblage. International Symp. stratigraphy mineral res. Gondwana system, AMU. Aligarh., 264-287.

Suttner, L.J and Dutta, P.K. (1986). Alluvial Sandstone Composition and Paleoclimate, I. Framework Mineralogy. Journal of Sedimentary Petrology., 56(3):329-345.

Trevena, A.S. and Nash. W.P . (1981). An electron microprobe study of detrital feldspar. Journal of Sedimentary Petrology., (51):137-150.

Veevers, J. J. (2004). Gondwanaland from 650-500 Ma assembly through 320 Ma merger in Pangea to 185-100 Ma breakup: Supercontinental tectonics via stratigraphy and radiometric dating. Earth –Science Reviews., 68:1-132.

Veevers, J. J. and Powell, C. M. C.A. (1987). Late Paleozoic glacial episodes in Gondwanaland reflected in Transgressive-regressive depositional sequences in Euramerica. Geological Society America Bulletin.,98:475-487.

Veevers, J. J. and Tewari, R. C. (1995). Gondwana master basin of Peninsular India between Tethys and interior of Gondwanaland province of Pangea.Memoir Geological Society of America., 187: 1-73.

Jour. Indian Association of Sedimentologists, Vol. 34, Nos. 1 & 2. (2017), pp. 39-57

Geochemical Characteristics of Proterozoic Carbonate Lithofacies of Indravati Basin, Chhatisgarh, Central India: Implication of Depositional and Diagenetic History

RAJEEVA GUHEY[1] AND MAHENDERKOTHA[2]
[1]Department of Geology, Govt. N. P.G. College of Science, Raipur, Chhattisgarh
[2] Department of Earth Science, Goa University, Goa
Email: guheygeol@gmail.com

Abstract: The intra-cratonic Proterozoic Indravati Basin, Central India, located on the south eastern margin of the Bastar craton is represented by a Lower clastic and the Upper carbonate succession. The upper carbonate succession is represented by two formations namely the Kanger Limestone Formation (the non-stromatolitic platform) which is overlain by the Jagdalpur Formation (the stromatolitic carbonate platform). Present work provides new field and petrological observations and high precision selected trace and REE data from carbonates in order to interpret the depositional conditions of these rocks. The two carbonate lithofacies (A & C) identified on the basis of their field occurrences, distinctive petrographic and geochemical characters. The lithofacies A is a bedded micritic limestone, devoid of any allochems and the lithofacies-C is a dolomitized, stromatolite bearing limestone. Detailed petrographic observation and geochemical characters suggest an early to late diagenesis involving the processes of compaction, dissolution, cementation, recrystallization and replacement. The trace element geochemistry from number of samples shows that they are characteristic of shallow water deposits. Although a similar pattern of REE abundances resembling to that of modern seawater has been observed for all the carbonate samples with depleted LREE, the greatly enriched HREE and negative Eu anomaly, the positive Ce anomaly deviates from the modern seawater patterns. All the carbonate samples display a distinctive negative Eu anomaly. The La N/Yb N ratio of 3.64 for Lithofacies A and 3.31 for Lithofacies C samples indicates a relatively moderate degree of REE fractionation. The trace and rare earth geochemistry together with sedimentological data strongly support deposition of Kanger (lower bedded limestone) in subtidal condition and Jagdalpur (upper stromatolitic) carbonate Formation in shallow marine intertidal-supratidal condition. The change in depositional and diagenetic conditions is further substantiated by factor analysis of the geochemical data which clearly differentiates the two carbonate lithofacies.

Keywords: REE, Proterozoic carbonates, Geochemistry, Indravati, palaeoenvironment, Diagenesis.

INTRODUCTION

The Indravati Basin, covering an area of 9000 km^2 in Kanker Baster and Dantewara districts of Chhattisgarh and Koraput of Orissa (Fig.1), representing good outcrops of the Proterozoic Indravati Group of sediments, is one of the important Purana basins adjacent to Proterozoic Chhattisgarh Basin, and has been studied over last few decades. However, it is particularly in the last few years their have been a surge of research, in part on age determination and depositional environments and the age of the both Chhattisgarh and Indravati basins. Mainkar et al.(2004) proposed La-ICPMS, U-Pb age 620 $\pm$ 30 Ma on the basis of Tokapal and Bhejripadar kimberlite pyroclastics within Kanger Formation. Mukherjee et al., 2012 did U-Pb isotopic analyses (LA MC-ICPMS) of the zircons from the Birsaguda tuff, within the Jagdalpur Formation point to closure of the basin at 1001 ± 7 Ma.

Although, the geochemical nature of sediment has been better utilized in the interpretation of the depositional setting and diagenesis in Phanerozoic sequences leading generation of large data bases, the geochemical data on even well-defined sedimentary suits of Precambrian, Proterozoic sequences are very limited. The present global correlation based on carbon isotope profile curve and trace element geochemistry for origin and chronostratigraphic? implications on Indravati Basin is still lacking. The present study reports geological, petrographic and geochemical (selected Trace and REE+Y) data in order to test firstly, the compatibility of a marine precipitate origin for the carbonates and secondly compatibility with microbial involvement in carbonate precipitation and stromatolite construction.

Trace metal concentrations recorded in carbonate sediments are commonly used for palaeoenvironmental reconstruction through examination of redox-sensitive

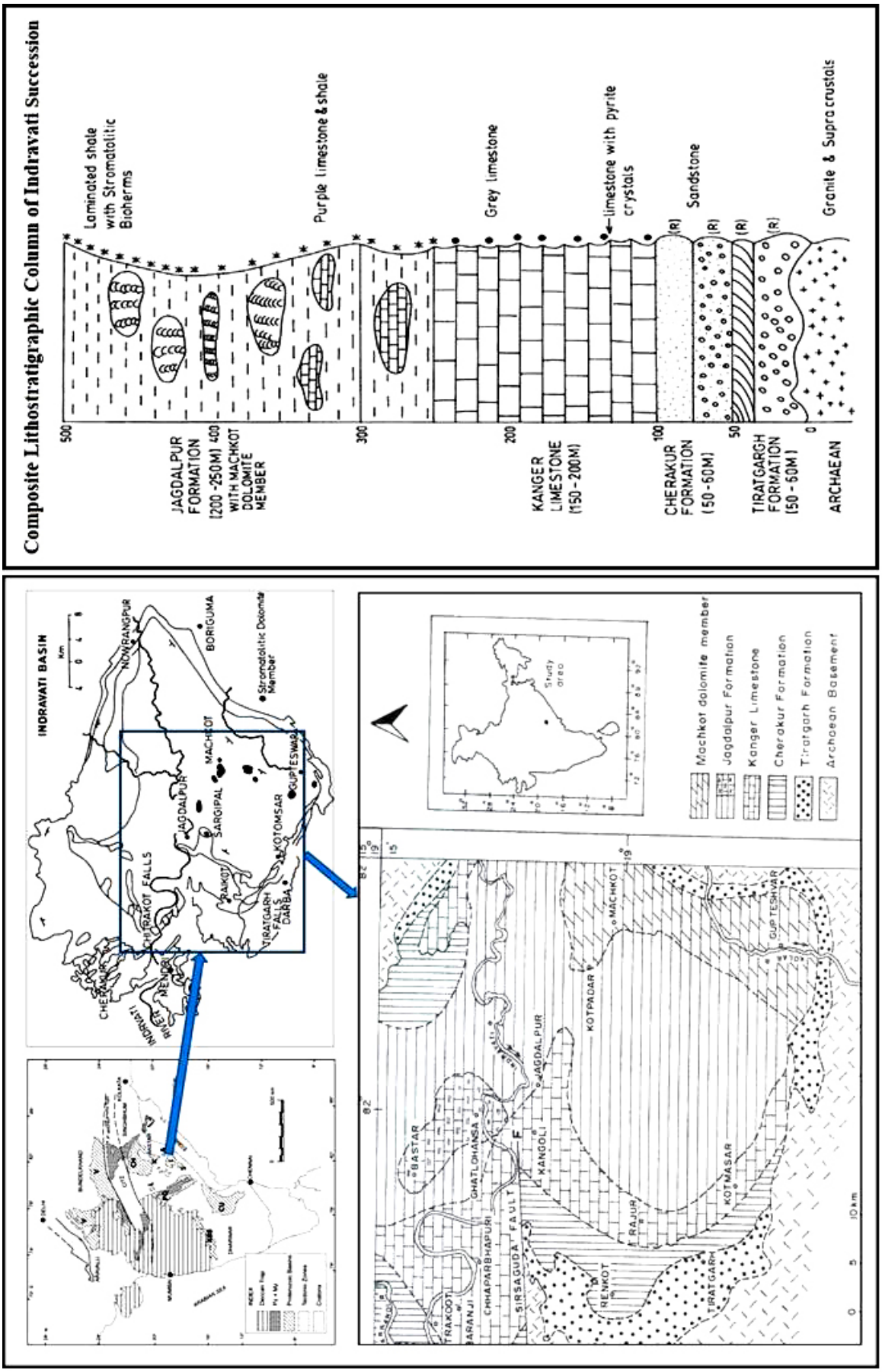

Fig. 1. Geology map and stratigraphic section of Indravati basin showing lithofacies and sampling locations.

elements that may become enriched under low-oxygen or euxinic water conditions (e.g. Brumsack, 2006; Algeo and Maynard, 2004). REE concentrations in carbonates is also used to reconstruct the chemistry of ancient seawater masses (Wright et al., 1987; Olivier and Boyet 2006; Webb and Kamber, 2000). Although REE concentration of carbonate rocks is relatively lower than that of the siliciclastic sediments, but their relative proportions are similar to those of terrigenous sediments (Balashov et al., 1964; Haskin et al., 1968, Ronov et al., 1974; Jarvis et al., 1975). Haskin et al. (1966) and McLennan et al. (1979) suggests that the carbonate phase may carry considerable portions of REE content of carbonate rocks and the incorporation of REE into carbonate minerals and the their behaviour during diagenesis was studied by Parekh et al. (1977), Scherer and Seitz (1980), and Shah and Waserburg (1985)

Therefore, the study of the trace and REE geochemistry combined with field description and the thin-section petrographic study is the appropriate means of characterizing the carbonate lithofacies. Their distribution in modern shallow seawater differs significantly from that of all known input sources. Modern and ancient carbonate rocks have been shown to record reliable marine REE signatures (Webb and Kamber, 2000). The data can also be used to test whether the Precambrian marine environment was reducing and whether terrestrial weathering was already significantly influencing marine chemistry.

GEOLOGICAL SETTING

The Indravati Group rocks unconformably overlie the Precambrian Gneissic Complex and are essentially horizontally bedded with low dips from 5 to 10 degrees. Ball (1877) and King (1881) were the earliest to describe the general geology and stratigraphy of these rocks. They have noted that these sedimentary rocks have resemblance to the Kurnool or Cuddapah Formations. The informal stratigraphic nomenclature first proposed by Crookshank (1963) was later revised by Dutt (1963), Schnitzer (1969), Krupanidhi (1970), Sharma (1975) etc. The most recent classification of lndravati basin was proposed by Ramakrishnan (1987) (Table 1). The stromatolite assemblages have been studied by Schnitzer (1971), Jairaman & Banerjee (1980), Jha et al. (1999), Guhey & Wadhwa (1993), Moitra (1999), and Guhey et al.(2011) from carbonate rocks of Indravati and Chhattisgarh Basins. These stromatolites can be correlated with upper Vindhyans and a tidal flat depositional environment (Subtidal to Intertidal) was suggested for their deposition.

Table 1. Geological succession of Indravati Basin(Ramakrishnan,1987).

	Formation	Member	Lithological Description
Indravati Group (Proterozoic)	**Jagdalpur Fm.**	Calcareous Shales with purple and gray stromatolitic dolomite (Machkot Dolomite Member)	Consists of shale, limestone and dolomite. Stromatolites are restricted to Upper part of the Jagdalpur Formation. The shale is ferruginous at places but calcareous; found with and within the Jagdalpur limestone as capping and intercalations. Limestone is hard and compact, pinkish to buff in colour, stromatolitic in nature and very well exposed.
	Kanger Limestone	Purple limestone Gray limestone	Consists of limestone. The upper part of this formation gradually becomes argillaceous in nature. The Limestone is hard and compact and breaks with conchoidal fracture and varies in colour from grayish grey to dark grey. Due to the major fault of Sirisguda, the limestone is greatly affected particularly in thickness and disposition. Burrowing structure and speleothemes are observed.
	Cherakur Fm.	Purple shale with arkosic sandstone and chert pebble conglomerate grit.	Mainly arenaceous unit consists of shales with chert pebble conglomerate, grit, arkosic sandstone and siltstone. Shales, abundant in mica (muscovite) content with prominent bedding, are used as roofing slabs.
	Tirathgarh Fm.	Chitrakoot member Mendri member	Comprises of two units (lower coarse clastic Mendri Member unit with subarkose, conglomerate, orthoquartzites and the upper fine clastic Chitrakoot Member with of sandstone/siltstones with shale interbeds. Sandstone display cross-bedding and ripple marks.
	---------- Unconformity ----------		
	Archaean		Granites and supracrustal

The sedimentary succession of the Indravati Basin, designated as Indravati Group is represented by four formations viz. Tiratgarh, Cherakur, Kanger and Jagdalpur Formations (Ramakrishnan,1987). The detailed stratigraphy and lithological characters of the Indravati succession are given in Table 1 and the general geology of the study area in Fig.1.

Following Kah et al. (2001), carbon isotope data of Indravati carbonate indicates that they appears to have been deposited during the Mesoproterozoic-Neoproterozoic transition (~1.25 to ~0.85 Ga), a period characterized by moderately positive ä13C values (~4.) (Maheswari et al., 2005). Two broad carbonate lithofacies (A & C) separated with a shale lithofacies (lithofacies B) are identified (represented by Kanger and Jagdalpur Formations) based on the field observations. The lithofacies A is represented by a well laminated/bedded black/gray pyrite bearing lime mud (belonging to Kanger limestone of Ramakrishnan, 1987), the lithofacies B represented by the purple gray calcareous shale and lithofacies C is purple gray stromatolitic dolomite belong to the Jagdalpur Formation (Table 2). Important sedimentary structures present in the study area include the depositional (bedding and stromatolites of various types), post-depositional/erosional structures (desiccation cracks, karstic features, stylolites, veinlets etc.) and the deformational (minor faults).

MATERIALS AND METHODS

In all 27 representative samples collected from various levels of the stratigraphic succession (Fig.1), which include 15 samples from Kanger Limestone (lithofacies-A), 2 samples from the calcareous shale (lithofacies-B) and 10 samples from the stromatolitic limestone (Lithofacies-C) of the Jagdalpur Formation were collected for the detailed mineralogical, petrographic and geochemical analyses.

The mineralogical composition of the various rock samples was determined by XRD and the thin sections were examined under the petrological microscope for their texture, framework composition and diagenetic modifications. The trace and rare earth element (REE) concentrations were determined by Perkin Elmer ICP-MS instrument (Elan DRC II Model) at the NGRI laboratories, Hyderabad. The JLs (Limestone) standard was used for the comparison and estimation of variation. The precisions of the elemental (trace and rare earth) data are well within accepted levels (< 6% RSD) with comparable accuracies (Balaram, 1993) of variation. The Eu and Ce were calculated following the formulae of McLennan 1989.

MINERALOGY AND PETROGRAPHY

Petrographic observation and XRD analyses of carbonate rock shows the predominantly calcite mineralogy of Lithofacies A and calcite with dolomitization confined to Lithofacies-C. The presence of chert could be indicative of late diagenetic replacement.

Different representative lithotypes of carbonate sequence of Indravati Group were identified on the basis of field and thin section petrography. The textural terminologies of Folk (1962) and Dunham (1962) have been followed in the study. Thin section petrography reveals the presence small allochem (calcareous algal filamental particles/carbonate intraclasts), micrite sized particle components. The main orthochemical constituents include the micrite, sparry calcite cement, pseudospar/neomorphic spar, replacement dolomite, pyrite etc. were present.

Various environmentally significant carbonate microfacies identified based on the detailed petrography include: i) Bedded or Laminated Micrite: occurs in Lithofacies A and consists of continuous laminae made-up of micrite alternating with a fine clastic grains are arranged parallel to laminae (Plate.1.1 & Plate.2.1). The laminated structures are produced by the construction of microbial mat through cyanobacteria. Bedded micrite contains alternate black organic layer and white crystalline layer and clear crystalline calcite layer with occasional presence of pyrite crystals, ii) Structureless micrite: occurs in lithofacies A and consist of micrite without laminations, so it's name given structureless micrite. (Plate2.2), iii) Pelmicrite: occurs in lithofacies A and contains small rounded grains of homogeneous micrite cemented by calcite and occasionally by silica (Plate.2.3), iv) Intramicrite/Intrasparite: is characteristic of lithofacies C and consists of elongated fragments of partly lithified carbonate mud. Reworking of desiccated sediments on tidal flats produces Intramicrite/ Intrasparite, and v) Dolomitized stromatoliticmicrite/ Dolospar: is representative of lithofacies C and characterized by partial fabric selective to non fabric selective replacement of stromatolitic micrite (Plate.2.4 to 2.6). In fabric selective replacement, dolomitization occurs parallel to algal lamination (Locality: Junaguda village, (Plate 1.6 & Plate.2.5)). Dolomitized rhombs represent euhedral to subhedral shape with clouded cores (Plate.2.6). The partial dolomitization gradually turns to total dolomitization towards the younger part of the succession (Locality: Gupteshwar village). Dolomite rhombs are tightly packed and forming idiotopic mosaic of euhedral dolomite and here stromatolitic structure is totally obliterated (Plate.2.6). Replacement nature of dolomite is characterized by the presence of dolomite rhombs along joints, fracture and algal laminations, clouded cores of micrite within the dolomite rhombs, progressive dolomitization obliterating the primary textures and structures and coarse crystal size of dolomite in comparison to calcite matrix. The source of Mg for extensive dolomitization in the area is supposed to be within the basin, as trapped brines in the subsurface.Dolomitization is more common to stromatolitic limestone of Jagadalpur formation and it commonly replaces micrite and shows patchy

Table 2. Summary of geochemical parameters of Indravati carbonate succession.

	Lithofacies - A				Lithofacies - B				Lithofacies - C				All Samples			
	Mz	Min	Max	σ	Mz	Min	Max	σ	Mz	Min	Max	σ	Mz	Min	Max	σ
B	16.12	12.99	19.41	1.86	18.74	16.81	20.67	2.73	17.19	12.77	22.36	2.73	16.91	12.77	22.36	2.46
Mn	292.40	65.05	472.32	117.64	335.25	213.51	456.99	172.17	206.62	126.36	296.08	61.82	247.92	65.05	472.32	101.59
Sc	0.22	0.10	0.59	0.14	0.38	0.17	0.59	0.30	0.15	0.06	0.42	0.09	0.19	0.06	0.59	0.14
V	15.57	5.39	50.61	13.41	30.44	10.48	50.40	28.22	14.63	5.63	42.29	8.60	16.15	5.39	50.61	12.24
Cr	9.87	5.12	28.68	7.01	19.11	7.40	30.83	16.57	9.95	4.19	27.94	6.13	10.60	4.19	30.83	7.34
Co	0.53	0.21	1.06	0.28	1.50	0.27	2.73	1.74	0.56	0.21	1.58	0.33	0.62	0.21	2.73	0.52
Ni	14.24	5.54	44.73	11.75	30.65	11.27	50.02	27.40	12.72	4.08	39.94	8.72	14.61	4.08	50.02	11.81
Cu	1.24	0.81	2.33	0.45	0.98	0.91	1.05	0.11	0.83	0.58	1.26	0.20	0.99	0.58	2.33	0.36
Zn	22.13	10.11	31.28	6.52	35.43	21.90	48.96	19.13	15.57	8.99	36.19	6.64	19.47	8.99	48.96	9.14
Rb	25.29	4.52	102.12	29.02	59.27	17.72	100.82	58.76	26.36	6.49	87.01	19.54	28.40	4.52	102.12	26.63
Sr	211.93	25.85	323.28	81.47	115.31	36.99	193.64	110.77	62.41	29.56	116.90	31.62	121.71	25.85	323.28	92.03
Y	12.32	8.77	23.17	4.65	16.95	9.31	24.59	10.81	8.69	2.86	19.69	4.10	10.64	2.86	24.59	5.23
Zr	304.49	75.23	1077.40	290.97	655.93	241.53	1070.34	586.06	311.28	84.28	1146.86	258.00	334.30	75.23	1146.86	294.89
Nb	64.66	15.80	223.03	61.42	126.69	57.24	196.14	98.22	58.53	16.62	218.19	49.60	65.85	15.80	223.03	57.60
Cs	2.22	0.38	9.40	2.71	5.97	1.31	10.63	6.59	2.48	0.47	11.20	2.58	2.65	0.38	11.20	2.95
Ba	283.37	1.59	657.53	301.36	502.07	449.45	554.68	74.41	129.16	48.39	386.49	83.58	213.90	1.59	657.53	218.63
Hf	8.63	2.00	31.09	8.46	19.47	7.11	31.83	17.48	9.02	2.37	33.95	7.68	9.65	2.00	33.95	8.74
Ta	0.34	0.09	1.18	0.32	0.42	0.42	0.43	0.01	0.37	0.11	0.65	0.18	0.36	0.09	1.18	0.23
Pb	1.34	0.78	2.73	0.57	1.45	1.10	1.80	0.49	1.08	0.87	1.49	0.20	1.21	0.78	2.73	0.40
Th	1.87	0.50	6.53	1.77	3.86	1.42	6.31	3.46	1.71	0.46	6.26	1.42	1.93	0.46	6.53	1.72
U	0.86	0.36	2.50	0.69	1.57	0.65	2.50	1.31	0.78	0.25	2.74	0.61	0.87	0.25	2.74	0.68
La	8.76	4.79	24.74	6.23	16.03	6.98	25.08	12.80	6.60	1.80	22.19	4.92	8.10	1.80	25.08	6.25
Ce	28.07	12.58	79.10	20.84	60.18	22.40	97.95	53.42	26.01	7.25	86.84	19.57	29.30	7.25	97.95	23.38
Pr	2.39	1.33	6.45	1.60	4.29	1.79	6.78	3.53	1.73	0.49	5.70	1.25	2.17	0.49	6.78	1.64
Nd	10.16	5.79	26.51	6.44	17.49	7.43	27.54	14.21	7.12	2.02	22.08	4.84	9.01	2.02	27.54	6.54
Sm	1.94	1.34	4.26	0.92	2.88	1.36	4.41	2.16	1.13	0.36	3.17	0.68	1.56	0.36	4.41	1.01
Eu	0.04	0.03	0.07	0.01	0.05	0.03	0.07	0.03	0.02	0.01	0.05	0.01	0.03	0.01	0.07	0.02
Gd	2.07	1.32	4.70	1.07	3.27	1.57	4.98	2.41	1.40	0.42	3.75	0.80	1.79	0.42	4.98	1.12
Tb	0.26	0.18	0.56	0.12	0.40	0.20	0.59	0.28	0.17	0.05	0.44	0.09	0.22	0.05	0.59	0.13
Dy	2.72	1.84	5.84	1.28	4.18	2.04	6.31	3.02	1.85	0.55	4.79	1.03	2.35	0.55	6.31	1.39
Ho	72.82	48.05	153.76	33.21	110.87	57.33	164.41	75.72	51.56	16.07	132.68	28.46	63.83	16.07	164.41	36.42
Er	67.53	41.64	146.28	32.49	104.17	52.22	156.12	73.47	48.83	14.56	128.20	27.59	59.86	14.56	156.12	35.02
Tm	58.16	35.10	130.70	29.11	89.52	42.31	136.73	66.77	42.31	12.62	120.47	25.98	51.68	12.62	136.73	31.70
Yb	1.54	0.96	3.53	0.79	2.45	1.17	3.74	1.82	1.08	0.31	2.99	0.65	1.35	0.31	3.74	0.85
Lu	1.48	0.92	3.42	0.77	2.30	1.08	3.53	1.73	1.00	0.26	2.88	0.63	1.28	0.26	3.53	0.82
Th_U	2.06	1.27	2.61	0.39	2.36	2.20	2.53	0.24	2.13	1.73	2.37	0.21	2.12	1.27	2.61	0.29
La_Th	5.52	3.79	9.50	1.73	4.45	3.98	4.92	0.67	4.00	2.89	4.68	0.53	4.60	2.89	9.50	1.32
SREE	259.81	156.84	596.44	136.19	421.93	199.31	644.55	314.83	192.54	57.23	542.48	117.52	234.44	57.23	644.55	147.08
Eu(an)	0.06	0.05	0.11	0.02	0.05	0.05	0.05	0.01	0.04	0.04	0.05	0.00	0.05	0.04	0.11	0.02
La/Yb	3.64	2.47	4.73	0.66	4.29	4.05	4.53	0.34	3.96	3.31	5.01	0.44	3.87	2.47	5.01	0.55
La/Lu	0.58	0.39	0.75	0.10	0.70	0.67	0.74	0.05	0.66	0.56	0.80	0.07	0.63	0.39	0.80	0.09
Ce(an)	1.53	1.25	1.76	0.17	1.82	1.66	1.99	0.23	2.00	1.88	2.28	0.10	1.81	1.25	2.28	0.26
Gdsn/Gd*	1.17	0.97	1.24	0.08	1.22	1.21	1.24	0.02	1.27	1.20	1.30	0.03	1.23	0.97	1.30	0.07
Ndsn/Ybsn	2.23	1.48	2.62	0.33	2.40	2.22	2.57	0.24	2.26	1.88	2.57	0.19	2.26	1.48	2.62	0.25
Dysn/Ybsn	1.16	0.95	1.29	0.09	1.12	1.10	1.14	0.03	1.14	1.03	1.26	0.07	1.15	0.95	1.29	0.08
Y/Ho	0.17	0.15	0.19	0.01	0.16	0.15	0.16	0.01	0.17	0.15	0.19	0.01	0.17	0.15	0.19	0.01
Pr/Pr*	0.82	0.77	0.88	0.04	0.76	0.73	0.79	0.04	0.71	0.66	0.74	0.02	0.76	0.66	0.88	0.06

an- anomaly; sn-shale normalized; Mz = Mean (Average); σ= standard Min = Minimum; Max= Maximum

Bedded limestone, Kanger limestone, Locality: Badanjī.

Intercalation of Calcareous Shale unit within limestone. Locality: Near Kangoli

Stromatolitic limestone showing stylolite veins and karst topography,(sink holes and Natural bridge) Locality: Jagdalpur Town

Isolated Bioherm of dolomitic limestone, Jagdalpur Formation, at the basin margin,can be comparable to Modern Shark Bay, Locality Junaguda

Plate 1. Field Photographs.

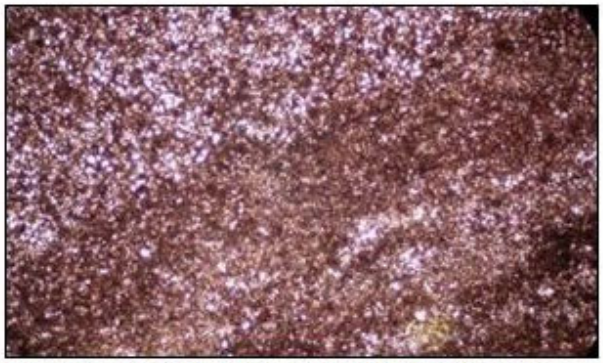

1. Laminated micrite with alternate light and dark micro-crystalline layers at upper stratigraphic horizon. Redstained grains are or calcite. Light, unstained grains correspond to dolomite & quartz.

2. Structureless micrite or massive micrite is composed of micrite without any visible structures like bedding, algal lamination etc.

3. Stained slide of Stromatolitic Micrite. Calcitic micrite is pink stained, the white is silicious.

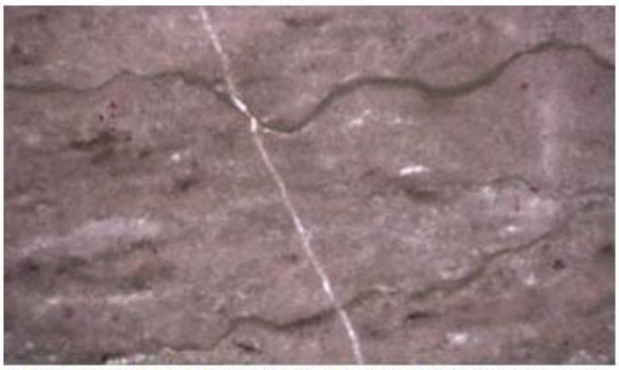

4. Laminated algal micrite showing stylolitic boundaries. Also seen in the section a quartz filled vein.

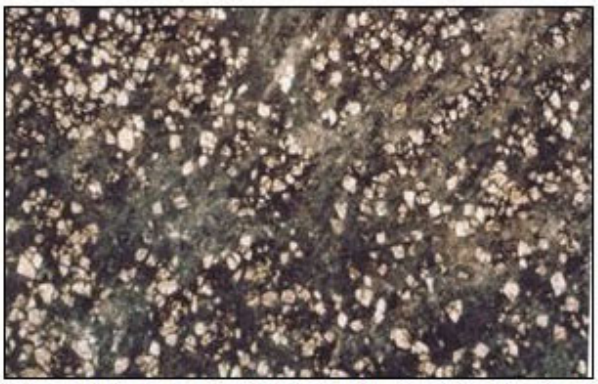

5. Microdolospar, a result fabric selective (algal laminae) dolomitization in stromatolitic dolomicrite at Loc.Junaguda.

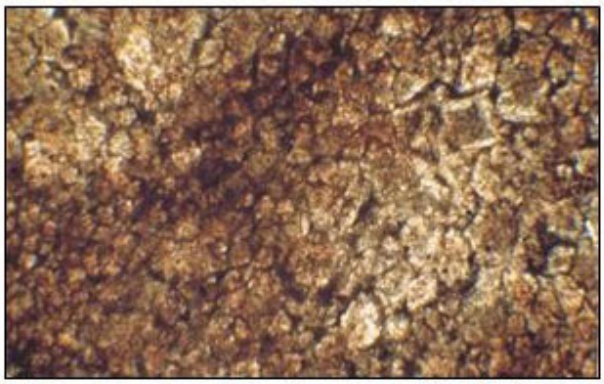

6. Dolospar representing replacement origin of dolomite resulted in formation of idiotoic mosaic of euhedral dolomite Jagdalpur Fm. Sample Loc. Gupteshwar.

Plate 2. Photomicrographs.

distribution and enhances porosity of rock. The dolomitic rhombs exhibit fabric selective (idiotopic) to pervasive (xenotopic) mosaic (Plate.2.6) that strongly suggestive of burial diagenesis. Geochemical investigations of Jagdalpur formation reveal low Sr, higher Mn content that suggest reducing condition and support burial diagenesis of dolomite. The source of Mg^{+2} for dolomitization was probably the underlying thick shale succession. It is suggested that the conversion of smectite to illite during increasing burial releases Mg^{+2} as well as Fe+2 which might be responsible for dolomitization.

GEOCHEMISTRY

Trace element data are widely considered as useful indicators of source area, tectonic setting and depositional environments (Taylor and McLennan, 1985; Bhatia,1985, Culler et all,1988; Algeo and Maynard 2004; Brumsack 2006; Maravelis and Zelilis, 2010). In the same way, REE concentrations have also been used in the reconstruction of the chemistry of ancient seawater masses during the formation of carbonates (Wright et al., 1987; Olivier and Boyet, 2006; Webb and Kamber, 2000 etc.). The trace elements in sedimentary rocks mostly reside in (a) as accessory mineral fraction, (b) adsorbed in exchangeable clay mineral sites and in clay mineral structure and (c) as organic complexes (Totten & Hanan, 1998). Non-clay minerals like quartz, feldspar in clastic rocks and contain very low concentration of trace elements. Most investigations on sedimentary carbonate rocks and minerals although reported in general a lower total REE, however, carbonate REE patterns are similar to clastic sedimentary rocks. Selected trace elements and REE analyzed for all the Indravati samples and their relative variation has been presented in Table 3. Cs, Ba, Rb, Sr, Cr, V, Sc, Ni, Ga, Co, Cu and Pb are depleted compared to PAAS for all the samples. The mean content of Ce & Y for the two carbonate units (Lithofacies A & B) is much less than that of PASS (80.00).

Strontium

Sedimentary geochemists prefer to use Sr as tool for facies analysis, while petroleum geochemists use Sr for identification of oil basins associated with carbonates. Generally Sr concentration is more in sea water than in fresh water and therefore, it reflects the nature of depositional basin water characteristics. Sr content in the present samples ranges from 25.85 to 323.28 ppm with a mean content of 211.93 ppm for Lithofacies A and 29.56 to 116.90 ppm with a mean content of 62.41 ppm for Lithofacies B (Table 3). In the present samples Sr shows a positive correlation with Mn (r = 0.521) and Cu (r = 0.398) while showing negative correlation with Ta (r= -0. 387). No correlation of Sr is observed with ∑REE.

Lead, Zinc and Nickel

The uniform presence of Pb, Zn and Ni in the present samples is interesting. Generally pelagic clays show higher concentration of Zn than near shore. The relatively lower concentration of Zn (mean ppm of 22.13 for Lithofacies-A and 15.57 for Lithofacies-B) in these rocks are related to shallow near shore phase. Nickel is very stable in aqueous solutions and capable of migration over long distance. The weathering of source rock gives rise to Fe, Ni and Si.

As the aqueous solution sinks Fe oxidizes and precipitates as ferric hydroxides, and then loses water ultimately to form goethite and hematite in which small amounts of Ni ions are trapped. In the present samples the presence of iron oxide coatings on various particles and presence of goethite (x-ray data) can be related to the consistent presence of Ni. Generally, deep see sediments show higher concentration of Ni up to 1000 ppm, whereas shallow water sediments show low concentration (Davies, 1972). The lower values of Ni (5.54 to 44.73 with a mean content of 14.24 ppm for Lithofacies-A and 4.08 to 39.94 with a mean content of 12.72ppm for Lithofacies- B) in the present samples can be related to shallow water environment of deposition.

Other Elements

The other trace elements analyzed include V, Cr, Co, Cu, Ga, Rb, Y, Zr, Nb, Cs, Ba, Hf, Ta, Th, U and REE which have been used in the interpretation of origin and provenance. The summary of the distribution of these elements and their interrelationships are shown in Tables 3 & 4. In general, the elements with low water rock coefficients and low residence time values including Zr, Hf, Ga, Y, Th, Nb, Be and REE are strongly excluded from natural waters and remain in the oceans for time less than average ocean mixing times. Consequently, it is likely that these elements are transferred quantitatively into sedimentary rocks and hence give best information regarding source rock composition. Therefore, their distribution in the sedimentary rocks is most useful for understanding the origin of the sediments. The high field strength elements (HFSE) such ZE, Y and Th are resistant to weathering compared to other trace elements (Taylor & McLennon, 1988). The present carbonate samples while showing a relatively high abundance of Zr, Y and Th display a very low concentration of Co, Sc and U. Relatively a greater variation in Ba, V and Rb is observed in Lithofacies A as compared to that of Lithofacies B. The strong positive correlation of Th with ∑REE (r= 0.967) corresponds to the relationship of REE and Th for upper crustal sediments (McLenna et al., 1980). The La/Th ratios (Fig.2) of the Indravati samples are slightly higher than those of Post-Archean or Archaean.

Table 3. Correlation coefficient matrix of Geochemical data of Indravati carbonates.

	B	Mn	Sc	V	Cr	Co	Ni	Cu	Zn	Rb	Sr	Y	Zr	Nb	Cs	Ba	Hf	Ta	Pb	Th	U	Th/U	La/Th	SREE	Eu/Eu	La/Yb	La/Lu	Ce/Ce	Gd/Gd	Nd/Yb	Dy/Yb	Y/Ho
B	1.00	-0.39	0.12	0.21	0.20	0.11	0.19	-0.13	0.16	0.20	-0.06	0.15	0.23	0.23	0.22	0.14	0.23	0.11	0.24	0.22	0.25	0.05	-0.24	0.16	-0.26	0.15	0.15	0.15	0.33	0.07	-0.10	0.01
Mn	-0.39	1.00	0.06	-0.08	-0.06	0.28	-0.01	0.10	0.27	-0.10	**0.52**	0.18	-0.11	-0.13	-0.07	-0.04	-0.10	-0.36	0.14	-0.08	-0.07	-0.16	**0.60**	0.10	**0.46**	-0.32	-0.37	**-0.44**	**-0.42**	-0.19	0.18	0.00
Sc	0.12	0.06	1.00	**0.96**	**0.93**	**0.76**	**0.97**	0.14	**0.85**	**0.95**	-0.16	**0.96**	**0.94**	**0.95**	**0.93**	**0.62**	**0.94**	**0.65**	**0.41**	**0.96**	**0.95**	**0.52**	-0.22	**0.98**	-0.13	**0.60**	**0.48**	0.03	0.06	**0.52**	-0.31	**-0.74**
V	0.21	-0.08	**0.96**	1.00	**0.97**	**0.77**	**0.99**	0.06	**0.78**	**0.99**	-0.34	**0.90**	**0.98**	**0.97**	**0.97**	**0.59**	**0.98**	**0.69**	0.35	**0.98**	**0.97**	**0.55**	-0.36	**0.95**	-0.30	**0.68**	**0.59**	0.24	0.23	**0.55**	-0.37	**-0.73**
Cr	0.20	-0.06	**0.93**	**0.97**	1.00	**0.79**	**0.98**	0.03	**0.77**	**0.98**	-0.32	**0.89**	**0.98**	**0.97**	**0.97**	**0.53**	**0.98**	**0.67**	0.38	**0.98**	**0.97**	**0.53**	-0.34	**0.95**	-0.27	**0.64**	**0.55**	0.26	0.20	**0.47**	**-0.47**	**-0.73**
Co	0.11	0.28	**0.76**	**0.77**	**0.79**	1.00	**0.82**	-0.09	**0.75**	**0.78**	-0.25	**0.72**	**0.78**	**0.73**	**0.81**	**0.44**	**0.79**	0.32	**0.45**	**0.78**	**0.74**	**0.49**	-0.21	**0.77**	-0.14	**0.43**	**0.39**	0.20	0.14	0.33	-0.36	**-0.58**
Ni	0.19	-0.01	**0.97**	**0.99**	**0.98**	**0.82**	1.00	0.05	**0.83**	**0.99**	-0.31	**0.92**	**0.98**	**0.98**	**0.98**	**0.58**	**0.98**	**0.67**	**0.41**	**0.99**	**0.98**	**0.55**	-0.33	**0.97**	-0.27	**0.67**	**0.58**	0.22	0.20	**0.53**	-0.40	**-0.77**
Cu	-0.13	0.10	0.14	0.06	0.03	-0.09	0.05	1.00	0.37	0.01	**0.40**	0.19	0.01	0.07	-0.01	0.36	0.01	0.09	0.35	0.04	0.07	0.00	0.10	0.13	0.12	-0.03	-0.09	-0.31	-0.14	0.12	0.14	-0.11
Zn	0.16	0.27	**0.85**	**0.78**	**0.77**	**0.75**	**0.83**	0.37	1.00	**0.76**	0.07	**0.84**	**0.78**	**0.79**	**0.78**	**0.61**	**0.78**	0.36	**0.61**	**0.80**	**0.82**	0.29	-0.07	**0.85**	-0.10	**0.51**	**0.41**	-0.03	0.04	**0.51**	-0.13	**-0.65**
Rb	0.20	-0.10	**0.95**	**0.99**	**0.98**	**0.78**	**0.99**	0.01	**0.76**	1.00	**-0.39**	**0.90**	**0.99**	**0.98**	**0.98**	**0.55**	**0.99**	**0.72**	0.36	**0.99**	**0.97**	**0.58**	-0.38	**0.95**	-0.32	**0.70**	**0.62**	0.29	0.25	**0.53**	**-0.43**	**-0.76**
Sr	-0.06	**0.52**	-0.16	-0.34	-0.32	-0.25	-0.31	**0.40**	0.07	**-0.39**	1.00	0.00	-0.34	-0.30	-0.36	0.00	-0.34	**-0.39**	0.10	-0.31	-0.27	-0.35	**0.75**	-0.13	**0.80**	**-0.54**	**-0.67**	**-0.86**	**-0.75**	**-0.40**	0.15	0.29
Y	0.15	0.18	**0.96**	**0.90**	**0.89**	**0.72**	**0.92**	0.19	**0.84**	**0.90**	0.00	1.00	**0.89**	**0.90**	**0.88**	**0.55**	**0.89**	**0.56**	**0.46**	**0.91**	**0.92**	**0.44**	-0.08	**0.98**	0.01	**0.49**	0.36	-0.05	-0.06	**0.39**	-0.37	**-0.66**
Zr	0.23	-0.11	**0.94**	**0.98**	**0.98**	**0.78**	**0.98**	0.01	**0.78**	**0.99**	-0.34	**0.89**	1.00	**0.99**	**0.99**	**0.56**	**0.99**	**0.70**	0.37	**0.99**	**0.98**	**0.57**	-0.38	**0.95**	-0.30	**0.70**	**0.61**	0.27	0.24	**0.52**	**-0.44**	**-0.76**
Nb	0.23	-0.13	**0.95**	**0.97**	**0.97**	**0.73**	**0.98**	0.07	**0.79**	**0.98**	-0.30	**0.90**	**0.99**	1.00	**0.98**	**0.58**	**0.99**	**0.73**	0.38	**0.99**	**0.99**	**0.56**	-0.37	**0.96**	-0.28	**0.69**	**0.60**	0.23	0.21	**0.53**	**-0.44**	**-0.78**
Cs	0.22	-0.07	**0.93**	**0.97**	**0.97**	**0.81**	**0.98**	-0.01	**0.78**	**0.98**	-0.36	**0.88**	**0.99**	**0.98**	1.00	**0.51**	**0.99**	**0.63**	0.35	**0.99**	**0.98**	**0.50**	-0.35	**0.94**	-0.29	**0.68**	**0.61**	0.30	0.23	**0.51**	**-0.42**	**-0.75**
Ba	0.14	-0.04	**0.62**	**0.59**	**0.53**	**0.44**	**0.58**	0.36	**0.61**	**0.55**	0.00	**0.55**	**0.56**	**0.58**	**0.51**	1.00	**0.56**	**0.56**	0.36	**0.58**	**0.52**	**0.65**	-0.28	**0.57**	-0.18	**0.49**	0.38	-0.07	0.13	**0.51**	-0.08	**-0.54**
Hf	0.23	-0.10	**0.94**	**0.98**	**0.98**	**0.79**	**0.98**	0.01	**0.78**	**0.99**	-0.34	**0.89**	**0.99**	**0.99**	**0.99**	**0.56**	1.00	**0.70**	0.36	1.00	**0.98**	**0.57**	-0.38	**0.95**	-0.30	**0.70**	**0.61**	0.28	0.24	**0.52**	**-0.44**	**-0.77**
Ta	0.11	-0.36	**0.65**	**0.69**	**0.67**	0.32	**0.67**	0.09	0.36	**0.72**	**-0.39**	**0.56**	**0.70**	**0.73**	**0.63**	**0.56**	**0.70**	1.00	0.09	**0.71**	**0.65**	**0.73**	**-0.48**	**0.62**	**-0.40**	**0.61**	**0.54**	0.27	0.34	**0.42**	**-0.40**	**-0.68**
Pb	0.24	0.14	**0.41**	0.35	0.38	**0.45**	**0.41**	0.35	**0.61**	0.36	0.10	**0.46**	0.37	0.38	0.35	0.36	0.36	0.09	1.00	0.38	**0.42**	0.13	-0.10	**0.44**	-0.01	0.14	0.08	-0.02	0.04	0.17	-0.18	-0.32
Th	0.22	-0.08	**0.96**	**0.98**	**0.98**	**0.78**	**0.99**	0.04	**0.80**	**0.99**	-0.31	**0.91**	**0.99**	**0.99**	**0.99**	**0.58**	1.00	**0.71**	0.38	1.00	**0.99**	**0.56**	-0.36	**0.97**	-0.27	**0.68**	**0.59**	0.23	0.21	**0.52**	**-0.43**	**-0.76**
U	0.25	-0.07	**0.95**	**0.97**	**0.97**	**0.74**	**0.98**	0.07	**0.82**	**0.97**	-0.27	**0.92**	**0.98**	**0.99**	**0.98**	**0.52**	**0.98**	**0.65**	**0.42**	**0.99**	1.00	0.47	-0.33	**0.97**	-0.26	**0.67**	**0.57**	0.23	0.20	**0.52**	**-0.41**	**-0.75**
Th/U	0.05	-0.16	**0.52**	**0.55**	**0.53**	**0.49**	**0.55**	0.00	0.29	**0.58**	-0.35	**0.44**	**0.57**	**0.56**	**0.50**	**0.65**	**0.57**	**0.73**	0.13	**0.56**	**0.47**	1.00	**-0.59**	**0.50**	-0.35	**0.54**	**0.47**	0.30	0.33	0.35	**-0.41**	**-0.63**
La/Th	-0.24	**0.60**	-0.22	-0.36	-0.34	-0.21	-0.33	0.10	-0.07	-0.38	**0.75**	-0.08	-0.38	-0.37	-0.35	-0.28	-0.38	**-0.48**	-0.10	-0.36	-0.33	**-0.59**	1.00	-0.18	**0.74**	**-0.49**	**-0.55**	**-0.75**	**-0.73**	-0.32	0.29	0.38
åREE	0.16	0.10	**0.98**	**0.95**	**0.95**	**0.77**	**0.97**	0.13	**0.85**	**0.95**	-0.13	**0.98**	**0.95**	**0.96**	**0.94**	**0.57**	**0.95**	**0.62**	**0.44**	**0.97**	**0.97**	**0.50**	-0.18	1.00	-0.11	**0.58**	**0.47**	0.08	0.04	**0.47**	**-0.39**	**-0.74**
Eu/Eu*	-0.26	**0.46**	-0.13	-0.30	-0.27	-0.14	-0.27	0.12	-0.10	-0.32	**0.80**	0.01	-0.30	-0.28	-0.29	-0.18	-0.30	**-0.40**	-0.01	-0.27	-0.26	-0.35	**0.74**	-0.11	1.00	**-0.69**	**-0.76**	**-0.82**	**-0.95**	**-0.63**	-0.15	0.32
La/Yb	0.15	-0.32	**0.60**	**0.68**	**0.64**	**0.43**	**0.67**	-0.03	**0.51**	**0.70**	**-0.54**	**0.49**	**0.70**	**0.69**	**0.68**	**0.49**	**0.70**	**0.61**	0.14	**0.68**	**0.67**	**0.54**	**-0.49**	**0.58**	**-0.69**	1.00	**0.94**	**0.52**	**0.63**	**0.87**	-0.02	**-0.62**
La/Lu	0.15	-0.37	**0.48**	**0.59**	**0.55**	**0.39**	**0.58**	-0.09	**0.41**	**0.62**	**-0.67**	0.36	**0.61**	**0.60**	**0.61**	0.38	**0.61**	**0.54**	0.08	**0.59**	**0.57**	**0.47**	**-0.55**	**0.47**	**-0.76**	**0.94**	1.00	**0.63**	**0.68**	**0.81**	-0.01	**-0.61**
Ce/Ce*	0.15	**-0.44**	0.03	0.24	0.26	0.20	0.22	-0.31	-0.03	0.29	**-0.86**	-0.05	0.27	0.23	0.30	-0.07	0.28	0.27	-0.02	0.23	0.23	0.30	**-0.75**	0.08	**-0.82**	**0.52**	**0.63**	1.00	**0.77**	0.33	-0.21	-0.28
(Gd/Gd*)sn	0.33	**-0.42**	0.06	0.23	0.20	0.14	0.20	-0.14	0.04	0.25	**-0.75**	-0.06	0.24	0.21	0.23	0.13	0.24	0.34	0.04	0.21	0.20	0.33	**-0.73**	0.04	**-0.95**	**0.63**	**0.68**	**0.77**	1.00	**0.56**	0.16	-0.20
(Nd/Yb)Sn	0.07	-0.19	**0.52**	**0.55**	**0.47**	0.33	**0.53**	0.12	**0.51**	**0.53**	**-0.40**	**0.39**	**0.52**	**0.53**	**0.51**	**0.51**	**0.52**	**0.42**	0.17	**0.52**	**0.52**	0.35	-0.32	**0.47**	**-0.63**	**0.87**	**0.81**	0.33	**0.56**	1.00	**0.39**	**-0.51**
(Dy/Yb)sn	-0.10	0.18	-0.31	-0.37	**-0.47**	-0.36	**-0.40**	0.14	-0.13	**-0.43**	0.15	-0.37	**-0.44**	**-0.44**	**-0.42**	-0.08	**-0.44**	**-0.40**	-0.18	**-0.43**	**-0.41**	**-0.41**	0.29	**-0.39**	-0.15	-0.02	-0.01	-0.21	0.16	**0.39**	1.00	0.30
Y/Ho	0.01	0.00	**-0.74**	**-0.73**	**-0.73**	**-0.58**	**-0.77**	-0.11	**-0.65**	**-0.76**	0.29	**-0.66**	**-0.76**	**-0.78**	**-0.75**	**-0.54**	**-0.77**	**-0.68**	-0.32	**-0.76**	**-0.75**	**-0.63**	0.38	**-0.74**	0.32	**-0.62**	**-0.61**	-0.28	-0.20	**-0.51**	0.30	1.00

Correlations (Indravati_Data.sta). Marked (in bold) correlations are significant at $p < .05000$; N=27 (Casewise deletion of missing data); sn-shale normalized

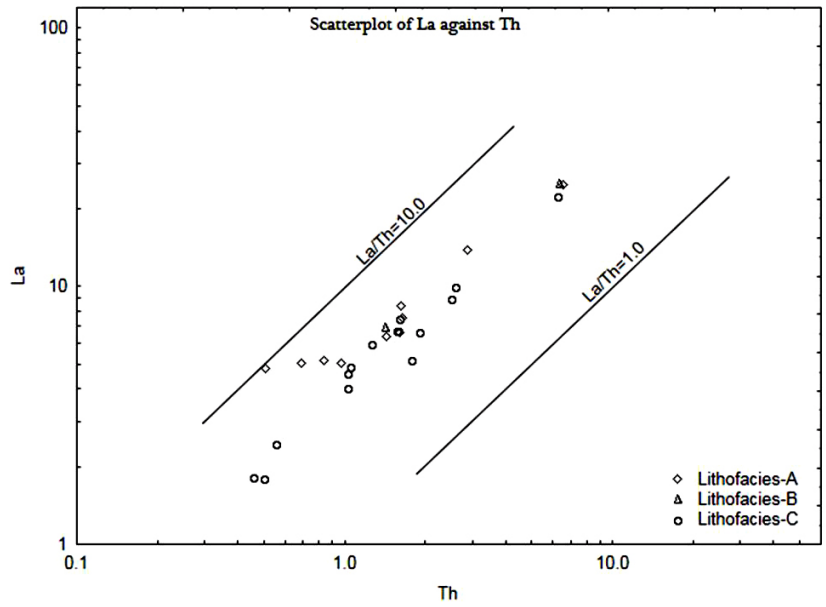

Fig. 2. Plot of La vs. Th for Indravati carbonates showing good correlation.

Rare Earth Elements (REE)

The rare earth elements (REE) are a group of 14 elements from La to Lu that exhibits generally similar chemical behaviour. Owing to their electronic configurations, these elements form ions that are nearly all trivalent, with smoothly decreasing ionic radii. Notable exceptions are stabilization of Ce^{4+} and Eu^{2+} under appropriate oxidizing and reducing conditions, respectively. Goldschmidt (1954) was first to suggest that the constant distribution of REE in sedimentary rocks is the result of homogenizing effects of sedimentary processes and therefore, the REE pattern of sedimentary rocks reflect the continental crustal abundances.

The concentration of REE is generally low in limestone than the shale, which suggest that the marine carbonate phase contains significantly lee REE than the terrigenous materials (Piper, 1974). Higher abundance of REE in clastic sediment is due to the presence of the clay fractions, because REE are readily accommodated in the clay structure (McLennan, 1989). Seawater contributes low REE to the sediments whereas the terrigenous sediment contains high REE abundance, not-similar to seawater-like pattern (Nothdurft et al., 2004).

The generally higher prevalence in nature of even atomic numbers is manifested by ratios of magnitude between neighboring pairs of elements. Consequently, comparisons among the REE are facilitated by normalizing analytical values to an appropriate reference, such as Chondrite, but for sedimentary rocks the preferred reference is either Post-Archaen Average Shale (PASS) or the North American Shale Composite (NASC), representatives of the average upper crust (Gromet et al., 1984, Condie, 1991). With respect to such a reference certain fractionation effects may enhance the light REE (LREE) or the heavy REE (HREE), and those may be quantified by the ratio of normalized $La_n/Lu_n>1$ (La/Lu>9.63) or $La_n/Lu_n<1$ respectively. Curvature in an REE plot may document an enhancement of the middle REE (MREE) with respect to both LREE and HREE. The resulting "hat-shaped" REE plat may be quantified by a ratio such as $2GD_n/(La_n/Lu_n)>1$.

REE Distribution of the Indravati Carbonate Succession

In the present study the REE have been analyzed with an objective of understanding their distribution in the carbonate lithofacies of Indravati Group, their provenance and depositional/diagenetic processes. The PAAS normalized REE patterns of sea water exhibit significant LHREE depletion, negative Ce anomaly, slight positive La anomaly (De Baar et al, 1991; Bau and Dulski, 1996) and super chondritic Y/Ho ratios (Bau, 1996). The Indravati carbonate samples show a variable REE +Y patterns resembling in some aspect to seawater pattern (ex. Significant LREE deletion) while deviating from the seawater patterns (in having a positive Ce anomaly and very low Y/Ho ratios) (Fig.3). The total concentration of REE (ΣREE) in the present sample varies from 57.23 to 644.55 with a mean content of 234.44. Both the carbonate lithofacies (Lithofacies A & C) display the total REE content of 259.81 and 192.54 ppm respectively (Table 4) which is more than the crustal average of 151.10 (after Mason and Moore, 1982). The PAAS normalized REE patterns (Fig. 4) of these rock samples are very similar to each other, (i) being significantly depleted in the LREE relative to the HREE - show a moderate degree of rare earth element fractionation when

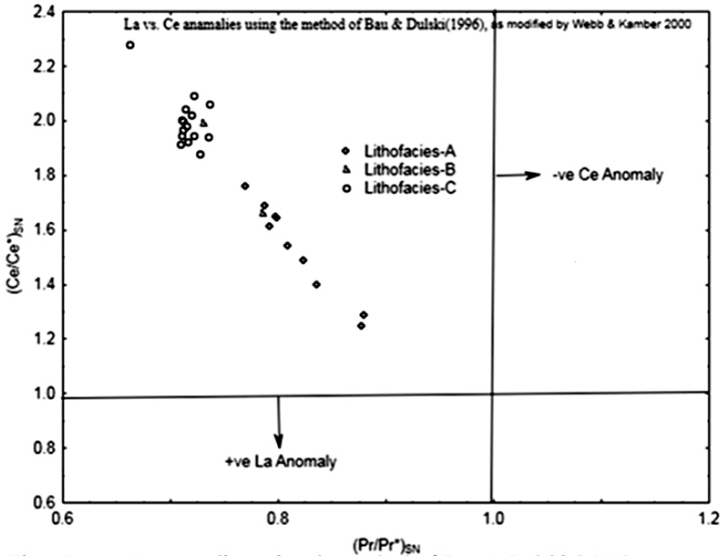

Fig. 3. La vs. Ce anomalies using the method of Bau & Dulski (1996), (modified by Webb & Kamber, 2000) differentiating the Indravati carbonates Lithofacies.

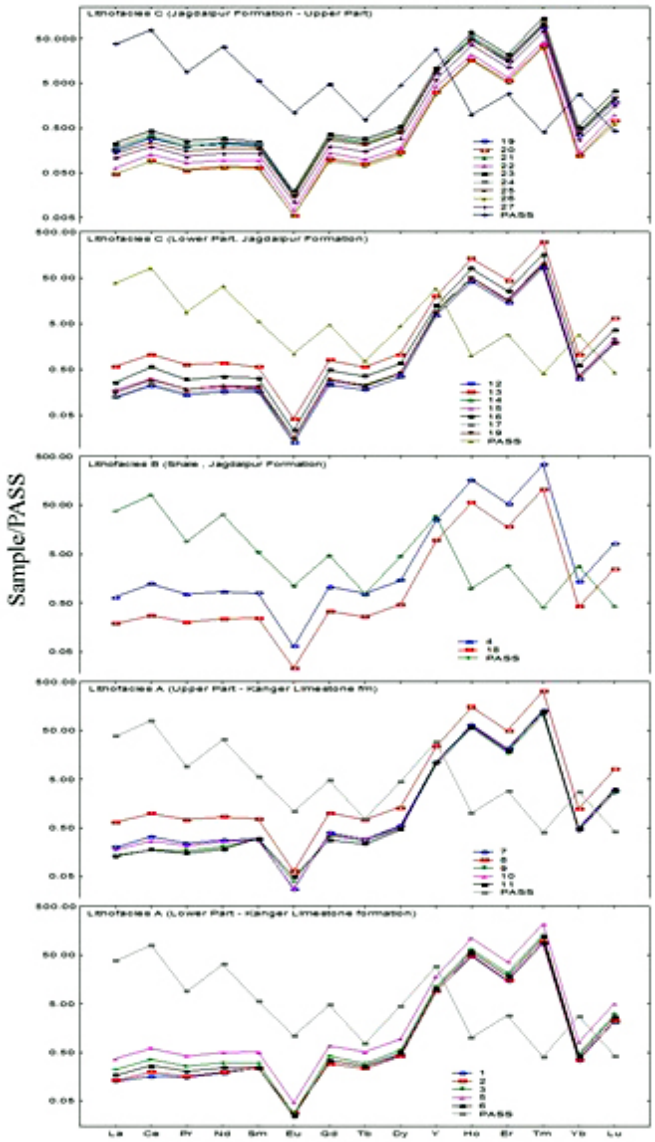

Fig. 4. PASS normalized REE+Y patterns of Indravati carbonates.

Table 4. Results of Factor Analysis of Indravati Carbonate Sequence

A. Factor Loadings (Varimax normalized)			
Variables	**Factor1**	**Factor2**	**Factor3**
B	0.1650	0.2427	-0.1741
Mn	0.0746	-0.6407	0.1678
Sc	**0.9798**	0.0106	0.0764
V	**0.9583**	0.2100	0.0092
Cr	**0.9568**	0.1925	-0.0921
Co	**0.7998**	0.0649	-0.0745
Ni	**0.9794**	0.1711	0.0005
Cu	0.1409	-0.3358	0.5467
Zn	**0.8626**	-0.1310	0.2969
Rb	**0.9586**	0.2531	-0.0476
Sr	-0.1281	**-0.9016**	0.1385
Y	**0.9642**	-0.1315	0.0050
Zr	**0.9627**	0.2354	-0.0578
Nb	**0.9675**	0.2041	-0.0268
Cs	**0.9500**	0.2315	-0.0645
Ba	0.6185	0.0347	0.4525
Hf	0.9613	0.2391	-0.0573
Ta	0.6444	0.3866	0.0097
Pb	0.4646	-0.1429	0.1094
Th	**0.9752**	0.1961	-0.0354
U	**0.9659**	0.1720	-0.0370
Th/U	0.5352	0.3808	0.0858
La/Th	-0.2102	**-0.8198**	0.0693
La/Yb	0.5824	0.6161	0.3669
La/Lu	0.4694	**0.7180**	0.3115
Y/Ho	**-0.7617**	-0.2395	-0.1505
(Eu/Eu*)sn	-0.1030	**-0.9144**	-0.2890
(Ce/Ce*)sn	0.0639	**0.9067**	-0.1290
(Gd/Gd*)sn	0.0443	**0.8866**	0.2521
(Nd/Yb)sn	0.4542	0.4549	0.6611
(Dy/Yb)sn	-0.4259	-0.0580	**0.7141**
(Pr/Pr*)sn	0.0168	**-0.9111**	0.1778
∑REE	**0.9901**	-0.0019	0.0057
∑LREE	-0.0238	0.0143	0.4516
∑HREE	**0.9870**	-0.0463	-0.0007
EigenValues	18.7382	6.0926	2.2833
Expl.Var	17.4715	7.3118	2.3307
%Total variance	49.91	20.89	6.66

B. Varimax Normalized Factor Scores			
Sample No	**Factor1**	**Factor2**	**Factor3**
1	-0.5164	-2.2293	0.8434
2	-0.3963	-1.0695	0.1608
3	-0.0533	-0.2719	2.2797
4	2.8033	-0.1520	0.1691
5	0.6897	-0.5675	0.5114
6	0.0354	-0.6155	0.7051
7	0.0548	-0.6805	2.2989
8	2.4955	0.3186	-0.2831
9	-0.3454	-1.9456	-0.4004
10	-0.0191	-0.6689	0.6146
11	-0.2713	-2.5298	-2.9292
12	-0.6654	0.5115	-0.3715
13	2.2303	0.7823	-0.5751
14	-0.3853	0.8230	-0.3170
15	-0.4103	0.7429	0.2006
16	0.2938	0.8282	-0.4880
17	-0.6327	0.3248	-0.4251
18	-0.1292	-0.1799	0.3755
19	-0.4812	0.8095	0.4927
20	-1.1630	0.9411	0.0656
21	-0.1026	0.8132	-0.6320
22	-1.0690	0.6546	0.2995
23	0.3000	0.6054	-0.5133
23	-0.2438	0.8082	0.1846
25	-0.3048	0.5140	-1.5207
26	-1.1100	0.8253	-0.3965
27	-0.6040	0.6076	-0.3495

(Marked (bold) loadings are >.700000)

sn - shale normalized

Total Variance Explained: 77.5%

compared to source rock, as indicated in their $(La/Yb)_N$ ratio of 3.64 for Lithofacies A and 3.31 for Lithofacies C samples, (ii) flat LREE and enriched HREE and (iii) a strong negative europium anomaly which is more pronounced in Lithofacies A. and (iv) a mild positive Ce anomaly. Relatively lower GD_N/Yb_N mean ratios (0.97 to 1.24; mean-1.17 for Lithofacies A and 1.20 to 1.30; mean-1.27 for Lithofacies B).

The concentration of REE in the present samples when compared to PAAS (ΣREE of PAAS) is 180; the Carbonate Lithofacies A & C show 259.81 & 192.54; the Lithofacies B (Calcareous Shale) show 421.93) is due to the presence of fine-grained clay minerals that contain high REE among the eroded materials and possibly the micrite (carbonate mud) and algal grains. Although, their REE is concentration high, the variability in terms of bulk rare earth elements and LREE/HREE ratio for all the samples is low. The change in the elemental concentration of ∑REE varying from 57.23 to 644.55 for the entire sequence as seen in the present samples (Table 3) reflect a relatively unstable tectonic conditions under which they have been evolved.

REE Anomalies

The most distinctive deviations from regular behaviour of the REE are "anomalous" levels of Ce and Eu. Understanding the origin of the depletion in Eu and Ce, relative to the other normalized REE in clastic sedimentary rocks is fundamental to most interpretations of crustal composition and evolution. A deviation of Ce and Eu may be quantified as ratio to Ce^* and Eu^* respectively by interpolating neighboring REE $\{Ce_{an} = Ce_n/[(La_n)(Nd_n)]^{1/2}$ and $Eu_{an} = Eu_n/[(Sm_n)(Gd_n)]^{1/2}\}$.

Eu Anomaly

Almost all the post-Archaen sedimentary rocks (except volcanogenic sediments) are characterized by Eu depletion (Taylor & McLennan, 1985). The negative Eu anomaly in some of these rocks indicates preferential removal of feldspar due to weathering (Nesbitt et al., 1996). The samples have a lower mean value Eu/Eu* (0.06 for Lithofacies A and 0.04 for Lithofacies B) compare to PASS/NASC representing the typical post-Archean submature sediments derived from differentiated upper continental crustal provenance (Eriksson et al., 1992). Though the rare earth elements are known to be immobile in weathering and erosion, Eu has slightly higher mobility than other REE (Albarede and Semhi, 1995).

Ce Anomaly

The possibility that Ce anomaly could be used as a possible indicator of redox conditions in natural water masses and their associated sediments, and that such sediments were preserved as reliable indicator of palaeo-redox in ancient oceans, attracted a good deal of attention in recent years (Wright et al., 1987, 88; Nothdurft et al., 2004). The Ce anomalies in marine carbonate rocks have been considered as suitable indicator of understanding the palaeo-redox conditions (Liu et al., 1988). In many past studies the palaeo-oceanographic conditions have been interpreted using the Ce behavior in the marine phases (Grandjean et al., 1987; Liu et al., 1988; German and Elderfield, 1990; Nath et al., 1997). Although. Negative Ce anomaly reveals the inclusion of REE directly from seawater or pore water under oxic-condition, the precise measurements and careful estimation of Ce anomalies in marine sediments give important aspects of the geological input and redox conditions at the time of deposition (MacLeaod and Irving, 1996). The prominent feature observed in REE distribution in present day waters and palaeo-seas is a negative Ce anomaly. If an oxic-suboxic boundary is encountered in a basin, the Ce anomaly reduces sharply to zero as Ce is re-mobilized (Sholkovitz et al. 1992). In general, strongly negative to zero Ce_{an} anomalies, and more rarely a weakly positive Ce_{an} are prominent features of REE distribution in a wide variety of modern and ancient sedimentary environments. In general the depletion of Ce relative to neighboring REE is one of the characteristic feature of seawater and marine carbonates deposited in the deep sea regions due to scavenging of Ce^{+4} by Mn oxides (Elderfield, 1988). The seawater Ce/Ce* values ranges from <0.1 to 0.4 (Elderfield and Greaves, 1982; Piepgras and Jacobson, 1992) whereas an average shale PASS/NASC Ce/Ce* is equal to 1 (Murray et al., 1991). In the present samples the value of Ce anomaly(Ce/Ce*) varies from 1.25 to 1.76 with mean value of 1.53 for lithofacies A and 1.88 to 2.28 with mean value of 2.00 for lithofacies B indicating a weakly positive Ce anomaly differing from that of the many ancient and modern sedimentary environments. The Ce/Ce* values show a negative correlation with Mn (r = -0.438) and Sr (r = -0.860) possibly suggesting the role of both redox conditions and digenesis leading to dolomitization responsible for the variation in Ce anomaly. The negative correlation between Mn and Ce/Ce* may also indicate reduction of Ce by MnO_2 (Viers and Wasserburg, 2004). The study of Takahashi et al. (2005) shows that the oxidation by Mn oxides is more plausible mechanism to produce Ce(IV)in soil horizon. The negative correlation of Ce/Ce* with Mn in the present samples could result not only from weathering process, but also by low oxygen fugacity during progressive dolomitization. The seawater signatures of the REE in the present samples are possibly masked by the abundant presence of micrite and clays and further the effect of early diagenesis and dolomitization cannot be ruled out.

STATISTICAL INTERPRETATION

The geochemical data on the Indravati Carbonate sequence has been subjected to statistical analyses for characterization of the two carbonate lithofacies. The

present study makes use of the Factor Analyses by extracting three varimax normalized factors explaining about 77.5% total variance. The results of the factor analysis are given in Table 4. The first factor explaining 49.9% total variance is display strong positive loadings of Sc, V, Cr, Co, Ni, Zn, Zr, Nb, ∑REE and ∑HREE whereas the Y/Ho ratio is the only variable showing negative relation with Factor1. The Factor1 has been related to the formation of organic complexes during the formation of the carbonates and explaining the enrichment of HREE over LREE. The Factor2, explaining 20.89% of total variance showing strong negative loadings of Sr, Eu/Eu*, Ce/Ce*, Gd/Gd* and Pr/Pr* variables and is related to the effect of diagenesis leading to depletion of LREE. The plot of factor scores of Factor1 vs. Factor2 (Fig. 5) show a clear discrimination of the lithofacies and suggesting change in the variation of depositional and diagenetic conditions of the Indravati Carbonate succession.

DISCUSSION

Shale-normalized REE+Y patterns of shallow seawater proxies have been described from both modern and ancient sedimentary environments. Suitable proxies viz. microbial carbonates, BIF, certain skeletal carbonates and pristine phosphides are primarily characterized by: (i) uniform LREE depletion; (ii) a positive La anomaly; (iii) a distinctively high Y/Ho ratios (higher than 44) and (iv) minor positive GD and Er anomalies (Alibert& McCulloch, 1993; Bau and Dulski, 1996). Further, these features are illustrated by an REE+Y pattern of average Holocene microbial carbonate that serve as a proxy for contemporary seawater owing to uniform seawater/carbonate partition coefficient (Web and Kamber, 2000). The concentration of Ce is additionally controlled by marine oxygenation levels whereas that of Eu also depends upon (i) co-precipitation with Fe-oxyhydroxides, (ii) input from high-temperature (>250°

Table 5. Lithofacies and depositional environments of Indravati carbonates.

Lithofacies and Lithology	Environment of Deposition
Lithofacies B and C Purple dolomitic shale, Pelmicrite and flat Pebble conglomerate, Purple, gray stromatolitic dolomite	**Intertidal to Supratidal**
Lithofacies A Limestone (Bedded micrite, pelmicrite etc.) Purple gray and black bedded micrite, sporadic occurrence micrites.	**Intertidal**

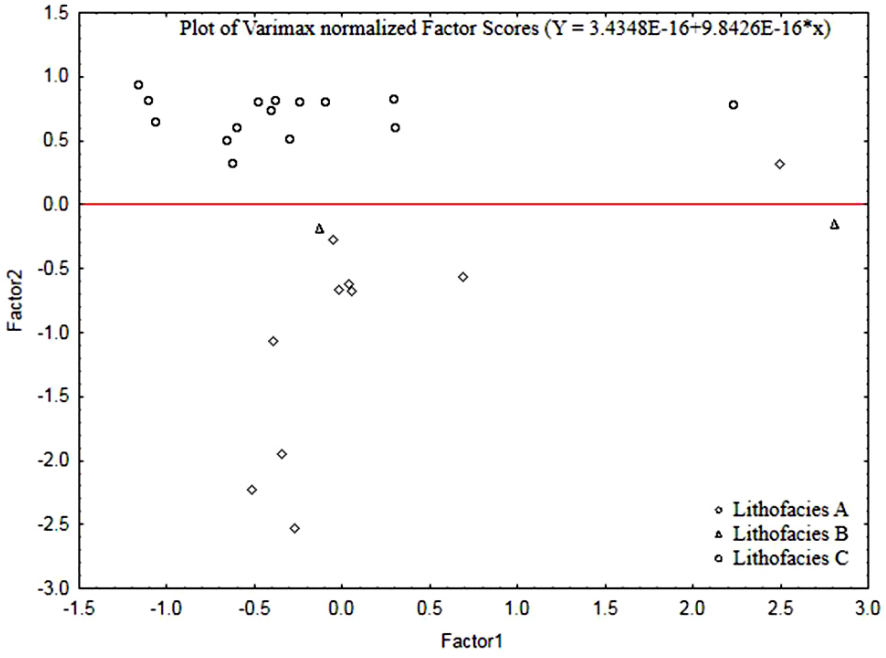

Fig. 5. Plot of Varimax normalized factor 1 vs. factor 2 differentiating the Indravati carbonates lithofacies.

C) hydrothermal sources (Michard and Albarede, 1986) and (iii) more locally the Early Archaen weathering sources that are enriched in Eu relative to post-Archaen shale (Gao and Wedepohl, 1995). However, genuine REE + Y patterns can be obscured in marine precipitates by contamination with siliciclastic or volcanic detritus, both of which contain a number of robust and different trace element signatures. Such contamination, as well as subsequent diagenetic and/or metamorphic overprinting, must be addressed before preserved patterns are interpreted.

The variations in the REE abundance patterns in Indravati carbonates are attributed to two factors: contamination with continental materials and post depositional diagenetic processes. The summary of the geochemical character of the carbonate facies is presented in Table 4. The Indravati Carbonates uniformly show REE+Y patterns characterized by LREE depletion, Lower Y/Ho ratios, positive Ce_{SN} and Er_{SN} and negative Eu anomalies (Table 3 and Fig.5). Although presence siliciclastic materials in the present samples is not observed in thin sections, due to very fine (micritic) nature of these carbonates, the LREE depletion and very low values of Y/Ho ratios and the relatively higher REE concentrations (particularly in lithofacies A & B) suggest mixing of shale. Although, the observed REE +Y patterns reflect some siliciclastic contamination but the relatively lower values of Sc and Th contradicts it. Furthermore, the samples show consistent +ve Ce, -ve Eu and +veer anomalies, all of which suggest somewhat different depositional waters unlike seawater. The chondrite/ PASS normalized REE pattern for seawater in general indicates that seawater shows a large depletion of Ce compared with the concentration of the other REE (Henderson, 1996). Ce is the only element among the mostly trivalent REEs, that can be oxidized to a tetravalent state. It is most likely removed from seawater by particulate scavenging (Buat-Menard and Chesselet, 1979) and is also fractionated into ferromanganese deposits (Glasby, 1973; Piper, 1974). In the present samples the weakly positive Ce anomaly could be due to the anoxic nature of the seawater and also low content of available Mn. The negative correlation of Mn with Ce/Ce* (r=-0.438) supports the anoxic nature of seawater.

Other features of the REE in seawater are the decreasing enrichment with increasing atomic number of the LREE, and the relatively constant, although somewhat enriched, pattern of the HREE (Table 5). The latter feature, as observed in the present carbonate samples can be explained by the formation of more stable inorganic and organic complexes by the HREE than by the LREE (Goldberg et al., 1963; Sillen and Martell, 1964).

The petrographic and XRD observations suggest the presence of calcite and dolomite in the present samples. The calcite exhibit fine grained (micrite or dolomicrite) and the dolomite crystals show a variable medium to coarse grained, anhedral to well-defined euhedral crystals (Plate.II-5 & 6). It is clear from petrography that the dolomite is of secondary origin (diagenetic replacement/recrystallization). In some samples the dolomite has been preferentially replaced by quartz, whereas the finely laminated sediments remain dolomite, suggesting that the initial sediments were more stable. The preservation of delicate lamination (Plate II-1) further supports this stable nature of carbonates. Though the original carbonates may have been calcitic or dolomitic, the diagenetic process (essentially the recrystallization and replacements) may have affected the original REE + Y pattern of the Indravti carbonates. Although, many previous studies (Tan and Hudson, 1971; Banner et., 1988; Zhong and Mucci, 1995 etc) have found that the diagenesis or early dolomitization have least effect on the REE concentrations, However, Nothdurft et al (2004) found that the dolomitization of Devonian limestones associated with basement-involved, mineralizing diagenetic fluids did alter original marine REE + Y patterns, primarily influencing on the abundance of Ce and Y content. Hence, the nature of the diagenetic fluid during dolomitization controls the degree of alteration of the REE + Y pattern. Additionally, subsequent dolomite/dolomite recrystallization may or may not alter aspects dolomite geochemistry (Land, 1992; Machel, 1997). The somewhat different REE+Y patterns (unlike the seawater) of the present samples suggest partly due to the fine non-carbonate components and the effects of the late diagenetic (burial) dolomitization which has greatly affected the REE + Y patterns and also the occurrences of various trace elements with relatively higher content of Zr, Ni, Ba and Ce. Further, the relatively higher content of Ho, Er, and Tm reported in the present study could be attributed to the presence of some silt sized heavy minerals of Zircon, Monazite? etc which also supported by higher content of Zr. Larger concentration of Ho, Er and Tm in xenotime and monazite are known to occur worldwide in many ancient and recent placer deposits, uranium ores, and weathered clay deposits (ion-adsorption ore). (http://reehandbook.com), although presence of the xenotime, monazite in the present samples is not observed due to their fine silt-size. The overall REE + Y patterns also comparable with those of Bau et al., 1996 for the Mediterranean samples differentiating the oxic v/s anoxic conditions (Fig.4f). Although, in general, the concentrations of the REE+Y in the present samples closely resembles to that of the upper crustal composition, the derivation of the framework composition of the present samples from a mixed source of origin is clearly evident from the plot of varimax normalized factor scores based on the chemical parameters wherein a clear discrimination of the two carbonate lithofacies (lithofacies A & C) is visualized. The Intervening calcareous lithofacies-B is seen separating the carbonate facies.

Depositional History of Indravati succession represented by two carbonate lithofacies (Table 5) separated by a shale lithofacies are interpreted based

on the field characteristics including the nature of the weathering surface and sedimentary structures observed suggest that deposition of the black and grey bedded micrite of lithofacies A, in tidal flat low energy environment of deposition (subtidal). While the lithofacies B consists of purple shale that gradually grading into lithofacies C that is composed of stromatolites and dolomitic micrite indicates a marine intertidal to supratidal flat environment. Desiccation cracks and mud pebbles in lithofacies C further supports their upper tidal to supratidal zone of deposition. Petrographic studies suggest that dolomitization is of secondary origin (as evidenced by stained sections showing clouded cores of dolomite crystals; larger size of dolomite crystals etc). The zonational/inclusions within the large euhedral dolomite crystals are supportive presence of Mn and Fe, that were introduced during late burial diagenesis. The some-what different REE+Y patterns, positive Ce anomaly and negative Eu anomaly and enriched HREE further supports the effect of burial diagenesis relatively at slightly higher temperatures. The significant LREE depletion compared with seawater, probably has several causes. Preponderance of basaltic REE sources in general (Condie, 1993) could have contributed this feature, but the sea water removal processes have greater potential to affect the slope of marine REE patterns. Bau and Moller (1993) and Alibert and McCullum (1993) have suggested that HREE enrichment relative to LREE could reflect higher CO2 pressure and hence different marine pH, favoring HREE stability in the water column. More efficient removal LREE in estuaries presently occurs with organic/clay complexation or carbonate complexation in estuaries where salinity increase from 2% to 10% (Hoyel et al., 1984). The persistent positive Ce anomalies in the present samples can be interpreted as a strong indication of insufficient free O to oxidize Ce to (IV) state. Under sufficiently oxidizing conditions Ce is removed very early with Fe oxides in the river water (Skolkovitz, 1992). Importantly, where such oxyhydroxide complexes were preserved as in case of Devonian estuarine carbonate sediments (Nothdurft et al, 2004), they have a positive Ce anomaly.

CONCLUSIONS

1. The carbonates comprising mainly of fine grained calcite and dolomite (fine to coarse grained) devoid of much detrital minerals display the effects of dissolution, recrystallization and replacement processes of diagenesis that is characteristic of burial diagenesis leading to dolomitization.

2. The slight variation in the PASS normalized REE+Y patterns from that of seawater are interpreted as the effect of the late stage burial diagenesis and possibly due to the minor content of non-carbonate fraction in the carbonates.

3. The HREE enrichment suggests higher CO_2 pressure and hence different marine pH (higher), and positive Ce anomaly in the carbonates are related to the oxygen deficient conditions during the deposition and/or subsequent diagenesis of the carbonates.

4. Depositional environments of Indravati carbonates can be interpreted on the basis of petrographic observation as Intertidal depositional environment for lithofacies A and Intertidal to Supratidal environment for the lithofacies B & C. The presence of desiccation cracks, various solution features and mud pebbles in lithofacies C are indicative of supratidal depositional environment and mixing of freshwater. The variation in the depositional conditions for the different lithofacies is also supported from the results factor analysis the total chemical data that clearly separate the two carbonate lithofacis and characterizes the varying depositional and diagenetic conditions of the carbonate succession.

The interpretation of each lithofacies discussed above indicates that Indravati carbonates were deposited within a broad, shallow sea marginal environment comprising of intertidal to supratidal flats.

***Acknowledgements*:** The author RG is grateful to the CGCOST for providing financial support and thankful to the Principal, Govt. NPG College of Science for extending necessary facilities. KM is thankful to the Goa University for the necessary help towards completing this work.

References

Albarede, F. (1995). Introduction to Geochemical Modeling. University Press, Cambridge, 554p.

Albarede, F and Semhi, K. (1995). Patterns of elemental transport in the bed load of the Meurthe River (NE France). Chem. Geol., 122, 129-145.

Algeo TJ, and Maynard JB (2004) Trace-element behavior and redox facies in core shale in upper Pennsylvanian Kansas-type cyclothems. Chem. Geol. 206, 289–318.

Alibert. C., and McCulloch, M. T. (1993). Rare earth element and neodymium isotopic compositions of the banded iron-formations and associated shale from Hamersley, Western Australia. Geochim. Cosmochim. Acta 57, 187-204.

Balaram, V. (1993). Characterization of trace elements in environmental samples by ICP-MS. Atomic Spectroscopy, 14(6): 174-179.

Ball, V. (1877). On the geology of the Mahanadi basin and its vicinity. Rec. Geol. Surv. India. 10(4), 167-186.

Balashov, Y. A., Ronov, A. B., Migdisov, A. A. and Turanskya, N. V. (1964). The effect of climate and

facies environment, on the fractionation of rare earths during sedimentation. Geochem. Int., 2: 951-969

Banner J. L. (1988). Rare earth element and Nd isotopic variations. in regionally extensive dolomites from the Burlington Keokuk. Formation (Mississippian): implications for REE Mobility. during carbonate diagenesis.. Jour. Sed. Petrol., 58, 415-432.

Bau, M. (1999). Scavenging of dissolved yttrium and rare earths by precipitating iron oxyhydroxide: Experimental evidence for Ce oxidation, Y-Ho fractionation, and lanthanide tetrad effect. Geochim. Cosmochim. Acta 63, 67–77.

Bau, M., Dulski, P., (1996). Distribution of yttrium and rare earth elements in the Penge and Kuruman iron formation, Transvaal Supergroup, South Africa: Precambrian Research, 79, 37-55.

Bau, M., Dulski, P. and Möller, P. (1995). Yttrium and Holmium in South Pacific Seawater: Vertical Distribution and Possible Fractionation Mechanisms. Chem. Erde. 55, 1–5.

Bau, M and Moller, P. (1993). Rare earth element systematic of the chemically precipitated component in Early Precambrian iron formations and the evolution of the terrestrial atmosphere-hydrosphere-lithosphere system. Geochim. Cosmochim. Acta, 57, 2239–2249.

Bhatia, M.R. (1983). Plate tectonics and geochemical composition of sandstones: Journal of Geology, 91, 611-627.

Brumsack H.J. (2006). The trace metal content of recent organic carbon- rich sediments: implications for Cretaceous black shale formation. PalaeogeogrPalaeoclimatolPalaoecol 232:344–361.

Buat-Menard, P. and Chesselet, R. (1979). Variable influence of the atmospheric flux on the trace metal chemistry of oceanic suspended matter. Earth Planet. Sci. Lett., 42, 399- 411.

Chatterjee N, Das N, Ganguly M and Chatterjee B (1990). Stromatolite based biostratigraphic zonation of Chandi Formation, Raipur Group, Chhattisgarh Supergroup in and around Dhamdha, Nandani area, District Durg, M.P.Geol. Surv. Ind. Spl. Publ.No. 28. 400-410.

Crookshank, H. (1963). Geology of Southern Bastar and Jeypore from the Bailadilla Range to the Eastern Ghats., Mem. Geol. Surv. India. 87, 149.

Condie, K. C. (1993). Chemical composition and evolution of the upper continental crust: contrasting results from surface samples and shales. Chemical geology, 104, 1-37.

Cullers, R.L., Barrett, T., Carlson, R. and Robinson, B., (1987). Rare earth element and mineralogic changes in Holocene soil and stream sediment: a case study in the Wet Mountains, Colorado, USA: Chemical Geology, 63(3-4), 275-297.

Davies, P. J. (1972). Trace element distribution in reef and sub reef rocks of Jurassic age in Britain and Switzerland. Jour. Sed. Petrol., 42(1), 183-194

De Baar, H.J.W., Schijf, J. and Byrne, R.H. (1991). Solution chemistry of the rare earth elements in seawater: European Journal of Solid State Inorganic Chemistry, 28, 357-373.

De Baar, H. J. W., German, C. R., Elderfield, H. and Gaans, P. V. (1988). Rare earth element distribution in the anoxic waters of Cariaco Trench. Geochim. Cosmochim. Acta, 52, 1203–1221.

Dunham, R. J. (1962). Classification of carbonate rocks according to depositional texture. In: Classification of carbonate rocks. Vol.1, (Ed. By W.E. Ham), 108-121, AAPG, Tulsa.

Dutt, N. V. B. S. (1963). Stratigraphy and Correlation of lndravati Series (Purana Group) Bastar district, M.P. Jour. Geol. Soc. India. 4, 35-49

Elderfield, H., Greaves, M.J., (1982). The rare earth elements in seawater: Nature, 296, 214-219.

Eriksson, K.A., Taylor, S.R. and Korsch, R.J. (1992). Geochemistry of 1.8-1.67 Ga mudstones and siltstones from the Mount Isa Inlier, Queensland, Australia: Provenance and tectonic implications. Geochim. Cosmochim. Acta, 56, 899-909.

Folk, R. L. (1962). Spectral sub-divisions of limestone types. In: Classification of carbonate rocks. .1, (Ed. By W.E. Ham), 62-84, AAPG, Tulsa.

Gao, S and Wedepohl, K. H. (1995). The negative Eu anomaly in Archaean sedimentary rocks-implications for decomposition, age and importance of their granitic sources. Earth and Planet. Sc. Lett., 133, 81-94.

German, C. R. and Elderfield, H. (1990) Application of the Ce anomaly as a paleoredox indicator: The ground rules. Paleoceanography 5, 823–833.

Glasby, G.B., 1973. Mechanism of enrichment of the rarer elements in marine manganese nodules. Mar. Chem., 1, 105-125.

Goldberg, E.D., Koide, M., Schmitt, R.A. and Smith, R.H., 1963. Rare earth distributions in the marine environment. J. Geophys. Res., 68, 4209—4217.

Goldschmidt, V.M., 1954. Geochemistry. Oxford University Press, Oxford, 730 pp.

Grandjean, P., Capetta, H., Michard, A and Albarede, F. (1987). The assessment of REE patterns and $^{143}Nd/^{144}Nd$ ratios in fish remains: Earth and Planet. Sc. Lett., 84, 181-196.

Guhey, R., Sinha, D., Tewari, V.C.(2011**).** Meso-Neoproterozoic Stromatolites from the Indravati and Chhattisgarh Basins, Central India. In:STROMATOLITES: Interaction of Microbes with Sediments, 21-42 (Ed. By Tewari V.C. and Seckbach, J. Springer Science + Business Media.

Guhey,R. and Wadhwa,N.P. (1993): Stromatolites from Raipur limestone around Nandini, District Durg, M.P. Ind. Jour. Earth Sci., 20 (1) 42-49.

Haskin, L. A., Haskin, M. A. and Wildeman, T. R. (1968). Relative and absolute terrestrial abundances of the rare earths. In: L.H. Ahrens(editor), Origin and sitribution of the elements. Pergamon, Oxford. 889-912.

Haskin, L.A. and Schmitt, R.A., (1976). Rare-earth distributions. In: P.H. Abelson (Editor), Researches in Geochemistry, 2. J. Wiley and Sons, New York, N.Y., 234-258.

Haskin, L. A., Wildeman, T. R., Frey. F. A., Collins, K. A., Heedy, C. R. and Haskin, M. A. (1966). Rare earths in sediments. J. Geophy. Res., 71, 6091-6105.

Holser, W. T. (1997). Evaluation of the application of rare earth elements to paleoceanography. Paleo. Paleo. Paleo. 132, 309-323.

Jairaman R.G. and Banerjee D.M. (1980). Preliminary studies of stromatolites from Raipur area, Chhattisgarh Basin, Geol. Surv. Ind. Misc. Publ. No. 44, 57-67.

Jarvis, J. C., Wildeman, T. R. and Banks, N. G. (1975). Rare earths in the Leadville Limestone and its marble derivates. Chem. Geol., 16: 27-37.

Kah, L.C., Lyons, T.W. and Chesley, J.T. (2001). Geochemistry of a 1.2 Ga carbonate-evaporite succession, northern Baffin and Bylot islands: implications for Mesoproterozoic marine evolution. Precambrian Res., 111, 203-236.

King, W. (1881). The geology of the Pranhita- Godavari Valley. Mem. Geol. Surv. India. 18 (3): 73-77.

Krupanidhi, K.V.J.R. (1970). The Purana rocks of Jagdalpurtahsil, Bastar district, M.P. Symposium on Geology and Mineral Resources of M.P. Ujjain. 3 (Abstract).

Land, L. S. (1992). The quantum theory of dolomite stabilization: does dolomite stabilize by 'Ostwald Steps'? In: Dolomite-from Process and Models to Porosity and Reservoirs, 1992 National Conference of Earth Science, Banff, Alberta, Canadian Soc. Petrol. Geologists and Faculty of Extension of University of Alberta.

Liu, X. and Byrne, R. H. (1998). Comprehensive investigation of yttrium and rare earth element complexation by carbonate ions using ICP-Mass spectrometry. J. Sol. Chem. 27, 803–815.

Liu, Y.G., Miah, M. R. U., and Schmitt, R. A. (1988). Cerium: a chemical tracer for palaeo-oceanoic redox conditions. Geochim. Cosmochim. Acta, 52: 1361-1371.

Machel, H. G. (1997). Recrystallization versus neomorphism, and the concept of 'significant recrystallization' in dolomitic research. Sed. Geolo., 113, 161-168.

Mac Leod, K.G.. and Irving, A.J., (1996). Correlation of cerium anomalies with indicators of paleoenvironment: Journal of Sedimentary Research, 66, 948-955.

Maheshwari, A., Sial, A. N., Guhey, R., and Fereeira, V. P. (2005). C-isotope Composition of Carbonates from Indravati Basin, India: Implications for Regional Stratigraphic Correlation. Gondwana Research (Gondwana Newsletter Section) V. 8, No. 4, pp. 603-610.

McCulloch, M.T. and Wasserburg, G.J., (1978). Sm-Nd and Rb-Sr chronology of continental crust formation: Science, 200, 1003-1011.

McLennan, S. M. (1989). Rare earth element in sedimentary rocks: Influence of provenance and sedimentary processes. Geochemistry and Mineralogy of Rare Earth Elements, Vol. 21 (Lipin, B. R. and McKay, G A., eds.), 169–200, Mineral Society of America.

McLennan, S. M., Fryer, B. J. and Yound, G. M. (1979). The geochemistry of the carbonate-rich Espanola Formation (Huronian) with emphasis on the rare earth elements. Cam. J. Earth Sci., 16: 230-239.

McLennan, S.M., Nance, W.B. and Taylor, S.R., (1980). Rare earth element-thorium correlations in sedimentary rocks, and the composition of the continental crust. Geochim. Cosmochim. Acta, 44, 1833-1839.

Michard, A and Albarede, F. (1986). The REE content of some hydrothermal fluids. Chemical geology, 55, 51-60.

Moitra, A.K. (1999). Biostratigraphy study of stromatolites and microbiota of Chhattisgarh Basin, M.P., India, Palaeontologia Indica Geol. Surv. Ind.51, 95P.

Nath, B.N., Bau, M., Ramalingeswara Rao, B., Rao, Ch.M. (1997). Trace and rare earth elemental variation in Arabian Sea sediments through a transect across the oxygen minimum zone: Geochimica et CosmochimicaActa, 61(12), 2375-2388.

Nothdurft, L.D., Webb, G.E. and Kamber, B.S. (2004). Rare earth element geochemistry of Late Devonian reefal carbonates, Canning Basin, Western Australia: Confirmation of seawater REE proxy in ancient limestones: Geochimica et Cosmochim. Acta, 68, 263-283.

Olivier, N. and Boyet, M. (2006). Rare-earth and trace elements of microbialites in Upper Jurassic coral- and sponge-microbialite reefs. ChemiGeol 230, 105–123.

Parekh, P.P., Moller, P., Dulski, P. and Bausch, W. M. (1977). Distribution of trace elements between carbonate and non-carbonate phases of limestone. Earth Planet. Sci. Lett., 34 39-50.

Piepgras, D.J., Wasserburg, G.J. and Dasch, E.J. (1979). The isotopic composition of Nd in different ocean masses. Earth Planet. Sci. Lett. 45: 223-236.

Piper, D.Z., (1974). Rare earth elements in the sedimentary cycle: a summary. Chem. Geol, 14: 285-304.

Ramakrishnan, M. (1987). Stratigraphy, sedimentary environment and evolution of the Late Proterozoic Indravati Basin, Central India. Geo. Surv. India. 139-160.

Schere, M. and Seitz, H. (1980). Rare earth element distribution, in Holocene and Pleistocene corals and their redistribution during diagenesis. Chem. Geol., 28: 279-289.

Schnitzer, W.A.(1971). Das jungpracambrium Indiens (Purana System). Erlanger Geol.Abhi, 85, 1-44.

Schnitzer, W. A. (1969). Die Jung-algonkischen Sedimentationsraume Peninsula-Indians. N. Jb. Geol. Palaeont. Abn. 33: 191-198.

Shah, H. F. and Waserburg, G.J. (1985). Sm-Nd in marine carbonate and phosphates: Implications of Nd isotopes in seawater and crustal ages. Geochim. Cosmochim. Acta, 49: 503-518

Sharma, V. P. (1975). Note on the stratigraphic classification of the Purana rocks of Bastar district, Madhya Pradesh. Geol. Surv. India Misc. Publ. 25(1), 171-175.

Sholkovitz, E. R. (1990). Rare earth elements in marine sediments and geochemical standards. Chemical Geology, 83, 333-347.

Sholkovitz, E. R. (1992). Chemical evolution of rare earth elements: Fractionation between colloidal and solution phases of filtered river water. Earth Planet. Sci. Lett., 114, 77-84.

Sillen, L.G. and Martell, A.E., (1964). Stability constants of metal-ion complexes. Chem. Soc. London, Spec. Publ, 17: 754 pp.

Takahashi, Y., Yuita, K., Kihou, N., Shimizu, H. and Nomura, M (2005). Determination of the Ce(IV)/Ce(III) ratio by XANES in soil horizons and its comparison with the degree of Ce anomaly. Phy. Scr., 115, 936-939.

Tan, F. C and Hudson, J. D. (1971). Carbon and oxygen isotope relationships of dolomites and co-existing calcites, Great Estuarine Series(Jurassic), Scotland. Geochim. Cosmochim. Acta, 35, 755-767.

Taylor, S.R., McLennan, S. (1985). The Continental Crust: Its Composition and Evolution: Blackwell, Oxford, 312 p.

Viers, J and Waserburg, G. J. (2004). Behaviour of Sm and Nd in a laterite soil profile. Geochim. Cosmochim, Acta., 698, 2043-2054.

Walker, T. L. (1900). A geological sketch of the central portion of the JeyporeZamindari Vizagapatam district. General report for 1899- 1900. Geol. Surv. India. Mise Publ. 166-176.

Webb, G. E. and Kamber, B. S. (2000). Rare earth elements in Holocene reefalmicrobialites: A new shallow seawater proxy, Geochim Cosmochim Acta 64, 1557-1565.

Wright, J., Schrader, H., and Holser, W. T. (1987). Paleoredox variations in ancient oceans recoded by rare earth elements in fossil apatite. Geochim. Cosmochim. Acta, 51, 631-644.

Zhang, J. and Nozaki, Y. (1996). Rare earth elements and yttrium in seawater: ICP-MS determinations in the east Caroline, Coral Sea, and South Fiji basins of the western South Pacific Ocean. Geochim. Cosmochim. Acta 60, 4631-4644.

Zhang, P. S., Tao, K. J., Yang, Z. M., Yang, X. M. andSong, R. K. (2003). Rare earths, niobium and tantalum minerals in Bayan Obo ore deposit and discussion on their genesis. J Rare Earths 20(2):81–86.

Zhon, S and Mucci, A. (1995). Partitioning of rare earth elements (REEs) between calcite and seawater solutions at 25^{o} and 1 atm, and high dissolved REE concentrations. Geochim. Cosmochim. Acta, 59, 443-453.

http://reehandbook.com.

Jour. Indian Association of Sedimentologists, Vol. 34, Nos. 1 & 2. (2017), pp. 59-62

Depositional Environments of Vempalle Formation along Western Margin of Cuddapah Basin: Interpretations of Borehole Data

R.V. Singh, H.S.Rajaraman, V.Rajagoplan, and M.B.Verma
Atomic Minerals Directorate for Exploration and Research, Department of Atomic Energy,
Hyderabad-500 016
Email: rvsingh.amd@gov.in

Abstract: Litho-facies study in Vempalle Formation using borehole cores revealed five major facies. They are lower impure dolostone (Facies-A), quartzite (Facies-B), chert laminated dolostone (Facies-C), purple shale (Facies-D) and upper cherty dolostone (Facies-E) in the order of superposition. Presence of abundant clastic component such as quartz, feldspar and argillaceous materials in the older dolostone facies indicate the terrigenous supply from the nearby provenance followed by shallowing of basin to form quartzite (Facies-B). Further, gradual increase in the depth of basin during the deposition of Facies-C, D and E resulted in the precipitation of chert dominated dolostone. The oscillation in the basin i.e. frequent exposure to the surface environment is evidenced by presence of wave ripples, dissolution cavities and desiccation cracks. Further, association of biological activity during the deposition of dolostone of Vempalle Formation is witnessed in the form of colonies of oncolithic, stratiform and columnar stromatolite structures. All the above observation envisages a Tidal Flat environment of deposition for Vempalle Formation, wherein mixing of fresh water derived from the continental part was involved for the development of dolostone.

Keywords: Depositional Environments, Vempalle Formation, Cuddapah Basin.

INTRODUCTION

The Cuddapah Basin is one of the important Proterozoic basins in India, which is considered as store-house of many mineral deposits. Vempalle Formation of Papaghani sub-basin in the southwestern margin of the Cuddapah Basin is significant for hosting strata-bound uranium mineralization, wherein a sizable deposit has been established by Atomic Minerals Directorate for Exploration and Research. Vempalle Formation rests above the Gulcheru quartzites with gradational contact. Vempalle Formation is dominantly a calcareous sequence represented by dolostone along with minor proportion of quartzite and shale. Vempalle Formation developed over a stretch of 185 km in the southern margin of Cuddapah Basin has been studied for litho-facies variation and uranium potential (Vasudev Rao et al., 1989; Majumdar et al., 1991; Roy, 1990). The northern extent of similar Vempalle Formation is exposed from Julakalva-Gudipadu over a stretch of 46 km form present study area. The results of lithofacies studies are presented with special reference to environment of deposition.

GEOLOGICAL SETTING

The investigated sector along Julakalva-Gudipadu in Papaghani sub-basin is located in southwestern part of the Cuddapah Basin (Fig. 1). The basin hosts sedimentary successions ranging in age from Palaeo proterozoic to Neo proterozoic, and associated volcanic rocks resulting a total thickness of about 12 km. These rocks rest unconformably over basement rocks consisting of granites, granite gneisses and greenstone belts. The lithostratigraphy of the Cuddapah basin is divided into Papaghani, Chitravati, Nallamallai, Srisailam and Kurnool Groups from base to top, composed dominantly of argillaceous and arenaceous sediments with subordinate calcareous units (Nagaraja Rao et al., 1987).

In the studied sector, the uranium mineralized dolostone is exposed as isolated hills. Geomorphologically, the mineralized dolostone occupy the erosional valley bounded by hill ranges of fairly resistive Gulcheru Formation in the west and cherty dolostone in the east. The hills developed in the Cherty dolostone are mostly conical shaped and present a rugged topography. Strike of the Vempalle dolostone varies from N-S to NNE-SSW with varying dip of 11°-28° towards east to east-south-east(Rajaraman et al., 2012). The Vempalle sediments are cross-cut by WNW-ESE to E-W trending strike slip faults (Tripathi et al., 2012). In the upper part of Vempalle Formation, basic sills are interbedded with the cherty dolostone. Dolerite dykes of E-W trend intrude the Vempalle Formation (Fig.1).

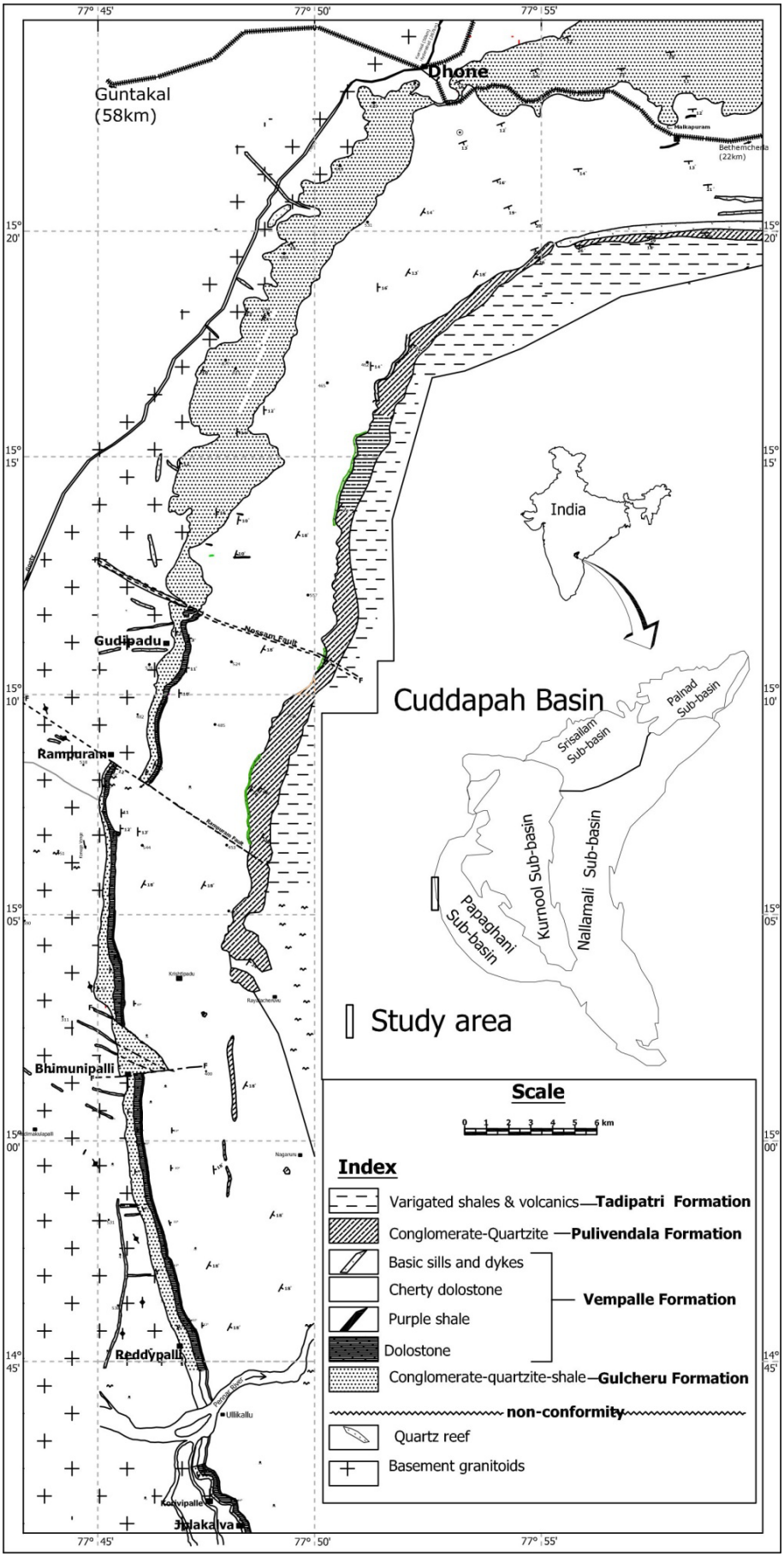

Fig. 1. Geological map of Korivipalle – Gudipadu sector.

LITHOFACIES IN VEMPALLE FORMATION

The dolostone of the Paleo-proterozoic Vempalle Formation along the western margin of Cuddapah Basin in Julakalva-Gudipadu sector over 46 km strike length is explored by core drilling for stratiform carbonate hosted uranium mineralization. Geological mapping and study of borehole cores of ~9000m revealed the five distinct facies variation in the Vempalle Formation and interpreted on the basis of composition, grain-size, sedimentary structures and stromatolites. They are lower impure dolostone (Facies-A), quartzite (Facies-B), chert laminated dolostone (Facies-C), purple shale (Facies-D) and upper cherty dolostone (Facies-E) in the order of superposition. A sketch showing the vertical variation of lithofacies of Vempalle Formation is shown in figure 2. Detailed description of these facies is presented below.

The facies-A rests above the Gulcheru Formation with a gradational contact and consists of massive to laminated, pale to dark grey dolostone. Intercalation of dolomitic wackstone (>10% grains) to dolomitic mudstone (<10% grains) with silt and sand grains and columnar and stratiform stromatolites have also been observed. The succession begins with dolomitic mudstone and passes into dolomitic wackstone containing occasional fenestral structures. This facies also contains lot of irregular clastic bands, consisting of quartz, feldspar and argillaceous materials. This facies also show cross-bedding with mud-draped bottom sets and foresets characteristics to tidal sand waves.

Facies-B overlies the facies-A and has a thickness of 50cm to 1.50m. It consists mainly of medium grained quartz (>90%) with minor siliceous and ferrugenous cement. Planar cross bedding and current ripples are well developed in this facies. It is overlain by the 4-6m thick chert laminated dolostone (facies-C) consisting of thinly laminated chert bands in alternation with dolomitic mud stone (<10% grains). Besides, facies - C also contains very fine grained (<1mm) pyrite dissemination. Purple shale (facies - D) has a uniform thickness of ~22m throughout the study area and consists mainly of reddish brown, thinly laminated shale with occasional specularite along bedding plane. The facies-D is overlain by laminated upper cherty dolostone (facies-E) comprising chert bands (2 - 60cm thick)and thin brownish silt / shale bands (<1 - 30cm). Facies-E has huge thickness up to 1400m. Many chert bands are composed of well-rounded, mustard size siliceous oolite, which show concentric rings at places. Besides, chert also occurs in the form of nodules and lenses in facies-E. Primary sedimentary structures such as wave ripples, fenestrae, dissolution cavities, desiccation cracks, breccia, colonies of round to oval shaped oncolithic and columnar stromatolite structures are pervasive in facies-E. Besides, many thin cross-bedded units with mud drapes and group of small-scale cross-bedded units

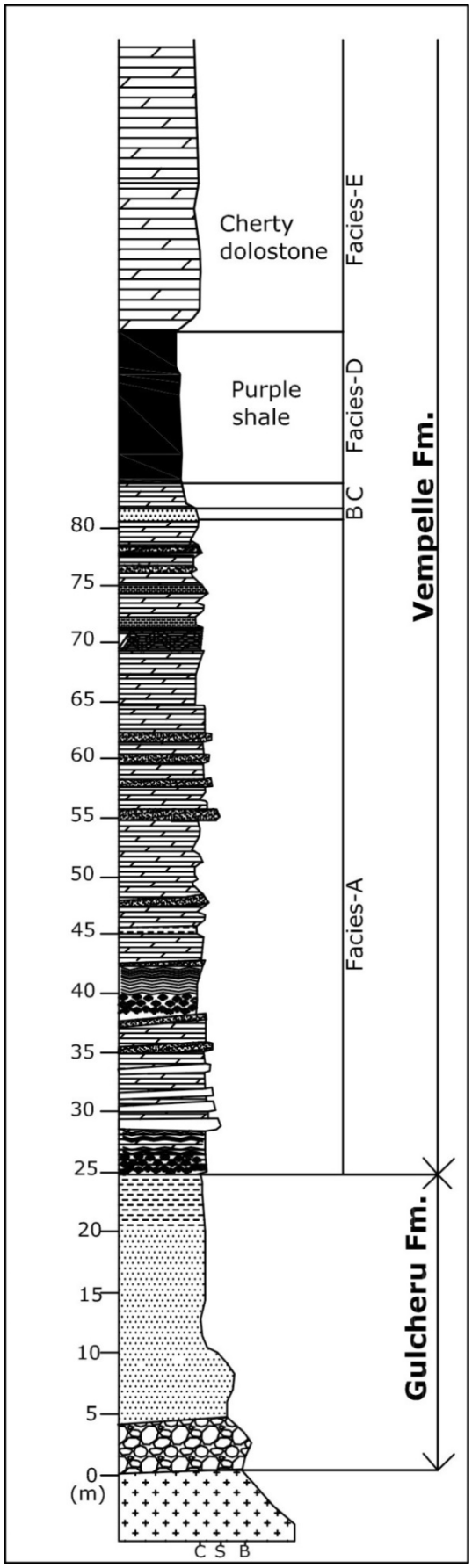

Fig. 2. Vertical lithofacies variation in Vempalle Formation.

with mud-draped bottom sets and foresets are observed on outcrops in facies-E.

The identified facies of the Vempalle Formation shows lateral discontinuity. Facies-A, facies-B and facies-D are developed from Julakalva in the south to Gudipadu in the north over 46 km stretch; whereas, the facies-C gradually tappers from south to north up to 18km stretch only and not developed in the north of Bhimunipalle. Further, northern continuity of facies-A, B and D is delimited by the WNW-ESE trending Nossam Fault. The youngest facies of Vempalle Formation i.e. upper cherty dolostone (facies-E) directly overlies the Gulcheru Formation in north of Gudipadu showing overlapping relationship.

Facies-A of Vempalle Formation rests above the arenaceous to argillaceous Gulcheru Formation with gradational contact. Facies-A starts with purple and grey colored, laminated stromatolitic dolostone and are dominantly dolomitic mudstone and passes into dolomitic-wackstone. A grey, fine grained, columnar dolostone with stromatolites of about 2m thick overlies the laminated unit. This is overlain by a 2m thick grey, medium grained, stratiform stromatolite bearing dolostone with current ripples, desiccation cracks, current bedding and thin layers of grey siltstone.

DISCUSSION AND CONCLUSIONS

The Vempalle Formation occurring along the western margin of Cuddapah Basin is dominantly calcareous with minor argillaceous and arenaceous units. Evidence of repeated sub aerial exposure are present in the litho-units of Vempalle Formation in the form of dessication cracks at different levels. Repetitive changes in sea level causing cyclic deposition of sediments on carbonate platforms, are well documented from the western margin of Cuddapah Basin in this paper. The lower part of the Vempalle Formation consists of facies-A and C representing intertidal to supratidal environment of deposition. Siliciclasitc influx in the form of arenite eventually led to progradation of the tidal complex as inferred by thin laterally continuous arenite in between facies-A and C. Low-relief stromatolites, parallel microbial laminae and fine grained carbonate particles suggest low-energy, shallow-water conditions. Presence of a lot of clastic components, fenestrae, vugs, desiccation cracks and breccias in the facies-A, C and E favors sub-aerial exposure during deposition under shallow marine tidal flat environment, especially belonging to the peritidal-siliciclastic carbonates. Facies-B being highly matured, quartz rich may indicate their deposition in upper shore. The purple shale facies-D appears to be deposited in shallow sub-tidal environment.

The thinly laminated and laterally continued purple shale i.e. facies-D may represent shallow subtidal environment below fair weather wave base in which shale could accumulate from suspension with increase in siliciclasitc influx. The thickest facies-E of Vempalle Formation is the cherty dolostone facies that also contain number of bands of shale and stromatolites. It displays greater facies variability, with an outer shelf marked by a stromatolite-rich peritidal carbonate complex. The alternate cherty dolostone and shale indicate the continuous cyclic change in environment of deposition. Increase in thickness of litho-units from west to east and decrease in the frequency and size of coarser detrital quartz and sand laminae within the carbonate indicate that the hinterland was nearer to west. Thus, the overall facies association of the Vempalle Formation shows shoaling upward trends. Prevalence of clastic components, cross-beds with mud drape leads to the conclusion that the dolostone of study area formed in a *Tidal Flat* environment wherein mixing of fresh water derived from the continental part was involved.

Acknowledgements: The authors are thankful the Director, Atomic Minerals Directorate, Department of Atomic Energy, Hyderabad for permitting to publish this work.

References

Majumdar, A., Shrivastava, V.K., Agarwal, M., Banerjee, D.C. and Kaul, R. (1991). Uranium mineralization in the northern part of Papaghani sub-basin of Cuddapah Super group, Andhra Pradesh, India. Expl. Res. Atom. Min., 4, 39-47.

Nagaraja Rao, B., Rajurkar, S., Ramilingaswamy, G. and Ravindra Babu (1987) Stratigraphy, structure and evolution of the Cuddapah Basin, In: Purana Basins of Peninsular India. Geol. Soc. Ind. Mem.6, 33-86.

Rajaraman, H.S., Mukundhan, A.R., Ramesh Kumar, K., Achar, K.K. and Umamaheswar, K. (2012). Regional facies variations in the Vempalle Formation of Cuddapah Basin: Implications on uranium exploration. Expl. Res. Atom. Min., 22, 103-112.

Roy, M., Dhana Raju, R., Vasudeva Rao, M. and Vasudeva, S.G. (1990). Stromatolitic uraniferous dolostone of the Vempalle Formation, Cuddapah Super group, Andhra Pradesh, India: Nature and bearings of stromatolites on uranium mineralization. Expl. Res. Atom. Min.,3, 103-113.

Tripathi, V. and Saha, D. (2013). Plate margin paleostress variations and intracontinental deformations in the evolution of the Cuddapah Basin through Proterozoic. Precam. Res., 235, 107-130.

Vasudev Rao, M., Nagabhushana, J.C. and Jeyagopal., A.V. (1989). Uranium mineralization in the Middle Proterozoic carbonate rock of the Cuddapah Super group, southern peninsular India. Expl. Res. Atom. Min., 2. 29-38.

Jour. Indian Association of Sedimentologists, Vol. 34, Nos. 1 & 2. (2017), pp. 63-73

Petrography, Clay Mineralogy and Heavy Mineral Distribution of Gondwana Sediments of Palar Basin, South India - Implications on Palaeoclimate and Provenance

R. Subin Prakash* and S. Ramasamy
Department of Geology, University of Madras, Guindy Campus, Chennai- 600025
*E-mail: suban5geo@gmail.com

Abstract: Palar Basin is a pericratonic rift basin located along the south eastern tip of India. An integrated study involving petrography, clay mineralogy and heavy mineral analysis of sandstone, shale and ironstone from the basin has been carried out to decipher their tectonic setting, provenance and paleoclimate. Texturally the samples are mature, well sorted, rounded to subrounded, contain monocrystalline grains showing straight to undulose extinction along with few polycrystalline quartz. Based on framework composition, the sandstones are classified as quartz arenite and sublitharenite types. A moderate content of feldspar especially plagioclase, orthoclase, perthite and microcline may imply rapid deposition of sediments from a nearby source rock. In modal analysis of sandstone, quartz ranges from 83.06 to 96.55% with an average of 89.17%. The feldspar content varies from 3.03 to 11% with an average of 7.17%. Rock fragments in the studied samples range from 0.41 to 9.12% with an average of 3.88%. The detrital mode suggests that the sandstone deposited in the continental recycled orogen provenance and stable cratonic (Passive Margin) interior such as those are derived from the exposed basement shield area of uplifted basement rocks. This is generally in agreement with the intracratonic, pull-apart origin of the east coast basins.

The heavy mineral suite displays rounded to subrounded as well as euhedral or angular grains of ilmenite, magnetite, zircon, tourmaline, garnet, rutile, sillimanite, kyanite, and staurolite in decreasing order of abundance. The calculated ZTR indices range from 73.42 to 95.16% with an average of 83.21%. The ZTR index and abundance of heavy minerals reflects that the samples have attained a moderate to high mineralogical maturity and these sediments have been originated mainly from granitic and metamorphic source areas with broad drainage basin.

Clay mineral assemblage point out the dominance of rock derived minerals (illite and chlorite) over soil derived clay minerals (kaolinite and smectite). The high content of illite indicates that the sediments were derived from pre-existing rocks (granite and gneisses), subjected to physical weathering over chemical weathering in a temperate climate (Hot/ Humid).

Keywords: Palar Basin, Gondwana, palaeoweathering, Provenance, Sandstone, Heavy mineral

INTRODUCTION

The detrital sediments are controlled by the source rock composition, weathering and diagenetic process (Armstrong- Altrin, 2009). The source rocks composition and characteristics are well recorded in sedimentary rocks (Armstrong- Altrin et al. 2004; Armstrong- Altrin and Verma, 2005; Sinha et al. 2007). Petrographic studies provide information on provenance, paleoclimate, effects of transportation and chemically deposited minerals during sedimentation and diagenesis. Provenance studies are based on modal analysis of detrital framework grains (Dickinson and Suczek, 1979; Dickinson et al., 1983). Sandstone detrital modes also provide information about the tectonic settings of depocentres (Dickinson et al., 1983). Heavy minerals have been used in deciphering the provenance (Krynine, 1946) and tectonic settings (Van Andel, 1959) of the western Himalayan Foreland basin (Singh et al., 2004). The heavy mineral suites are not only controlled by the provenance, but also by weathering, transportation, deposition and post-depositional alteration (Morton, 1985). The clay mineral study is a reliable tool for evaluation of source rock modifications during tectonism and reconstruction of paleoenvironmental conditions in siliciclastics (Chamley, 1989). The clay minerals have undergone alteration due to weathering, sedimentation, diagenesis and metamorphism (Chaudari and Kalitha, 1985).

Numerous studies on bio-litho stratigraphy, clay mineralogy, geochemistry, hydrogeology, depositional environments and tectonic evolution of the Palar Basin based on the scanty outcrops have been carried out by various researchers (Sastri et al., 1974; Venkatachala and Rajanikanth, 1988; Rangaraju et al., 1993; Tripathi and Vijaya, 1997; Ramasamy et al., 2011; Mazumder et al., 2013). The most recent and a detailed bio – lithostratigraphic study based on the subsurface samples from the first exploratory well covering the entire sedimentary column drilled in the basin by ONGC has

thrown much light on the evolutionary history of the basin (Basavaraju et al. 2016). However studies on petrography, clay mineralogy and heavy mineral studies are scarce. Hence the present investigation was taken up to understand the paleoclimatic conditions, tectonic settings and provenance characteristics.

STUDY AREA

The Palar Basin is one of the pericratonic rift basins located along the eastern coast of southern India. It covers an area of about 18,300 sq.km extending to Andhra Pradesh. The rift axis is oriented in a N – NNE direction, located in Tamil Nadu and adjoining Andhra Pradesh with its northern part extending into offshore. The northern side is separated from the adjacent Pennar Basin by Nayudupeta high and in the south by Chengalpattu high from the Cauvery Basin (Fig. 1). The basement (Sastri et al. 1974) is composed of an Archaean metamorphic complex overlain by the Gondwana sediments. The tectonic initiation of the Palar Basin was around the Lower Permian in N-S oriented linear troughs. In the southern part the older Ongur Formation (Lower Gondwana) deposited in a fluvio-glacial environment with a marine influence directly over the Precambrian crystalline rocks (Mazumder et al., 2013). Lithologically this formation consists of splintery gray and greenish shale with ferruginized sandstone. However, this formation is not recorded in the subsurface section of an exploratory well drilled by ONGC where Arani Formation of middle Jurassic sediments directly overlies the basement (Basavaraju et al. 2016). The continental separation between India and Antarctica during middle Jurassic resulted in the formation pull apart rift systems of Cauvery, Palar, Pennar and Krishna Godavari, ultimately leading to a series of horst and graben features. Palar Basin has evolved on the landward side of a zone of basement high and in all probability underlain by a thin continental crust which had undergone a small attenuation during Gondwana fragmentation. This basin is a single low with no horst and graben architecture within it (Rangaraju et al., 1993; Basavaraju et al., 2016).

The Sriperumbudur Formation represented by the Upper Gondwana sequence (Valanginian – Barremian age; Basavaraju et al., 2016), are characterized by lacustrine deposits with marine intercalations. The succeeding Satyavedu Formation (Aptian – Albian age; Basavaraju et al., 2016) has got deposited under fluvial/ lacustrine conditions with marine intercalations (Table 1). Satyavedu Formation consists of ferruginous sandstone with plant fossils. Probably towards the end of early Cretaceous during Late Aptian – Early Albian, rifting ended after which the area suffered widespread positive movements (Rangaraju et al., 1993; Basavaraju et al., 2016). This change has led to the uplift with no surface development of any post rift sedimentation. Late Cretaceous and Paleogene sediments are not found in the basin. The Satyavedu Formation is overlain by lateritic sandstone, cobbles, pebbles, boulders and surface alluvium of Pleistocene – Recent age. There are two major unconformities in the basin, one across Jurassic – Cretaceous boundary and the other spanning from Late Albian to Pliocene (Basavaraju et al., 2016).

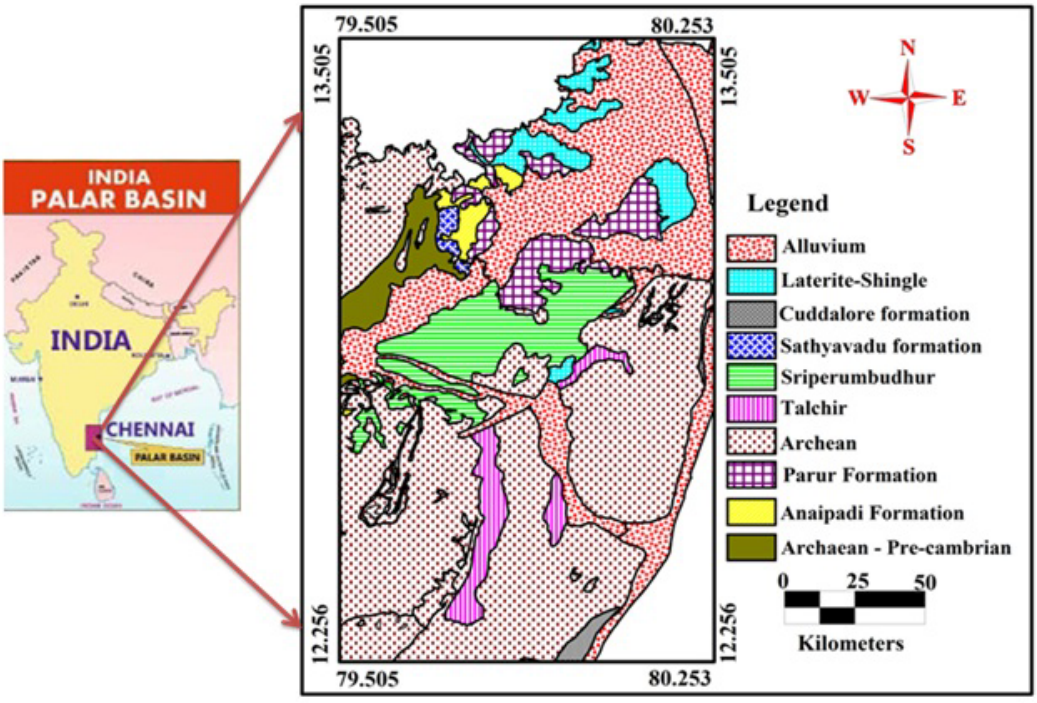

Fig. 1.Geological map showing the study area (Ramasamy et al., 2000).

Table 1. The new stratigraphy of the Palar Basin based on the subsurface studies Basavaraju et al. 2016.

Age	Formation	Thickness	Lithology	Environment
Pleistocene- Recent	Conjeevaram	50 – 100 m	Alluvium, laterite and pebbles, cobbles	Continental
~~ Late Albian to Pliocene ~~~~~~~~~~~~~~~~~~				
Aptian - Albian	Sathyavedu	350 m	Sandstone with Intercalations of shale	Lacustrine with marine intercalations
Valanginian - Barremian	Sriperumbudur	500 m	Sandstone, siltstone and minor intercalations of claystone/shale	Lacustrine with marine
~~ 5 Ma equivalent to Berriasian stage ~~~~~~~~~~~~~~~~~~				
Middle –Late Jurassic	Arani	1400 m	Sandstone with intercalations of shale	Lacustrine with marine intercalations

MATERIALS AND METHODS

Petrography

A total of 32 samples of sandstone, shale and ironstone were collected from three different exposures of Ongur, Sriperumbudur and Satyavedu Formations. A detailed petrography study was carried out on 21 thin sections. Modal analysis was done on 13 samples, with a minimum of five hundred framework grains counted from each thin section, except matrix and cement. In sandstone, the point counts were done following Gazzi-Dickinson (Gazzi, 1966; Dickinson, 1970) and traditional methods, which manages to minimize the effect of grain size (Ingersoll et al. 1984).

Heavy Mineral Analyses

A total of 20 samples were selected for modal analysis of heavy minerals. Bromoform liquid (sp.gr.2.89 gm/cm^3) was used to separate heavy minerals. The samples are mildly crushed and sieved using 80,100 and120 ASTM sieve meshes. The sediments in the 120 mesh were used for heavy mineral separation. After separation of heavy minerals, they were mounted on a glass slide with Canada balsam for microscopic examinations.

Clay Mineralogy

Twelve samples were selected for the clay mineral study. The clay rich samples were ground under standard conditions using an agate mortar. The samples were treated with hydrogen peroxide (H_2O_2) for 24 hours in order to remove organic matter. Clay deflocculating was done by successive washing prior to the separation of the clay fraction (<2 ìm). For each sample, two X-ray analyses were performed, first after air drying and the second after solvation by ethylene glycol (4hr, 80°C). Qualitative mineralogy of the clay sample is determined by the standard interpretation procedure of XRD data. The standard interpretation procedure of XRD data (Brindley and Brown, 1980 and Moore and Reynold, 1989) is used to determine the qualitative mineralogy of the clay samples. The oriented and glycolated slides were scanned from 2-30° (2-θ). X-Ray diffraction was performed using a computer controlled Joel powder diffractometer system model 8031 with Cu k (radiation).

RESULTS

Petrograhy of Sandstone

Populations of quartz were determined by the method proposed by Basu et al. (1975), and classification and tabulation of grain types were done following the traditional methods (Ingersoll et al. 1984).

The framework mineralogy of the clastic rocks indicates that these rocks are composed of quartz followed by feldspar, rock fragments with minor amounts of chlorite, glauconite, zircon, garnet and opaques. Texturally these sandstones are matured and well sorted. Quartz is the main framework grain, subangular to subrounded, monocrystalline with subordinate polycrystalline grains. Polycrystalline grains are composed of more than 5 grains and show crenulated and long fabric. Quartz grain shows undulatory extinction with, long as well as straight extinction. The rock fragments are sedimentary and igneous with subordinate metamorphic particles.

Framework parameters (Dickinson, 1985) and detrital modes of sandstones are given in Tables 2 and 3 respectively. Quartz is dominant in the entire section; ranges from 83.06 to 96.55% with an average of 89.17%. Monocrystalline quartz ranges from 67.71 to 92.31% with an average of 78.89% and the polycrystalline quartz range from 3.09 to 21.19% with an average of 11.85%. A variety of undulose and non-undulose quartz also present in the samples. Undulose quartz ranges from 75.77 to 95.60% with an average of 83.83%, while non-undulose quartz, ranges from 1.15 to 11.97% with an average of 4.78%.

The second abundant mineral is feldspar followed by rock fragments. Most of the rock fragments are derived from sedimentary, igneous and metamorphic source. Prior to plotting, the necessary minerals (quartz,

Table 2. Expansion of terms pertaining to Modal composition.

Qm nu	Non-Undulose monocrystalline quartz
Qm u	Undulose monocrystalline quartz
Qpq	Polycrystalline quartz
Qpq> 3	Qpq>3 crystal units per grain
Qpq 2-3	Qpq 2-3 crystal units per grain
Cht	Chert
Qp	Polycrystalline quartzose (or calcedonic) lithic fragments (Qpq+Cht)
Qt	Total quartzose grains (Qm+Qp)
Q	Total (Qm non+Qm un) and Qpq used for folk (1980)classification (Qm+Qpq)
P	Plagioclase feldspar
K	Potassium feldspar
F	Total feldspar grains (P+K)
Lv	Volcanic-metavolcanic rock fragments
Ls	Sedimentary rock fragments
Lsm	Metasedimentary rock fragment
L	Unstable (siliclastic) lithic fragments (Lv+Ls+Lsm)
Lt	Total siliciclastic lithic fragments (L+Qp)
RF	Total unstable rock fragments and chert used for Folk (1980) classification

Table 3. Recalculated modal Composition of Palar Basin sandstone samples.

Samples	Q	F	R	Qm	F	Rt	Qt	F	Rt	Opq	F	R	Qpq	Qmu	Qm nu
PB1	93.64	3.95	2.42	86.96	8.09	4.95	88.04	7.42	4.54	40.66	36.81	22.53	8.52	80.6	10.88
PB4	83.07	7.81	9.12	67.71	14.9	17.39	71.05	13.36	15.59	26.27	34.03	39.70	12.68	76.73	10.59
PB7	84.26	9.98	5.76	68.3	20.09	11.61	72.8	17.24	9.96	34.26	41.67	24.07	16.3	75.77	7.93
PB8	86.35	8.74	4.91	73	17.29	9.71	75.98	15.38	8.64	31.52	43.84	24.64	12.7	81.46	5.84
PB9	83.06	11.00	5.93	69.32	19.93	10.75	71.03	18.82	10.15	16.11	54.50	29.38	7.26	89.96	2.78
PB12	84.98	10.03	4.99	71.32	19.15	9.53	73.88	17.44	8.68	25.49	49.75	24.75	10.79	89.21	0
PB13	87.74	9.79	2.47	77.6	17.89	4.51	78.15	17.45	4.4	10.24	71.69	18.07	3.09	88.36	8.55
PB14	87.65	7.65	4.69	76.77	14.4	8.83	78.02	13.63	8.35	19.65	49.82	30.53	6.44	81.59	11.97
VK1	94.69	3.85	1.46	86.72	9.63	3.65	89.92	7.3	2.78	70.59	21.32	8.09	21.19	78.81	0
VK3	96.55	3.03	0.41	92.31	6.77	0.92	93.33	5.87	0.8	66.67	29.33	4.00	12.5	87.5	0
VK6	91.48	6.03	2.49	80.3	13.94	5.76	84.3	11.11	4.59	56.38	30.87	12.75	19.4	79.45	1.15
P12	88.30	8.30	3.40	80.75	13.66	5.59	84.34	11.11	4.55	54.41	32.35	13.24	18.14	81.86	0
SV2	96.13	3.31	0.55	92.22	6.67	1.11	92.55	6.38	1.07	36.36	54.55	9.09	4.4	95.6	0

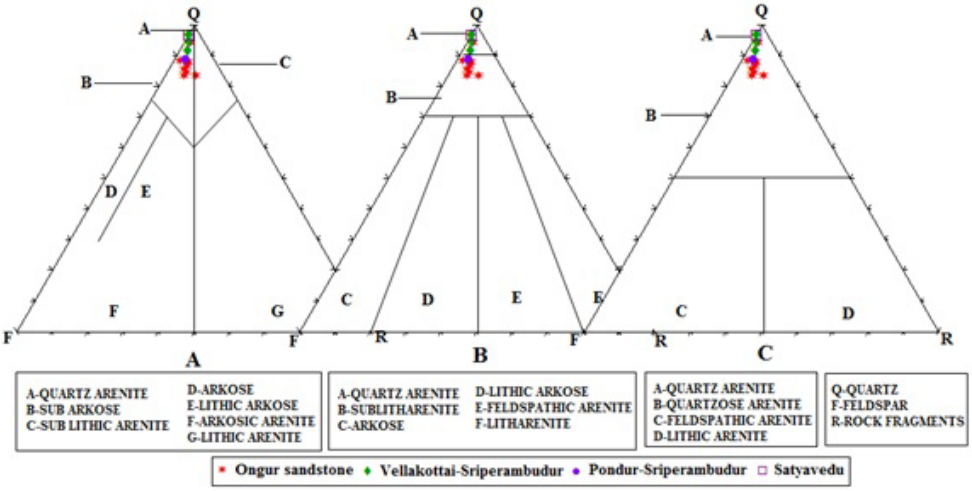

Fig.2. Triangular plot of Q-F-R of Ongur, Sriperumbudur and Sathyavedu sandstone samples (A) after Pettijohn et al. 1972, (B) after Folk, 1980 and (after James et al. 1986).

Table 4. Distribution of Heavy Minerals in Palar Basin samples.

Sample No.	Zircon	Tourmaline	Rutile	Garnet	Silimanite	Staurolite	Kyanite	Ilmenite	Magnetite	ZTR INDEX
PB1	53.49	8.36	4.56	12.04	1.65	0	0.13	4.31	15.46	82.775
PB4	41.53	19.35	2.26	2.68	1.69	0.14	0	10.17	22.18	93.333
PB6	47.19	8.84	3.21	15.06	2.61	0	0	3.61	19.48	77.025
PB7	41.33	8.08	0.24	10.21	2.38	0	0	13.06	24.7	79.772
PB8	41.28	8.72	0.58	16.86	1.45	0	0	10.17	20.94	73.421
PB9	37.21	10	1.03	10.74	0.59	0.15	0.29	9.41	30.58	80.387
PB12	38.75	10.16	0.82	13.46	1.65	0.27	0	10.71	24.18	76.378
PB13	36.98	17.09	0.98	9.38	0.7	0	0.28	8.54	26.05	84.161
PB14	40.06	6.34	2	9.18	1.34	0.17	0.17	10.02	30.72	81.674
VK1	13.47	5.97	1.5	2.87	0	0	1.12	11.85	63.22	83.995
VK3	14.3	4.28	1.34	2.2	0	0	0.24	47.44	30.2	89.088
VK4	12.84	13.46	2.45	4.28	0	0	0.61	12.84	53.52	85.464
VK6	13.18	21.96	1.01	2.7	0	0	1.01	20.28	39.86	90.692
VK8	10.95	2.95	1.35	1.62	0	0	0.27	39.19	43.67	88.973
P12	24.28	15.04	0.54	5.07	0	0.18	2.36	15.57	36.96	83.969
P14	20.36	3.14	1.23	5.03	0	0.11	0	48.32	21.81	82.792
V11	11	3.95	1.55	0.6	0	0.24	0	69.38	13.28	95.156
SV1	1.93	2.76	1.38	1.93	0	0	0	74.86	17.14	75.875
SV2	1.56	1.91	0.52	1.21	0	0	0	90.12	4.68	76.731
SV3	3.86	4.17	2.16	2.47	0	0	0	72.38	14.96	80.490

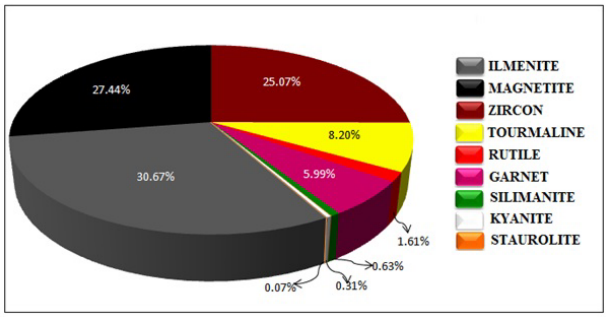

Fig.3. The distribution of Heavy Minerals in the Palar Basin sandstone samples.

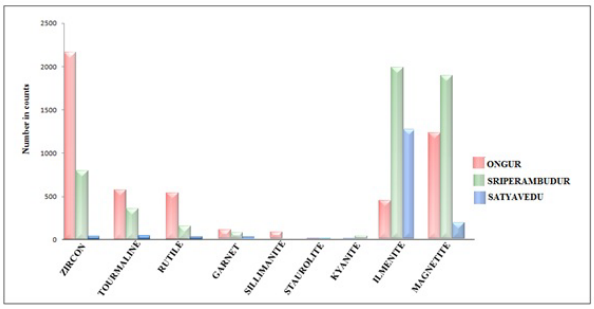

Fig.4. Heavy Mineral counts in the Ongur, Sriperumbudur and Satyavedu sandstone samples.

feldspar and rock fragments) were recalculated to 100%, ignoring cement and other detrital minerals (Pettijohn et al. 1972; Folk, 1980).

Heavy Minerals

The heavy mineral suite consists of zircon, tourmaline, rutile, garnet, sillimanite, staurolite, kyanite, ilmenite, and magnetite (Table 4) (Fig. 3). The heavy mineral assemblage consists of ultra-stable minerals: zircon, tourmaline and rutile and moderately stable minerals : garnet, sillimanite, staurolite and kyanite. However the opaque concentration dominates the entire assemblage. The presence of heavy mineral assemblage shows the variation of abundance in one formation to another (Fig. 4).

The zircon content ranges from 1.56 to 53.49% with an average of 25.48% and is present in all the samples. Some of the zircon grains show randomly distributed inclusions of opaque and non-opaque minerals. Tourmaline content ranges from 1.91 to 21.96% with an average of 9.11%. Tourmaline grains are elongated and irregular in shapes with termination in ends. Striations and partings are common. Rutile is dark red, brownish red to yellowish brown and shows weak pleochroism. Refractive index is high and the grains are subrounded to slender prismatic grains with well-developed termination or breakage patterns. Rutile varies from 0.24 to 4.56% with an average of 1.61%. Garnets have high relief, isotropic nature, euhedral, rounded, subrounded or irregular grains with an uneven or conchoidal fracture. It ranges from 0.60 to 16.86% with an average of 6.68%. Silimanite shows high relief and moderate birefringence, and varies from 0.59 to 2.61% with an average of 1.57%. Kyanite shows zoning with play of colors, moderately rounded and elliptical grains. Kyanite varies from 0.13 to 2.36% with an average of 0.75%. Staurolite is light yellow, showing low birefringence and high relief. It ranges from 0.11 to 0.27% with an average of 0.18%.

The common varieties of opaque are magnetite and ilmenite. The grains are mostly subrounded to rounded. Ilmenite ranges from 3.61 to 90.12% with an average of 30.73%. Magnetite is varying from 4.68 to 63.22% with an average of 28.25%. The ZTR indices calculated range from 73.42 to 95.16% with an average of 83.21% for the Palar Basin samples. ZTR index is a method of determining degree of weathering of source rocks both chemically and mechanically. The high ZTR index of the Palar Basin samples reveals a moderate to high mineralogical maturity and high weathering index in the source area.

Clay Mineralogy

The clay content shows significant differences in mineral composition (Table 5). The identified clay minerals are illite, chlorite, kaolinite, montmorillonite, smectite and sepiolite. Illite is identified by XRD peak values at 10 Å and 3.3 Å; Kaolinite at 7Å, 3.55 Å and 2.3 Å. The kaolinite is clearly distinguishable from the chlorite peak at 3.5 Å. Using slow scanning, chlorite is identifiable at peak values of 3.5 Å, 4.7 Å and 14 Å. Montmorillonite is identified with basal reflections at 5.7 Å and 8.5 Å. The sediments in general consist of the high amount of illite and followed by chlorite and kaolinite. Small amount of smectite is identified in the Ongur samples with its characteristic at 17 Å. The fibrous clay sepiolite is present in the studied samples, and is identified by using the distinctive peak at 12.3 Å.

DISCUSSION

The collective study of petrography, clay mineralogy and heavy mineral distribution of the Gondwana sediments of the Palar Basin bring out valuable information about the provenance, paleoclimate, tectonic settings and diagenesis.

PALAEOCLIMATE

The compositions of the clastics are widely used to interpret the weathering process in the source area. The degree of weathering is a function of climate and tectonic uplift. Increased intensity of chemical weathering infers decreased tectonic activity and /or increased warm and humid conditions in the source region (Jacobson et al. 2003). In the Q-F-R diagram (Suttner et al. 1981), the samples fall in the metamorphic source area with humid climate (Fig. 5). This diagram suggests sources of metamorphic and plutonic rocks with humid or arid conditions in the provenance. Another supportive Q-F-R diagram (Dickinson, 1985), reveals that most of the samples fall in the field of humid and semi-humid climate (Fig. 6). In the bivariate plot of Suttner and Dutta (1986) of Log-Log QP/F+R Vs Qm+Qp/ F+R (Fig.7) considered more sensitive to climatic control, the studied samples fall in the field of semi-humid and humid climate. These diagrams suggest that the source area must be predominantly a combined metamorphic and granitic terrain subjected to high intensity of physical weathering over chemical weathering under a humid climate. Morton

Table 5. List of clay minerals identified in the different Palar Basin shale samples.

S.No.	Study Area		Sample No.	Untreated Clay Mineralogy	Glycolated Clay Mineralogy
1.	Ongur		PB 2	Illite, Chlorite, Kaolinite, Smectite, Montmorillonite	Illite, Chlorite, Kaolinite, Montmorillonite
2.			PB3	Illite, Chlorite, Kaolinite, Smectite	Illite, Chlorite, smectite, Montmorillonite
3.			PB5	Illite,Chlorite	Illite, Chlorite, Kaolinite, Montmorillonite
4.			PB10	Illite, Chlorite, Kaolinite, Smectite	Illite, Chlorite, Kaolinite, Smectite, Montmorillonite
5.			PB11	Illite, Chlorite, Kaolinite, Smectite	Illite, Chlorite, Kaolinite, Smectite, Montmorillonite
6.	Sriperumbudur	Vellakotai	VK2	Chlorite, Illite, Kaolinite	Chlorite, Illite, Kaolinite, Montmorillonite
7.			VK5	Chlorite, Illite, Kaolinite	Chlorite, Illite, Kaolinite, Montmorillonite
8.			VK7	Chlorite, Illite, Kaolinite	Chlorite, Illite, Kaolinite, Montmorillonite
9.		Vellum	V9	Illite, Chlorite, Kaolinite	Illite, Chlorite, Kaolinite
10.			V10	Illite, Chlorite, Kaolinite, Sepiolite	Illite, Chlorite, Kaolinite, Sepiolites, Montmorillonite
11.		Pondur	P13	Kaolinite, illite, Chlorite,Sepiolite	Kaolinite, illite, Chlorite, Montmorillonite
12.	Satyavedu		SV4	Illite, Chlorite, Kaolinite, Sepiolite	Illite, Chlorite, Kaolinite, Montmorillonite

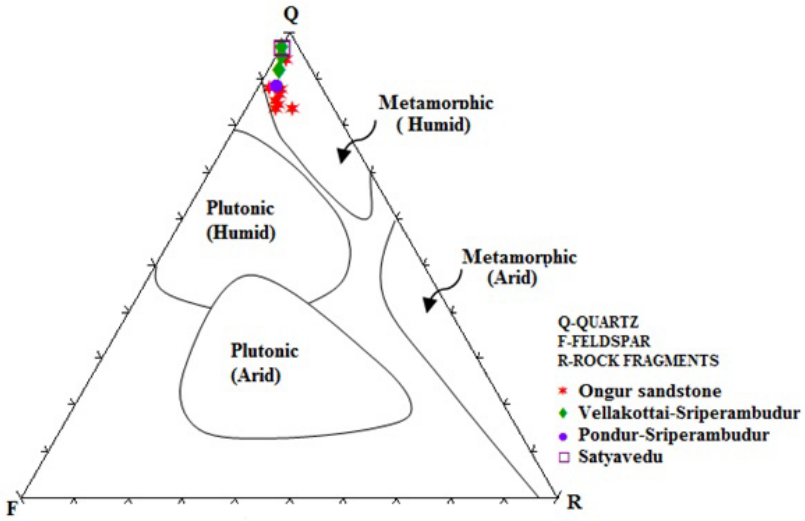

Fig. 5. The effect of source rock on the composition of the Palar Basin sandstones using Suttner et al., 1981 diagram.

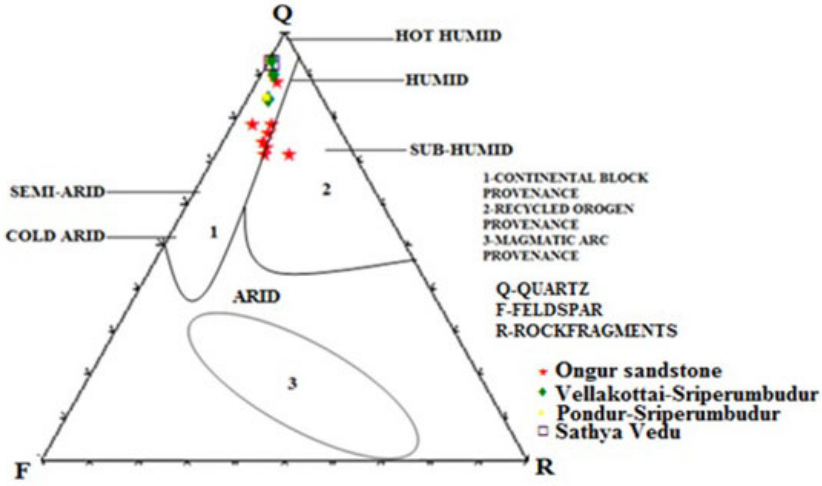

Fig. 6. Triangular plot of QFR of Ongur, Sriperumbudur and Sathyavedu sandstone samples (after Dickinson, 1985).

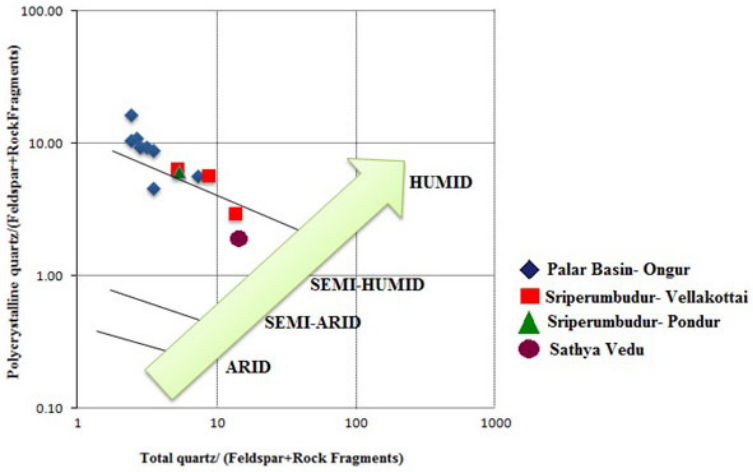

Fig. 7. Bivariate Log-Log plot of the ratio of polycrystalline quartz to feldspar+rock fragments against the ratio of total quartz to feldspar +rock fragments for interpretation of palaeoclimate from the Palar Basin sandstone samples (after Suttner and Dutta, 1986).

(1985) stated that heavy mineral suites are not only controlled by the provenance, but also affected by the source area weathering and process of transportation, deposition and post-depositional alteration. The high value of the ZTR index (73.42 to 95.16%) reveals that Palar Basin samples have attained a moderate to high mineralogical maturity (Fig. 10).

The study reveals the dominance of rock derived minerals (illite, chlorite) over soil derived clay minerals (kaolinite and smectite). The soil derived minerals are subordinate suggesting the predominance of physical weathering over chemical weathering. Fibrous clay (sepiolite) and kaolinite assemblage are indicative of both semi-arid and semi-humid paleoclimate in the source area terrain. In Ongur Formation, illite clay is high, whereas moderate content of illite is noticed in Satyavedu and Sriperumbudur Formations. The presence of high content of illite is reflective of temperate climate (Froth and Truck, 1974). The abundance of illite clay in the Ongur Formation suggests that the source area experienced a temperate climate where physical weathering was dominant, which produced sufficient quantities of rock derived mineral (illite). In the Sriperumbudur Formation depletion in illite content could be due to climate warming, which reduces the supply of illite with a corresponding increase in soil derived minerals, especially kaolinite and smectite.

In the Ongur Formation, the supply of pedogenic mineral (smectite and kaolinite) is influenced by a decreasing supply of rock derived minerals (illlite). During Cretaceous, warm climate may have produced more pedogenic mineral (Smectite) than the rock-derived mineral. The study reveals that smectite mineral is absent in the Satyavedu and Sriperumbudur Formations. The majority of the studied samples contain chlorite, possibly formed to a smaller extent in soils by weathering of micas and montmorillonite. Another soil derived clay mineral, the kaolinite is present throughout the section. The occurrence of kaolinite indicates a source region, which experienced intense weathering under possible tropical conditions (Biscaye, 1965). The fibrous clay sepiolite is present in Satyavedu and Sriperumbudur samples and is not recorded in Ongur samples. Fibrous clays (Sepiolite and Palygorskite) form under semi-arid conditions in calcareous pedogenic crusts (Millot, 1970) and these minerals can later get reworked by wind or water from the subaerial lacustrine or paralic environments.

PROVENANCE

Based on the petrography, the samples are classified into quartzarenite and sublitharenite (Fig. 2). For provenance study several petrographical techniques were used (Wanar and Adbel-Maguid, 2006). Based on the modal percentages, framework grains such as monocrystalline quartz, polycrystalline quartz, undulose quartz, non-undulose quartz, feldspar and rock fragments are used to construct different tridraws. Dickinson et al. (1983) demonstrate that provenance and tectonic settings of sandstone can be deciphered by considering the Q-F-R and Qm-F-Rt diagrams. The technique used (Basu et al. 1975) shows plotting of polycrystalline quartz versus undulatory to non-undulatory monocrystalline quartz (Fig. 8). Through this plot, it is inferred that low rank metamorphic source rock released quartz grains to sandstone samples. The triangular plots Qt-F-Rt (after Dickinson et al. 1985) and Qm-F-Rt, (Dickinson, 1985), suggest the continental block provenances with sources of stable craton and uplifted basements and recycled orogen provenance of the studied samples (Fig. 9)**.** These diagrams point out that the source terrain had a mixed provenance of sedimentary strata with subordinate igneous rocks and their metamorphic derivatives that exposed near to the basin. Well rounded and rounded quartz grains suggest an evidence of reworking of sediments. The studied monocrystalline grains show strong undulose extinction (more than 5 degrees of stage rotation) which they derived from strained source rocks, such as a metamorphic source; however, this is still not diagnostic evidence because igneous quartz may also exhibit undulose extinction (Scholle, 1979; Adams et al., 1984). Well rounded and rounded quartz, monocrystalline quartz with uniform or straight extinction, inclusions of Sillimanite, rutile and zircon needles, polycrystalline grains with 5 crystals of straight to slightly curved inter-crystalline boundaries, low content of plagioclase and k-feldspar characterize the Palar basin samples. They are derived from metamorphic, igneous and reworked sediments of different grades subjected to both long and short distances of transport. The recycled orogen provenance suggests that the framework grains of the sandstone have been derived predominantly from low lying granite and gneissic sources. The framework petrography of sandstone exhibits (a) higher percentage of quartz (b) predominance of monocrystalline grains (c) feldspar affinity, (d) a paucity of rock fragments and low F/R ratio suggests the sediment deposited in a passive continental margin tectonic setting. The presence of ultrastable, metastable and opaque minerals, euhedral, angular and sub-rounded grains of zircon, rutile with reddish and dark boundaries, suggested an evidence of metamorphic source which were derived from acidic igneous and sedimentary rock types.

The presence of illite and chlorite in the studied sample is possibly derived from metamorphic rocks of green schist facies and or weathering products of igneous rocks. The presence of sepiolite fibrous clay is indicative of granitic and low grade metamorphic rocks with seasonal warm and humid climatic conditions. The smectite clay mineral also points out the igneous origin of the clay mineral. The smectite clay mineral originates either from volcanic activity or during pedogenesis (Chamley, 1989).

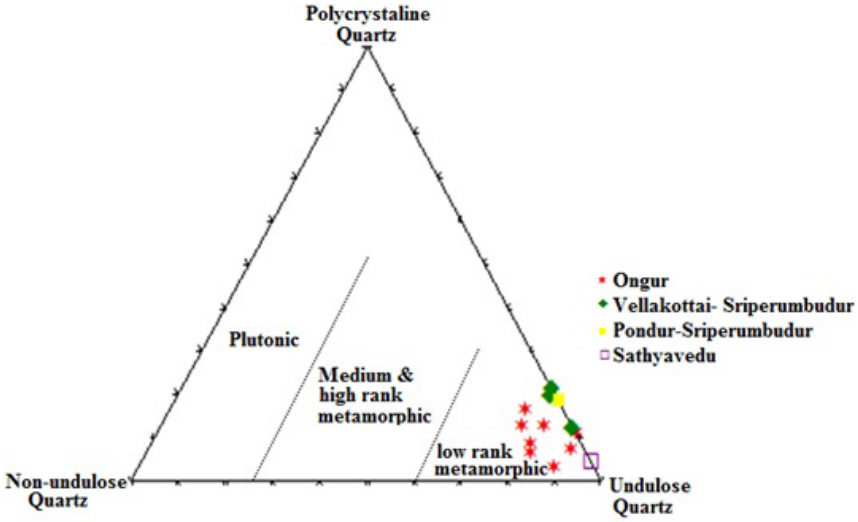

Fig.8. Triangular plot of detrital quartz types of the Palar Basin sandstones (after Basu et al. 1975).

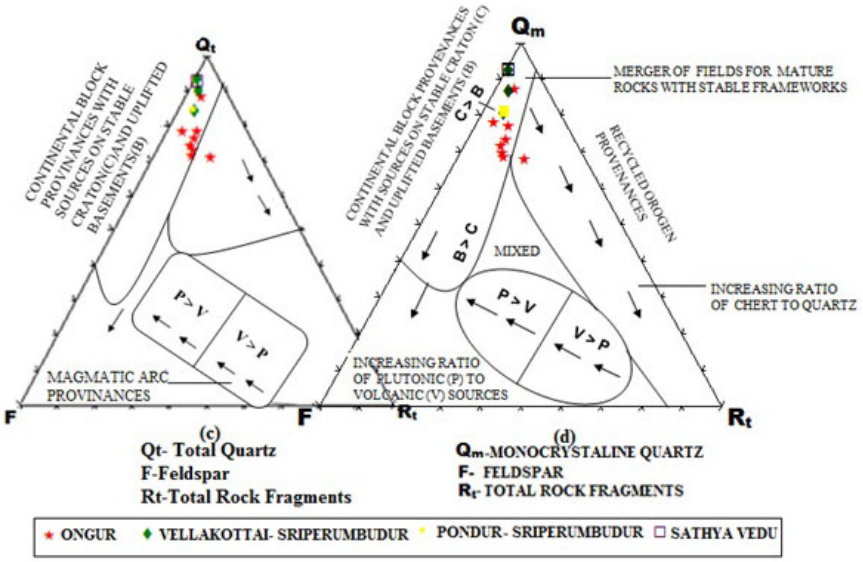

Fig.9. Triangular plot of Qt-F-Rt and Qm-F-Rt of Ongur, Sriperumbudur and Satyavedu sandstone samples (after Dickinson, 1985).

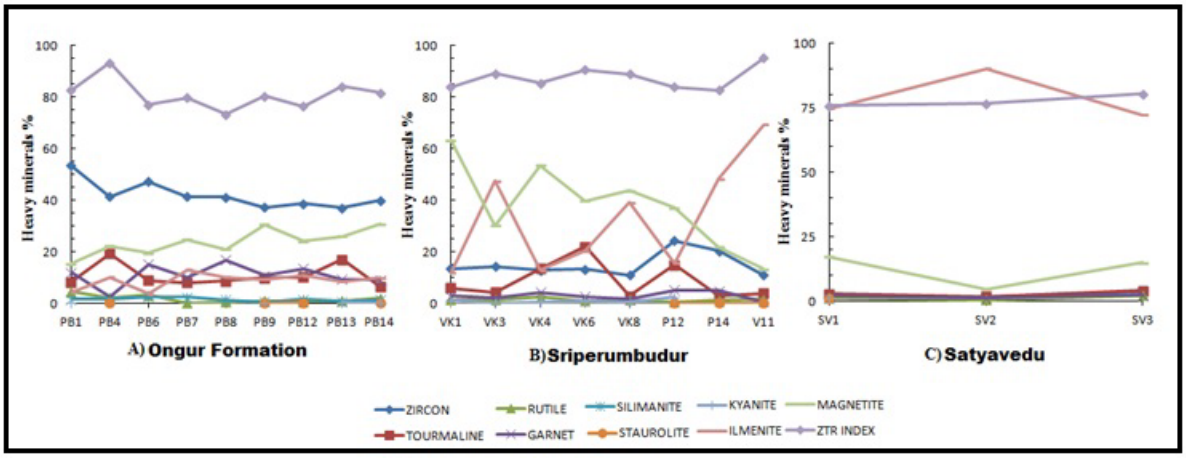

Fig.10. Distributive trend of Heavy Minerals and ZTR Index in Ongur, Sriperumbudur and Satyavedu sandstone samples.

CONCLUSIONS

This study reports the first account of petrographic analysis, heavy minerals and clay mineralogy of the clastic rocks of Gondwana sediments of the Palar Basin. The data have been used to interpret the palaeoweathering conditions and provenance characteristics of the sediments. Petrographic study shows that the sandstones are dominantly quartz arenite and sublitharenite varieties. Modal analysis of framework grain constitutes enrichment of quartz, and depleted content of feldspar and rock fragments. Among the quartz grains, monocrystalline quartz is volumetrically higher than the polycrystalline quartz. And the amount of sedimentary rock fragments is higher than those of igneous and metamorphic rock fragments. The data reveal that the clasts were mainly from igneous and metamorphic sources along with considerable percentage from sedimentary provenance.

Further, these studies also show that the samples were derived from a provenance of continental block and recycled orogen source terrains. The heavy mineral suite consists of stable (zircon, tourmaline and rutile) and metastable (sillimanite, staurolite, and kyanite) indicating dominantly low grade metamorphic source rocks from which they got released. The presence of varieties of heavy mineral also supported multiple source rocks (sedimentary, igneous and metamorphic). The heavy mineral suites, characterized by rounded as well as euhedral varieties of zircon suggest an igneous source. The clay mineral assemblage consists of illite, chlorite, kaolinite, montmorillonite, smectite and sepiolite. Illite is found volumetrically dominant suggesting a temperate climate where physical weathering prevailed over chemical weathering. The presence of illite and chlorite is possibly derived from the metamorphic rocks of green schists facies or the weathering product of igneous rocks. The QFR and Log-Log Qp/F+R Vs Qm+Qp/F+R plots also support the semi-humid and humid climate. The heavy minerals also substantiate that the sediments were sourced from a mixed provenance comprising metamorphic, igneous, and sedimentary rock. ZTR strongly support a low to moderate relief in the provenance or moderate to high mineralogical maturity.

Acknowledgement: This work has been carried out in the Department of Geology, University of Madras, Guindy Campus, Chennai-25. We thankfully acknowledge the support of the DST-INSPIRE Fellowship, Ref No. DST/INSPIRE Fellowship/2014:dt.1st July 2014-07-12.

References

Adams, A.E., Mackenzie, W.S., Guilford, C. (1984). Atlas of sedimentary rocks under the microscope: New York, Halsted Press, John Wiley & Sons, 104 p.

Armstrong-Altrin, J.S. (2009) Provenance of sands from Cazones,Acapulco, and Bahía Kino beaches, Mexico. Revista Mexicana de Ciencias Geológicas., 26, 764–782.

Armstrong-Altrin, J.S., Lee, Y.I., Verma, S.P., Ramasamy, S. (2004). Geochemistry of sandstones from the upper Miocene Kudankulam Formation, Southern India: implications for provenance, weathering, and tectonic setting. Jour. Sed. Res., 74, 285–297.

Armstrong-Altrin, J.S., Verma, S.P. (2005). Critical evaluation of six tectonic setting discrimination diagrams using geochemical data of Neogene sediments from known tectonic settings. Sediment. Geol., 177, 115–29.

Basavaraju, M.H., Jaiprakash, B.C., Chidambaram. L., M. Ayyadurai (2016). Biostratigraphy and Depositional Environments of Subsurface Sediments in Well Arani-A, Palar Basin, Tamil Nadu. Jour.Geol.Soc.India, 88, 407-420.

Basu, A., Young. S., Suttner, L., James, W., Mack, G.(1975). Re-evaluation of the use of undulatory extinction and crystallinity in detrital quartz for provenance interpretation. Jour. Sediment. Petrol. 45, 873–882.

Biscaye, P.E. (1965). Mineralogy and sedimentation of recent deep sea clay in the Atlantic Ocean and adjacent seas and oceans. Geol. Soc. America, Bulletin., 76, 803–832.

Brown, G., Brindley, G.W.(1980). X-ray diffraction procedures for clay mineral identification. In G. W. Brindley and G. Brown, Eds., Crystal Structures of Clay Minerals and their X-ray ldentification., Mineralogical Society, London, 305-359.

Carozzi, A.V. (1993). Sedimentary petrography: Englewood Cliffs, New Jersey, PTR Prentice Hall, 263 p.

Chamley, H. (1989). Clay Sedimentology, 623. (Springer-Verlag, Berlin).

Choudri, R.S., Kalita, C.K. (1985). X-ray study of clay mineralogy of the Krol Formation of the Mussorie Hills, Kumaon Himalaya, India., Jour. Earth Sci. 12, 239-249.

Dickinson, W.R. (1970). Interpreting deterital modes of greywacke and arkose. Jour. Sediment. Petrol., 40, 695 –707.

Dickinson, W.R. (1985). Interpreting provenance relation from deterital modes of sandstones, Zuffa,G.G.(ed), provenance of arenites. NATO ASI Series, Reidel Publ.Co., Dordrecht, 333-361.

Dickinson, W.R., Beard, L.S., Brokenridge, G.R., Ergavee, J.L., Ferguson, R.C., Inman, K.F., Knopp, R.A.,

Lindberg, F.A., Ryberg, P.T. (1983). Provenance of North America Phanerozoic sandstone in relation to tectonic setting. Geol. Soc. America, Bulletin., 94, 222–235.

Dickinson, W.R., Suczek, C.A. (1979). Plate tectonics and sandstone compositions. Bulletin. Am. Assoc. Petrol. Geol. 63, 21–71.

Folk, R.L. (1980). Petrology of sedimentary rocks., Austin, Texas Hemphill Publishing, 159p.

Froth, H.D., Truck, L.M. (1973) Fundamentals of Soil Sciences (5th Ed.). Wiley Eastern Pvt. Ltd., New Delhi, 454p.

Gazzi, P. (1966). Le arenarie del flysch sopracretaceo dell'Appennino modensese: Correlazioni con il flysch di Monghidoro. Miner. Petrographica Acta, v.12, pp.69-97.

Ingersoll, R.V., Bullard, T.F., Ford, R.L., Grimm, J.P., Pickle, J.D., Sares, S.W. (1984). The effect of grain size on detrital modes: a test of the Gazzi–Dickinson point-counting method. Jour. Sediment. Petrol. 54, 103–116.

Jacobson, A.D., Blum, J.D., Chamberlain, C.P., Craw, D., Koons, P.O. (2003). Climate and tectonic controls on chemical weathering in the New Zealand Southern Alps.Geochim. Cosmochim. Acta., 37, 29–46.

James, K., Lorente, M.A., Pindell, J. (Eds.). The geology and evolution of the region between north and south America, Geology society of London, Special Publication.

Krynine, P.D. (1940). Petrology and genesis of the Third Bradford sand. Bulletin. Pennsylvania Stat. Coll. 29, 134.

Millot, G.(1970) Geology of clays, Springer. Berlin 499.

Moore, D.M And Reynolds, R.C. (1989). X-Ray diffraction and the identification and analysis of clay minerals. Oxford University Press, Oxford 332.

Morton, A.C.(1985). Heavy mineral in provenance studies, "Provenance of Arenites" (Ed Zuffa B.B), D. Rediel Publication Company, New Jersey, pp.249-277.

Mazumder, S., Pangtey, K.K.S., Mitra, D.S. (2013). Delineation of a possible subsurface ridge in onshore Palar Basin based on morphotectonic studies and its implications.10th Biennial international conference and exposition.

Pettijohn, F.J., Potter, P.E., Siever, R. (1972). Sand and Sandstone. Springer-Verlag, New York, 618.

Ramasamy, S.M., Kumanan, C.J., Selvakumar, R., Saravanavel, J. (2011). Remote sensing revealed drainage anomalies and related tectonics of South India, Tectonophysics, 501, 41-51.

Rangaraju, M.K., Agarwal, A., Prabhakar, K.N. (1993). Tectonostratigraphy, structural styles, evolutionary model and hydrocarbon prospects of Cauvery and Palar Basins, India. In: Biswas et al. (Eds.), Proc.2nd Seminar on Petroliferous Basins of India., 1, 371-388. Indian Petroleum Publishers, Dehradun-248001, India.

Sastry, V.V., Raju, A.T.R., Singh, R.N., Venkatachala, B.S. (1974). Evolution of the Mesozoic sedimentary basins on the east- coast of India. APEA Journal, 29-41.

Schieber, J.(1986). Stratigraphic control of rare- earth patterns types in mid- Proterozoic sediments of the Belt Super Group, Mountana, U.S.A. Implication for basin analysis Chem. Geol., 54, 135-148.

Scholle, P.A. (1979). Memoir 28: A color illustrated guide to: constituents, textures, cements, and porosities of sandstones and associated rocks: Tulsa, Oklahoma, The American Association of Petroleum Geologists, pp. 201.

Suttner, L.J., Basu, A., Mack, G.H. (1981). Climate and the origin of quartz arenite. Jour. Sediment. Petrol. 51 (4), 1235–1246.

Suttner, L.J., Dutta, P.K. (1986). Alluvial sandstone composition and paleoclimate. Framework mineralogy. Jour. Sediment. Petrol. 56, 329–345.

Singh, B.P., Pawar, J.S., Karlupia, S.K. (2004). Dense mineral data from the north western Himalayan foreland sedimentary rocks and recent sediments: Evaluation of the hinterland. Jour.Asian Earth. Sci. 23, 23-25.

Sinha, S., Islam, R., Ghosh, S.K., Rohtash Kumar., Sangode, S.J. (2007). Geochemistry of Neogene Siwalik mudstones along Punjab re-entrant, India: Implications for source area weathering, provenance and tectonic setting. Curr. Sci. 92, 1103-1113.

Tripathi, A., Vijaya, A. (1997). Biostratigraphic age determination of Sriperumbudur Formation in borehole PBSD-1, Palar Basin, Tamil Nadu: a re-assessment. Jour. Palaeont.Soc. India, 42, 101-116.

Wanar, H.A., Abdel-Maguid, N.M. (2006). Petrography and geochemistry of the Cambro-Ordovician Wajid Sandstone, southwest Saudi Arabia: Implications for provenance and tectonic setting. Jour.Asian Earth. Sci. 27, 416-429.

Van Andel, T.H. (1959). Reflections of the interpretations of heavy minerals analysis, Jour. Sediment. Petrol., 29, 163-174.

Van De Kamp, P.C., Leake, B.E. (1995). Petrology and geochemistry of siliciclastic rocks of mixed feldspathic and ophiolitic provenance in the Northern Apennines, Italy. Chem.Geol. 122, 1-20.

Venkatachala, B.S., Rajanikanth, A. (1988). Stratigraphic implication of Late Gondwana floras in the east coast. Paleobotonist., 36, 183-196.

Jour. Indian Association of Sedimentologists, Vol. 34, Nos. 1 & 2. (2017), pp. 75-92

Commonality of Sedimentary facies of Andaman Flysch in South Andamans and Great Nicobar Island: Implications for depositional model in southern part of Andaman basin

SANDIP KUMAR ROY AND SANTANU BANERJEE
Department of Earth Sciences, IIT Bombay, Powai, Mumbai-400076, India
Email: jovialchap@gmail.com, santanu@iitb.ac.in

Abstract: Andaman Flysch comprises five facies, viz thick sandstone, heterolithics, shale, thin sandstone and conglomerate-gritty sandstone in South Andaman Island and Great Nicobar Islands. The first three are the common facies to both the islands. The thin sandstone facies occurs in South Andaman while the conglomerate-gritty sandstone facies occurs in the Great Nicobar Island. Thick sandstone facies are dominating in both the locations, repeating vertically in quick succession. Pene_contemporaneous deformation features, occurring with periodicity in the south Andaman Island are attributed to seismic activity. A general lowering of grain size, variation in facies association and sedimentary structures, from the north to the south suggests sediment supply from the north. A north-south, arc-parallel presence of the Andaman Flysch is envisaged. However, carbonaceous shale and conglomerate-gritty sandstone facies in the Great Nicobar represents sediment input from North Sumatra. In South Andamans, the Andaman Flysch represents submarine channel to lobe transition zone, while in Great Nicobar Island, they represent distal lobes.

Keywords: Andaman Flysch, Nicobar, Facies, channel-levee, lobe.

INTRODUCTION

The Andaman and Nicobar islands represent an uplifted accretionary prism on the edge of a fore arc. It came into existence following the breakup of the Gondwanaland, the northward flight of the Indian plate, its anticlockwise rotation, impingement beneath the Eurasian plate since Late Cretaceous time (Fig.1, Table1). The major tectonic elements are outlined as outer arc, Andaman trench, accretionary prism, trench slope break or structural high, fore-arc, volcanic arc and back-arc (Weeks,1967; Curray et al., 1979; Curray, 2005, Roy, 1983; Mishra and Roy, 1984; Roy,1992 ; Roy and Das Sharma, 1993; Roy and Banerjee, 2016) (Fig. 1). A standardized stratigraphy of the basin, on the basis of outcrop studies in the Andaman and Nicobar group of islands, exemplifies the vertical and lateral variation in litho_facies succession (Roy and Das Sharma, 1993; Pal et al., 2003) (Table 1). In this succession, the Andaman Flysch, a deep marine, silici_clastic sequence is increasingly gaining focus for hydrocarbon exploration in view of its distinguished presence as a major reservoir all along the island arc chain and in the adjoining fore-arc.

Published sedimentological studies on the Andaman Flysch on the main Andaman group of islands used the Bouma sequence and classical submarine fan model (Shanmugam and Moiola, 1988,1995; Shanmugam, 1997, 2006) to describe the flysch in South Andamans (Chakraborty and Pal, 2001; Pal et al., 2003; Mukhopadhyay et al.,2003 ; Bandopadhyay, 2012).). The objectives of the present study involves a) identification, classification and detailed bed by bed process interpretation of the constituent facies of the Andaman Flysch in South Andaman Islands and Great Nicobar islands, b) identification of commonality of constituent facies in South Andaman islands and Great Nicobar islands, and variations thereof, c) developing a depositional model for the Andaman Flysch in the southern part of the Andaman-Nicobar arc chain (Figs. 2 & 3).

Near vertical exposures in short stretches, exposed at several places on the arc chain was utilized for detailed bed by bed examination of the Flysch. Lithological logging of beds, bed thickness, bed boundary conditions, grain size, colour, sedimentary structures, were recorded mainly for their vertical stacking and to a certain extent for lateral variations.The sedimentary facies of the Andaman Flysch has been logged, in various positions in detail for the first time in Great Nicobar island, and compared with similar, logged facies at four outcrop positions South Andamans.

GEOLOGICAL BACKGROUND AND TECTONIC SETTING

Following the breakup of Gondwanaland, the swift northward flight of the Indian plate, its anticlockwise rotation and oblique subduction beneath the SE Asian plate led to the evolution of the Andaman basin (Roy,

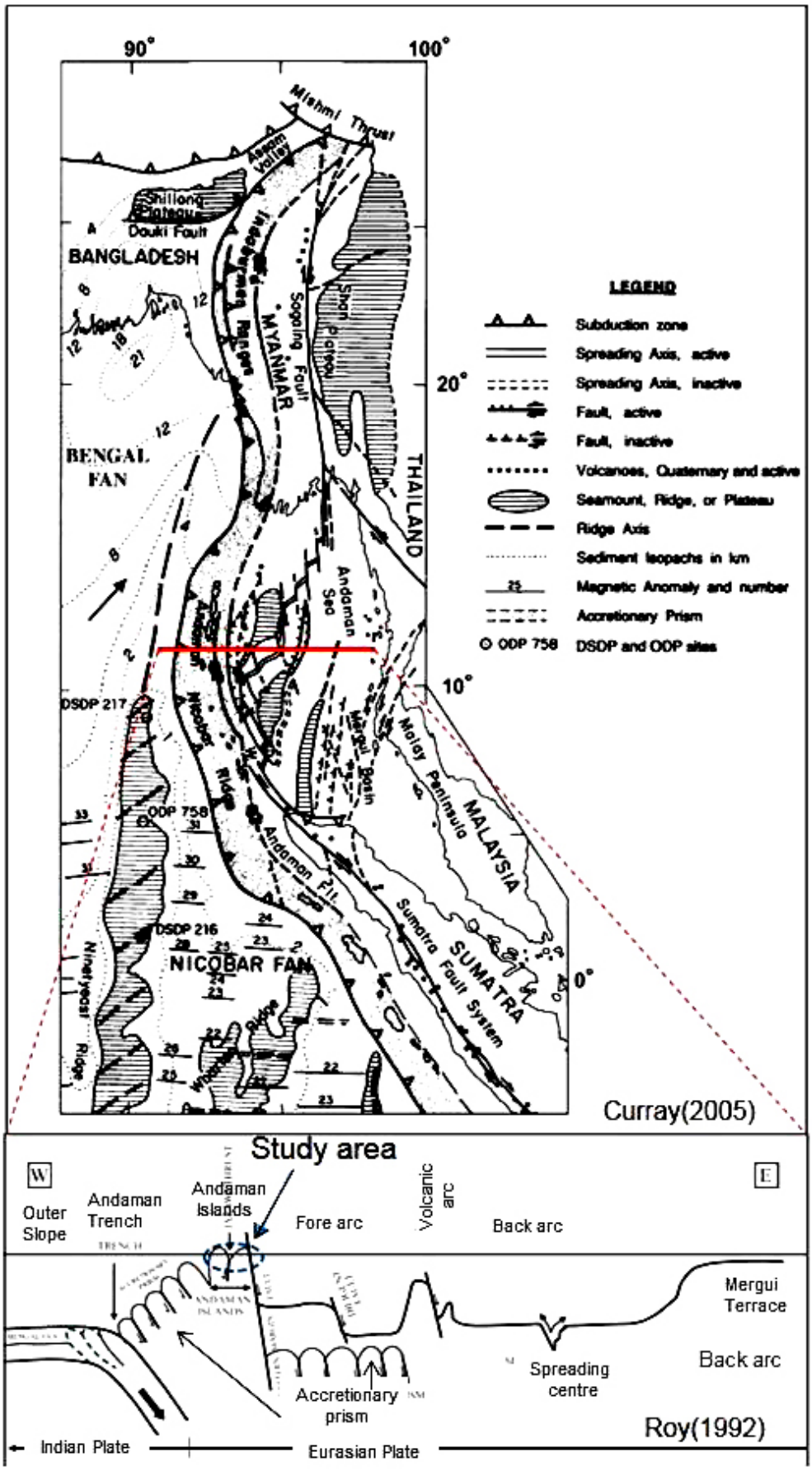

Fig. 1. Tectonic Map and Tectonic elements map of the Andaman sea region.

Table 1. Stratigraphy of Andaman basin (from outcrop data, altered after Roy,1983; Pal et al ,2003).

Stratigraphic unit	Age	Lithology
Unconformity	Pleistocene ro Recent	Beach, tidal falt deposits, mudstones, coral reefs, raised beaches.
	Pliocene	Foraminiferal mudstones, calcareous sandstones, siltstones.
Archipelago Group	Early-Mid Miocene	White nannoforam chalk,volcanic ash, calcareous sandstones, mudstones, siltstones.
Unconformity	Early Miocene	Calcareous sandstones, conglomerates, marl, siltstones
Unconformity		
Andaman flysch Group	Late Eocene to Oligocene	Massive to plane laminated, buff to light grey coloured fine to coarse grained sandstones with or without clay clast and concretions. Sand-shale alternations, shale and conglomerates.
Unconformity		
Mithakhari Group	Late Cretaceous to Paleocene	Darkgrey, compact shales.Coarse grained ophiolite derived greenish sandstones and polymictic conglomerates with extraneous ophiolite clasts, mud clasts, sandstone and limestone clasts.
Unconformity	Late Cretaceous	Pink radiolarian cherts, jaspers, quartzites, white limestones and Marbles.
Unconformity		
Ophiolite Group		Oceanic basement - Ophiolite suite

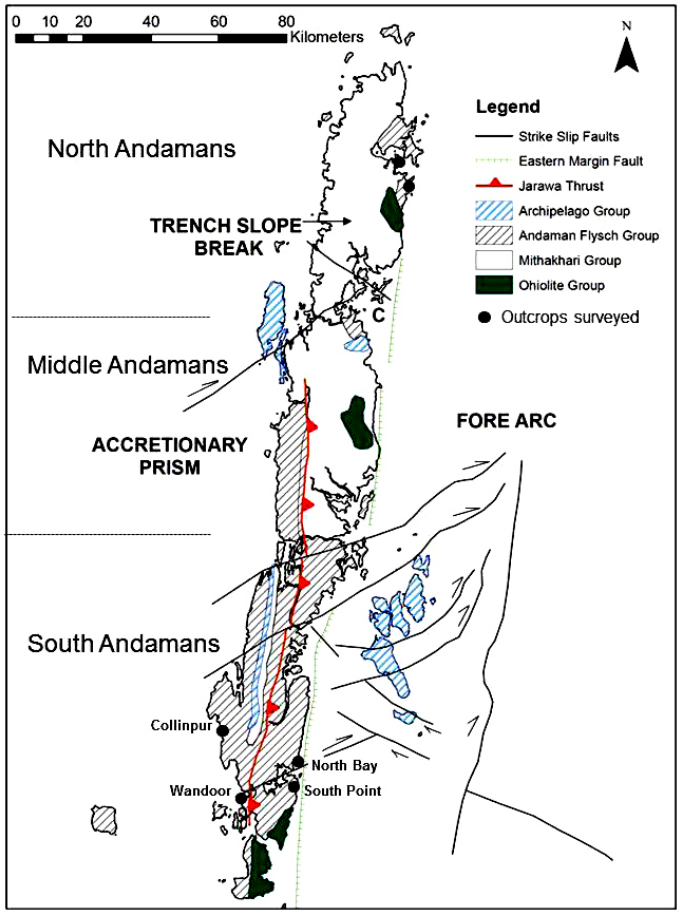

Fig. 2. Geological map of Andaman Islands with reffered outcrop positions.Map altered after,Roy and Chopra(1987), Roy and Das Sharma(1993) and Pal et al(2003).

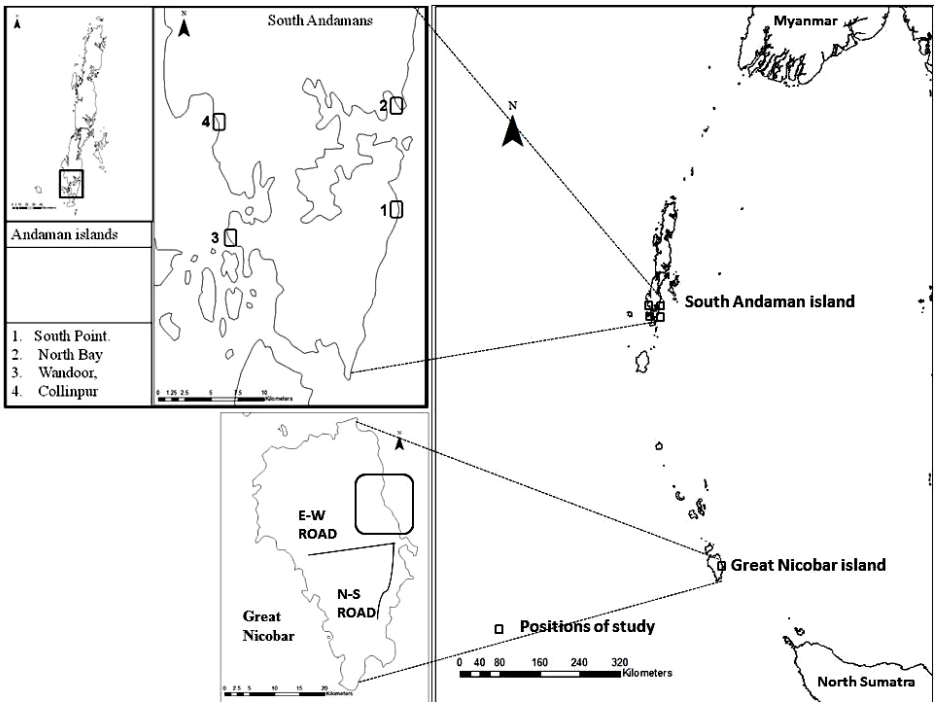

Fig. 3. Location map of study areas, South Andaman island and Great Nicobar islands.

1983, 1992; Roy and Das Sharma, 1993; Curray, 2005). Since late Cretaceous to present, each increment of subduction, witnessed scrapping of sediment floor of the Indian plate at the trench and its accretion to the SE Asian plate as under thrusted fold packets, one beneath the other, from east to west (Fig.1). This plate convergence led to outgrowth of the accretionary prism and formation of a narrow ridged fore-arc. By the late Oligocene time, step up in the rate of convergence resulted in the emergence of the Andaman Islands, basement uplift through thrusting and the development of a regional Pre-Neogene unconformity in the fore-arc (Roy, 1982; Mishra and Roy,1984; Roy and Banerjee, 2010). During the Neogene time, compressive forces due to plate interaction led to formation of NW-SE, SE-NW wrench faults, a trans tensional pull apart basin in the back -arc and the upliftment of the Ritchie's Archipelago in the Forearc and few islands in the Nicobar area (Roy, 1983, 1992; Roy and Chopra, 1987; Roy and Das Sharma, 1993; Curray, 2005).

In South Andamans, good exposures of the Andaman Flysch occurs in the east coast of Andamans, viz South Point ($11^0$39'0.06''N, $92^0$45'06''E) and North Bay($11^0$42'0.78''N, $79^0$45'28''E) and the west coast ie Collinpur and Wandoor /North Wandoor ($11^0$37'0.4''N, $92^0$36'13''E) in the present day intertidal zone. In the Great Nicobar island, the Flysch exposures have been noted in the eastern part of the island along road cuts along N-S ($06^0$57'N, $93^0$55'E) and E-W roads ($07^0$00'N, $93^0$54'E) (Fig. 3).

FACIES ANALYSIS OF ANDAMAN FLYSCH, SOUTH ANDAMAN AND GREAT NICOBAR ISLAND

From observations of outcrops, four broad sedimentary facies with associated sub facies were identified and classified for the Andaman Flysch in South Andamans, includes thick-bedded sandstone, heterolithics and thin-bedded tabular sandstone and shale (Figs. 4 & 5). These facies have been divided into sub-facies on the basis of finer characteristics. In Great Nicobar island, the first three named facies of the South Andamans, viz thick-bedded sandstone, heterolithics and shale are present (Figs. 6 & 7). Additionally conglomerates - gritty sandstone facies is also found in Great Nicobar (Figs.6 & 7). While, in South Andamans, the thick-bedded sandstone facies can be divided into massive sandstone, faintly laminated sandstone, planar laminated sandstone with mud clasts,, massive sandstone with random clasts and massive sandstone with slumps, in Great Nicobar, only the massive sandstone variety is present (Figs. 4,5,6,7, 8A,B,C,D, Table 2). In heterolithics, exhibiting sand-shale intercalations is common to both the islands. However, heterolithics in the South Andaman Island may exhibit convolute laminae. In shale facies, laminated shale is common in the two islands while convolute laminated shale is observed only in South Andamans. Matrix-supported conglomerates with extraclasts and green gritty sandstones are limited to Great Nicobar islands.

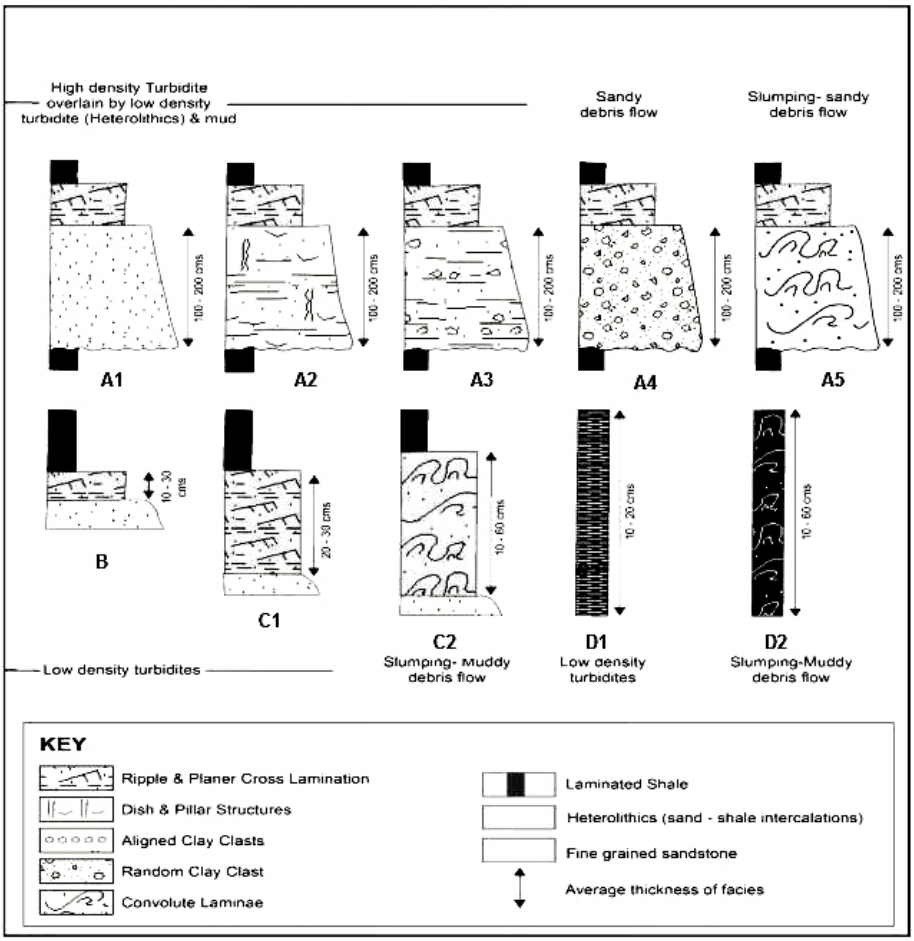

Fig. 4. Sedimentary Facies of Andaman Flysch, South Andaman island.

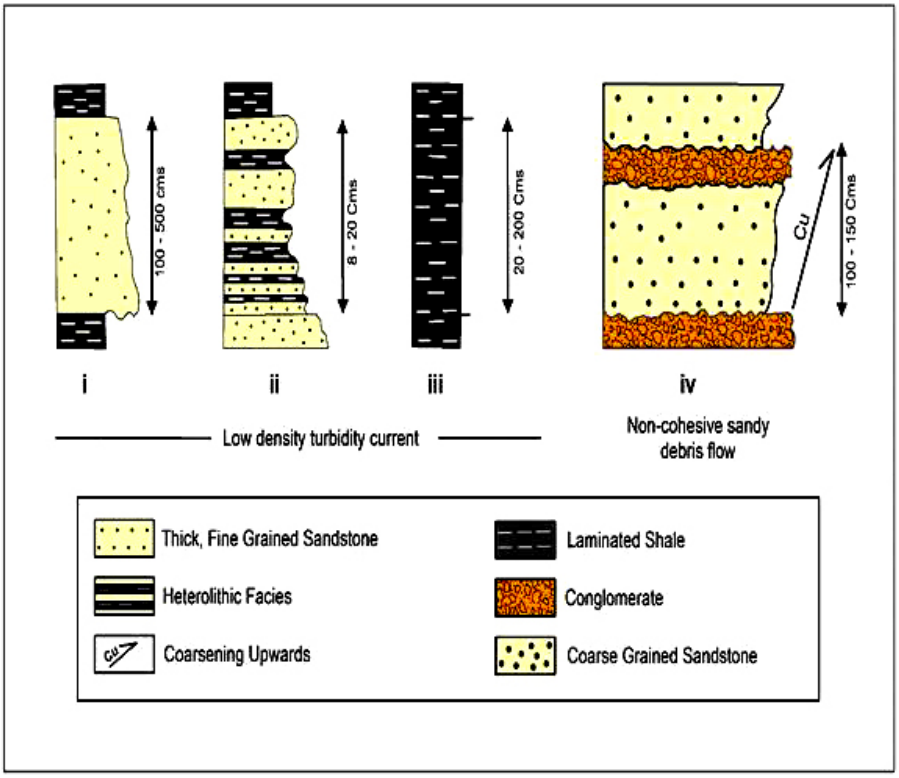

Fig 5. Sedimentary Facies of Andaman Flysch, Great Nicobar island.

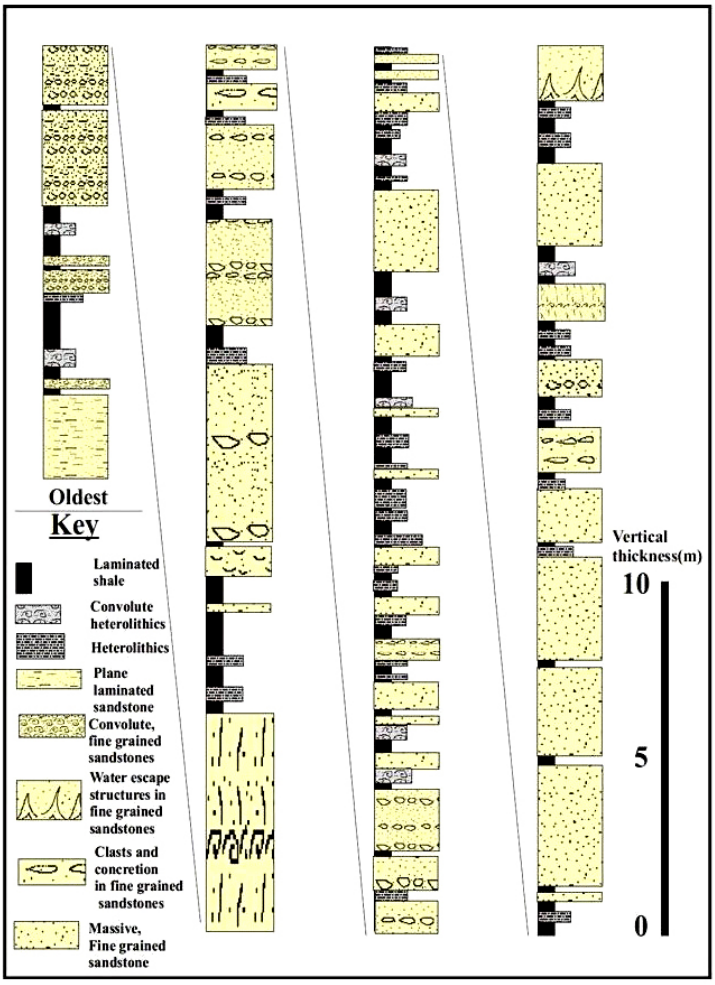

Fig. 6. Sedimentological Log of Andaman Flysch, South Point, South Andaman island.

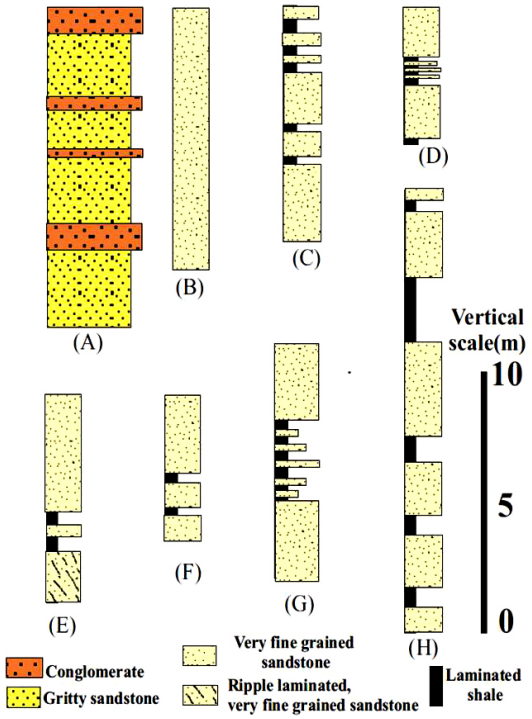

Fig. 7. Sedimentological Log of Andaman Flysch, Great Nicobar island.

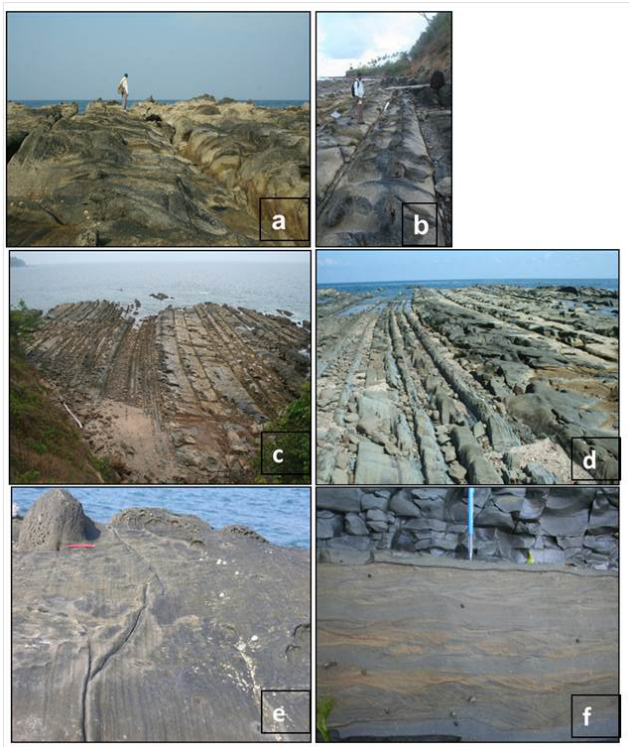

Fig. 8A. Photographs of sedimentary facies of Andaman Flysch, South Andaman island.a. Amalgamated beds of thick sandstone facies,SouthPoint. b. Clustered floating concretions in a thick sandstone facies,SouthPoint. c. Cluster of thick bedded sandstone facies on theleft and right portion of the Andaman flysch with intervening heterolithic facies in the centre of the photo.The former are attributed to channel facies in a deep water environment with the latter being tied to levees and overbank areas,SouthPoint. d. Vertically dipping Andaman flysch with jutting out sandstone units alternating with shale units, heterolithics (depressed portions in photo).Thick bedded sandstone facies are towards the right of the photograph,SouthPoint. e. Planer laminations passing through concretions in a thick bedded apparently massive sandstone facies,South Point. f. Heterolthic facies capped by shale facies, North Wandoor.

Fig. 8B. Photographs of sedimentary facies of Andaman Flysch, Great Nicobar island.a. 1.5 m ,massive, thick sandstone facies of Andaman flysch, N-S Road.Great Nicobar island. b. A metre thick heterolithic facies, overlain and underlain by thick sandstone facies. N-S Road. Great Nicobar island. c. Highly carbonaceous shale facies, a metre thick, in a faulted section, E-W Road, Great Nicobar island. d. Quartz pebbles in the Conglomerate-gritty sandstone, Joginder nagar, Great Nicobar island. e. Conglomerate-gritty sandstone facies.Joginder nagar, Great Nicobar island. f. Flute casts at the base of thick , massive sandstone facies.

The sedimentary facies constituents of the Andaman Flysch were differentiated on the basis of bed definition, bed contacts, bed relationships, sedimentary structures, sorting, grain size and bioturbation.

Facies1: Thick-Bedded Sandstones.

These are essentially fine-grained, light grey to khaki, well-sorted sandstones. The average and maximum thickness of the sandstone beds are 1.0 m and 5.5 m respectively. The beds may thin out laterally. Internally the beds exhibit no grading. The sandstone beds exhibits a sharp and undulating basal contact with most other facies. The soles of the sandstone beds are characterized by profuse prod and groove casts and flute casts. The width of the flute casts may be as big as ~25 mm and relief of the flute casts vary between a few mm and a few cm. Dish and pillar structures have been observed in a few sandstone beds in South Andamans. The upper contact of the facies with other facies is usually gradational with heterolithics. It is divided into four or five (see below) sub facies, viz. massive sandstone, faintly laminated sandstone, planar laminated sandstone with mud clasts, massive sandstone with random mud clasts and massive sandstone with slumps. Only the massive sandstone sub facies have been observed in both the South Andaman and the Great Nicobar islands. Bioturbation was observed in some of the sandstones.

These sandstones are very fine – fine grained, moderate to well sorted sandstone. They are dirty (matrix rich 20-30%) sandstones of lithic wacke composition. The quartz is mostly monocrystalline (monocrystalline: polycrystalline=80:20), having undulose extinction. The rocks contain plagioclase and a host of rock fragments like metamorphic rock fragments, orthoquartzites, chert, plenty of opaques (15% of rock composition) and a few bent muscovite flakes. The feldspars are in an advanced stage of degradation to sericite. The composition of the sandstone is typical of subaqueous gravity flow deposits.

Sub-facies 1A: Massive Sandstone

Massive, structure less, fine-grained sandstone with moderate sorting, no apparent grading to occasional grading, scoured base and gradational top with abundant dish and pillar structures are the characteristic features of the sub-facies in South Andamans. Average thickness of the sandstone beds is around 1 m, while several stacked beds of 5m have also been observed in South Andamans. Dewatering structures like dish and pillar structures and soft sediment deformation structures are commonly observed. Slump folds, water escape structures; convolute beds are present at recurrent intervals in South point, South Andamans.

In Great Nicobar, this is the most frequently occurring facies. Bed sizes commonly runs from an m to 4-5 m. It has an orange hue when it is weathered by water, unlike the khaki appearance of the fine grained sandstone in South Andamans. It is usually massive, devoid of perceptible sedimentary structures within the bed. Distinct scour marks, prod marks, skip marks, bounce marks at the base of the bed are conspicuous. Occasional tabular cross bedding has been observed with clay and dark minerals marking the fore sets. Bed top is gradational to planar with the overlying heterolithics facies or shale facies. The scoured bed base occasionally overlies a shale facies of the earlier depositional cycle. The sandstone beds are, very fine-grained, grading to siltstone in Great Nicobar.

Interpretations: Deposition of these massive sandstones represents rapid dumping of sand due to flow unsteadiness in collapsing single surge currents (Lowe, 1982). These sediment gravity flows are attributed to high density turbidity currents with rapid fallout from sediment suspensions (Walker, 1978; Lowe, 1982). Rapid deposition of such massive sands due to non-uniformity in prolonged quasi-steady high density turbidity currents have also been advocated for such deposits (Kneller and Branney, 1995). The dish and pillar structures are attributed to liquefaction in a fluidized sediment flow and corroborate rapid sediment deposition.

Sub-facies 1B: Faintly Laminated Sandstone

These are essentially very fine- to fine-grained, occasionally medium-grained, light grey to khaki, poorly-sorted, fine-grained sandstones with a thickness range of 1-7 m. They have an undulating basal contact with underlying shale the upper contact usually with sand–shale intercalation is gradational. The thickness of the sandstone beds frequently decreases laterally. These sandstones may exhibit massive nature to crude or faint planar lamination. Dish structures and pipes have been observed in a few sandstone beds. The lower contact is erosional and is often riddled with prod, flute and groove casts. This sub-facies is present only in South Andamans. They are very similar to facies 1A excepting that indistinct, faint planar laminae.

Interpretations: These thick-bedded facies represent rapid deposition from a waning sediment gravity flow/ high density turbidity currents (Lowe, 1982; Hadlari, 2009). Erosive bases of the beds and planar laminae indicate turbulence (traction deposits).The added lateral continuity of these beds, lenticular geometry along with described attributes promote mid fan depositional lobe setting for this facies. The erosive bases of these facies marked by flutes and tool marks.

Sub-facies 1C: Planar Laminated Sandstone with mud Clasts

With average thickness of 1-2 m, this fine-grained facies possess planar laminae (similarity with sub facies 1B), with aligned mud clasts of various shapes, sizes, orientations being distinct. The mud clasts, often covered by concretions, are oriented parallel to bedding plane within the facies.. The diameter of the rounded clasts ranges from 30 cm to 50 cm. The elongated clasts are usually oriented parallel to the lamination and may be 30 cm long. The sandstone is fine to medium-grained and is moderately sorted. Unidirectional flute marks is distinct at the base of sandstones. The flutes are up to 10 cm in length and have a width up to 7.5cms on an average.

Interpretations: Thick-bedded sandstone exhibiting planar laminae and aligned clasts, with an erosional base with flute marks at base is attributed to deposition from high density turbidity currents (Lowe, 1982). Several of these thick sandstone facies, bunched together, exceeding several metres may be related to amalgamation of beds because of recurrent high-density turbidity current flow. The continuation of planar laminae through the concretions, indicate their secondary diagenetic origin.

Sub-facies 1D: Massive Sandstone with Random Mud Clasts

Fine-grained massive sandstone with conspicuous floating mudclasts defines this sub- facies. The clasts, rounded in nature vary from mm scale to as much as 10 cm in diameter. This facies is abundant in South Andamans. Usually 1 m in thickness, this facies show vertical repetitions in South Andamans.

Interpretations: Cohesive debris flow is implied for beds with random floating clasts. The large clay clasts are assumed to be supported by the buoyancy and cohesiveness of the clay-water matrix. The deposition involves a sudden freezing (laminar flow) (Lowe, 1982). The presence of floating clasts in matrix-supported sandstone is indicative of matrix strength which is the principal particle support mechanism in debris flows (Hampton, 1972; Middleton and Hampton, 1973; Shanmugam and Moiola, 1995). The failure of the floating clasts to settle to the base is also evidence for flow strength (Shanmugam and Moiola, 1995).This facies has been interpreted as products of sandy debris flow. Presence of random clasts in both fine and coarse-grained sandstone along with or without mud clasts has been a striking feature of the Andaman Flysch. Occurrence of clasts in sandstone either in abundance, moderation and rarity is unique to this facies.

Sub-facies 1E: Massive Sandstone with Slumps

Light grey, fine-grained, massive, with no distinct sorting, this sub-facies is characterized by convolute laminae. The sub-facies with distinct convolute laminae appear in periodic intervals in a vertical stack of Andaman Flysch in South Andamans. The convolute laminae are sometimes restricted to part of the usually, m- scale beds. The convolute laminae are characterized by a relatively tight antiformal part and broad sagged (synformal) part. The convolutions are often capped by and underlain by undeformed portions of the massive sandstone facies. The facies is often very variable in thickness 1-10 m.

Interpretations: This facies is attributed to debris flows as a result of slumping in a sandy debris flow (Shanmugam and Moiola, 1995). The diagnostic feature of this facies is contorted and convolute bedding; internal deformation in the form of recumbent and asymmetric folding, with undisturbed facies above and below and occasional sigmoidal imbricate slices (i.e., duplexes,) (Shanmugam and Moiola, 1995). The thicker facies units are attributed to massive, amalgamated units.

Facies 2: Heterolithic Facies

This facies exhibits planar- and climbing ripple-laminated sandstone of mm- to cm-scale, intercalated with shale of similar thickness. The facies occurs above the thick bedded sandstone facies with a planar contact. They equate to the Tc division of Bouma (1962) with ripple or wavy laminae in fine-grained sandstone (Bouma, 1962). Upwards, this facies gradationally passes into pelagic or hemi pelagic shale. A fining upward trend, with well-developed current ripples, climbing ripples and planar laminations is a definitive aspect of this facies. A series of alternating, cm-scale, fine sand and shale intercalations define this common facies of the Flysch in both South Andamans as well as in the Great Nicobar outcrops. Climbing ripple cross lamination has been frequently observed in many beds in very fine-grained sandstone, at South point, South Andamans.

Flaser, wavy and lenticular bedding are well observed in interaction of fine sands and shales in Wandoor, Wandoor north and Collinpur in South Andamans.

Sub-facies 2a: Sand-silt / Shale Intercalations with Planar and Ripple Laminae

Thin cm-scale alternations between sandstone and shale are one of the most common facies at different outcrops of South Andamans. The facies is overall fining upward in nature. The sandstone beds exhibits sheet

geometry. The fine-grained sandstones exhibit transitions from planar laminae to ripple laminae. Climbing ripple laminae are often observed **(Fig. 8C).** Each facies unit has mm-cm scale sand shale units. The shale unit is 5-10 cm in thickness and each sand unit varies from 8-20 cm with facies.

Unlike South Andamans, the heterolithics comprise cm-scale, thin, sand shale alternations in Great Nicobar Island. Facies thickness varies from 50 cm to 3 m. In Great Nicobar, the shale is organic rich and carbonaceous in nature. Average thickness of this facies varies from 30-50 cm, with each individual lamina of sand and shale being 5-10 cm each. They often have a diffused contact with the overlying shale facies and a diffused to sharp contact with underlying coarse-grained massive/ clay clast filled sandstone.

Interpretations: The facies represents waning energy conditions in a turbid flow regime. Plane parallel laminations with occasional ripples are attributed to traction currents with suspension, suggesting fluctuating energy at the end of each flow or cycle. The planar laminations capped by ripple laminations can be classified as Tb and Tc divisions of Bouma (1962).The climbing ripple drift is attributed to a combination of traction (ripple creation) and rapid fallout of sediment from suspension (Middleton and Hampton, 1973; Lowe, 1982; Mulder and Alexander, 2001). Some ripples are draped with mud layers with fluctuating energy conditions. Shanmugam (2006) considered these climbing ripples, as a product of bottom current reworking. Parallel laminated sandstones record the upper flow regime beds that formed during passage of the flow, the ripple cross lamination recording flow deceleration experienced in the tail of the flow (Hadlari et al., 2009).

Sub-facies 2b. Sand-shale Intercalations with Convolute Laminae

The facies comprising alternations of sandstone and shale is marked by convolute laminae, recumbent folding, tight isoclinal folds, and asymmetric folding. The sandstone beds in this facies are fine-grained, up to 10 cm thick and are planar laminated. Flame structures, distorted, contorted facies are common. Each shale and sandstone unit in the facies varies from mm to cm scale (between 5 and 20 cms in thickness, averaging 8cm). Dish and pillar structures are common. Loading of sand into underlying shale is characteristic in this facies in Collinpur, South Andamans. The imbricate slices of 10-20 cm, sand –shale intercalations are observed in this facies.

Interpretations: Various soft sediment deformation features like slumps, flame structures, dish and pillar structures are the hall mark of this heterolithic facies. These heterolithics comprising of thin alternations of fine-grained sandstone and shale imply a quiet deposition per se, which have been subjected to dewatering. This facies is attributed to sedimentary slumping in a muddy regime.

Fig. 8C. Photographs of penecontempraneous deformation structures in Andaman Flysch, South Andaman island. A. Wavy and convolute lamination in Heterolithics, SouthPoint. b. Burst out structures in an inverted sequence in heterolithics, NorthWandoor. c.Load casts of sandstone within shale facies, Collinpur. d. Convolute facies with sandstone balls and load casts

Facies 3. Shale

This facies comprises dark grey shale with horizontal silt laminae. Bedding contact is diffused with the heterolithic facies below and is erosive at the top. The massive sandstone facies usually overlie this facies. These shales are carbonaceous in the outcrops of Great Nicobar islands.

Sub-facies 3A. Laminated Shale

The facies is characterized by dark grey to black massive to planar laminated shale with occasional silt inter beds. Thickness of the shale bed ranges from a few cm to a few m, with no hint of bioturbation. The facies is marked by a planar basal contact with underlying sand-shale alternations and an erosive top, overlain by younger sandy channel facies. The thickness of the facies usually varies from 15 cm to 2 m. In the top part of the South point section, South Andamans, a 6-10 m-thick black shale bed serves as a marker bed. In Great Nicobar, they are found both along the North-South Road and the East west road, the only two roads in the Great Nicobar Island and carbonaceous in nature.

Interpretations: This facies has been attributed to waning energy conditions with operating thin traction and heavy suspension sedimentation in a low density turbidity flow regime. Plane laminated, jet black shale, represent pelagic to hemi pelagic settling of mud in a deep water environment (Shanmugam and Moiola, 1995). In places, the plane laminated shale is entrenched between the coarse massive sands, attributed to waning of energy at the end of each cycle with suspension settling processes acting on it.

Sub-facies 3B. Shale with Convolute Laminations

In South Point section of South Andamans, a highly contorted two m- thick shale bed with an underlying, 50-60 cm scale convolute sand-shale alternations were observed. Convolute laminae are well entrenched in Collinpur and Wandoor in South Andamans in thin, cm-scale intercalations of sand and shale. The size of the beds varies from few cm to 1 m.

Interpretations: The shale is pelagic to hemi pelagic in nature. This facies has been attributed to sedimentary slumping in a muddy system and is a part of the debris flow process (Shanmugam and Moiola, 1995). The presence of massive to plane laminated beds above and below the convolute beds indicates products of muddy slumps.

Facies 4: Thin Bedded Sandstones

The facies is characterized by tabular, blocky, sheet-like sandstone beds consisting of medium- to coarse-grained moderately sorted sandstones. The sandstone beds are 10-30 cm thick on an average. The sandstone exhibits faint to distinct planar laminae near the base, overlain by ripple laminae. These beds usually have sharp basal contacts, occasionally exhibits convolute laminae internally. The soles of the sandstone beds exhibit prod and groove casts. The facies gradationally passes upward to sand-shale alternation/ heterolithic facies.

Interpretations: Traction related planar and ripple laminae are attributed to turbidity currents (Bouma, 1962; Middleton and Hampton, 1976; Lowe, 1982; Mutti, 1992; Amy et al., 2005). The prod and groove casts at the soles of the sandstone beds represents erosional nature of the currents at the initial stage (Shanmugam, 2006). This facies represents products of a low density sediment gravity flow or a low density sediment gravity flow (Hadlari et al., 2009) equated with the deposition by traction and fallout processes associated with various stages of sedimentation of waning low density turbidity currents (Mutti,1992).

Facies 5: Conglomerates to Gritty Sandstone

Quartz pebbles, well rounded sandstone clasts, mudstone clasts in matrix -supported conglomerates, underlain by coarse gritty sandstone characterize this facies at Vijaynagar/ Joginder nagar areas of Great Nicobar Island. Coarse gritty sandstone with pellets of well-rounded quartz clast, are found in a coarsening upward cycle of gritty sandstone overlain by coarse conglomerates. The thickness of this facies ranges from 1 to 1.5 m. The gritty sandstones occasionally have a greenish hue.

Interpretations: These conglomerates/gritty sandstones are attributed to non-cohesive debris flow, rapidly deposited by frictional freezing (Pickering et al., 1986). Erosive bases suggest a channel environment; chaotic layers in clast-supported conglomerates suggest slump deposits. The significant presence of these conglomerates at one place represents the erosive power of the carrying current with implied slope and proximity to provenance. These conglomerates and coarse grained sandstones possibly represents channel lag deposits or a highly proximal sediment source in a slope setting.

DISCUSSION

As compared to existing literature on South Andaman islands, data on the Nicobar islands are few (Rink, 1847; Rink and Stoliczka, 1870; Oldham,1885; Ray,1982; Karunakaran et al., 1975; Babu Madhavan, 1997). The first reference to geology of Nicobar Islands came through its work on stratigraphic superposition as Brown Coal Formation (equivalent to Brown Coal formation of Sumatra), igneous rocks and Older Alluvium respectively (Rink, 1847; Hochsetter, 1869) respectively in order of succession. The close similarity between the

Brown Coal Formation of Rink (1847) and sandstone shale alternations around Port Blair, South Andamans (known as Andaman Flysch) emerged from studies by Rink and Stoliczka (1870). The stratigraphy and Geology of the Nicobar Island, by Karunakaran et al. (1968, 1975), Ray (1982) placed the Andaman Flysch of Eocene-Oligocene age, underlain by the Mithakhari Group and overlain by the Archipelago Group. They recognized the presence of huge thickness of Andaman Flysch right from North Andaman Islands to Galathea Bay, the southernmost part of the Nicobar Island.

Submarine sediment density flows of the Andaman Flysch were studied till date through detailed observations by a number of workers with emphasis on specific positions (Chakraborty and Pal, 2001; Pal et al., 2003; Mukhopadhyay et al., 2003; Bandopadhyay, 2012).The Flysch facies have not been addressed by earlier workers in terms of connectivity and to this detail, as addressed here. The difficulty in tracing facies architecture over long distances, complex tectonics and remoteness of outcrop positions have all served as hindrances to the understanding of the facies architecture of the Andaman Flysch. Yet, bed by bed facies presence in a vertical sequence, spread laterally over several outcrop positions have helped in understanding the spread of facies architecture and the flow processes. The Andaman Flysch is present all along the arc chain as observed along outcrops on the trench slope break or the Andaman Islands. The Andaman Flysch is recorded all along the arc chain, right from North Andamans to the Great Nicobar in the south (Roy et al., 2011). The grain size of all the constituents facies of the Andaman Flysch decreases from very coarse grained (North Andamans) to coarse-medium grained (Middle Andamans) to fine grained (South Andamans), to very fine grained –silt grade in Great Nicobar (Roy and Banerjee, 2010; Roy et al., 2011). The grain-size variation suggests of an open marine fan system running longitudinally from North to South along the fore-arc and subduction zone. The Flysch is a sand rich clastic system with coarser clastics in the North and progressively finer equivalents in the southern part of the arc chain. Six arc-parallel outcrop positions of Andaman Flysch on the trench slope break have been subject to detailed process sedimentology. Five sedimentary facies, identified from the outcrops from the South Andamans and the Great Nicobar Island has entailed conceptualisation of the depositional model of the Andaman Flysch in the southern part of the arc trench system.

The present study recognizes four broad facies of Andaman Flysch, in the South Andaman Islands viz thick bedded sandstones, heterolithics, shale and thin tabular sandstone (Table 2). The first three have also been observed in the Nicobar Islands additionally with a conglomerate-gritty sandstone facies. Collectively, the five sedimentary facies, identified from the outcrops from the South Andamans and the Great Nicobar Island highlights the depositional domains of the Andaman Flysch, in the southern part of the Andaman-Nicobar arc trench system. The gritty sandstone-conglomerate facies is endemic to Great Nicobar only, the rest being common. Shale in Great Nicobar is highly carbonaceous, which is not noticeable in counterparts in South Andamans. Using field classification (Pickering et al., 1986; Ghibaudo, 1992) of subaqueous gravity flow deposits, these five facies can be defined more easily. The thick massive sand facies, which is occasionally cross-stratified at the bottom part equates to mS and xS codes of Ghibaudo (1992) and disorganized sands (B1) and organized sands (B2) respectively of Pickering et al. (1986). The heterolithic facies behaves as graded sandy mud (gySM) of Ghibaudo (1986) and organized, sand mud couplets (C2) of Pickering et al.(1986). The laminated shale qualifies as laminated to graded mud (lgM) of Ghibaudo (1992) and organized muds and clays E2 of Pickering et al. (1986). Convolute facies (thick sandstone, heterolithics) are taken care of F2 chaotic deposits (Pickering et al., 1986). Conglomerates and pebbly sands classify as disorganized gravels and pebbly sands A1 of Ghibaudo (1992) and as mGyS , massive gravelly sand of Pickering et al. (1986). Thin bedded tabular sands (<30cms in thickness) could not be well defined by either classification.

The thick, massive sandstone of South Andamans has inherent, basic similarity with the same facies in Great Nicobar. At both locations, they are poorly sorted, both have abundant clay matrix in them. Both have scoured bases with flute marks, groove marks and a gradational top with the heterolithics and both having similar bed thickness. These thick massive sandstones (sub facies 1a) are attributed to waning sediment gravity flow with rapid suspension fallout from a sizable volume of sediments, with an implied long distance transport (Stow and Johansson, 2000) .They represent 90% of the facies of Andaman flysch in Great Nicobar in terms of appearance. The other sub-facies in the same class of thick sandstone facies in South Andamans, namely faintly laminated sandstone, planar laminated sandstone with mud clasts, massive sandstone with random clasts and massive sandstone with slumps, have not been observed from the outcrops of Andaman Flysch in the Nicobar section. While the first two facies have been thought of being products of high density turbidity current (Lowe, 1982), the next two have been visualized to be products of cohesive debris flows and slumping. Usual sedimentary cycles comprise thick bedded sands, overlain by heterolithic and shale. The cycles are repetitive with cycle size usually of am in thickness to as much as 5-12 m in a few cases, with thicknesses exceeding 1m attributed to bed amalgamation. The base of each cycle is scoured with flute marks, grove marks and the top of each cycle is scoured again with the base of a younger cycle.

The heterolithic facies is the distinct facies in both South Andamans as well as Nicobar section. Its

Table 2. Tabulated facies of Andaman Flysch.

South Andamans					
Facies	**Sub facies**	**Average Vertical Facies Thickness(cm)**	**Sedimentary Structures**	**Inferred Depositional Process**	**Remarks**
Thick bedded sandstone	Massive sandstone	100-200	flute marks,groove marks,	high density turbidity current	Present in Great Nicobar.
	Faintly laminated sandstone	100-200	faint planer laminations, flute marks,	high density turbidity current	
	Planar laminated sandstone with mud clasts and concretions	100-200	planer laminations,flute marks,	high density turbidity current	
	Massive sandstone with random mud clasts	100-200	flute marks,groove marks,	sandy debris flow	
	Massive sandstone with slumps.	100-200	convolute laminations	slumping- sandy debris flow	
Heterolithics	Sand-shale intercalations with planar and ripple laminae	20-30	Planer and climbing ripple laminae	Low density turbidity current	Present in Great Nicobar.
	Sand-shale intercalations with convolute laminae	10-60	convolute laminations	slumping- muddy debris flow	
Shale	Laminated shale		planer laminations,	Low density turbidity current	Present in Great Nicobar.
	Shale with convolute laminations		convolute laminations	slumping- muddy debris flow	
Thin bedded sandstones		10-30	planer laminations,	Low density turbidity current	

Great Nicobar					
Facies	**Sub Facies**	**Average Vertical Facies Thickness (cm)**	**Sedimentary Structures**	**Inferred Depositional Process**	**Remarks**
Thick bedded sandstone	Massive sandstone	100-500	flute marks,groove marks,	Low density turbidity current	Present in South Andamans.
Heterolithics	Sand-shale intercalations with planar and ripple laminae	8-20	Planer and climbing ripple laminae	Low density turbidity current	Present in South Andamans.
Shale	Laminated shale	20-200	planer laminations,	Low density turbidity current	Present in South Andamans.
Conglomerates -Gritty sandstones		100-150		Non cohesive debris flow	

distinguished presence just above the massive sandstone facies, planar lamination (usually) are attributed to bottom currents in a turbidity flow regime. They represent distal facies in a basin floor regime due to traction and fallout processes (Mutti et al., 1999). Heterolithics with convolute laminations flame structures, water escape features are attributed to fluidization- liquefaction events of unconsolidated sediments (Kundu et al., 2011, Roy and Banerjee, 2016). It represents slumping in a muddy regime linked to tsunamis or due to an earthquake (Shiki, 2000). Convolute heterolithic sub-facies occur at cyclic intervals of 15th-30 th bed in South Andaman outcrops. Yet this sub-facies has not been observed in the Nicobar outcrops of Andaman Flysch.

The genesis of shale facies is linked to hyperpycnal flows to dilute turbidity flows and termed as pelagics and hemiplegic's when deposited in a deep water regime. Thick shale facies are attributed to terminal facies of a turbidity current regime or parts of a levee regime in a channel-levee combine in deep water settings. Pene contemporaneous deformational features have been observed with periodicity in facies of Andaman Flysch in south Andamans. The same was not observed in the Great Nicobar. Soft sediment deformation features like slumps structure/folds, convolute bedding or lamination, load and flame structures, pseudo nodules/ball and pillow structures and dish and pillar structures have been observed with periodic regularity in these facies and independent of facies specifics (Roy and Banerjee, 2016).

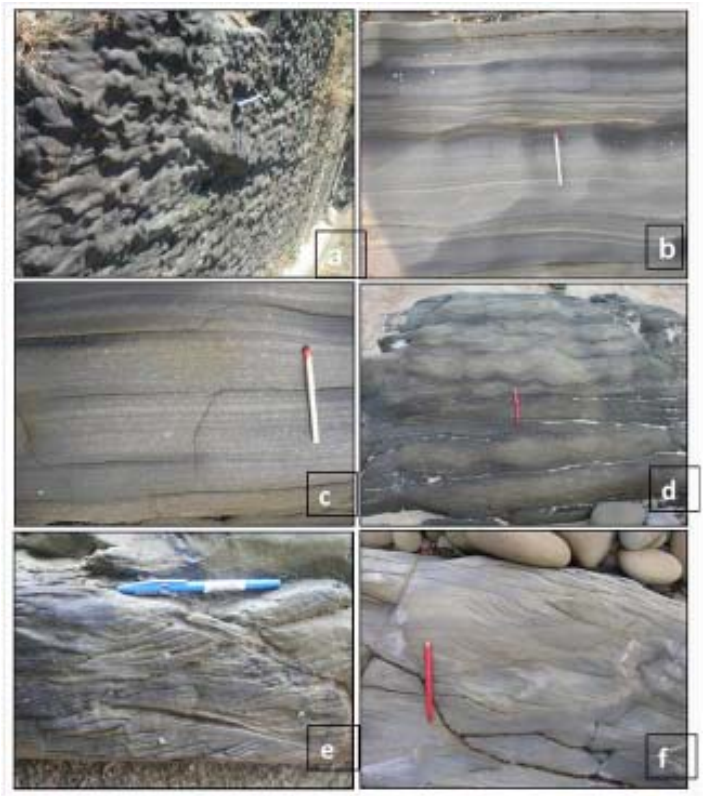

Fig. 8D. Photographs of sedimentary structures of Andaman Flysch, South Andaman island. a. Flute marks at the base of thick sandstone facies,SouthPoint. b.Planer and Ripple cross lamination in heterolithic facies,SouthPoint. c.Planer lamination in heterolithic facies, SouthPoint. d. Planar and wavy laminationin heterolitic facies, Wandoor. e.Stacked, symmetrical, wave ripple cross lamination attributed to oscillatory flow in afine grained thick sandstone facies due to possible storm events, Wandoor. f. Climbing ripple lamination in heterolithic facies, SouthPoint.

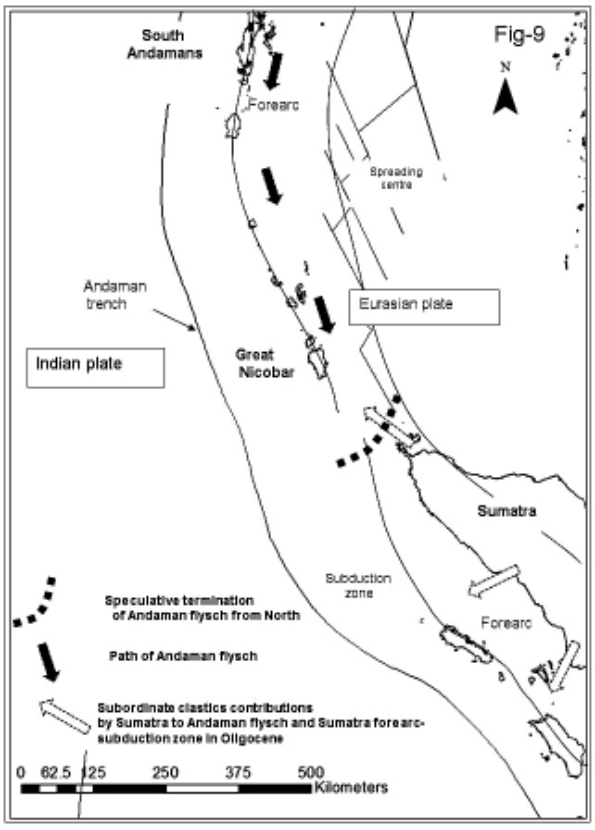

Fig. 9. Conceptual depositional model of Andaman Flysch between SouthAndaman and Great Nicobar island.

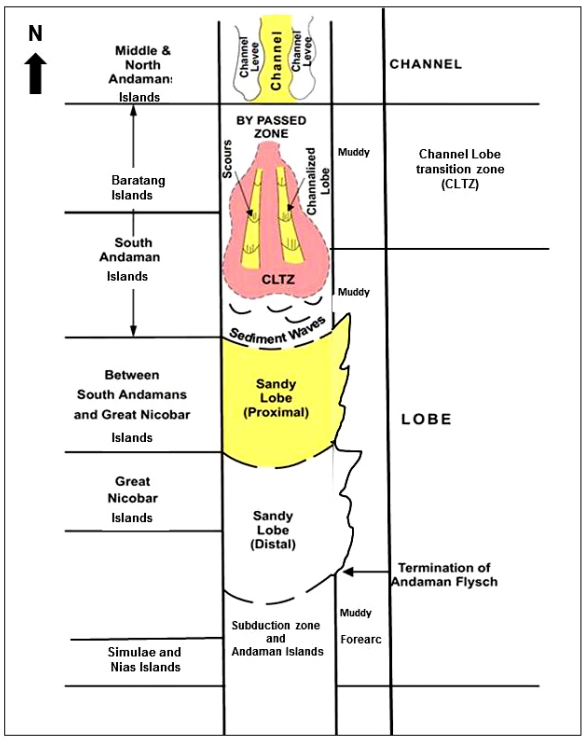

Fig. 10. Spatial Distribution of Channel, channel lobe transition complex and lobes of Andaman Flysch.

Syn depositional deformation structures like flame structures, ball and pillow structures, burst out structures, convolute lamination, have been observed in recurrent intervals in the thick sandstone, heterolithic and shale facies every 15-30 m apart, particularly in South point and Flame and ball and pillow structures were particularly conspicuous in Collinpur (Fig. 8d). The periodicity of these syn depositional deformation features in practically 30 m apart in South Point, South Andamans are indicative of seismic activity close to the plate boundary affecting the deposition, attributed to slumps in a debris flow process due to earthquakes and Tsunamis (Shanmugam, 2006). The Andaman Flysch outcrops being positioned on a rising subduction complex in proximity to convergence of two oceanic plate boundaries (Roy, 1992; Roy and Das Sharma, 1993), are in a highly tectonic active zone. The outcrops in South Andamans are very close to the arc parallel, N-S trending Jarawa thrust. Frequent periodic earthquakes in the region are the possible cause of the convolute facies manifested by syn sedimentary deformation structures. Hence it is proposed to attribute them as seismites (Van Loon, 2002; Bose et al., 1997).

The vertical facies organization of the Andaman Flysch in both South Andaman Islands and the Nicobar islands show remarkable similarity in terms of vertical sedimentary cycle repeatability. Each Andaman Flysch cycle begins with massive sandstone with an erosive base, overlain by heterolithic facies which is capped by the pelagic to hemi pelagic shale. The entire cycle is usually 1-2m. The above standard sedimentary, fining upward cycle is indicative of high density turbidity currents (massive sandstone facies) overlain by heterolithics and shale (low density turbidites). Periodic presence of massive sand stone with random clasts and contorted beds of massive sands, heterolithics and shale brings in a change of process interpretation to debris flows and slumping respectively which interrupt the turbidity flow process.

Ancient channel deposits can either be erosional, depositional or erosional-depositional (Nomark, 1970; Mutti and Nomark, 1987). Most sandstone beds in South Andamans are sheet-like. Variability of bed thickness though observed, is not translated to facies pinch outs. Series of fining upward sedimentary cycles are observed with planar erosive bed bases. The coarse Flysch equivalents, observed in North Andamans, are envisaged as proximal deposits, on the basis of the evidence of the architectural elements. From spatial position of the Andaman Flysch in South Andamans, it is envisaged as deposited far away from provenance. A distal end of channel lobe transition zone (CLTZ, Bouma, 1985; Wynn, 2002) is envisaged for the South Andaman area (Figs. 9 & 10). Bunching of massive, thick sand rich facies interspersed with shale rich zones are attributed as channel –levees at the top of a prograding lobe complex which has cut the top part of the lobe. In Great Nicobar outcrops of the Andaman Flysch, of a distal sandy lobe **(Figs. 9 & 10)** marked by facies, grading from very fine grained sandstones to siltstones to shales.

CONCLUSIONS

i) Five broad sedimentary facies in four outcrop sections of the Andaman Flysch in South Andamans, and Great Nicobar islands promote a case of subaqueous gravity flows. The Andaman Flysch in South Andaman is fine-grained with four major facies with their sub-facies, the broad facies are: thick sandstones (amalgamated beds), thin tabular sandstones, heterolithic facies and the shale facies. In great Nicobar Island, within the Andaman Flysch exposures, the first three mentioned facies of South Andaman Island along with a conglomerate-gritty sandstones facies makes distinguished presence.

ii) Thick sandstones with planar laminations and thick massive sandstones with/without aligned clasts are interpreted to be deposited from high density turbidity currents. Thick sandstones with random are attributed to sandy debris flow. Thin tabular sandstones and plane and ripple laminated, heterolithic facies are interpreted due to low density turbidity currents. The laminated shale facies are hemiplegic's in a deep water realm. The Conglomerates are attributed to non-cohesive debris flows.

iii) Vertical stacking of preponderance of sand rich facies, with intervening clay rich facies in the South Andamans with and fining upward cycles, erosive bases, and occasional pinching out suggests a progradation of lobe of a sand-rich deep water clastic deposit on a basin floor, separated by levees. The Andaman Flysch in South Andamans is envisaged as a product of lobe progradation within a channel lobe transition zone (CLTZ) while the equivalents in Great Nicobar represent distal submarine lobes. Sheet like geometry, non-erosive bed bases, lack of pinching out of units support lobe presence in both the areas with some scoured beds in South Andamans attributed to CLTZ.

iv) Thick sandstones (amalgamated beds) and heterolithic facies of Andaman Flysch present in both South Andaman and Great Nicobar Island show a variation in grain size. In the former it is essentially fine grained, while in the latter it is grading from very fine to silt grade. This is attributed to an envisaged, north-south, arc-parallel progression of the Andaman Flysch along the eastern edge of the islands (trench slope break) and the fore arc.

References

Amy, L.A., Talling, P.J., Peakall, J., Wynn, R.B., Arzola,Thynne. (2005). Bed geometry used to test recognition criteria of turbidites and (sandy) debrites.Sedimentary Geology, 179, 163-175.

Babu Madhavan, B., Venkataraman, G., Krishna Mohan, B., and Shah, S. D., (1997). Revealing the geology of the Great Nicobar Island, Indian Ocean, by the interpretation of Airborne Synthetic Aperture Radar images - International Journal of Remote Sensing, 18 (13), 2723-2742.

Bandhopadhyay, P.C. (2012). Reinterpretation of age and environment of deposition of Paleogene turbidites in the Andaman and Nicobar islands, Western Sunda Arc. Journal of Asian Earth Sciences, 45, 126-137.

Bouma,A.H (1962). Sedimentology of some flysch deposits. Amsterdam, Elsevier, 168p.

Bouma, A.H (1985): Introduction to submarine fans and related turbidite systems. In: Bouma, A, Nomark, W, Barnes, N (Eds), Submarine fans and related Turbidite systems. Spriger-Verlag, New York, 351 pp.

Bose,P.K, Banerjee,S.and Sarkar, S.(1997): Slope controlled seismic deformation and tectonic framework of deposition of Koldahashale, India. Tectonophysics, 269:151-169.

Chakraborty, P.P. and Pal, T. (2001). Anatomy of a fore arc submarine fan: Upper Eocene–Oligocene Andaman Flysch Group, Andaman Islands, India. Gondwana Research, 4, 477-486.

Curray, J. R. (2005). Tectonics and history of the Andaman Sea region. J. Asian Earth Sci. 25, 187–232.

Curray, J.R., D.G. Moore, Lawver, L.A., Emmel, F.J. , Raitt, R.W. , Henry M., Kieckhefer, R. (1979). Tectonics of the Andaman Sea and Burma. In, Geological and geophysical investigations of continental margins, AAPG Mem. 29, 189-198.

Ghibaudo, Guido. (1992). subaqueous sediment gravity flow deposits: practical criteria for their field description and classification. Sedimentology, 423-454.

Hadlari, T., Tylosky,SA., Lemiyux,Y., Zantwoort,WG., and Catuneanu,O. (2009). Slope and submarine fan turbidite show a fine variation in terms of grain size.facies of the Upper Devonian Imperial Formation, Northern Mackenzie mountains, NWT. Bulletin of Canadian Petroleum Geology, 57(2), , 192-208.

Hampton, M. A. (1972). The role of subaqueous debris flow in generating turbidity currents: Jour. Sedimentary Petrology, 42, 775- 793.

Hochsetter, F.von. (1869).Geology and physical geography of the Nicobar Island. Translated in part byStiliczka.Rec.Geol.Surv.Ind.2, 59.

Karunakaran, C., Roy, K.K., Saha, S.S. (1968). Tertiary sedimentation in the Andaman Nicobar Geosyncline. Jour. Geol. Soc. Ind. 9, 32-39.

Karunakaran ,C., Roy, K.K., Sen, C.R., Saha, S.S., and Sarkar, S.K.(1975).Geology of Great Nicobar island. Journal of the Geological Society of India, 16, 2, 135-142.

Kneller, Benjamin. C., Branney, Michael.J.(1995). Sustained high density turbidity currents and the deposition of thick massive sands. Sedimentology, 42,607-616.

Kundu, K., Matin, A., Mukul, M., Eriksson, P.G., 2011. Sedimentary facies and soft-sediment deformation structures in the Late Miocene Pliocene Middle Siwalik subgroup, Eastern Himalaya, DarjilingDistrict, India. Journal of the Geological society of India 78, 321–326.

Lowe, D.R. (1982). Sediment gravity flows II. Depositional models with special reference to the deposits of high density turbidity currents. Journal of Sedimentary Petrology, 52, 279-297.

Middleton, G. V. and Hampton, M.A.(1973). Sediment gravity flows: mechanics of flow and deposition in Middleton, G.V. and Bouma, A.H. eds., Turbidites and deep water sedimentation: Proceedings of the Pacific section society of Economic Paleontologists and Mineralogists, Los Angeles, 1-38.

Misra, T.C. and Roy, T.K. (1984). Exploration in Andaman forearc basin: its evaluation, facies trend and prospects- a review. Proc. 5th Offshore South East Asia Conf. (OFFSEA 84), Singapore 1984, South East Asia Petroleum Expl. Soc. (SEAPEX), 4-66-4-83.

Mukhopadhay, B., Chakraborty, P.P., Paul, S. (2003). Facies clustering in turbidite successions: case study from Andaman Flysch Group, Andaman Islands, India. Gondwana Research, 6, 918-925.

Mulder, T. and Alexander,J. (2001) . The physical character of subaqueous sedimentary density flows and their deposits. Sedimentology 48, 269-299.

Mutti,E.(1985). Turbidite systems and their relations to depositional sequences. G.G. Zuffa(Ed).Prvenance of Arenites. D.Reidel Publishing.

Mutti,E.(1992).Turbidite sandstones: Milan, Italy, Agip special publication, 275p.

Mutti, E. and Nomark,W.R. (1987). Comparing examples of modern and ancient turbidite systems: problems and concepts.In : Legget, J.K, Zuffa,G.G (Eds), Marine Clastic Sedimentology, London, Graham and Trotman, 1-38.

Nomark,W.R. (1970). Growth patterns of deep sea fans. AAPG Bull.54 (11), 2170-2195.

Nomark, W.R. (1978) . Fan valleys, channels and depositional lobes on modern sub marine fans.: characters for recognition of sandy turbidite environments. AAPG Bull.62 (6), 912-931.

Oldham,R.D. (1885).Notes on the Geology of Andaman islands. Rec. Geol. Surv. Ind 18(3), 136.

Pal, T., Chakraborty, P.P., Gupta, T.D. and Singh,C.D. (2003). Geodynamic evolution of the outer arc forearc belt in the Andaman Islands, the central part of Burma-Java subduction complex: Geological Magazine v 140, 289-307.

Pickering, Kevin., Stow, Dorrik., Watson, Mike, Hiscott and Richard. (1986). Deep water facies, processes and models: A review and classification scheme for modern and ancient sediments. Earth Science Reviews, 23, 75-174.

Ray, K.K. (1982).A review of the Geology of Andaman and Nicobar islands. Geological Survey of India Miscellaneous Publication 42(2), 110-125.

Rink, P.H. (1847). Die Nikobar Inseln. Eine Geographische Skizze, mit speciieller Beru¨ksichtigung der Geognosie, Kopenhagen. Translated Selections, Records Government India LXXVII, 540.

Rink, P.H. and Stoliczka (1870). Die Nicobar Inseln, Kopenhagen Translated sections. Rec. Gov. of India 77, 105,153.

Roy, S. K. (1992). Accretionary prism in Andaman Forearc. Geol. Surv. Ind. Spl. Pub 29, 273-278.

Roy, Sandip, K., and Banerjee Santanu. (2010).From Chaos to apparent calm. The saga of tectonics and sedimentation in Andaman basin: 2010 GSA Denver Annual Meeting (31October–3 November,) (Abstract).

Roy, S. K. and Das Sharma, S. (1993). Evolution of Andaman Fore arc Basin and its hydrocarbon potential. Proc. Second Seminar on Petroliferous Basins of India, vol 1.S K, Biswas et al(eds).

Roy, Sandip. Kumar and Banerjee Santanu. (2016). Soft Sediment Deformation Structures in Andaman Flysch, Andaman Basin:Evidence for Paleogene Seismic Activity in the Island Arc. Berita Sedimentologi, 35, 55-64, May, Indonesia.

Roy, Sandip. Kumar, Paul, Swagata., Sadhu, Rajib and Banerjee Santanu. (2011). Provenance and tectonic setting of a coarse grained Flysch: Case study from the Andaman Flysch at trench slope break, North Andaman islands. GSA Minneapolis Annual Meeting, Oct 11 th,.(Abstract, Poster session). Geological Society of America Abstracts with Programs. 43, 5, 432.

Roy, T. K .(1983).Geology and hydrocarbon prospects of Andaman Nicobar Basin. Petroleum Asia Journal, Nov, 37-50.

Roy, T. K. and Chopra, N. N. (1987).Wrench faulting in Andaman Forearc basin. 19th Annual OTC in Houston, Texas, AprTI 27-30,.

Shanmugam G. (2006). Deep water processes and facies models: implications for sandstone petroleum reservoirs.Elsevier, Amsterdam.

Shanmugam, G. and Moiola R.J.(1995). Reinterpretation of depositional processes in a classic flysch sequence (Pennsylvanian Jackfork group), Ouachita Mountains, Arkansas and Oklahoma. AAPG Bull 79, 672-695.

Shiki, T., Cita, M.B. and Gorsline, D.S. (2000). Sedimentary features of seismites, seismo-turbidites and tsunamites—an introduction Sedimentary Geology, 135 (2000) vii–ix.

Stow Dorrik A.V., Johansson and Melissa. (2000). Deep-water massive sands: nature, origin and hydrocarbon Implications. Marine and Petroleum Geology 17 (2000) 145-174.

Van Loon, A.J., (2002). Soft-sediment deformations in the Kleszczów Graben (central Poland). [In:] P.K. Bose, S. Sarkar & P.G. Ericksson (Eds), Rift basins: sedimentology and palaeontology – Chanda Memorial Issue. Sedimentary Geology 147, 57–70.

Walker, Roger. G. (1978).Deep-Water Sandstone Facies and Ancient Submarine Fans: Models for Exploration for Stratigraphic Traps'. AAPG Bull 62, 6, June, 932-966.

Weeks, Austin.L, Harbison, R.N., Peter.(1967).Island arc system in Andaman sea. AAPG Bull 9, September.

Wynn, Russel.B, Kenyon, Neil. H., Masson, Douglas.g, Stow, Dorrik.A.V., Weaver and Phillip,P.E. (2002). Characterization and recognition of deep water channel-lobe transition zones. AAPG Bull, 86, 8, 1441-1462.

Jour. Indian Association of Sedimentologists, Vol. 34, Nos. 1 & 2. (2017), pp. 93-101

Change in Depositional Environment of Maharashtra Coast, Central West Coast of India

VOLVOIKAR S. P.[1] AND NAYAK G. N.[2]
1. National Institute of Oceanography, Dona Paula, Goa
2. Goa University, Taleigao Plateau, Goa
Email: samida2010@gmail.com; gnnayak@unigoa.ac.in

Abstract: Deposition of organic matter in nearshore and offshore regions largely depends upon the contribution from terrestrial inputs. Rivers are the major pathways of organic matter to these regions. Any change in fluvial or estuarine inputs therefore will significantly affect the biogeochemical processes operating in nearshore and offshore environments. Significant change in distribution patterns of grain size, organic carbon, TOC/TN ratio, diatom assemblages and carbon isotope ratio values have been noted in the cores collected from Khonda creek, Dudh creek, Vaitarna estuary, Amba estuary, Kundalika estuary, Rajapuri creek and Savitri estuary. All these estuaries and creeks located along central west coast of India indicated a transition from river dominated depositional environment in the past to marine dominated depositional environment in recent years. Since these estuaries and creeks are the pathways of terrestrial material load to eastern Arabian Sea region, decrease in input of terrestrial material load over time has significantly affected the biogeochemical processes operating in this region.

Keywords: Creeks, Deposition**,** Estuaries, Organic matter, Sediments

INTRODUCTION

Coastal regions are the important sites of biogeochemical transformations including biological production, sediment retention and nutrient transformation (Bianchi, 2007). An estimate of over 80% of global burial of organic carbon occurs in margins adjacent to the rivers (Berner, 1982; Hedges, 1992; Hedges and Keil, 1995). Deposition of organic matter largely depends upon contributions from marine and terrestrial sources in coastal regions. Recent studies have highlighted coastal and nearshore areas as important sites where both terrigenous and marine derived organic matter is actively recycled (Aller, 1998; Aller et al., 2004; Blair et al., 2003, 2004; Gordon and Goni, 2003; Stein and Macdonald, 2004). The elevated sediment accumulation rates and the input of recalcitrant organic matter from terrigenous sources both contribute to the efficient sequestration of carbon in the coastal regions (Goni et al., 2005). Information about processes controlling the delivery of organic matter to coastal sediments and mechanisms that underlie their preservation is therefore important to our understanding of global biogeochemical cycles (Canuel et al., 1997).

Rivers draining into the sea are the major pathways of terrestrial input (organic and clastic matter) to coastal and near shore regions. Any change in riverine freshwater input and associated material load therefore directly influence the coastal and offshore regions. Intertidal mudflat and mangrove sediments within estuaries and creeks are known to act as repositories, which store signatures of such changes effectively in different geochemical phases. Study of variation in marine and terrestrial organic matter sources within these sediments provide important information on changes in riverine inputs from past to present. And this information can be used to understand its possible influence on biogeochemical processes operating in the off shore regions. However, impact of such changes will be significant on global level, only if they occur on a larger geographical area for similar time frame and this needs to be assessed.

Rivers supplying freshwater and terrestrial organic and inorganic particulate and dissolved material to Arabian Sea are rapid, short and swift flowing and having hardly any delta formations as compared to those rivers in the east. It is suggested that, in addition to large rivers, smaller rivers also significantly contribute to the overall global carbon budget. Thus, studies should be carried out on smaller rivers to better understand the influence of environmental changes on coastal regions. However, earlier studies carried out along west coast of India emphasized on metal pollution (Fernandes and Nayak, 2012a, b; Siraswar and Nayak, 2011 Fernandes et al., 2011; Kumar and Edward, 2009; Nair and Ramchandran, 2002; Nair and Sujatha, 2012; Harikumar et al., 2009; Ram et al., 2003). Significant work has also been carried out to understand sources and factors controlling metal distribution (Singh and Nayak, 2009; Pande and Nayak, 2013a, b; Volvoikar and Nayak, 2013a,

b; Singh et al., 2013), distribution and association of metals within clay fraction (Volvoikar and Nayak, 2014) and bioavailability of metals (Volvoikar and Nayak, 2015; Dessai and Nayak, 2009). Limited studies that were carried out on margins and near shore areas of west coast of India also focused mainly on pollution aspect (Karbassi and Shankar, 2005).

Maharashtra state located along the west coast of India harbors a number of westward flowing rivers. It is the state with highest number of dams in India. Coastal Maharashtra is also one of the most rapidly industrializing and urbanizing regions of India. Thus, mudflat and mangrove sediment cores of Vaitarna estuary (Volvoikar et al., 2014), Kundalika estuary (Pande and Nayak, 2013), Rajapuri Creek (Pande, 2014), Savitri estuary (Pande, 2014), Vashishti estuary (Pande, 2014), Amba estuary (Pande et al., 2014), Dudh creek (Volvoikar and Nayak, 2013a) and Khonda creek located along the coast of Maharashtra state have been studied (Table 1) individually to understand changes in depositional environment from past to present (Fig. 1). In this paper an attempt is made to understand the processes operating all along the coast of Maharashtra state and its significance based on the results of our earlier studies.

STUDY AREA

The coast of Maharashtra is characterized by pocket beaches flanked by rocky cliffs, estuaries, bays and mangroves at some places; while mudflats are found mainly along estuaries and creeks (Nayak, 2005). The coast is affected by medium to high tidal range. In addition to spring and neap tides, semi diurnal tides, seem to have more impact on the tidal estuaries and creeks (Karlekar, 1993). The narrow strip of land between the Arabian Sea and the Sahyadri hills of Maharashtra state is known as Konkan coast. The rocky Konkan coast of Maharashtra is characterized by impressive sea cliffs, sea caves and shore platform at number of places (Mate, 1993). The dominant geomorphic process in the region is terrestrial erosion resulting from high relief (Deswandikar, 1993). Common mangrove species reported from this region are *Avicennia alba*, *Avicennia marina* and *Sonneratia apetala*. *Avicennia officinalis*, *Rhizophora mucronata* and *Rhizophora apiculata* (Naskar and Mandal, 1999). The region is the part of the Deccan volcanic province (DVP) or Deccan Trap. The basaltic terrain has an undulating topography with landforms typical of the DVP (Shankar and Mohan, 2006). The Deccan Trap basalts have uniform tholeiitic composition, are dark green to black volcanic rocks with a wide variety of textural character (Wensink, 1973). In the Northwestern part these tholeiitic basalts show notable picritic and alkali occurrences. They are largely microporphyritic with phenocrysts of plagioclase, subordinate augite and rare olivine (Sano et al., 2001, Sen, 2001). The sediments within the estuary and creeks along this coast will be influenced by the mineral and chemical composition of rocks within the catchment area.

Table 1. Details of sampling locations of sediment cores.

Estuary/ Creek	Name of the Place	Station Location	Core Length (cm)
Khonda Creek	Aagwan	19º57'33.1"N; 72º46'07.1"E	42
Dudh Creek	Murbe	19º44'43.9"N; 72º42'39.6"E	56
Vaitarna Estuary	Chikaldongri	19º28'56.3"N; 72º46'58.7"E	102
Amba Estuary	Dharamtar	18º41‘47.60"N; 73º12‘41.05"E	50
Kundalika Estuary	Revdanda	18º32‘20.76"N; 72º56’11.41"E	66
Rajapuri Creek	Nandale	18º32’55.39"N; 73º00’30.59"E	98
Savitri Estuary	Bankot	17º59‘4.54"N; 73º3’53.18"E	100

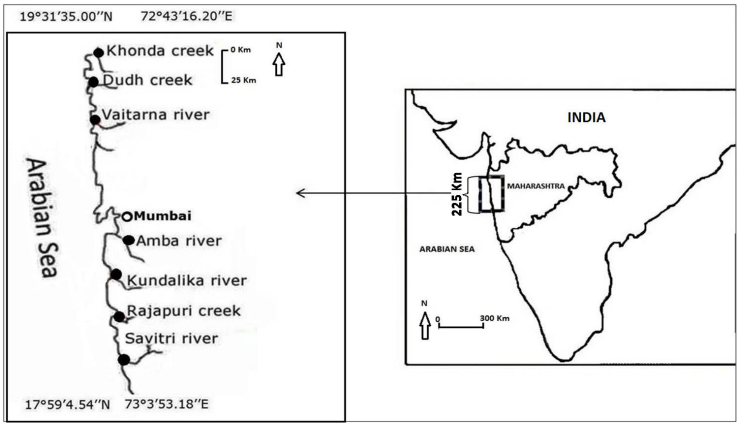

Fig. 1. Study area map of Maharashtra coast.

MATERIALS AND METHODS

Sediment cores were collected using hand operated PVC corer. Following the collection, sub sampling was done at 2 cm interval with the help of a plastic knife in case of all the cores uniformly. The sub-samples were immediately sealed in clean plastic bags, labeled and stored in ice box and transferred to the laboratory. Sampling stations were located using hand held Global Positioning System (GPS). Sediments were oven dried at 60°C in the laboratory. Portion of the dried sample was powdered and homogenized using an agate mortar and pestle. Un-ground sediment samples were used for the analysis of sediment components (sand: silt: clay) and study of diatoms. While, powdered and homogenized samples were used for the estimation of total organic carbon, bulk sediment chemistry, TOC/TN and bulk sedimentary stable carbon ($ä^{13}C_{org}$). In-order to determine the sand: silt: clay ratio, pipette analysis was carried out following Folk (1968). The organic carbon in sediment sub-samples was estimated using the method given by Gaudette et al. (1974) also known as Walkey-Black method. The method utilizes exothermic heating and oxidation with potassium dichromate ($K_2Cr_2O_7$) and concentrated sulphuric acid (H_2SO_4). Total decomposition of sediments for metal analyses was carried out, wherein 0.3 g of finely powdered sediment sample was digested in open Teflon beaker. 10 ml of 7:3:1 acid mixture of HF, HNO_3 and $HClO_4$ was added slowly to the sample. Care was taken to avoid excessive frothing. The mixture was kept overnight and later dried completely on a hot plate at 70° C. After drying, again 5 ml of the above mixture was added to the beaker and dried for 1 h in order to ensure complete digestion of the sediment. To this 2 ml of concentrated HCl was added and dried completely. To the dried sample 10 ml of 1:1 HNO_3 was added and warmed for few minutes. The solution was then made to 100 ml using Milli Q water and was then stored in pre-cleaned plastic bottle. The solution was then aspirated into flame atomic absorption spectrophotometer (AAS) (Varian AA240FS) for the analyses of the metals viz. iron (Fe), manganese (Mn), aluminium (Al), copper (Cu), zinc (Zn), cobalt (Co), nickel (Ni) and lead (Pb). Care was taken to avoid contamination at every step. While, for $ä^{13}C_{org}$ analysis, acid treated, powdered, oven dried sediment sub-samples were run on a Thermo-Finnigan Delta-V-Plus continuous flow isotope ratio mass spectrometer attached to an elemental analyzer (Thermo EA1112). Whereas, the homogenized and not powdered sediment samples were used for diatom isolation using the method described by Battarbee (1986).

RESULTS AND DISCUSSION

Significant change in distribution patterns of grain size, organic carbon, TOC/TN ratio, diatoms and isotopes were observed in the cores collected from Khonda creek (Fig. 2), Dudh creek (Fig.3) (Volvoikar and Nayak, 2013), Vaitarna estuary (Fig. 4) (Volvoikar et al., 2014), Amba estuary (Fig. 5) (Pande and Nayak 2013a), Kundalika estuary (Fig. 6) (Pande and Nayak, 2013b),

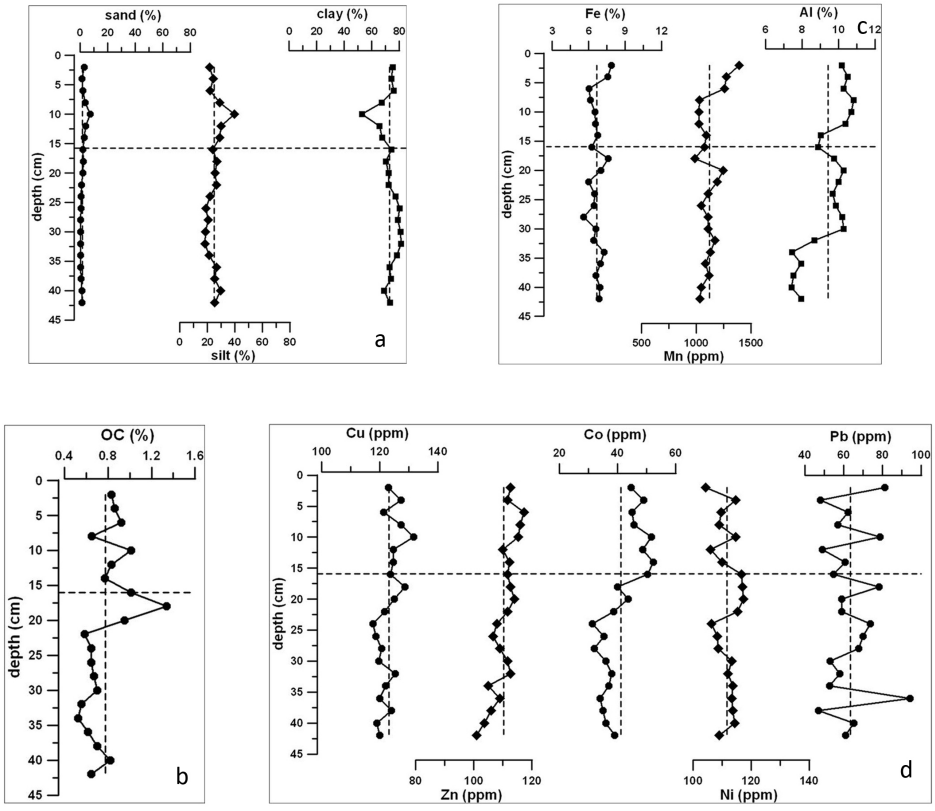

Fig. 2. Distribution of a. sediment components b. OC c. major and d. trace metals in Khonda creek.

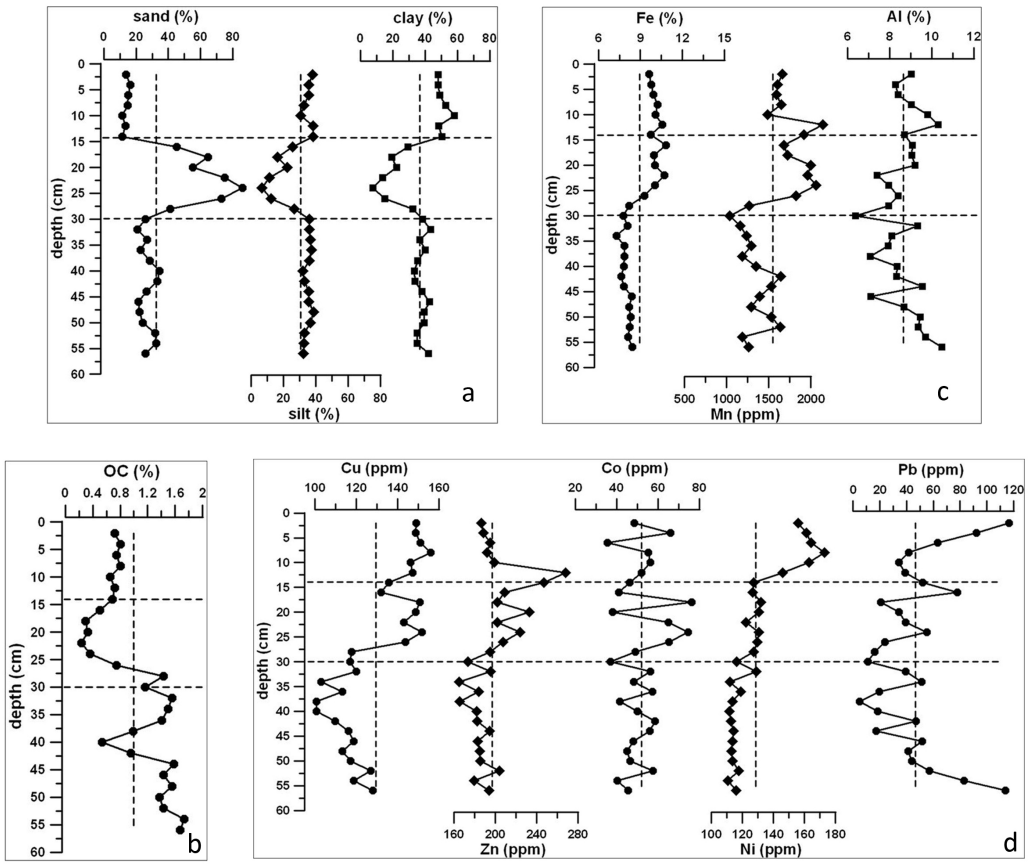

Fig. 3. Distribution of a. sediment components b. OC c. major and d. trace metals in Dudh creek (Volvoikar and Nayak, 2013).

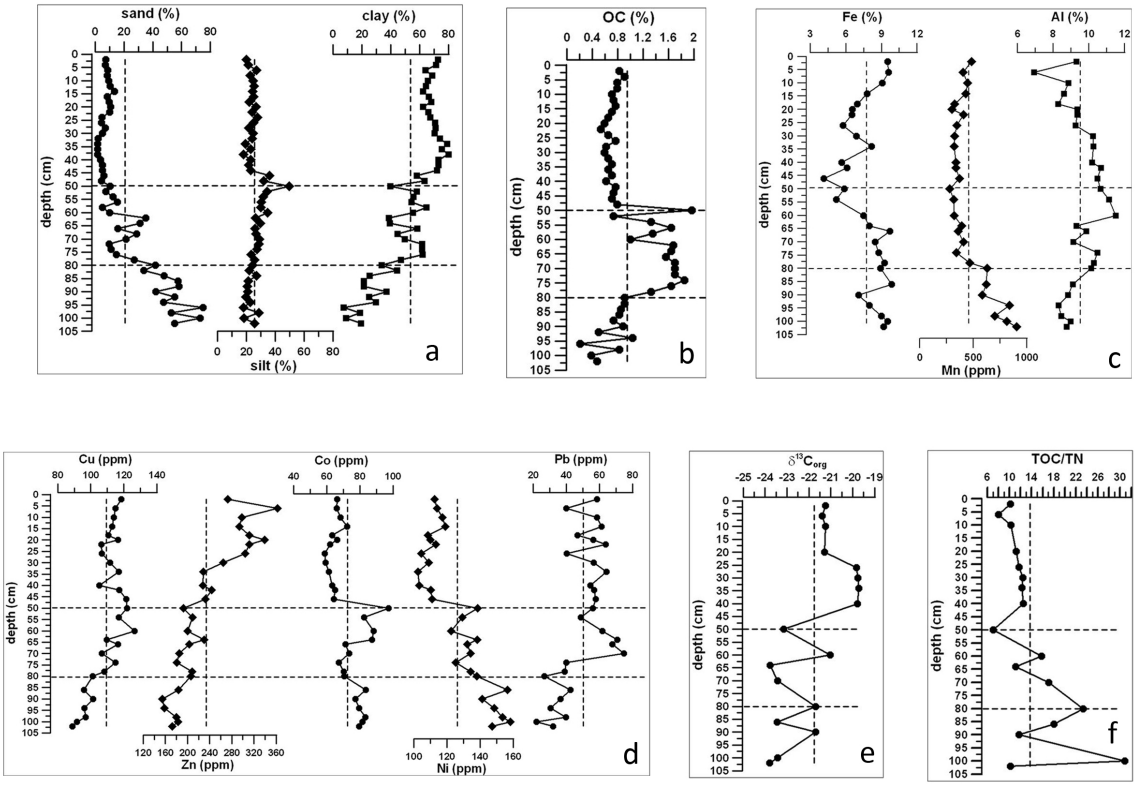

Fig. 4. Distribution of a. sediment components b. OC c. major and d. trace metals e. ä13C_{org} and f. TOC/TN in core collected from Vaitarna estuary (Volvoikar et al., 2014).

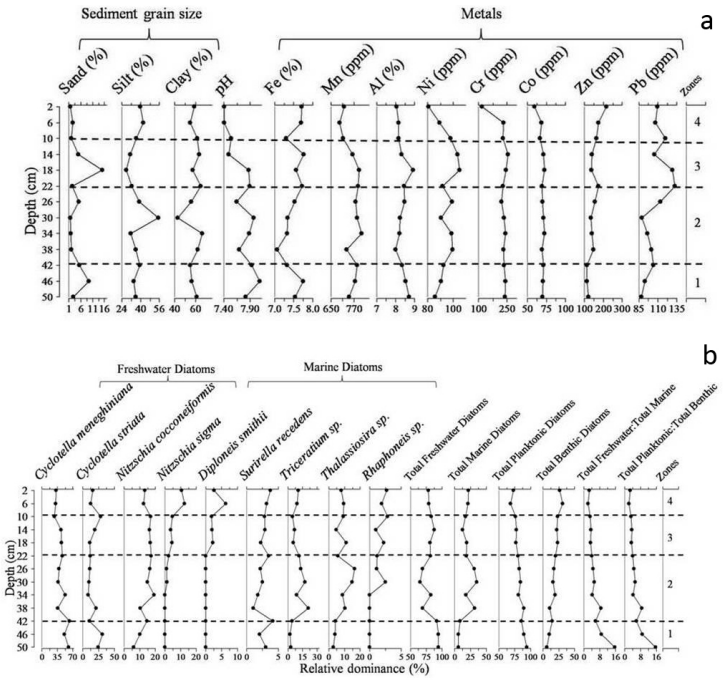

Fig. 5. a. Distribution of sediment components and metals b. diatoms in core collected from Amba estuary (Pande and Nayak, 2013a).

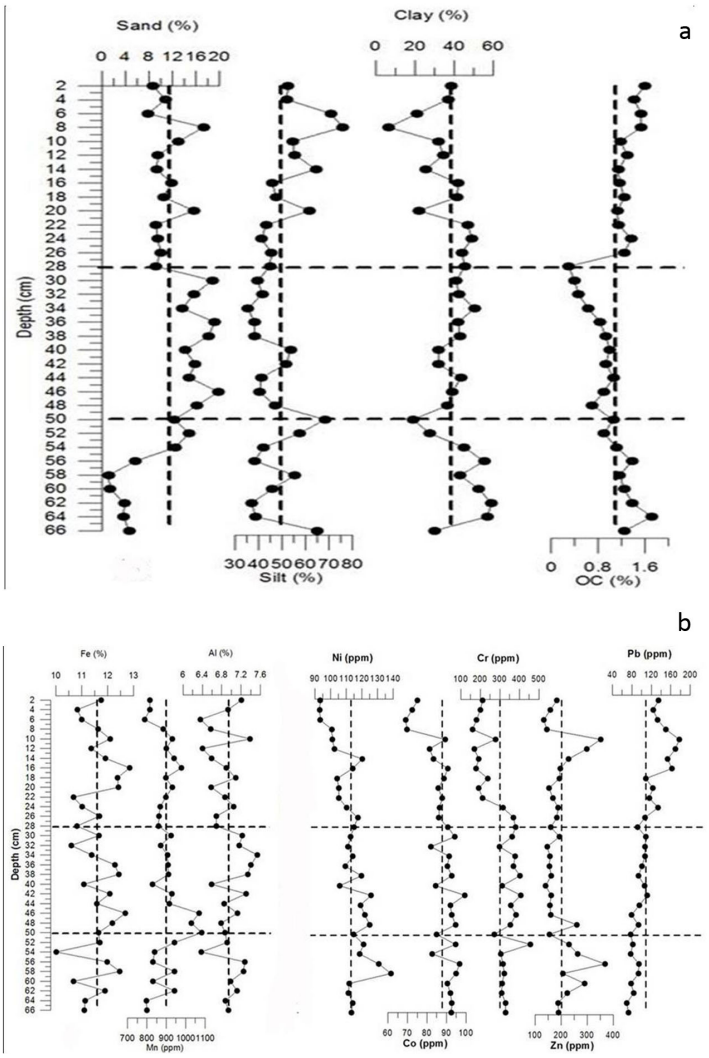

Fig. 6. a. Distribution of sediment components and b. metals in core collected from Kundalika estuary (Pande and Nayak, 2013b).

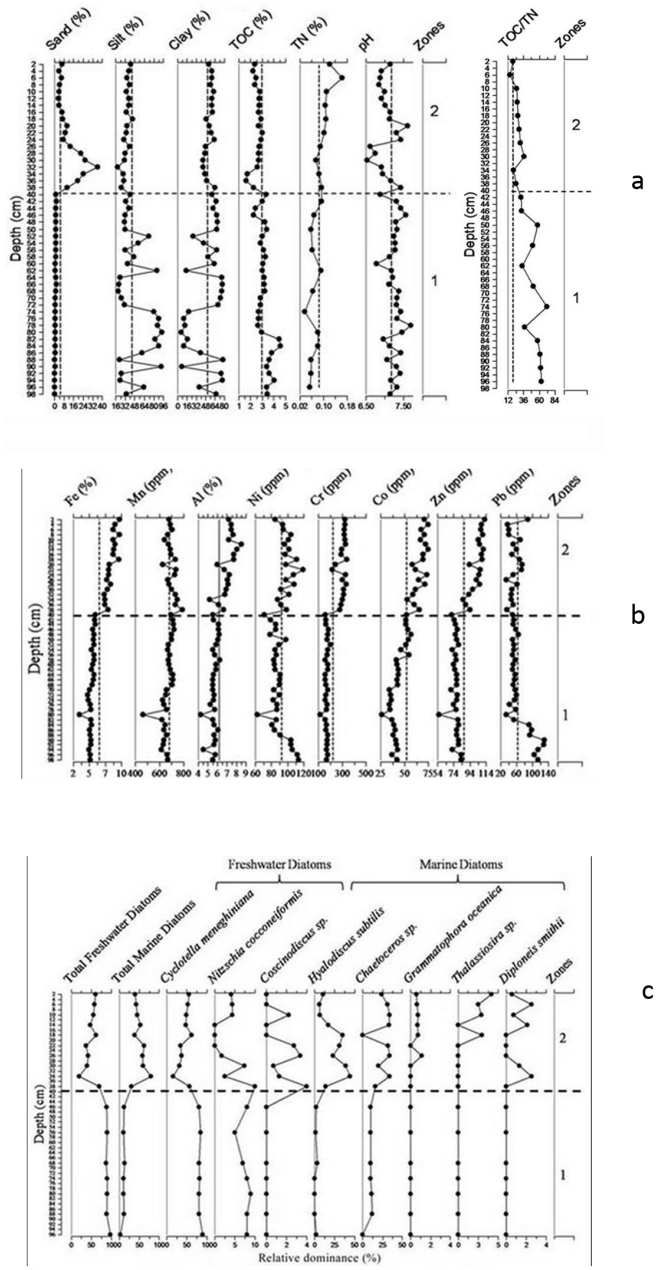

Fig. 7. a. Distribution of sediment components, OC, TOC/TN b. metals c. diatoms in core collected from Rajapuri creek (Pande et al. 2014a).

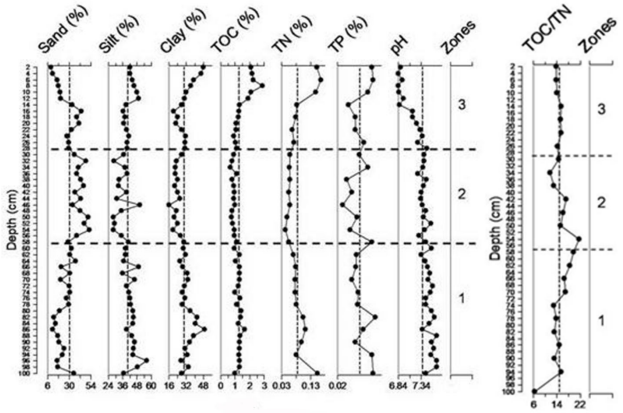

Fig. 8. a. Distribution of sediment components, OC, TOC/TN in core collected from Savitri estuary (Pande 2014).

Rajapuri creek (Fig. 7) (Pande et al 2014) and Savitri estuary (Fig. 8) (Pande 2014) present along the central west coast of India. Relatively higher deposition of fine sediments towards the bottom of the cores collected from Dudh creek (Volvoikar and Nayak 2013), Rajapuri creek (Pande et al 2014) and Savitri estuary (Pande 2014) pointed towards deposition under calm conditions in the past. Further, increased sand percentage noted in the middle section of the cores collected from Dudh creek (Volvoikar and Nayak 2013), Rajapuri creek (Pande et al 2014), Savitri estuary (Pande 2014) and Kundalika estuary (Pande and Nayak 2013b) suggested a change from calm to higher hydrodynamic conditions. In the top section of the cores higher percentage of fine sediment has been reported from Dudh creek (Volvoikar and Nayak 2013), Rajapuri creek (Pande et al 2014), Savitri estuary (Pande 2014), Vaitarna estuary (Volvoikar et al 2014) and Amba estuary (Pande and Nayak 2013a) suggesting a further change to calmer conditions in recent years. The type of organic matter deposited in estuaries along central west coast of India also showed a corresponding change. Wherein, the relatively higher TOC/TN ratio in the bottom sections of the cores collected from Rajapuri creek (Pande et al 2014), Savitri estuary (Pande 2014) and Vaitarna estuary (Volvoikar et al. 2014) indicated periods when sediment received relatively higher proportion of terrestrial organic matter in the past. Whereas, overall decrease in TOC/TN ratio in the top sections, suggested decrease in terrestrial input in the recent years. These results were also supported by diatom records in Amba estuary (Pande 2014), Rajapuri creek (Pande et al 2014) and Savitri estuary (Pande 2014) and stable carbon isotopic composition in Vaitarna estuary (Volvoikar et al 2014). Thus indicating a transition from river dominated to marine dominated depositional environment over the years within these estuaries. Metal concentration also showed increase towards surface of most of the cores, further providing supporting evidence for increased marine inundation in recent years (Volvoikar and Nayak 2014) all along the Maharashtra coast.

Since, all the estuaries transport a portion of the material derived from its catchment to the adjacent near shore region, such changes in sediment particles, organic matter, nutrients and metal input in almost all the studied estuaries and creeks of Maharashtra state should significantly affect the depositional environments of the near shore and offshore regions as well. It can therefore be strongly suggested that the biogeochemical processes in near shore and offshore regions of Maharashtra coast i.e. eastern Arabian Sea will also be widely affected.

FUTURE SCOPE

These studies were based on undated cores and age-dates needs to be investigated further for better understanding of time dependent changes in processes along the coast. In addition, earlier studies on terrestrial-marine influence in Rajapuri, Savitri and Amba estuaries were based on results of diatom studies, while that of Vaitarna estuary were based on stable carbon isotopic studies in addition to that of TOC/TN ratio. Similar studies should also be carried out on other estuaries and creeks present along west coast of India. The use of proxies should also be made uniform to get a precise knowledge and clear idea of recent changes in depositional environment along west coast of India. Such studies carried out all along the coast may help to establish whether the change as observed is controlled by global/ eustatic sea level rise or is controlled by local/regional factors resulting from reduction in precipitation, construction of dams, and diversion of fresh water.

Acknowledgement: We would also like to thank UGC and MoES for providing financial support to complete our research work. We would also like to thank Dr. Anant Pande for providing the details of the study locations.

References

Aller R C., (1998). Mobile deltaic and continental shelf muds as suboxic, fluidized bed reactors. Marine Chemistry 61, 143-155.

Aller R C, Hannides A, Heilbrun C. and Panzeca C. (2004). Coupling of early diagenetic processes and sedimentary dynamics in tropical shelf environments: the Gulf of Papua deltaic complex. Continental Shelf Research 24, 2455-2486.

Battarbee R W. (1986). Diatom analysis In: Berglund B E (ed.) Handbook of Holocene Palaeoecology and Palaeohydrology. Wiley Chichester, 527-570.

Berner R A. (1982). Burial of organic carbon and pyrite sulfur in the modern ocean: its geochemical and environmental significance. American Journal of Science, 282, 451-473.

Bianchi T S. (2007). Biogeochemistry of estuaries. Oxford University Press.

Blair N E, Leithold E L andAller R C. (2004). From bedrock to burial: the evolution of particulate organic carbon across coupled watershed-continental margin systems. Marine Chemistry 92, 141-156.

Blair N E, Leithold E L, Ford S T, Peeler K A, Holmes J C, Perkey D W. (2003). The persistence of memory: the fate of ancient sedimentary organic carbon in a modern sedimentary system, Geochimica et Cosmochimica Acta 67, 63-73.

Canuel E A, Freeman K. H. andWakeham S G., (1997). Isotopic compositions of lipid biomarker compounds in estuarine plants and surface sediments. Limnology and Oceanography 42 (7), 1570-1583.

Dessai D V G, Nayak G N. (2009). Distribution and speciation of selected metals in surface sediments, from the tropical Zuari estuary, central west coast of India. Environmental Monitoring and Assessment, 158, 117-137.

Deswandikar A. (1993). The sea cliffs of rocky coast between Kelshi and Dabhol. In Coastal Geomorphology of Konkan (Karlekar S. ed). Aparna Publications, Pune, 235-236p.

Fernandes L, and Nayak G N., (2012a). Geochemical assessment in a creek environment: Mumbai, west coast of India. Environmental Forensics, 13(1), 45–54.

Fernandes L, and Nayak G N., (2012b). Heavy metals contamination in mudflat and mangrove sediments (Mumbai, India). Chemistry and Ecology, 28(5), 435–455.

Fernandes L, Nayak G N, Ilangovan D, and Borole D V., (2011). Accumulation of sediment, organic matter and trace metals with space and time, in a creek along Mumbai coast, India. Estuarine, Coastal and Shelf Science, 91, 388–399.

Folk R L., (1968). Petrology of Sedimentary rocks. Austin, Texas: Hemphills, pp.177.

Gaudette H E, Flight W R, Toner L, and Folger D W., (1974). An inexpensive titration method for the determination of organic carbon in recent sediments. Journal of Sedimentary Petrology, 44, 249-253.

Goni M A, Yunker M B, Macdonald R W, and Eglinton T I., (2005). The supply and preservation of ancient and modern components of organic carbon in the Canadian Beaufort Shelf of the Arctic Ocean. Marine Chemistry 93, 53-73.

Gordon E S, and Goni M A., (2003). Sources and distribution of terrigenous organic matter delivered by the Atchafalaya River to sediments in the northern Gulf of Mexico. Geochimica et Cosmochimica Acta 67, 2359-2375.

Harikumar, P. S., Nasir, U. P., and Mujeebu Rahman, M. P. (2009). Distribution of heavy metals in the core sediments of a tropical wetland system. International Journal of Environment Science and Technology, 6 (2), 225-232.

Hedges J., (1992). Global biogeochemical cycles: progress and problems. Marine Chemistry 39, 67-93.

Hedges J I, and Keil R G., (1995). Sedimentary organic matter preservation: an assessment and speculative synthesis. Marine Chemistry 49, 81-115.

Karbassi, A.R., and Shankar, R. (2005). Geochemistry of two sediment cores from the west coast of India. International Journal of Environmental Science & Technology, 1(4), 307-316.

Karlekar S., (1993). The tidal landforms of Uran-Alibag-Murud coast. In Coastal Geomorphology of Konkan (Karlekar S. ed). Aparna Publications, Pune, 65p.

Kumar S. P. and Edward J K P., (2009). Assessment of metal concentration in the sediment cores of Manakudy estuary, south west coast of India. Indian Journal of Marine Science, 38(2), 235–248.

Mate I., (1993). The sea caves of Guhagar coast. In Coastal Geomorphology of Konkan (Karlekar S. ed). Aparna Publications, Pune, 259p.

Nair M N M, and Ramchandran K K., (2002). Textural and trace elemental distribution in sediments of Beypore Estuary (S-W Coast of India) and adjoining inner shelf. Indian Journal of Marine Sciences, 31, 295-304.

Nair M P, and Sujatha C H., (2012). Biogeochemical quality assessment of the sediments in Kerala coast. International Journal of Environmental Sciences, 3 (1), 707-719.

Naskar K, and Mandal R., (1999). Ecology and biodiversity of Indian Mangroves. Part I: Global status. Vol (1), 150-155, Published by: Daya Publishing House. ISBN 81-7035-191-X.

Nayak G N., (2005). Indian Ocean Coasts, Coastal Geomorphology. In Encyclopedia of Coastal Science (Schwartz ed). Springer press, 555p.

Pande A., (2014). Depositional environments and processes within mudflats and mangroves along central west coast of India. Ph.D Thesis, Goa University, India.

Pande A, and Nayak G N., (2013a). Depositional environment and preferential site of metal concentration in mudflats of dharamtar creek, west coast of India. Indian Journal of Geo-Marine Sciences 42(3), 360–369.

Pande A, and Nayak G N., (2013b). Understanding distribution and abundance of metals with space and time in estuarine mudflat sedimentary environment. Environ Earth Sci. doi:10.1007/ s12665-013-2298-y

Pande A, Nayak G N, Prasad V, Prakash Babu C., (2014). Geochemical and Diatom records of recent changes in depositional environment of a Tropical creek, Central west coast of India, Environmental Earth Sciences (DOI 10.1007/s12665-014-3799-z).

Ram A, Rokade M A, Borole D V, and Zingde M D., (2003). Mercury in sediments of Ulhas estuary. Marine Pollution Bulletin, 46, 846–857.

Sano T, Fujii T, Deshmukh S S, Fukuoka T, and Aramaki S., (2001). Differentiation processes of Deccan Trap Basalts: Contribution from geochemistry and experimental petrology. Journal of Petrology, 42 (12), 2175-2195.

Sen G., (2001). Generation of Deccan Trap magmas. P Indian AS-Earth, 110 (4), 409-431.

Shankar M N R, and Mohan G., (2006). Assessment of the groundwater potential and quality in Bhatsa and Kalu river basins of Thane district, western Deccan volcanic province of India. Environmental Geology, 49, 990-998.

Singh K T, and Nayak G N., (2009). Sedimentary and geochemical signatures of depositional

environment of sediments in mudflats from a microtidal Kalinadi estuary, Central west coast of India. Journal of Coastal Research, 25 (3), 641–650.

Singh K T, Nayak G N, Fernandes L L, Borole D V, and Basavaiah N., (2013). Changing environmental conditions in recent past—Reading through the study of geochemical characteristics, magnetic parameters and sedimentation rate of mudflats, central west coast of India. Palaeogeography Palaeoclimatology Palaeoecology. http://dx.doi. org/ 10.1016/j.palaeo.2013.04.008

Siraswar R, and Nayak G N., (2011). Mudflats in lower middle estuary for concentration of metals. Indian Journal of Marine Science, 40(3), 372–385.

Stein R, and Macdonald R W., (2004). The Organic Carbon Cycle in the Arctic Ocean. Springer, 363 pp.

Volvoikar, S. P., and Nayak, G. N. (2013a). Depositional environment and geochemical response of mangrove sediments from creeks of northern Maharashtra coast, India. Marine Pollution Bulletin, 69:223–227.

Volvoikar S P, and Nayak G N., (2013b). Evaluation of impact of industrial effluents on intertidal sediments of a creek. International Journal of Environmental Science and Technology, 10, 941–954.

Volvoikar S P, and Nayak G N., (2014). Factors controlling the distribution of metals in intertidal mudflat sediments of Vaitarna estuary, North Maharashtra coast, India. Arabian Journal of Geoscience, DOI 10.1007/s12517-013-1162-4

Volvoikar S P, and Nayak G N., (2015). Impact of industrial effluents on geochemical association of metals within intertidal sediments of a creek. Marine Pollution Bulletin**,** 99 (1), 94-103.

Volvoikar S P, Nayak G N, Mazumdar A, and Peketi A., (2014). Reconstruction of depositional environment of a tropical estuary and response of $ä^{13}C_{org}$ and TOC/TN signatures to changing environmental conditions. Estuarine Coastal Shelf Science, 139, 137-147.

Wensink H., (1973). Newer paleomagnetic results of the Deccan Traps, India. Tectonophysics, 17, 41-59.

Jour. Indian Association of Sedimentologists, Vol. 34, Nos. 1 & 2. (2017), pp. 103-119

Geochemistry of Mudflat and Mangrove Sedimentary Environments, within Tropical (Sharavati) Estuary, Karnataka Coast, India

MARIA C. FERNANDES AND G. N. NAYAK*
Department of Marine Sciences, Goa University, Goa, India, 403206
*E-mail: nayak1006@rediffmail.com, gnnayak@unigoa.ac.in

Abstract: Five sediment cores from Sharavati estuary were analysed for sediment components, organic carbon and selected metals with 2 cm interval. Progressive sorting of sediments was noted in the Sharavati estuary from the mouth to middle estuarine region. Sand in the vertical section showed overall decreasing trend which is compensated by increase in the finer sediments and organic carbon in recent years except in core F1. The data revealed prevalence of relatively higher and varying hydrodynamic energy conditions facilitating greater deposition of sand particles in the past, while, lower and stable hydrodynamic conditions in recent years seemed to have resulted in deposition of finer particles towards the surface. Metals in different sediment size fractions indicated their association with finer sediments. In addition Fe-Mn oxides played a major role in distribution of metals in sediments. Cobalt showed value almost equal to Apparent Effects Threshold (AET) in core G2 of upper middle region, suggesting risk of toxicity and high bioavailability of Co to sediment dwelling organisms. Risk Assessment Code (RAC) criteria also indicated high risk of Co in core G1 and shows medium risk in the other cores.

Keywords: Sediment core, Sharavati estuary, metals, speciation.

INTRODUCTION

An estuary is a transition zone, between land and sea, where there is large mixing of marine and fresh waters which results in large change of pH and salinity, thereby, redistributing sediments and enhancing the rate of sedimentation. Estuary is divided into lower, middle and upper regions. Lower is dominated by marine and upper by fresh water, middle representing mixing. The boundaries between the three transition zones vary with tides, season, and weather (Fairbridge, 1980). Distribution of sediments within estuaries is often classified on the basis of grain size which in turn helps in understanding the hydrodynamic conditions prevailing in the area. Low energy central mixing zone facilitates deposition of large quantity of finer sediments (Dalrymple et al., 1992). The estuarine mouth generally seems to be largely dominated with sand content whereas middle and upper region with finer sediments. Mudflats and mangroves are adjacent sub-environments along estuarine tidal flats in tropical region (Harbison, 1986). Mudflats cover large unvegetated areas that are exposed during low tide and submerged during high tide (Reineek, 1972). Mangroves, on the other hand, are salt tolerant shrubs and trees associated with a unique horizontal root network (Kumaran et al., 2004). They primarily consist of fine sediment deposits (<63 μm) and are influenced by tides, waves and fluvial processes (Lesueur et al., 2003). These fine sediments retain large organic matter and act as sink for a wide range of metals which show high affinity for fine grained sediments. In the present study, cores collected from micro tidal Sharavati estuary were investigated. Within the catchment area of Sharavati River, a hydroelectric dam named "Linganamakki" commissioned in 1964 has probably had its impact on the sediment distribution pattern in Sharavati estuary. Mudflats and mangrove generally are formed in the middle and lower estuarine region and are sensitive to changes in sea level and the effects of reclamation and industry. The metals accumulation in the sediments of estuaries is of major concern because of their toxicity, persistence and bio-accumulative nature and may be transferred to the overlying water column thereby entering into the food chain (Nemati et al., 2011; Díaz-de Alba et al., 2011). Further, the metals introduced by human activities show greater mobility and are associated with bioavailable sediment phases, such as, carbonates, oxides, hydroxides and sulfides (Passos et al., 2010; Heltai et al., 2005) while, those from weathering of rocks are less mobile. Major sources of metals in aquatic systems are the rock weathering and anthropogenic activities including industrial wastewater, drainage of land, atmospheric inputs, soil erosion, biological activities and urban wastes (Carman et al., 2007). Estimation of only total metal concentrations in sediments is not suitable to determine their mobility (Tüzen, 2003) as the bioavailability and prospective toxicity of the metals to

the biota depends on their chemical forms (Ahlf et al., 2009). Therefore, it has become a necessity to determine associations of the metals with different geochemical phases. Though sequential extraction procedure is complicated and lengthy, it provides adequate information related to the origin, occurrence, biological/ physicochemical aspects, mobilization and transport of metals. It emulates mobilization and retention of the metals in the aquatic ecosystems by changes such as, pH, redox potential and degradation of organic matter. In this paper an attempt is made to:

1) Study the distribution and abundance of sediment components, organic carbon and selected elements in sediments with time

2) Understand the depositional environment, post depositional processes

3) Understand the role played by different sediment size fraction in distribution of metals and

4) Understand the bioavailability of metals and their toxicity.

STUDY AREA

Karnataka coastline extends over a length of 320 km. For the present study, five sediment cores were collected from one of the large estuaries, along this coast. Sharavati River has catchment area 2985 km² and is one of the important rivers (Fig. 1) whose basin falls into two districts of Karnataka namely Uttara Kannada and Shimoga. A hydroelectric dam was commissioned in 1964 at Linganamakki, which has water spread area of 357 sq km. The length of the river is 128 km. The tidal influence is up to 15 km from the mouth towards upstream of the estuary. The soil texture is mainly clayey, sandy loam and sand distributed. The catchment area consists of grey granite, migmatites, granodiorite, metabasalts, greywacke, alluvium, and quartz chlorite schist with orthoquartzite are spread across the study area. Annual rainfall in the region ranges from 3521±619 mm (Honavar) 4339±1249 mm (Gerusoppa).

MATERIALS AND METHODS

Five sediment cores, three from mudflat and two from mangrove sedimentary environment from Sharavati estuary (Fig. 1) were collected. Mudflat cores are denoted by letter "F" and mangrove cores are denoted by letter "G". The cores were sub-sampled at 2 cm interval, homogenized, stored at 4°C and later oven dried at 60°C. A small quantity (5 g) of sediment was powdered. 10 g of the unground sample was analysed for sand, silt, clay (Folk, 1968) and a portion of powdered sample was analysed for organic carbon using the procedure by Walkley-Black method (1947), adopted and modified by Jackson (1958) and total metals were extracted by HF, HNO_3 and $HClO_4$ acid mixture (Jarvis and Jarvis, 1985). Further, two cores were selected for metals analysis in each of the different sediment size fraction viz. sand (4Ø); medium silt (6Ø) and clay (8Ø). Same procedure was also followed for reference standard 2702

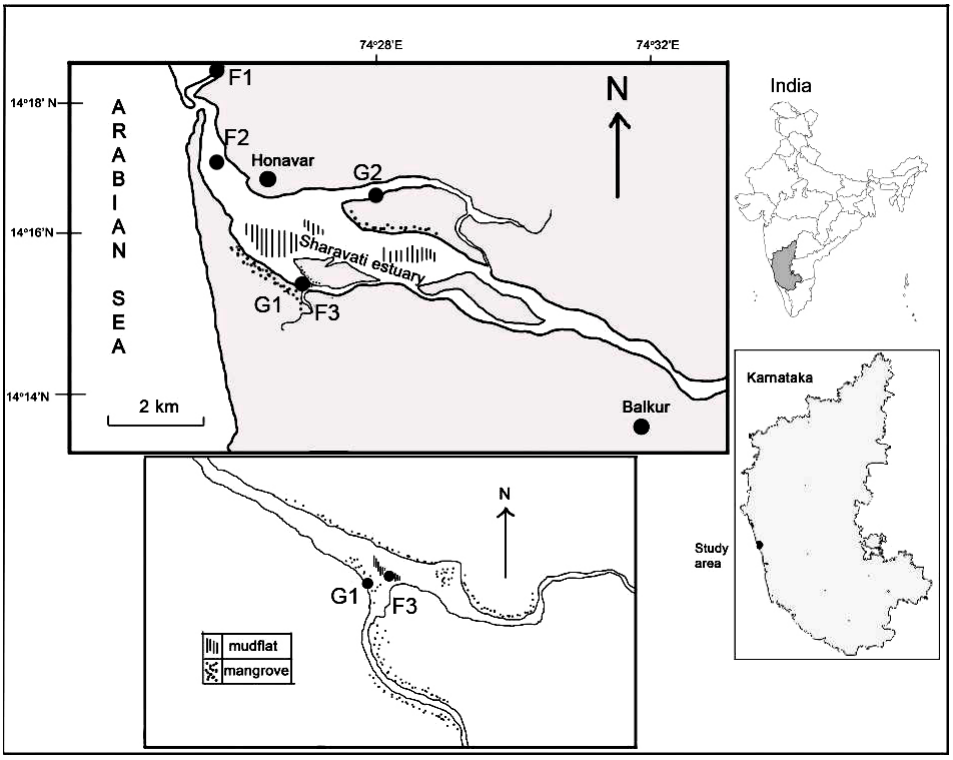

Fig. 1. Map showing locations of sediment core collection in Sharavati estuary.

obtained from National Institute of Standards and Technology (NIST) to ensure accuracy of the analytical method. Samples were analysed for eight different metals viz. Al, Fe, Mn, Ni, Zn, Cu, Co and Cr using Atomic Absorption Spectrophotometer (Varian AAS 240FS model, Australia). Internal chemical standards obtained from Merck were used to calibrate the instrument and recalibration checks were performed at regular intervals. Speciation studies were also carried out for selected samples of selected cores following the procedure given by Tessier et al., (1979), for Fe, Mn, Ni, Zn, Cu, Co and Cr. The procedure involves extraction of five phases, viz., Exchangeable, Carbonate, Fe–Mn oxide, Organic matter/sulphide bound and the Residual phase. Further, to understand the potential bioavailability or the risk of toxicity of the studied metals to the biota, the average (avg.) concentration of metals obtained after total acid digestion, as well as sequentially extracted bioavailable fractions (i.e. sum of exchangeable, carbonate, Fe - Mn oxide and organic bound) were compared with the Sediment Quality Values (SQV) following Screening Quick Reference Table (SQUIRT). SQUIRT was developed by NOAA for screening purposes. Based on SQUIRT, the guideline values are categorized into five classes, given by Buchman (1999), which elucidate the toxicity level of the metals. The implication of SQV is to achieve the information on toxicity of metals to the biota and understand the impact on environment (Attri and Kerkar, 2011). The Risk Assessment Code (RAC) as proposed by Perin et al. (1985) was calculated which indicates that sediment in exchangeable and carbonate fraction, if less than 1% of the total metal will be considered safe for the environment. On the contrary, sediment releasing in the same fraction more than 50% of the total metal has to be considered highly dangerous and can easily enter the food chain. The values are interpreted in accordance with the RAC percentage classifications. Pearson's correlation was obtained between the different parameters by using the computer software STATISTICA.

RESULTS AND DISCUSSION

Sediment Components and Organic Carbon

Five sediment cores were collected from Sharavati estuary namely F1 (Fig. 2), F2 (Fig. 3) and F3 (Fig. 4), from mudflat sedimentary environment and G1 (Fig. 5) and G2 (Fig. 6) from mangrove sedimentary environment. Core F1 and F2 were collected from the lower estuary, while, F3, G1 and G2 were collected from the middle estuary. Core F3 and G1 were collected adjacent to each other. On the basis of the distribution of sediment components, core F1 can be divided into two sections. Section 1 from 28 to 18 cm and section 2 from 18 cm to the surface. Core F2 can be divided into three sections. Section 1 from 60 to 36 cm; section 2 from 36 to 14 cm and section 3 from 14 cm to the surface. Core F3 can be divided into three sections; section 1 (46 – 22cm), section 2 (22 – 8 cm) and section 3 (8 – 0 cm). Core G1 can be divided into three sections; section 1 (40 – 22 cm), section 2 (22 – 6 cm) and section 3 (6 – 0 cm). Core G2 can be divided into two sections; section 1 (52 – 16 cm) and section 2 (16 – 0 cm). In mudflats, when the average values (Table 1) of sediment components and organic carbon of cores F1, F2 and F3 were compared, it is noted that all the three cores were highly dominated by sand content and organic carbon was found to be relatively higher in core F3 which was collected at the middle estuary as compared to cores F1 and F2 which were collected at the lower estuary. Among all the three mudflat cores, core F3 showed large range in variation of sand, silt, clay and organic carbon. Among all the studied cores in Sharavati estuary, sand showed an overall decreasing trend except core F1 which was collected from the north of mouth of river Sharavati. The source of sand for core F1 could be from river Badagani flowing from north side of mouth of Sharavati and a part of it entering the estuary. Silt and clay showed an overall increasing trend. Among the mangroves, when the average values of sediment components and organic carbon of cores G1 and G2 were compared, it is noted that the average sand content was higher in core G1 which was collected at lower middle region and mud content (silt + clay) was found to be higher in core G2 which was collected from the upper middle region. The average organic carbon was also found to be higher in core G2 and it also showed large range in variation of sand, silt and organic carbon. Higher deposition of mud content (silt + clay) reflects periods of calmer energy conditions which facilitated deposition of finer sediments. Core F1 maintained high sand values uniformly with time indicating availability of higher energy conditions throughout the core.

Table 1. Range and average values of sand, silt, clay and organic carbon (OC) in mudflats and mangroves.

Core	Sand			Silt			Clay			OC		
	Min	Max	Avg	Min	Max	Avg	Min	Max	Avg	Min	Max	Avg
F1	65	87	80	2	11	6	10	24	15	0.24	0.9	0.49
F2	53	94	78	0.07	29	8	4	32	14	0.03	1.5	0.44
F3	42	96	76	0.28	32	8	3	33	16	0.03	2	0.79
G1	59	94	82	0.01	13	4	6	34	14	0.06	2	0.41
G2	23	78	58	1	58	25	11	34	18	0.4	5	2

Sand is the major sediment component in all the five cores studied. Sand content in an area generally reflects high energy hydrodynamics due to its size and settling velocity. In core F1 (lower estuary), collected at the northern part of mouth of Sharavati estuary, sand showed higher than average values in section 1 as compared to core F2 (lower estuary) which was collected from the southern part of the mouth. Sand showed decreasing trend in core F2 (lower estuary) and F3 (middle estuary) from section 1 to 2, however, higher sand content was noted in section 3 at the surface of core F3. Among the mangrove cores, in core G1 (lower middle estuary), sand showed constant value with more than average line in section 1, fluctuating along the average line in section 2, and lower values in section 3. In core G2 (upper middle estuary), sand showed constant trend in section 1 and decreasing trend in section 2. When the average sand content in mudflat and mangrove cores were compared, higher sand content was noted in mangrove core G1 with 82% followed by F1 (80 %) > F2 (78 %) > F3 (76 %) > G2 (58 %). In general, mangroves environment is known to retain finer sediments as compared to the mudflats, however, higher sand content in core G1 could be due to the coarser material brought by the adjoining tributary. Sand content in mudflat cores F1, F2 and F3 reflects decreasing wave action towards the upstream of the estuary facilitating deposition of finer sediment. Therefore a progressive sorting of sediment is noticed from lower to the upper middle estuary as the tidal energy decreases away from the mouth. Higher mud (silt and clay) content in cores G2 and F3 reflects processes like flocculation of sediments which facilitate the deposition of finer sediments in the middle estuarine region due to the mixing of fresh water and saline water. Clay has a tendency to aggregate with each other forming large particles that settle at the bottom of the estuary. Higher sand percentage in section 1 of cores F2, F3, G1 and G2 suggest that sediments in the past were probably deposited in the high energy conditions. Decrease in the sand percentage from 14 cm could be due to reduced supply of coarser material due to the activities within the catchment area like building dams, change in rainfall pattern and runoff, and sea level changes bringing a change in sedimentation pattern. Sharavati River must have contributed significantly in the reduction of sand content. Dredging activities within the lower reaches must have also contributed for the distribution of sediment components (Huaiyang et al., 2004) as it amounts the resuspension and settling of finer sediments. Increase of clay percentage in the top section of these cores probably reflects a calmer energy conditions during their deposition (Dolch and Hass, 2008). The depth wise distribution pattern suggests the prevalence of relatively higher energy conditions facilitating greater deposition of coarser sediments in the past. Finer sediments towards the surface must have been deposited in lower hydrodynamic condition in the recent year. However, in case of core F1, it is noted that sand percentage is higher in section 2 and mud fraction is higher in section 1. Besides the hydrodynamic condition, sediment source also plays an important role in the distribution of grain size (Yang et al., 2008). The high sand percentage, almost 80 % throughout this core could be due tidal energy flushing the finer sediment component leaving behind the coarser ones.

Organic carbon profiles of all the cores showed similar distribution trend to that of the finer sediments indicating its association. Among the mudflat cores, higher average value was found in core F3, collected at the middle estuarine region, favouring its deposition. Organic carbon was found to be increasing from bottom to surface in cores F2 and F3 whereas in core F1, it showed decreasing trend. Among the mangrove cores, higher average organic carbon was noted in core G2 collected at upper middle estuarine region as compared to core G1. In core G1, it showed constant trend in section 1 and 2 and higher values at the surface, whereas, in core G2, it showed constant trend in section 1 and increasing trend in section 2. Organic carbon profile in all the cores (mudflat and mangrove) shows a similar trend to that of silt and clay though; in core G2 it shows association only with silt. It is well established that organic carbon is generally associated with the finer sediments as compared to the coarser sediments (Dessai et al., 2009) which is mainly due to surface area/volume ratio of the sediment grain (Muzuka and Shaghude, 2000). The decrease in the organic carbon with depth in cores F2, F3, G1 and G2 can be attributed to its degradation. In sandy marine sediments, oxygenated water can easily percolate through the coarser sediments leading to high rate of degradation as compared to the finer sediments (Singh and Nayak, 2009). Higher values of organic carbon in the upper sections of these cores indicate enhanced supply of organic material from the overlying water column or the organic matter are yet to undergo degradation. In mangrove core G2, highest percentage of organic carbon is noted (2%) as compared to other cores. This is probably due to additional organic matter supplied from the surrounding mangrove litter. It is observed that organic carbon in all the mudflat cores of minor estuaries also shows similar profile to that of finer sediment components indicating its association (Mayer and Xing, 2001; Falco et al., 2004).

Distribution of Metals in the Bulk Sediment

Major elements (Al, Fe and Mn)

In core F1, Al profile maintained a constant trend along the average line (Fig. 2). However, it showed higher values in section 1 as compared to section 2. Similar distribution pattern is also observed in case of Fe and to some extent Mn profiles. Al, Fe and Mn showed peak values at 20 cm depth. In core F2, Al showed lower values

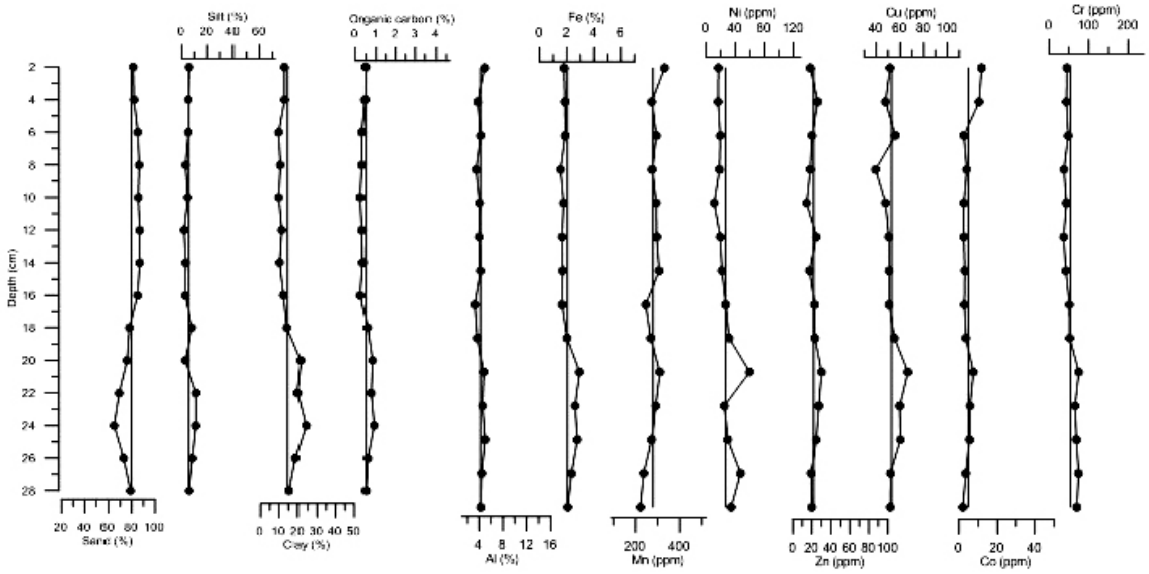

Fig. 2. Vertical profiles of sediments components, organic carbon and metals in core a) F1 (Sharavati estuary – lower region)

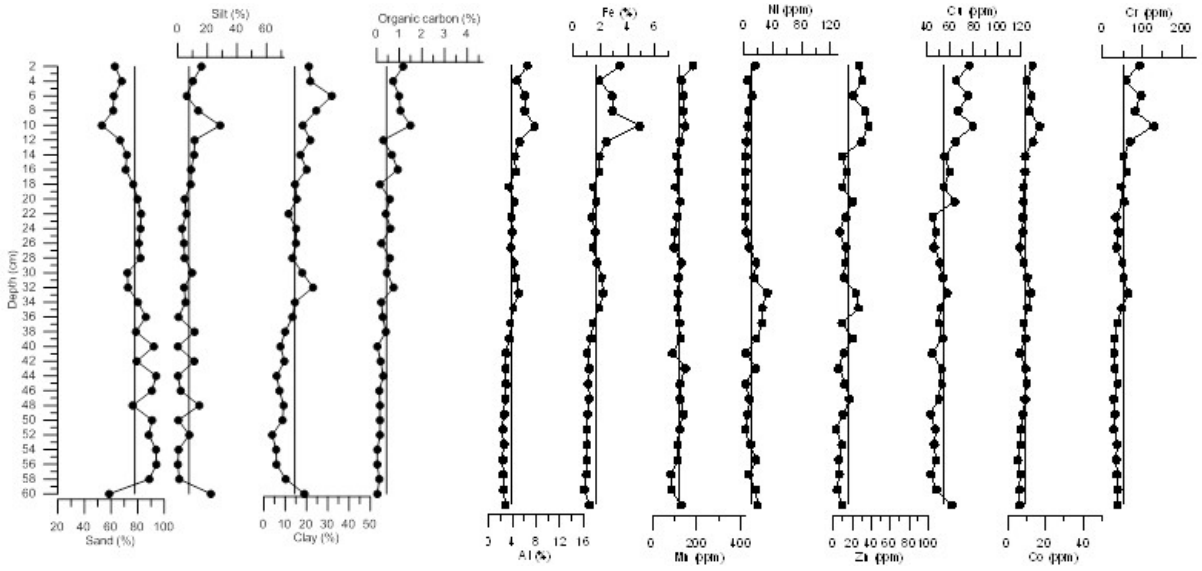

Fig. 3. Vertical profiles of sediments components, organic carbon and metals in core F2 (Sharavati estuary – lower region).

than the average in section 1. Further, it remained constant along the average line (Fig.3) in section 2. In section 3, it showed higher values. Similar profile was also observed in case of Fe. However, Mn profile maintained a constant trend throughout the core. In core F3, the distribution of Al shows an increasing trend in section 1 and 2 followed by a decreasing trend in section 3 showing positive peak value at depth 12 (prominent) and 4 cm (Fig. 4). Similar distribution pattern is also observed for Fe throughout the core and in section 1 and 2 in case of Mn. All the three elements maintain lower than average values in section 1 in core F2 and F3 and higher than average in section 2 in core F3. In section 3, Al and Fe, showed a peak at 4 cm depth in core F3 and at 10 cm depth in core F2 and then decrease. Mn, however, maintained a constant value in section 3. Higher values of Fe and Al, between 20 cm and 4 cm with peaks at 12 cm of Al, Fe and Mn and, at 4 cm of Fe and Al in core F3 and, peak at 10 cm depth of Al and Fe in core F2 indicate either additional input of sediments with these metals or remobilization of Fe and Mn during early diagenesis. Low values of metals at the surface are probably due to the removal of these ions from the sediments to the water column above, through diffusion processes (Badr et al., 2009). Like fine sediments, Al, Fe and Mn maintained higher values in section 1 for core

F1. Among the mangroves, in core G1, Al showed an increasing trend from section 1 to 3 with positive peak at 18 cm (prominent) and elevated values at the surface. Similar distribution pattern was also observed for Fe (Fig. 5). However, Mn showed similar distribution pattern to Al and Fe only in section 1 and 2 but having a prominent peak at 20 cm depth. In section 3 it exhibited constant trend. Peak values of Al and Fe coincides with peaks of clay and organic carbon and peak of Mn coincide with that of silt peak at 20 cm depth. In core G2, Al showed constant trend in section 1 (Fig. 6). Further, in section 2 it showed increasing trend up to the surface. Fe and Mn showed similar fluctuating distribution profiles with lower values than average line in section 1, whereas in section 2 they showed large increase. They showed higher value at 40 cm which coincides with peak of clay in section 1 and peaks at 8 and 4 cm which largely coincides with silt and organic carbon in section 2.

Minor elements (Ni, Zn, Cu, Co and Cr)

In mudflats, in core F1, Ni shows higher values than average in section 1 with a peak at 20 cm depth. Further, it shows a decreasing trend in section 2 (Fig. 2). Zn, Cu, Co and Cr show similar distribution trend to that of Fe indicating a similar source or remobilization. Cu and Co, however show higher values near surface like Mn. In core F2, Ni shows almost constant value in section 1 with slightly higher values between 38 and 32 cm depth where as in section 2 it shows lower values than average line (Fig. 3). Zn shows an increasing trend in section 1, remains constant in section 2 and shows an increasing values in section 3 having a peak value at 10 cm depth similar to Al and Fe. Similar distribution is also noticed by Cu, Co and Cr. It is further noted that Zn, Cu, Co and Cr show similar distribution to that of Al indicating their association with Al and natural source. Further, concentration of metals is also similar to that of Fe especially near surface which indicates precipitation of Fe oxyhydroxides and co-precipitation of metals in the top sections of the core (Selvaraj et al., 2010). In core F3, all trace metals show an increasing trend from section 1 to section 2 and decreasing trend in section 3 (Fig. 4). They show similar trend to that of Al, Fe and Mn, with peak value at 12 cm depth. Except Cr, all metals also show small peak at 4 cm. Among the mangroves, in core G1, all trace metals show similar distribution trend in section 1 which is almost constant to the average line, probably originating from the same source (Fig. 5). In section 2, Ni, Zn Cu and Cr show small peak at 18 cm which coincide with peaks of Al and Fe. Cu shows a peak at 12 cm which coincide with peaks of Al, Fe and Mn as well. In section 3, however they show slight increase similar trend to that of Al and Fe. In core G2, Ni and Cu show largely similar distribution trend to that of Fe and Mn indicating a diagenetic remobilization and enrichment towards surface (Fig. 6). However, Zn, Co and Cr show similar trend to that of Al indicating their association and lithogenous source.

The distribution of Al is largely governed by the distribution of finer sediments throughout the cores as Al is largely associated with Aluminosilicates. Similar distribution of Fe and Mn with Al indicate their common terrigenous source. Fe and Mn show largely similar distribution pattern in core G2, section 1 and 2 of core F3, indicating similar source and/or show similar early digenetic mobilization. The redox sensitive elements, Fe and Mn have been widely used to understand the diagenetic processes (Caetano et al., 2009). Normally, Fe^{2+} and Mn^{2+} species get precipitated in the top layers of sediment after being removed through the pore water of subsurface sediments (Klinkhammer et al., 1982) as observed at 10 cm depth in section 3 of core F2; at 12 and 4 cm of core F3; at 10 and 12 cm in in core G1 and in section 2 of core G2. Enrichment of Fe and Mn in top layers indicates the precipitation of these redox sensitive elements as oxides and hydroxides, and the low Fe and Mn content in the bottom layers reflect their dissolution (Pande and Nayak, 2013) and possible migration. It is noted that the distribution pattern of all studied trace metals except Co in core F1 and G1, Ni in core F2 and Cr in core F3 largely follows the distribution pattern of Al and Fe indicating similar source and post diagenetic processes. The exceptions viz. Co in core F1, Ni in core F2 and Cr in core F3, especially near surface follow the trend of Mn. Enrichment of metals towards the surface in cores F2, F3, G1 and G2 indicated either additional input received during recent years or diagenetic remobilizaition. The protected area of core G2 must have facilitated the deposition of sediments under relatively less violent hydrodynamic conditions thereby recording the changes in metal input from past to present. Decrease in fresh water inflow over a period of time is known to be one of the factors which may contribute to the gradual accumulation of metals along with finer sediments within the estuary (Ruiz and Saiz-Salinas, 2000). The metal input could also be from other sources like agriculture, domestic waste, industrial effluents etc.

Pearsons Correlation for parameters of bulk sediments

In order to understand the elemental association, correlation tests were carried out for the data set of F1, F2 and F3. Analysis of correlation coefficient among the different chemical components for core F1 shows a significant positive correlation of Al with clay (0.63), organic carbon (0.69), Fe (0.69) along with trace metals Cu (0.85) and Cr (0.87). In core F2 and F3, Al showed a significant correlation with finer sediments, organic carbon, Fe and Mn along with all trace metals (except Ni in core F2). In core F1, Fe showed significant positive correlation with finer sediments, organic carbon and trace metals (except Co). In core F2 and F3, Fe and Mn showed a significant positive correlation with finer

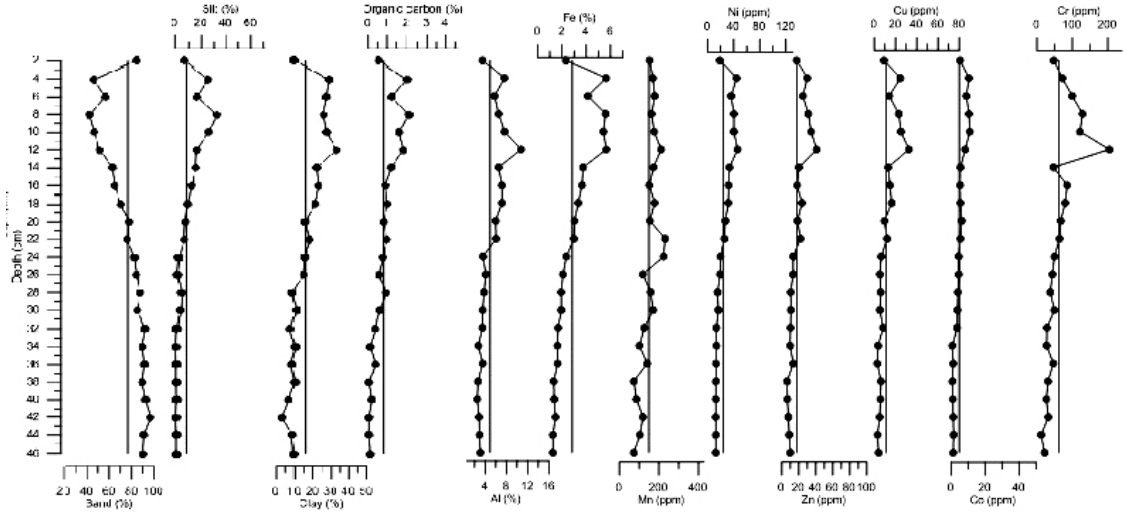

Fig. 4. Vertical profiles of sediments components, organic carbon and metals in core F3 (Sharavati estuary – lower middle region)

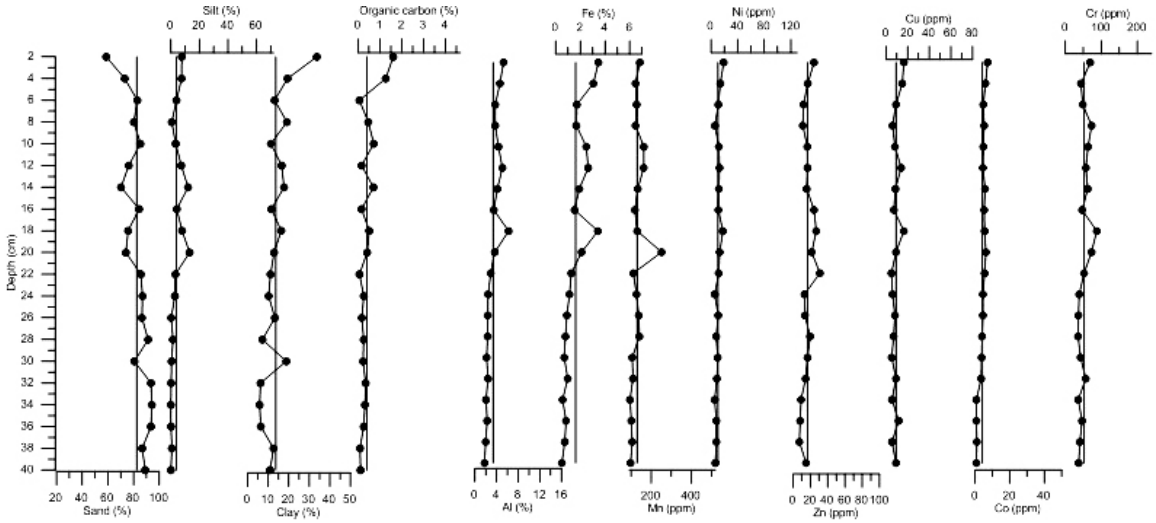

Fig. 5. Vertical profiles of sediments components, organic carbon and metals in core G1 ((Sharavati estuary – lower middle region)

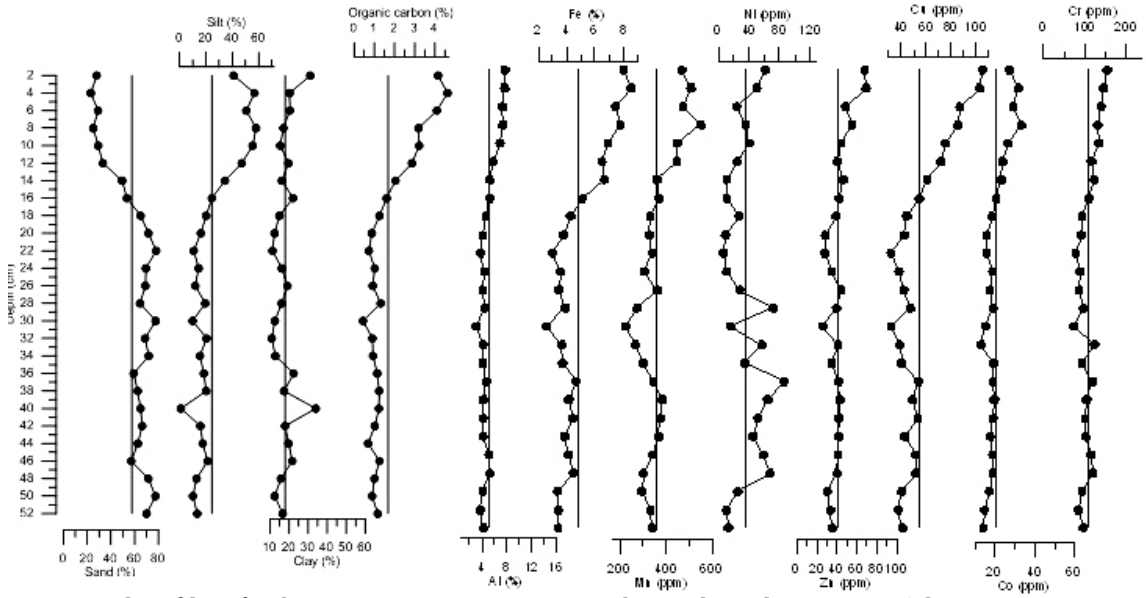

Fig. 6. Vertical profiles of sediments components, organic carbon and metals in core G2 (Sharavati estuary – upper middle region).

sediments, organic carbon and trace metals (except Ni in core F2). A significant negative correlation of sand with all other parameters was observed in all three cores. In core G1 and G2, Al showed significant positive correlation with finer sediments, organic carbon and Fe along with all the trace metals (except Ni in core G2). Further, in core G1, Fe cycling seems to play a major role in the trace metal distribution whereas Mn is associated with Co and Cr only. Therefore, the major controlling factors for the distribution of metals in mangrove core G1 are Al, Fe along with finer sediment components and organic carbon. In core G2, along with fine sediments, organic carbon, Al and Fe, Mn also played a role in distribution of trace elements. Ni in core G2 must be from different source.

Al indicates terrigenous input and is the major component in the clay lattice. Al exhibited signiûcant positive correlation with clay indicating its natural source. The association of Al with fine grained sediments in cores F1, F2, F3, G1 and G2 suggests that the sediments include detrital minerals dominated by phyllosilicates (Jonathan et al., 2004). Also, most metals show positive correlation with fine grained sediments in core F1 (except Mn and Co), F2 (except Ni), F3, G1 and G2 as they have greater affinity for adsorption of metals due to their large surface area as compared to the coarser grained sediment fraction (Mikulic et al., 2008). The strong correlation between these elements and organic carbon reveals an association in the form of organo-metallic complexes (Zourarah et al., 2009). A significant correlation of trace metals with Fe and Mn in core F3 and also in core F2 and G2 (except Ni) suggests that the distribution of trace metals was largely controlled by Fe and Mn cycle. In core F1, Mn and Co show weak correlation with finer sediments, organic carbon and also with Al, Fe indicating their input from different source. Core F1 collected from lower estuary receives input from river Badagani River flowing from north direction and joining Sharavati River at its mouth region, can be source for these metals which may be anthropogenic.

Distribution of Metals in Sediments of Different Particle Size (Sand, Medium Silt and Clay)

The distribution of metals within sediment will depend on the property of each sediment size fraction. Thus the study of metals associated with different size fractions is important to understand the role and its ability to fix metals within the sediments. Here, an attempt has been made to understand the distribution of metals in different sediment size fractions {viz. sand (4Ø), medium silt [silt+clay] (6Ø) and clay (8Ø)} on two cores F1 (mudflat) and G1 (mangrove) collected adjacent to each other in Sharavati estuary.

Sand fraction, in core F3 (Table 2a), decreases from the bottom to the surface i.e. from section 1 to section 3 of the core. This is also true in the case of Mn and Cu distribution. In core G1 (Table 3a), it is noticed that sand percentage decreases from the bottom up to the surface, similar to core F3. Similar distribution is also seen in case of Co in this core. In medium silt fraction, it is seen from table 2b for core F3, that the percentage of silt and organic carbon is higher in the upper two sections as compared to section 1. Similar distribution is also seen in case of the metals (except Zn and Cu). In section 2, it is observed that concentration of Al, Fe and Mn are higher which is also true in case of Cu and Co. In core G1 (Table 3b), it is noticed that all the metals are enriched in section 2 and 3 with higher concentration in section 2. However, in clay fraction, in core F3 (Table 2c) and core G1 (Table 3c) higher percentage of clay and organic carbon is observed in the upper two sections as compared to section 1. Similar distribution is also seen in case of the metals except Zn and Cu in core F3. However in section 2 of core F3, it is observed that the concentration of Al, Fe, Ni, Co and Cr are higher compared to section 1 and 3. In core G1, Al and Fe along with all metals (except Mn, Zn and Cu) were found to be higher in section 3.

Previous studies have demonstrated that grain size is a major factor in controlling sedimentary metal concentration (Lin et al., 2000; Neto et al., 2006). In the sand fraction, decrease in sand, Mn and Cu content from bottom to surface in core F3 (Table 2a) and; sand and Co in G1 (Table 3a) indicates association of these metals with sand grains. In the silt fraction, organic carbon and most of the metals are highly concentrated in section 2 and 3 compared to section 1 in both the cores (Table 2b, 3b). In the clay fraction, of core F3 (Table 2c), organic carbon and metals are highly concentrated in section 2 and 3 (except Zn and Cu). However Al, Fe, Ni, Co and Cr are higher in section 2.

From the above discussion, it is clear that the distribution of Cu is regulated by Mn coating on sand in core F3. Further, association of Al with other metals indicates lithogenic source and consists of feldspars in addition to quartz grains. Compared to silt and clay, role of sand is less in distribution of metals as particles in the size range of coarse silt to fine sand are generally composed of quartz and feldspars, which have relatively low metal concentrations (Ackerman, 1980). Silt in both the cores and clay in mudflat core along with organic carbon are responsible in retaining higher concentration of metals in section 2. Organic carbon increases with increasing finer fraction and decreases with increasing coarser fraction in the sediments (Kumar and Sheela, 2014) due to their similarity in settling velocity. Association of organic carbon with clay fraction is of particular significance in estuarine sediments. Greater accumulation of organic carbon is found in the case of clayey sediment due to larger surface area for the adsorption of organic carbon (Rajamanickam and Setty, 1973). Early diagenetic mobilization is responsible for higher concentration of metals in section 3 of mangrove sediments. However, in case of mudflat, metals are

Table 2. Average value of metals in three different sections with depth in: a) sand (4Ø), b) medium silt (6Ø) and c) clay (8Ø) fraction in mudflat core (F3).

(a)

Section	Sand (%)	OC (%)	Al (%)	Fe (%)	Mn (ppm)	Ni (ppm)	Zn (ppm)	Cu (ppm)	Co (ppm)	Cr (ppm)
3	57	1.5	3	1	93	20	7	5	3	121
2	64	1.2	3	1	119	13	4	7	3	39
1	89	0.3	3	1	136	11	6	9	3	45

(b)

Section	Silt (%)	OC (%)	Al (%)	Fe (%)	Mn (ppm)	Ni (ppm)	Zn (ppm)	Cu (ppm)	Co (ppm)	Cr (ppm)
3	20	1.5	9	7	69	57	115	133	12	309
2	13	1.2	15	8	82	57	135	145	14	274
1	1	0.3	4	4	35	37	137	137	9	71

(c)

Section	Clay (%)	OC (%)	Al (%)	Fe (%)	Mn (ppm)	Ni (ppm)	Zn (ppm)	Cu (ppm)	Co (ppm)	Cr (ppm)
3	23	1.5	13	7	98	49	226	273	12	332
2	23	1.2	15	7	70	77	166	229	13	514
1	10	0.3	9	4	59	28	550	791	8	153

Table 3. Average value of metals in three different sections with depth in: a) sand (4Ø), b) medium silt (6Ø) and c) clay (8Ø) fraction in mangrove core (G1)

(a)

Section	Sand (%)	OC (%)	Al (%)	Fe (%)	Mn (ppm)	Ni (ppm)	Zn (ppm)	Cu (ppm)	Co (ppm)	Cr (ppm)
3	71.56	0.98	2.13	0.58	111.00	5.13	12.75	13.13	4.25	28.00
2	78.96	0.40	1.89	0.44	94.00	1.19	11.00	11.38	6.31	53.25
1	89.15	0.23	1.71	0.43	107.88	1.09	10.81	6.63	8.94	31.38

(b)

Section	Silt (%)	OC (%)	Al (%)	Fe (%)	Mn (ppm)	Ni (ppm)	Zn (ppm)	Cu (ppm)	Co (ppm)	Cr (ppm)
3	6.37	0.98	7.90	3.98	119.43	28.67	123.09	49.86	18.59	120.22
2	6.46	0.40	10.11	4.33	151.54	32.54	128.76	78.09	23.36	266.19
1	0.68	0.23	1.43	0.38	42.56	5.63	85.44	53.75	10.00	31.06

(c)

Section	Clay (%)	OC (%)	Al (%)	Fe (%)	Mn (ppm)	Ni (ppm)	Zn (ppm)	Cu (ppm)	Co (ppm)	Cr (ppm)
3	22.07	0.98	9.75	5.30	172.63	46.13	242.63	87.13	23.75	167.00
2	14.58	0.40	8.89	3.01	131.63	39.31	184.56	93.75	16.69	128.00
1	10.16	0.23	4.54	2.93	180.81	28.91	495.20	205.58	21.65	88.86

probably diffused to water column due to higher rate of flushing compared to mangroves.

Metal Speciation in Sediments

Total metal concentration is usually measured to understand its metal load in sediments but it fails to explain the toxicity to sediment dwelling organisms. The study of elemental speciation in environment is a significant step to understand the potential environmental risk, mobility and bioavailability of pollutants (Tuzen, 2003). Therefore to know the processes governing metal accumulation and bioavailability, speciation study was carried out on redox sensitive elements (Fe and Mn) together with trace metals Ni, Zn, Cu, Co and Cr. Three cores were selected for metal speciation viz. F3 (Fig. 7), G1 (Fig. 8) and G2 (Fig. 9).

Iron (Fe) and Manganese (Mn)

From the speciation analyses, it was noted that, Fe was mainly found to be associated in the residual fraction in all the studied cores. Further, next to residual fraction Fe was associated with Fe-Mn oxide fraction. Fe concentration in the exchangeable, carbonate and organic bound are found to be very low. From the vertical variation it was noted that Fe in the bioavailable fractions was high at 28 cm depth in core F3 (Fig. 7); at 18 and 14 cm depth which decreased further at 10 cm and further remained almost constant up to the surface in case of core G1 (Fig. 8). Though high concentration of Mn was associated in the residual fraction considerable amount was available in exchangeable fraction in the studied cores. From the vertical variation it is noted that Mn in bioavailable fractions was highest at 14 cm and 18 cm depth which decreased further at 10 cm and 6 cm depth, later increased towards the surface in core G1.

Trace Metals

In all the studied cores, Ni, Zn, Cu, Co and Cr were largely associated with residual fraction. After residual fraction, Ni was associated with Fe-Mn oxide fraction, organic bound fraction and exchangeable fraction, respectively in core F3, G2 (Fig. 9) and G1, respectively. However, Zn was associated with Fe-Mn oxide fraction in all the studied cores, after residual fraction, while, Cu and Cr were associated with organic bound fraction, after residual fraction in the studied cores. Though large amount of Co was present in residual fraction, considerable amount was associated in the exchangeable fraction in core G1 and G2; and with Fe-Mn oxide bound in case of core F3.

Fe concentration was found to be very low in the bioavailable phases i.e., exchangeable, carbonate bound, Fe-Mn oxide and organic bound fractions when added together. Major quantity (> 80 %) of Fe (except in core G2) and Cr was found to be associated with the residual fraction in all the cores. Metals in this fraction are considered to be in inert phase which are stable and do not react during sedimentation and diagenesis, and therefore have less potential bioavailability as they cannot be mobilized (Tessier et al., 1979, Sarkar et al., 2014). Large amount of Fe associated with the residual fraction (Fraction 5) can thus be directly attributed to its high abundance in the earth's crust. This is probably due to relatively low mobility of this element as compared to Mn, as metals associated with this fraction cannot be remobilized under the conditions normally encountered in nature**.** Considerably higher amount of Mn was present in the bioavailable phases in core G2. The higher concentration of Mn in exchangeable fraction indicates weakly bound Mn, which is the most unstable and reactive (Passos et al., 2010). In G2 (Fig. 9), Mn associated with bioavailable fractions increased and that associated with residual fraction decreased from bottom to surface. While towards the surface of the core, increase of Fe and Mn in Fe-Mn oxide bound fraction is noted in G2. Reductive dissolution of Fe-Mn hydroxides in the suboxic zone, can release dissolved Mn (II) and Fe (II) to pore waters, potentially making them more bioavailable and mobile. These freshly formed Fe–Mn oxides are very efficient at scavenging a variety of metals. Further, decrease in concentration near surface indicates diffusion. If sediments are further disturbed by process of bioturbation or human interference like dredging, else a change in pH due to mixing of fresh water and marine water, redox conditions or degradation of organic matter can lead to release metals at the sediment water interface that is into the estuarine environment, causing a potential risk of toxicity to the organisms in case of cores G2. Considerable amount of Zn is present in Fe-Mn oxide fraction in all the cores (Volvoikar and Nayak, 2015). This could be due of adsorption of Zn by Fe-Mn oxides (Shuman, 1985). Considerable amount of Cu and Cr are present in the organic bound although they are largely associated in the residual fraction in all the cores as they are characterized by high stability constant with organic matter (Avudainayagam et al., 2003). Earlier studies elsewhere in marine sediments have also reported association of Cu with organic matter (Tokalioglu et al., 2000). Thus, solubility and mobility of Cu and Cr is largely controlled by organic matter mineralisation (Caplat et al., 2005) and that of Zn by the redox conditions. Among the studied metals Co is the only metal which is largely available in the labile fractions in core G2.

Risk Assessment

Comparison of average total metal concentration and sum of the bioavailable fractions (first four fractions) in sediments with SQUIRT's table.

Further, in order to understand the risk of metals to the sediment dwelling organisms and consequently to

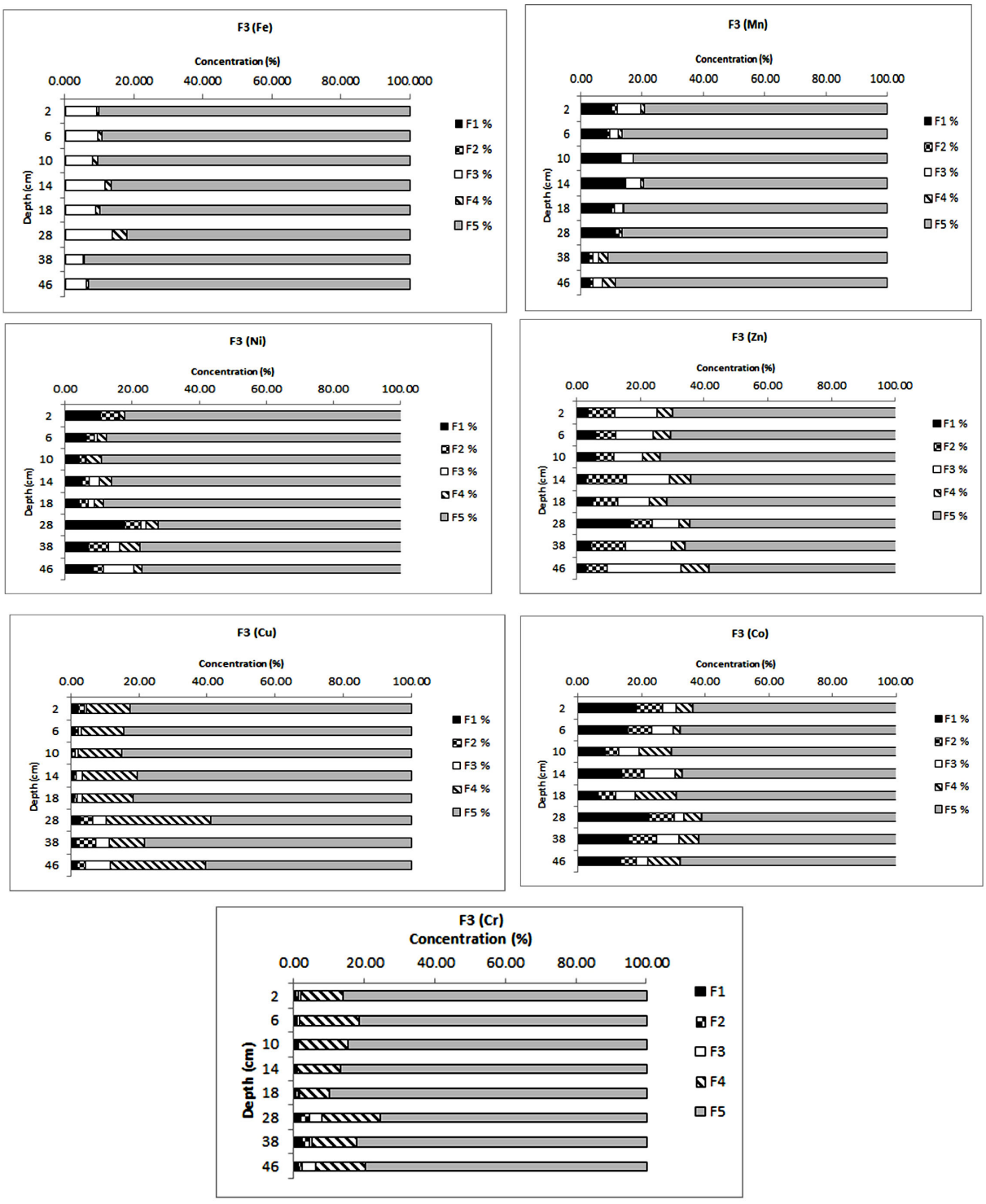

Fig. 7. Extractable contents of Fe, Mn, Ni, Zn, Cu, Co and Cr in Tessier sequential extraction protocol for core F3. F1 exchangeable fraction, F2 carbonate bound fraction, F3 Fe – Mn oxide fraction, F4 organic / sulfide bound fraction, F5 residual fraction.

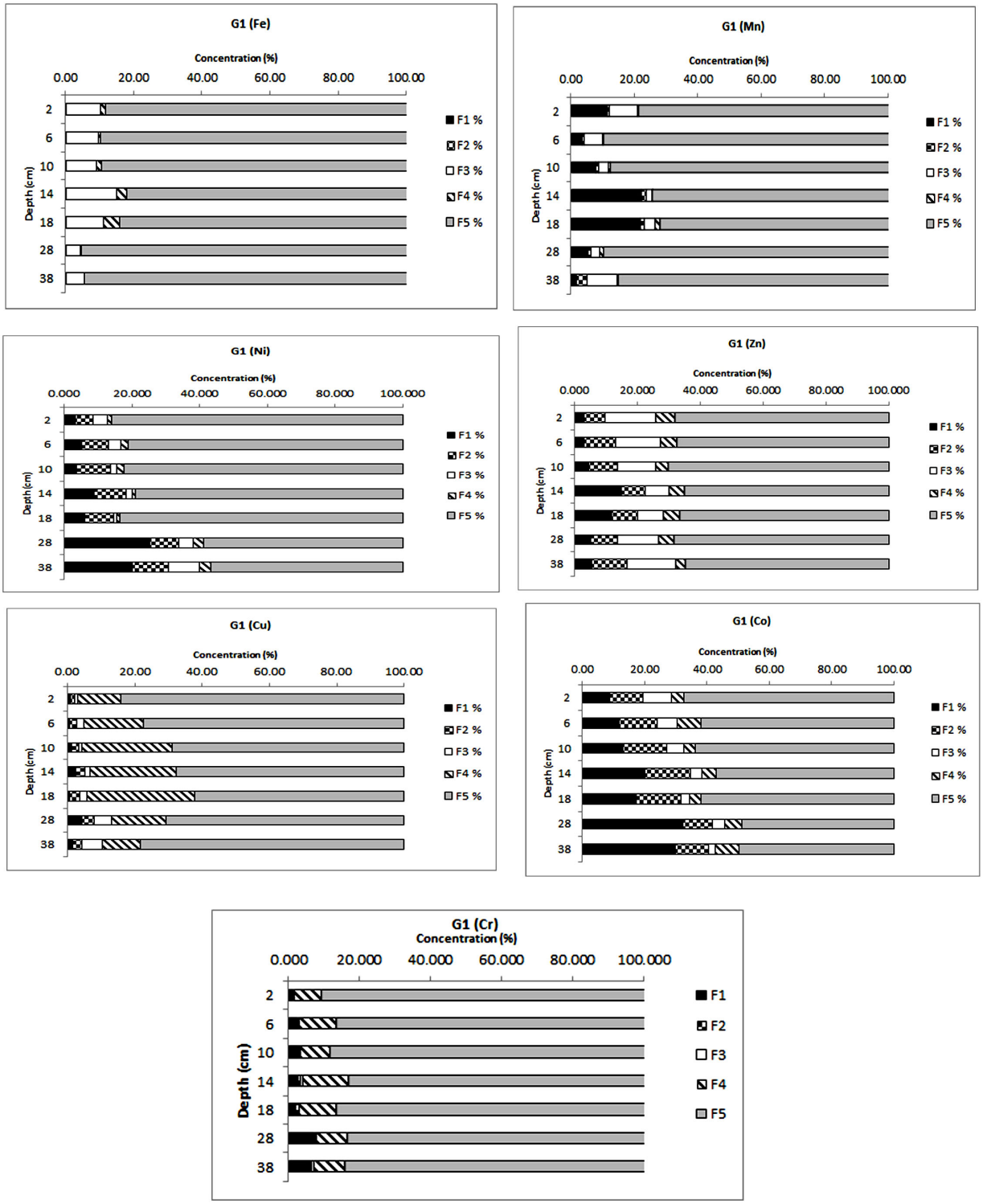

Fig. 8. Extractable contents of Fe, Mn, Ni, Zn, Cu, Co and Cr in Tessier sequential extraction protocol for core G1, F1 exchangeable fraction, F2 carbonate bound fraction, F3 Fe – Mn oxide fraction, F4 organic / sulfide bound fraction, F5 residual fraction.

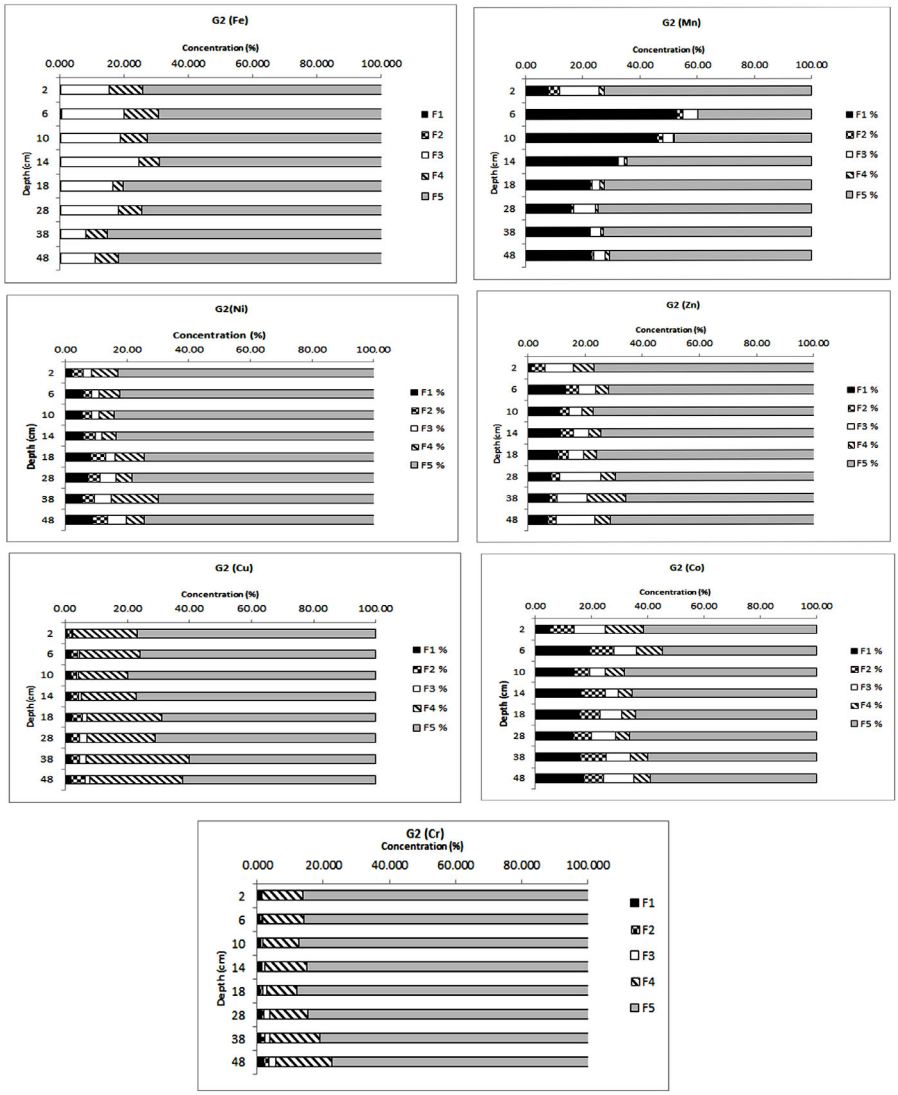

Fig. 9. Extractable contents of Fe, Mn, Ni, Zn, Cu, Co and Cr in Tessier sequential extraction protocol for core G2. F1 exchangeable fraction, F2 carbonate bound fraction, F3 Fe – Mn oxide fraction, F4 organic / sulfide bound fraction, F5 residual fraction.

the human population, the data of metals (Table 4) in the bioavailable fractions (F1 + F2 + F3 + F4) is compared with the sediment quality values (SQV) using SQUIRT (Screening Quick Reference Table). SQUIRT was developed by NOAA for screening purposes (Table 5a & b). The guideline values were categorized by Buchman (1999) into five classes namely TEL, ERL, PEL, ERM and AET. The average total metal concentration in sediments was compared with SQUIRT's table. In the total metal concentration, Mn exceeded the Apparent Effects Threshold (AET) value in core G2. Ni fell in the range between Effects Range Low (ERL) and Probable Effects Level (PEL) in core F3 and G2. Cu fell in the range between Effects Range Low (ERL) and PEL in core G2. Co exceeded the AET value in core G2. Cr fell in the range between Threshold Effect Level (TEL) and ERL in core F3; between ERL and PEL in core G2. However, metal concentration in core G1 was below the Threshold Effect Level (TEL).

Comparison of sum of average percentage of metals in F1 and F2 fraction in sediments with RAC criteria

The risk assessment code indicates the sediment which can release heavy metal in exchangeable and carbonate fractions given by Perin et al. (1985). Risk Code Assessment (RAC) values (Table 6) computed indicates no risk of Fe in the studied estuaries. Medium risk of Mn in core G1 and G2, whereas, low risk in core F3, Medium risk of Ni in cores F3 and G1, and low risk in core G2. Medium risk of Zn in F3, G1 and G2; Cu and Cr values shows low risk in all the studied cores. High risk of Co in core G1 and shows medium risk in the other cores.

In the sum of the bioavailable fractions, Co in core G2 is almost equal to the AET value. Cobalt in all the cores was mainly associated with exchangeable fraction and therefore indicates anthropogenic origin. Co in bioavailable fraction in core G2 exceeded AET

Table 4. Total concentration of metals, bioavailable fractions and sum of exchangeable (F1 %) and carbonate bound fraction (F2 %).

Core		Fe (%)	Mn	Ni	Zn	Cu	Co	Cr
F3	Total metal	3	149	24	17	11	5	62
	F1+F2+F3+F4	0.24	32	5	10	4	5	15
	F1+F2	0..043	10	11	14	3	21	2
G1	Total metal	2	130	11	17	9	4	52
	F1+F2+F3+F4	0.21	33	6	9	5	6	13
	F1+F2	0.074	12	19	16	4	31	4
G2	Total metal	2	364	36	42	55	20	107
	F1+F2+F3+F4	0.12	128	12	15	12	9	20
	F1+F2	0.023	29	10	12	5	22	2

Table 5a. Screening Quick Reference Table (SQUIRT) for metals in marine sediments (Buchman, 1999).

Elements	Threshold Effect Level (TEL)	Effects Range Low (ERL)	Probable Effects Level (PEL)	Effects Range Median (ERM)	Apparent Effects Threshold (AET)
Fe	-	-	-	-	22 % (Neanthes)
Mn	-	-	-	-	260 (Neanthes)
Ni	15.9	20.9	42.8	51.6	110 (Echinoderm Larvae)
Zn	124	150	271	410	410 (Infaunal community)
Cr	52.3	81	160.4	370	62 (Neanthes)
Cu	18.7	34	108.2	270	390 (Microtox and Oyster larvey)
Co	-	-	-	-	10 (Neanthes)

Table 5b. Sediment guidelines and terms used in SQUIRT.

Sediment Guidelines	
Threshold Effect Level (TEL)	Maximum concentration at which no toxic effects are observed
Effects Range Low (ERL)	10^{th} percentile values in effects or toxicity may begin to be observed in sensitive species
Probable Effects Level (PEL)	Lower limit of concentrations at which toxic effects are observed
Effects Range Median (ERM)	50^{th} percentile value in effects
Apparent Effects Threshold (AET)	Concentration above which adverse biological impacts are observed.

Table 6. Criteria for Risk Assessment Code (RAC) by Perin et al., 1985.

Risk Assessment Code (RAC)	Criteria (%)
No risk	< 1
Low risk	1 - 10
Medium risk	11 - 30
High risk	31 - 50
Very high risk	> 50

therefore suggesting a high risk of toxicity. Fe, Ni, Zn, Cu and Cr were mainly bound to the residual fraction and represented metals of natural origin. Also, the percentage of Fe and Mn along with Ni, Zn, Cu and Cr was very low compared to AET indicating no harm to the biota. However, Co associated with bioavailable fractions exceeded the AET suggesting risk of toxicity of Co to organisms (Fernandes et al., 2014) associated with the sediments of core G2 (upper middle region on Sharavati estuary).

CONCLUSIONS

The study of distribution of sediment components in general, indicated a decrease in deposition of coarser sediments and simultaneous increase in deposition of finer sediments from bottom to surface of cores except core F1. Thus suggested prevalence of relatively higher and varying hydrodynamic energy conditions facilitating greater deposition of sand particles in the past, while, lower and stable hydrodynamic conditions in recent years seemed to have resulted in deposition of finer particles towards the surface. Spatial variation in distribution of sediment components was attributed to the location of core samples from which they were collected. High average sand percentage in cores collected from lower region (core F2) and high mud content in cores collected from middle region (core G2) of Sharavati estuary was attributed to progressive sorting of sediments by tidal currents as well as decrease in the energy conditions away from the mouth. Organic carbon profiles of all the cores were similar to that of finer sediments profiles indicating similar settling velocity of the two and their association. Along this coast systematic distribution of sediment components in mangroves and large fluctuation in case of mudflats was noted. Therefore, variation in hydrodynamics affected mudflats and less in mangroves. The result indicated association of Al with sedimentary components such as silt and clay in all the cores. The similarity in distribution of Fe and Mn with Al at various depths further represented portion of alumina-silicate mineral bound fraction and / or weathered material of terrestrial source rock. Diagenetic enrichment of Fe and Mn was noted in all the cores. Distribution of trace metals namely Ni, Zn, Cu, Co and Cr was also studied. Large similarity in vertical distribution patterns of metals in most of the studied cores suggested that they were derived from the same source and / or had undergone similar post-depositional changes except for Mn, Ni and Co in some cores indicating their origin from a different source. Finer sediment and organic carbon was found to play a significant role in distribution of metals in all the cores. High Mn along with high sand content in core F1 and F3 indicate a Mn coating on coarser particle and further indicating an anthropogenic source. The study of metals in different sediment size fractions of mudflat (F3) and mangrove (G1) cores in the middle estuary revealed coarser sediments at the bottom section and finer sediments in the upper sections. However, the average sand content was relatively higher in the mangrove core. Metals are enriched in the upper sections indicating the role of finer sediments and organic carbon in their distribution. Relatively higher amount of Mn and Co was associated with exchangeable fraction in core G2 (Sharavati), indicating an anthropogenic input in recent years. Change in the pH conditions due to fresh water influx from the upper middle estuary has led to the diffusion of metals to the overlying water column. However, change in Eh conditions mobilises the metals associated with Fe-Mn oxide (fraction 3) and organic bound (fraction 4) as the conditions change from anoxic to oxic. Zn was largely associated with Fe-Mn oxide fraction, whereas, Cu and Cr with organic bound fraction. Cobalt showed value equal to Apparent Effects Threshold (AET) in core G2, thus suggesting its risk of toxicity and high bioavailability to sediment dwelling organisms. Also risk Assessment Code (RAC) criteria indicated medium risk of Co in core G2 (Sharavati).

References

Ackerman, F., (1980). A procedure for correcting the grain size effect in heavy metal analyses of estuarine and coastal sediments. Environmental Technology Letters, 1, 518-527.

Ahlf, W., Drost, W. and Heise, S., (2009). Incorporation of metal bioavailability into regulatory frameworks-metal exposure in water and sediment. Journal of Soils and Sediments, 9, 411–419.

Attri, K. and Kerkar, S., (2011). Seasonal assessment of heavy metal pollution in tropical mangrove sediments (Goa, India). Journal of Ecobiotechnoloy, 3(8), 09-15.

Avudainayagam, S., Megharaj, M., Owens, G., Kookana, R. S., Chittleborough, D. and Naidu, R. (2003). Chemistry of Chromium in Soils with Emphasis on Tannery Waste Sites. Reviews of Environmental Contamination and Toxicology, 178, 53–91.

Badr, N. B., El-Fiky, A. A., Mostafa, A. R. and Al-Mur, B. A., (2009). Metal pollution records in core sediments of some Red Sea coastal areas, Kingdom of Saudi Arabia. Environmental Monitoring and Assessment, 155, 509–526.

Buchman, M. F. (1999). NOAA screening quick reference tables. NOAA HAZMAT Report 99-111, Seattle, WA, Coastal protection and restoration division, national oceanic and atmospheric administration, pp 12.

Caetano, M., Prego, R., Vale, C., de Pablo, H. and Marmolejo-Rodrguez, J., (2009). Record of

diagenesis of rare earth elements and other metals in a transitional sedimentary environment. Marine Chemistry, 116, 36–46.

Caplat, C., Texier, H., Barillier, D. and Lelievre, C., (2005). Heavy metals mobility in harbour contaminated sediments: the case of Port-en-Bessin. Marine Pollution Bulletin, 50, 504–511.

Carman, C.M., Li, X.D., Zhang, G., Wai, O.W.H. and Li, Y.S., (2007). Trace metal distribution in sediments of the Pearl River Estuary and the surrounding coastal area, South China. Environmental Pollution, 147, 311–323.

Dalrymple, R. W., Zaitlin, B. A. and Boyd, R. (1992). Estuarine facies models: conceptual basis and stratigraphic implications. Journal of Sedimentary Petrology, 62(6), 1130-1146.

Dessai, D. V., Nayak, G. N. and Basavaiah, N., (2009). Grain size, geochemistry, magnetic susceptibility: Proxies in identifying sources. Estuarine, Coastal and Shelf Science, 85, 307–318.

Díaz-de Alba, M., Galindo-Riano, M.D., Casanueva-Marenco, M.J., García-Vargas, M. and Kosore, C.M., (2011). Assessment of the metal pollution, potential toxicity and speciation of sediment from Algeciras Bay (South of Spain) using chemometric tools. Journal of Hazardous Materials, 190, 177–187.

Dolch, T. and Hass, H. C. (2008). Long-term changes of intertidal and subtidal sediment compositions in a tidal basin in the northern Wadden Sea (SE North Sea). Helgoland Marine Research, 62, 3-11.

Fairbidge, R. W., (1980). The estuary: its definition and geodynamic cycle. In: Olausson, E., and Cato, I. (eds.), Chemistry and Biogeochemisry of Estuaries. Pp. 1-36.

Falco, G., Magni, P., Svuori, L. M. H. and Matteucci, G., (2004). Sediment grain size and organic carbon distribution in the Cabras lagoon (Sardinia, Western Mediterranean). Chemical Ecology, 20, 367–377.

Fernandes, M. C., Nayak, G. N., Pande, A., Volvoikar, S. P. and Dessai, D. R. G. (2014). Depositional environment of mudflats and mangroves and bioavailability of selected metals within mudflats in a tropical estuary. Environmental Earth Sciences, 72 (6), 1861-1875.

Folk R.L. (1968). Petrology of Sedimentary rocks. Hemphills, Austin, pp 177.

Harbison, P. (1986). Mangrove muds-A sink and source for trace metals. Marine Pollution Bulletin, 17, 246–250.

Heltai, G., Percsich, K., Halasz, G., Jung, K. and Fekete, I., (2005). Estimation of ecotoxicological potential of contaminated sediments based on a sequential extraction procedure with supercritical CO2 and subcritical H2O solvents. Microchemical Journal, 79, 231–237.

Huaiyang, Z., Xiaotong, P. and Jianming, P. (2004). Geochemical characteristics and sources of some chemical components in sediments of Zhujiang (Pearl) river estuary. Chinese Journal of Oceanology and Limnology, 22 (1), 34-43.

Jackson, M. L., (1958). Soil chemical analysis. New York: Prentice Hall.

Jarvis, I. J. and Jarvis, K., (1985). Rare earth element geochemistry of standard sediments: a study using inductively coupled plasma spectrometry. Chemical Geology 53, 335 - 344.

Jonathan, M. P., Ram-Mohan, V. and Srinivasalu, S., (2004). Geochemical variations of major and trace elements in recent sediments, off the Gulf of Mannar, the southeast coast of India. Environmental Geology, 45, 466–480. doi:10.1007/s00254-003-0898-7.

Klinkhammer, G. P., Heggie, D. T. and Graham, D. W., (1982). Metal diagenesis in oxic marine sediments. Earth and Planetary Science Letters, 61, 211–219.

Kumar, S. P. and Sheela, M. S., (2014). Comparative study of textural and chemical characteristics of riverine and estuarine sediments of a bar built estuary in Tamil Nadu, India. Research Journal of Chemical Sciences, 4(3), 27-31.

Kumaran, K. P .N., Shindikar, M. and Limaye, R. B. (2004). Mangrove associated lignite beds of Malvan, Konkan: evidence for higher sea level during the Late Tertiary (Neogene) along the West Coast of India. Current Science, 86(2), 335–340.

Lesueur, P., Lesourd, S., Lefebvre, D., Garnaud, S. and Brun-Cottan, J.C. (2003). Holocene and modern sediments in the Seine estuary (France): a synthesis. Journal of Quaternary Science, 18(3–4), 339–349.

Lin, S., Hsieh, I. J., Huang, K. M. and Wang, C. H., (2000). Influence of the Yangtze River and grain size on the spatial variations of heavy metals and organic carbon in the East China Sea continental shelf sediments. Chemical Geology, 182, 377–394.

Mayer, L. M. and Xing, B. S., (2001). Organic matter - surface area relationships in acid oils. Soil Science Society of Amerian Journal, 65, 250-258.

Mikulic, N., Orescanin, V., Elez, L., Pavicic, L., Pezelj, D., Lovrencic, I. and Lulic, S., (2008). Distribution of trace elements in the coastal sea sediments of Maslinica Bay, Croatia. Environmental Geology, 53, 1413-1419. 10.1007/s00254-007-0750-6.

Muzuka, A. N. and Shaghude, Y. W., (2000). Grain size distribution along the Msasani Beach, North of Dar es Salaam Harbour. Journal of African Earth Sciences 30, 417–426.

Nemati, K., Abu Bakar, N.K., Abas, M.R. and Sobhanzadeh, E., (2011). Speciation of heavy metals by modified BCR sequential extraction procedure in different depths of sediments from Sungai Buloh, Selangor, Malaysia. Journal of Hazardous Materials, 192, 402–410.

Neto, J. A. B., Gingele, F. X., Leipe, T. and Brehme, I., (2006). Spatial distribution of heavy metals in surficial sediments from Guana-bara Bay, Rio de Janeiro, Brazil. Environmental Geology, 49, 1051–1063.

Pande, A. and Nayak, G. N. (2013). Understanding distribution and abundance of metals with space and time in estuarine mudflat sedimentary environment. Environmnetal Earth Sciences, DOI 10.1007/s12665-013-2298-y.

Passos, E.A., Alves, J.C., Santos, I.S., Alves, J.P., Garcia, C.A.B. and Costa, A.C.S., (2010). Assessment of trace metals contamination in estuarine sediments using a sequential extraction technique and principal component analysis. Microchemical Journal, 96, 50–57.

Perin, G., Craboledda, L., Lucchese, M., Cirillo, R., Dotta, L. and Zanetta, M. L., et al.(1985). Heavy metal speciation in the sediments of northern Adriatic sea. A new approach for environmental toxicity determination. In Lakkas TD (Ed). Heavy metals in the environment, CEP consultants, Edinburg. Environmental Pollution, 110, 3-9.

Rajamanickam, G. V. and Setty, M. G. A. P., (1973). Distribution of phosphorus and organic carbon in the nearshore sediments of Goa. Indian Journal of Marine Sciences, 2, 84-89.

Reineek, H. E. (1972). Tidal flats. In: Rigby, J. K. and Hamblin, W. K. (Eds.), Recognition of Ancient Sedimantary Environments, Tulsa, Okla. Soc Econ Paleontol Mineral Spec Publ, 16:146 – 159.

Ruiz, J. M. and Saiz-Salinas, J. I., (2000). Extreme variation in the concentration of trace metals in sediments and bivalves from the Bilbao estuary (Spain) caused by the 1989-1990 drought. Marine Environmental Research, 49, 307-317.

Sarkar, S. K., Favas, P. J. C., Rakshit, D. and Satpathy, K. K. (2014). Geochemical Speciation and Risk Assessment of Heavy Metals in Soils and Sediments. Environmental Risk Assessment of Soil Contamination, edited by Maria C. Hernandez-Soriano, 918 pp, Publisher: InTech, http://dx.doi.org/10.5772/57295.

Selvaraj, K., Parthiban, G., Chen, C. T. A. and Lou, J. Y., (2010). Anthropogenic effects on sediment quality offshore southwestern Taiwan: assessing the sediment core geochemical record. Continental Shelf Research, 30, 1200-1210.

Shuman, L. M. (1985). Fractionation method for soil microelements. Soil Science, 140 (1), 11-22.

Singh, K. T. and Nayak, G. N., (2009). Sedimentary and Geochemical signatures of depositional environment of sediments in mudflats from a microtidal Kalinadi estuary, central west coast of Inida. Journal of Coastal Research, 25 (3), 641-650.

Tessier, A., Campbell, P. G. C. and Bisson, M. (1979). Sequential extraction procedure for the speciation of particulate trace metals. Analytical Chemistry, 51(7), 844–851.

Tokalioglu, S., Kartal, S. and Elçi, L., (2000). Determination of heavy metals and their speciation in lake sediments by flame atomic absorption spectrometry after a four-stage sequential extraction procedure. Analytica Chimica Acta, 413, 33–40.

Tuzen, M., (2003). Determination of heavy metals in soil, mushroom and plant samples by atomic absorption spectrometry. Microchemcal Journal, 74, 289-297.

Volvoikar, S. and Nayak, G. N. (2015). Impact of industrial effluents on geochemical association of metals within intertidal sediments of a creek. Marine Pollution Bulletin (in press).

Walkley, A. (1947). A critical examination of a rapid method for determining organic carbon in soil. Soil Science 63, 251–263.

Yang, S. L., Li, H., Ysebaert, T., Bouma, T. J., Zhang, W. X., Wang, Y. Y., Li, P., Li, M. and Ding, P. X. (2008). Spatial and temporal variation in sediment grain size in tidal wetlands, Yangtze Delta: On the role of physical and biotic controls. Estuarine, Coastal and Shelf Science, 77, 657-671.

Zourarah, B., Maanan, M., Robin, M. and Carruesco, C., (2009). Sedimentary records of anthropogenic contribution to heavy metal content in Oum Er Bia estuary (Morocco). Environmental Chemistry Letters, 7, 67–78. doi:10.1007/s10311-008-0138-1.

Jour. Indian Association of Sedimentologists, Vol. 34, Nos. 1 & 2. (2017), pp. 121-125

Geochemistry of Heavy Metals and CHNS Composition in the Sediments of Netravati River Basin: Insight into the Pollution Aspects

M.S. Ragi*, P. Saranya, A. Krishnakumar, B. Upendra, T.M. Liji,
K. Anoop Krishnan and D. Padmalal
Hydrological Processes (HyP) Group, ESSO-National Centre for Earth Science Studies (NCESS),
Ministry of Earth Sciences, Government of India, Trivandrum, 695011, India
*Email: ragims369@gmail.com

Abstract: The health of river basin systems in terms of sediment heavy metal distribution pattern is significant in recent times due to the natural and anthropogenic interventions. To map the impact of these interventions in view of pollution the knowledge of heavy metal geochemistry carbon, nitrogen, hydrogen and sulphur (CHNS) compositional outline is warranted. In view of this, this paper focuses on determining both qualitative and quantitative heavy metals and CHNS composition with respect to pollution in riverine sediments of Netravati River basin. Sediment samples from eight stations in the selected area of Netravati River basin collected during June 2015 (monsoon). The sediment metal pollution status attributed by using the enrichment factor and the geo-accumulation index. According to the enrichment factor calculations, the river sediments were treated under minor enrichment, with Cr, Cu, and Mn. The results of geo-accumulation index revealed that sediments of Netravati River were moderately polluted with Cr, Cu, Zn and Mn. Which are above threshold effect concentrations (TECs). The elemental distribution of elements (CHNS) in organic material is the indirect evidence of sedimentary materials origin and its characteristics. The percentage of CHNS in Netravati Riverine sediments ranges of 0.45-2.14, 0.53-1.73, 0.08-0.23 and 0.15-0.20, respectively. The C/N ratio ranges from 4.37-13.62 in riverine samples, implies the influence of organic matter from exogenous sources.

Keywords: Enrichment factor, Pollution, Heavy metals, Sediment, Netravati.

INTRODUCTION

Sediments act as carriers and sinks for contaminants, reflecting the history of pollution (Singh *et al*., 2005), catchment inputs into aquatic ecosystems (Mwamburi, 2003). Metals are a group of pollutants of ecological significance. Which are not removed from water by self-purification, but accumulate in suspended particulates enter the food web (Ghrefat and Yusuf, 2006). They always present in aquatic ecosystems and re-distribute among different components (Linnik and Zubenko, 2000). The sediments serve as a metal pool that releases to the overlying water by natural or anthropogenic processes, causing adverse effects to the ecosystems (Dickinson *et al*., 1996; Fatoki and Mathabatha, 2001). The field and laboratory experiment reveals that accumulation of heavy metals in tissues of animals depends on metal concentration in water.

The objectives of this study is (1) to determine concentrations of major and trace elements** in the Netravati River to assess the toxic to the aquatic environment (V, Cr, Ni, Cu, Zn, Ga, Rb, Sr, Y, Zr, Ba, and La)** (2) to determine carbon, hydrogen, nitrogen and sulphur percentages to account for the distribution of elements (3) comparing metal concentrations in Netravati sediment to the standard sediment quality. (4) to determine the enrichment factor and geo-accumulation index of the metals.

MATERIALS AND METHODS

Study area

The Netravati River (Bantwal-Uppinangadi Stretch), lies between N 12°50′22.8" - 13°11′38.2" and E75°02′34.0"-75°25.4′49.2" (Table 1). Netravati River originates at Bangrabalige valley, Yelaneeru Ghat of Kudremukh in Chikkamagaluru district, Karnataka, India at an elevation of 1000m. This river flows through the Dharmasthala and merges with the river Kumaradhara at Uppinangadi before joining to the Arabian Sea, south of Mangalore. Netravati River is the source of water supply for Bantwal and Mangalore cities. The total length of the river is 103 km from its source to the outfall and catchment area is about 3,657 sq. km.

Table 1. Location in Netravati River.

Sl. No.	Sample code	Geographical Position (GPS)		Location
		Latitude	Longitude	
1	NB 1	12°52'47.8" N	75°02'34.0" E	Bantwal
2	NB 2	12°53'56.4" N	75°02'45.2" E	Bantwal
3	NB 3	12°52'40.9" N	75°06'19.7" E	Bantwal
4	NB 4	12°51'23.0" N	75°09'18.3" E	Uppinangadi
5	NB 5	13°01'05.9" N	75°22'39.8" E	Dharmasthala
6	NB 6	13°00'29.4" N	75°21'11.3" E	Mundaje
7	NB 7	13°08'32.3" N	75°25.4' 49.2" E	Megur
8	NB 8	13°14' 45.89" N	75°20' 37.12"E	Kalasa

Sample Analysis

Carbon, hydrogen, nitrogen and sulphur concentrations in sediment samples were assessed using a CHNS Analyser (Elementary, Vario EL-Cube). Oxygen used for combustion of sample materials, and helium as carrier gas. In the presence of an excess of oxygen and combustion reagent, samples were combusted to elemental gases CO_2, H_2O, SO_2 and N_2. After homogenisation in the gas phase, they were first placed in a separation zone, and then in a detection zone. Major and trace element concentration were determined using (SiO_2, TiO_2, Al_2O_3, Fe_2O_3, MnO, MgO, CaO, Na_2O, K_2O, and P_2O_5, V, Cr, Ni, Cu, Zn, Ga, Rb, Sr, Y, Zr, Ba and La) XRF instrument.

GEOLOGY OF THE DRAINAGE BASIN

Archaean granitoid are exposed in the central part of the area. Charnockites (granulites) occur in the southern part and metavolcanic in the northeastern part. Ancient supra crustal (Sargur Group) rocks occur within the granitoid as enclaves around Sullia, Puttur and Dharmastala (Chousetty and Nagabasavasetty, 1971; Awasthi and Krishnamurthy, 1979). Proterozoic dykes (Balasubrahmanyan, 1975). Paleogene laterites capping on basement rocks, in the lower reaches of the river basin. Quaternary boulder-pebble beds and recent to sub-recent alluvium are present in the Netravati River basin.

RESULTS AND DISCUSSION

Nutrient Status

The elemental composition analysis of sediments attributes the distribution of elements (C, H, N, S) in organic and sedimentary materials origin and its characteristics. The nitrogen content in organic sediments of the river is in the range of 0.08 – 0.23% (Figs. 1-4). The percentage of carbon in Netravati River ranges of 0.45 – 2.14%. The hydrogen is in the range of 0.53 – 1.73% and the percentage of sulphur in Netravati River were recorded in the range of 0.15 – 0.2%. The C/N ratio infers the degree of sediment organic matter evolution in the presence of microorganisms. The C/N ratio ranged from 4.37 to 13.62 in river samples, imply an influence of organic matter from exogenous sources.

Sediment Geochemistry

The sediment samples consists of 44.42 to 79.11 SiO_2; 9.12 to 27.23 Al_2O_3; 0.31 to 1.02 TiO_2; 3.59 to 12.44 Fe_2O_3; 0.01 to 0.16 MnO; 0.41 to 1.58 CaO; 0.33 to 1.62 MgO; 0.36 to 1.51 Na_2O; 0.53 to 2.21 K_2O and 0.09 to 0.38 P_2O_5. Total iron is expressed as Fe_2O_3. Ni, from 25 to 134 ppm; Cu from 85 to 154 ppm; Zn from 28 to 110 ppm; Cr from 108 to 749 ppm; V from 98 to 198ppm; Ga from 4 to 36ppm; Rb from 22 to 60; Sr from 61 to 145; Y from 6 to 49; Zr from 115 to 0.14%; Ba from 1 to 422; and La from 9 to 41 (Table 2 & 3).

Enrichment Factor

Enrichment factor (EF) and Geoaccumulation index (I*geo*) (Covelli and Fontolan 1997; Chen *et al*., 2007) indicators are used for estimation of anthropogenic inputs. According to this technique, metal concentrations were normalised to metal concentrations of average shale (Mwamburi, 2003) or average crust (Gonzales-Macias *et al.*, 2006). The elements for normalisation are Aluminium (Al) (Chen *et al*., 2007) and Iron (Fe) (Ghrefat and Yusuf, 2006). In this study, Fe has been used as a conservative tracer to differentiate natural from anthropogenic components and we prefer to express the metal contamination with respect to the average shale to quantify the extent and degree of metal pollution. The average shale values (Fe 46,700, Cr 90, Cu 45, and Zn 95 ìg g l) are used Mwamburi (2003).

According to Chen *et al.* (2007), EF<1 indicates no enrichment, EF<3 is minor enrichment, EF=3–5 is moderate enrichment, EF=5–10 is moderately severe enrichment, EF=10–25 is severe enrichment, EF=25–50 is very severe enrichment, and EF>50 is extremely severe enrichment.

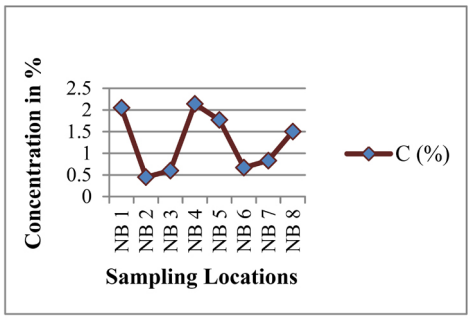

Fig. 1. Total Carbon (%).

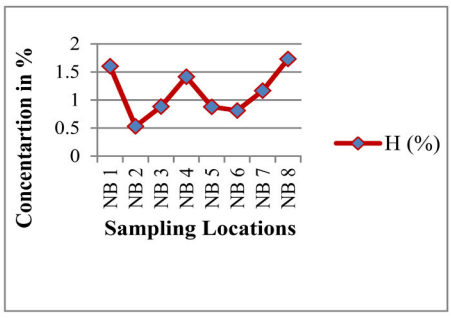

Fig. 2. Hydrogen (%).

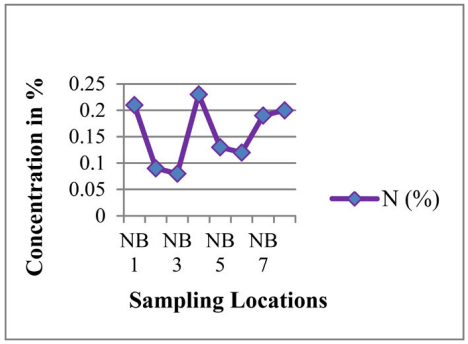

Fig. 3. Nitrogen (%).

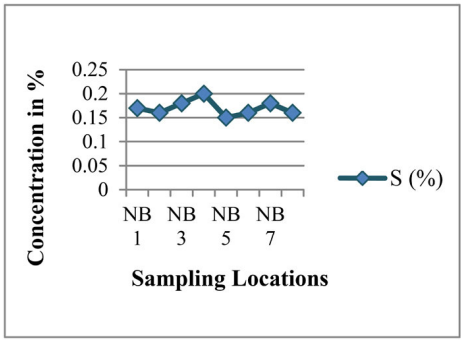

Fig. 4. Sulpher (%).

Table 2. Major element composition in the sediment samples (in wt.%).

Sl. No.	Sampling locations	SiO_2	TiO_2	Al_2O_3	MnO	Fe_2O_3	MgO	CaO	Na_2O	K_2O	P_2O_5
1	NB 1	79.11	0.31	10.08	0.01	3.59	0.75	1.06	1.51	0.53	0.38
2	NB 2	58.97	0.99	17.97	0.07	9.44	1.62	1.58	1.07	1.24	0.23
3	NB 3	44.42	1.02	27.23	0.04	10.57	1.38	0.69	0.39	1.15	0.21
4	NB 4	77.20	0.32	10.36	0.02	5.85	0.44	0.50	0.53	0.61	0.09
5	NB 5	70.30	0.35	12.68	0.02	8.88	0.33	0.41	0.36	1.20	0.11
6	NB 6	53.11	0.72	20.65	0.06	11.29	0.98	1.07	0.41	1.40	0.26
7	NB 7	60.85	0.78	14.38	0.11	12.23	1.25	1.40	1.00	2.21	0.21
8	NB 8	70.68	0.46	9.12	0.16	12.44	0.41	0.60	0.47	0.83	0.19

Table 3. Trace element composition of the sediment samples.

Sl. No.	Sampling locations	V	Cr	Ni	Cu	Zn	Ga	Rb	Sr	Y	Zr	Ba	La
1	NB 1	98	108	25	106	71	ND	24	128	6	116	99	12
2	NB 2	152	286	98	107	107	22	36	145	49	0.14%	340	39
3	NB 3	190	309	134	85	65	36	44	70	14	628	422	41
4	NB 4	127	224	35	87	28	ND	22	63	8	241	32	26
5	NB 5	146	266	32	154	70	4	32	70	11	191	216	26
6	NB 6	174	251	60	111	110	26	49	83	13	360	275	23
7	NB 7	178	295	81	122	86	10	60	113	23	267	417	18
8	NB 8	198	749	70	123	73	ND	27	61	13	115	1	9

***ND- Not detected/ Below detection limit**

The calculation of enrichment factors (**Fig. 5**) that Zn and Cr were enriched in sediments of Netravati River. Comparatively, Cr had the highest EF value (NB 8; 4.53) among the three metals (Cu, Zn, Cr) studied. Cr, Cu and Zn had minor enrichment (average value 2.48, 2.03 and 1.48, respectively). Elements with enrichment factors >1 are assumed to have originated from anthropogenic sources (Schroeder *et al*., 1987). Chromium is an essential trace element that can be toxic to aquatic biota at elevated concentrations.

Geoaccumulation Index

The geoaccumulation index (I*geo*) was used to assess metal pollution in sediments of Netravati River. Where *Cn* is the measured concentration of the heavy metal (*n*) in the sediments, *Bn* is the geochemical background value in the average shale of element *n*, and 1.5 is the background matrix correction factor due to lithogenic effects (Loska *et al*. 1997; Ghrefat and Yusuf, 2006; Gonzales-Macias *et al*., 2006; Chen *et al*., 2007). According to Loska *et al*., (1997) and Gonzales Macias *et al*., (2006), the contamination level may be classified on a scale ranging from 1 to 6 (I*geo*d"0= unpolluted, I*geo*<1=unpolluted to moderately polluted, I*geo*<2=moderately polluted, I*geo*<3=moderately to strongly, I*geo*<4= Strongly polluted, I*geo*<5= strongly to very strongly polluted, I*geo*>5=very strongly polluted).

The results of the geoaccumulation index (**Fig. 6**) reveal that sediments of the Netravati River are moderately polluted with Cu, Zn, Cr, and Mn.

Sediment Quality Guidelines

Sediment Quality Guidelines (SQGs) are significant for protection of benthic organisms in freshwater ecosystems and used to assess sediment ecosystem health. The threshold effect concentrations (TECs) and the probable effect concentrations (PECs) for sediment levels were reported by MacDonald *et al*., (2000). The TECs were intended to identify contaminant concentrations below which harmful effects on benthic organisms were not expected. The PECs were intended to identify contaminant concentrations above which harmful effects on benthic organisms were expected to occur frequently (MacDonald *et al*., 2000). In this study, metal concentrations in the Netravati River sediments are compared with threshold effect levels (TELs), effect range low values (ERLs), lowest effect levels (LELs), minimal effect thresholds (METs), which are included TECs, and probable effect levels (PELs), effect range

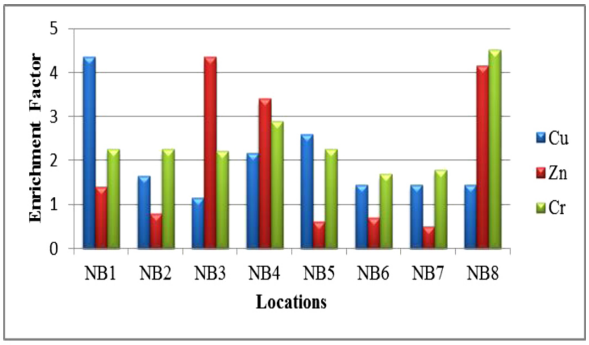

Fig. 5. Enrichment factors (EF) of Netravati sediments.

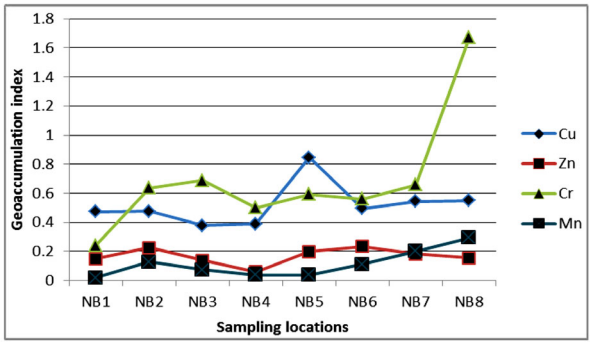

Fig. 6. Geoaccumulation Index (I*geo*) of Netravati sediments.

Table 4. Comparative trace metal concentrations in Netravati sediments and sediment quality guidelines.

		Metals			
		Cr	**Ni**	**Cu**	**Zn**
This study (ppm)		311	66.88	111.88	76.25
Threshold effect concentrations	TEL	37.3	18	35.7	123
	LEL	26	16	16	120
	MET	55	35	28	150
	ERL	80	30	70	120
Probable effect concentrations	PEL	90	36	197	315
	SEL	110	75	110	820
	TET	100	61	86	540
	ERM	145	50	390	270

TEL *Threshold Effect Level*, **LEL** *Lowest Effect Level*, **MET** *Minimal Effect Threshold*, **ERL** *Effect Range Low*, **PEL** *Probable Effect Level*, **SEL** *Severe Effect Level*, **TET** *Toxic Effect Threshold*, **ERM** *Effect Range Median*

median values (ERMs); severe effect levels (SELs), and toxic effect thresholds (TETs), which are included PECs. **Table 4** indicates that Cu, Ni and Cr concentrations in the Netravati River are above TECs. Ni and Cr concentrations are above then the PECs (except SEL for Ni). The Cu concentrations are above the range than SEL and TET. Whereas the range of Zn is below the TEC and PEC.

CONCLUSIONS

- The results indicate that Zn and Cr-enriched in the sediments of Netravati River.
- Cr, Cu and Zn had minor enrichment (average value 2.48, 2.03 and 1.48, respectively).
- Comparatively, Cr had the highest EF value among the three metals studied.
- Geoaccumulation Index infers that the Netravati sediments are moderately polluted with Cu, Zn, Cr, and Mn.
- Sediment Quality Guidelines (SQGs) indicates that Cu, Ni and Cr concentrations in the Netravati River are above TECs.
- Ni and Cr concentrations are above the PECs (except SEL for Ni). But for Cu PEL and ERM concentrations are above the range. The results of the study imply that continuous monitoring to be carried out to identify the long-term impact of the anthropogenic inputs, to ensure the health of water bodies.

***Acknowledgement*:** We are grateful to Dr. N. Purnachandra Rao, Director NCESS for providing laboratory and knowledge resource facilities.

References

Aswathi, S. K. and Krishnamurthy, K. V. (1979). Geology of parts of Puttur and Sullia taluks, South Kanara district, Karnataka. Progress report for the field season 1978-1979, Geol. Surv. India, Karnataka (South) Circle, 11p.

Balasubrahmanyan, M. N. (1975). The age of the South Kanara dykes, Mysore State., Geo. Surv. India Misc. Pub., 23, pp. 236-239.

Chen, C.-W., Kao, C.-M., Chen, C.-F., and Dong, C.-D. (2007). Distribution and accumulation of heavy metals in the sediments of Kaohsiung Harbor, Taiwan. *Chemosphere*, 66(8), 1431–1440.

Chousetty, V. C. and Nagabasavasetty, B. S. (1971). Magnetite quartzites of DharmastaIa, South Kanara District. Geol. Stud. Report. No. 46, Dept. Mines and Geol., Govt. Mysore, Bangalore, 13p.

Covelli, S., and Fontolan, G. (1997). Application of a normalization procedure in determining regional geochemical baselines. *Environmental Geology*, **30**(1/2), 34–45.

Dickinson, W.W., Dunbar, G.B., and Mcleod, H., (1996). Heavy metal history from cores in Willington Harbour, Newzealand. *Environmental Geology* 27, 59-69.

Fatoki O.S., and Mathabatha, S., (2001). An assessment of heavy metal pollution in the East London and Port Elizabeth harbours. Water SA 27, 233-240.

Ghrefat, H., and Yusuf, N. (2006). Assessing Mn, Fe, Cu, Zn, and Cd pollution in bottom sediments of Wadi Al-Arab Dam, Jordan. *Chemosphere*, 65, 2114 –2121.

Gonzales-Macías, C., Schifter, I., Lluch-Cota, D. B., Mendez-Rodriguez, L., and Hernandez-Vázquez, S. (2006). Distribution, enrichment and accumulation of heavy metals in coastal sediments of Salina Cruz Bay, Mexico. *Environmental Monitoring and Assessment*, 118, 211 –230.

Linnik, P. M. and Zubenko, I. B., (2000). The role of bottom sediments in the secondary pollution of aquatic environments by heavy metal compounds, *lakes and reservoirs. Res. Manage*., 5 (1), 11 – 21.

Loska, K., Cebula, J., Pelczar, J., Wiechula, D., and Kwapulinski, J. (1997). Use of enrichment, and contamination factors together with geoaccumulation indexes to evaluate the content of Cd, Cu, and Ni in the Bybnik water reservoir in Poland. *Water, Air and Soil Pollution*, 93, 347–365.

MacDonald, D. D., Ingersoll, G., and Berger, T. A. (2000). Development and evaluation of consensus-based sediment quality guidelines for freshwater ecosystems. Archives of *Environmental Contamination and Toxicology*, 39, 20 –31.

Mwamburi, J. (2003). Variations in trace elements in bottom sediments of major rivers in Lake Victoria's basin, Kenya. *Lakes Reservoirs Research Management*, 8, 5 –13.

Schroeder, W.H., Dobson, M., and Kane, K. D. M., (1987). Toxic trace elements associated with airborne particulate matter: A review. *J Air Pollut Control Assoc* 37(11):1267-1285.

Singh, K. P., Mohan, D., Singh, V. K., and Malik, A. (2005). Studies on distribution and fractionation of heavy metals in Gomti river sediments—a tributary of the Ganges. *Journal of Hydrology*, 312, 14-27.

Jour. Indian Association of Sedimentologists, Vol. 34, Nos. 1 & 2. (2017), pp. 127-139

Metal Enrichment in Core Sediments and their Possible Impact, the Ashtamudi Estuary, Southern Kerala, India

R. NAGENDRA[1], R. NAGARAJAN[2], T.N. PRAKASH[3] AND TIJU I VERGHEES[3]
[1]Department of Geology, Anna University, Chennai-600025, India.
[2]Department of Applied Geology, Curtin University Malaysia, Miri, Sarawak, Malaysia.
[3]National Centre for Earth Science Studies, Thiruvananthapuram-695011, India.
Email: geonag@gmail.com

Abstract: The investigation carried out on metals concentration in Ashtamudi estuarine core sediments reveals that, the pollution load index values in core 1 (AS 05) at mouth of estuary ranging from 1.56 to 1.95 with an average value of 1.72 and in core 3 (AS 17) at southern Kayal from 1.62 to 2.07; with an average 1.92 and in core 2 (AS 16) at central Kayal it ranged from 1.91 to 3.07 with higher average value of 2.33, which indicates that core 2 sediments are highly contaminated compare to that the core sediments core 1 and 3. The average enrichment factors of Cr 4.31; 3.47; 4.21 in core1, 2 and 3 respectively, Ni, 3.92; 3.49; 3.42 in core 1, 2 and 3 respectively and Cu 3.23 in core 2 are >2, suggesting contamination of these metals in the Ashtamudi estuary sediments. The adverse effect of the metals in the core sediments indicates that Ni concentration is recorded higher than the ERM values in all the three core sediments, Cu concentrations in core 2 and Cr concentrations in core 3, are potentially of concern, as they are between ERL and ERM with an effect of 93%, 87% and 83% respectively. Cu in core 1 and 3, Cr in 1 and 3 and Zn in core 2 and 3 concentration are recorded lower than the ERL value, whereas Pb concentration in core 1 shows that 13% of samples are recorded lower than the effects range.

Keywords: Geochemistry, metals enrichment, Ashtamudi estuary, Southern Kerala.

INTRODUCTION

Sediments are carriers of metals and they act as sinks for contaminants in aquatic environment, where they are the repository and potential source of metal pollutants. Metals are the environmental pollutants and their occurrence in sediments, water and biota indicates the existence of natural or anthropogenic sources (Nabi bidhendi et al., 2007; Jayaprakash et al., 2012, 2013; Nagarajan et al., 2014). Metals are present in atmosphere, water, soil, sediments and living organisms and their concentration is controlled by physical, chemical and biological processes. The Cr, Co, Cu, Fe, Mn, Mo, Pb, V, Sr and Zn, are essential for living organisms, however, metals are toxic even at low concentrations above the essential limits. These trace metals participate in biogeochemical cycles due to their mobility and frequently affect the ecosystems through bioaccumulation and bio-magnification processes and often they are potentially toxic to the bio-network (Sajwan et al., 2008). Sediment contaminated by metals affects the water quality and bioaccumulation of metals in aquatic organisms. Estuarine sediments, as basic components of environment, provide food for living organisms and serve as a sink and reservoir for organic and inorganic environmental contaminants. The aquatic sediments absorb persistent and toxic chemicals to levels higher than the water column concentration (Casper et al., 2004). Suspended particles with associated contaminants settle and become part of the bottom sediments (Ciszewski,1997; Viganó et al., 2003). In streams, rivers and estuaries, fine inorganic sediments, especially silts and clay, affect the habitat for microorganisms, macroinvertebrates and fish spawning, as well as fish rearing and feeding behaviour (Anandkumar et al., 2017). There are limited research data on sediment quality and estuarine health indicators in Ashtamudi estuary. The impact of potential inputs of trace metals to estuary from the catchment, surrounding area and within the estuarine itself causes the ecological imbalance.

GEOLOGICAL SETTING

The Precambrian rocks cover > 80% of the total area of Kerala (Rajan et al., 2005) and the Khondalite group is the predominant rock type in southern Kerala. The Palaeogene sedimentary formation of Kerala overlies the Precambrian, extending from Cape Comarin in the south to Manjeshwar in the north, which comprises of two facies of sediments (i) The continental facies; the Warkalli Formation- carbonaceous clays with lignite, China clays and friable sandstone (ii) The marine facies; the Quilon Formation-sandstone and carbonaceous clays with thin bands of fossiliferous limestone. Laterite; derived from the chemical weathering of either Precambrian crystalline or Palaeogene

sediments. They occur as cap rocks or iron hats over both the lithounits. The recent sediments include fringes of parallel sand bars, alluvial sands and lacustrine deposits. Polymict pebble bed separates these sediments from the Palaeogene sediments. In and around of the Ashtamudi estuary forms a geological segment of the Archaean crystalline basement, Palaeogene and Quaternary sedimentary sequences. The Archaean crystalline basement, are dominant in the eastern and southeastern parts of the Kallada River Basin. The Palaeogene sediments are enclave Sasthamkotta and Chelupola lakes. The Quaternary formations are represented on the southeastern side of the lake.

METHODOLOGY AND MATERIALS

Three sediment cores (Fig.1) were collected from the Ashtamudi estuary. The selected samples were washed thoroughly to remove salt and dried at 50^0C. The sediment samples were sieved by 230 mesh and < 63 microns is dried at 110^0C in order to remove moisture content. Pressed pellets were prepared by using collapsible aluminum cups (Govil,1985). These cups were filled with boric acid and about 1gm of the fine powdered sample (after LOI) is put on the top of the boric acid and pressed under a hydraulic press at 20 tons' pressure to obtain a 40 mm diameter pellet. Bruker model S4 Pioneer sequential wavelength-dispersive X-ray spectrometer equipped with a goniometer (which holds seven analyzing crystals) with 4kW Rh X-ray tube and 60 samples automatic loading system was used to measure different peaks and background counts for elements. Software used in computer is able to take care of dead time correction, background and line overlap corrections and matrix effects giving the output directly as the concentration in weight percentage or in ppm after converting the counts into concentration with the help of calibration curves. Major element concentrations were determined by X-ray fluorescence spectrometry as per the procedures given in Calvert (1990) at NCESS, Thiruvananthapuram. The major elements determined are: Si, Al, Fe, Ti, Ca, Na, K, Mg, Mn and P. Trace elements; Cr, Co, Ni, Cu, Zn,Ga, Rb, Y, Zr, Nb, Ba, La, Ce, Sm were analyzed using XRF.

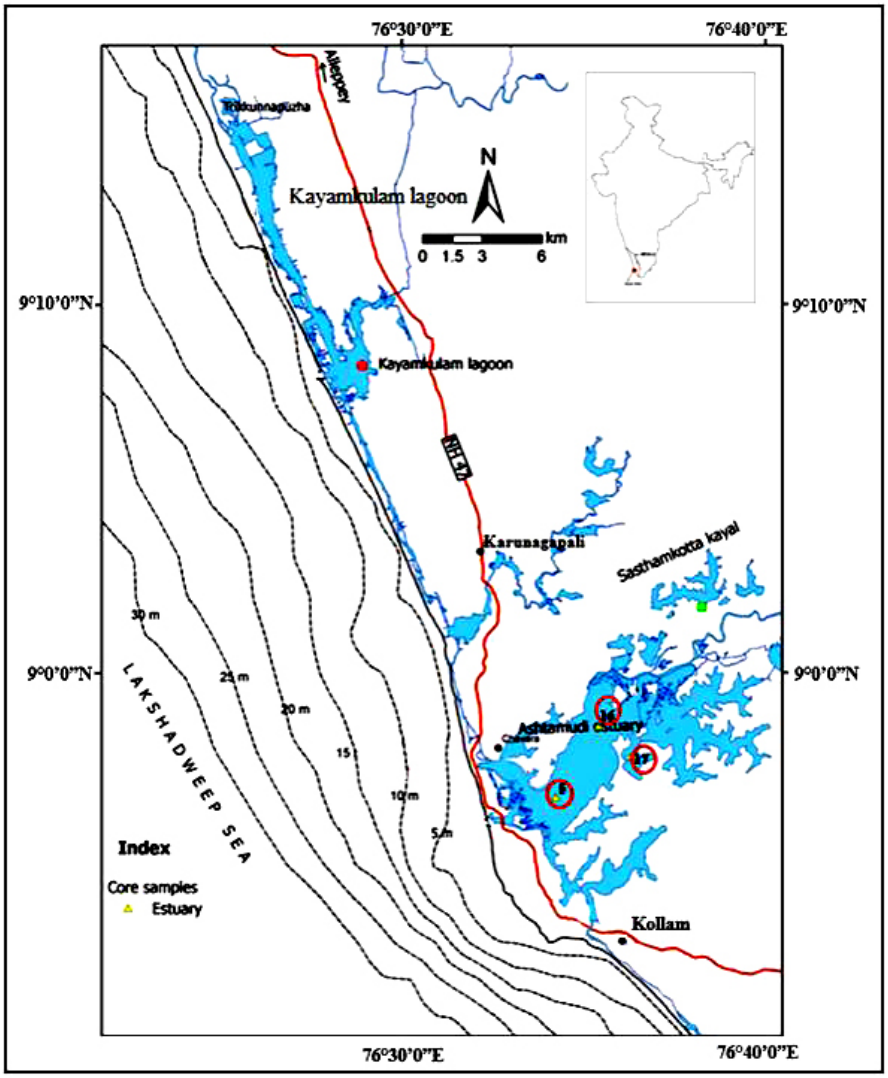

Fig. 1. Sediment core sample locations; AS 05, AS 16 and AS 17, Ashtamudi estuary.

RESULTS AND DISCUSSION

Distribution of Trace Metals

The average of trace metals contents has a significant variation; Mn 139-898 µg g^{-1}; Cr 146-193 µg g^{-1}; Ni 66-102 µg g^{-1}; Cu 13-144 µg g^{-1}; Zn 2-138 µg g^{-1}; Pb 41-72 µg g^{-1} and Co 9-14 µg g^{-1} respectively. The average lower values of Mn, Cr, Co, and Ni are recorded in core 1 sediments while the highest values of Mn, Ni, Cu and Zn are recorded in core 2 sediments. Core 3 sediments have the lowest values for Cu, Zn and the highest values for Cr and Co. The trace metals distributions and their variations among the cores are presented below in descending order,

Mn>Cr>Ni>Pb>Cu>Co [core 1 (AS 05) at mouth of estuary]
Mn>Cr>Ni>Cu>Zn>Co [core 2 (AS 16) at central Kayal]
Mn>Cr>Ni>Cu>Co>Zn [core 3 (AS 17) at southern Kayal]

The average Mn, Cr and Ni concentrations are recorded similar in decreasing order between the cores while Cu, Pb, Zn and Co concentrations and their distributions are varying between the cores. Concentrations of the metals have differences among them at different depths, which indicate that the source of input to the estuary is not uniform. Mn, Cr, Ni, Cu and Zn concentrations in the core-3 at southern Kayal estuary sediments are similar towards depth, whereas in the core 1 and core 2, these trace metals showing difference at different depths. Mn, Cr, Co and Pb concentrations in surface sediments of core 1 show a decreasing trend while Ni and Cu shows an increasing trend, which might be related to changes in the sources of these metals over the period. Cu-Zn and Mn-Cr content in sediment core 2 is showing uniform distribution with depth, which indicates their closeness and similarities of the source of these metals. All the elements in core 1 sediments show wider distribution over the period, which indicates the effect of variation in the source region and the location of the core in the estuary.

The concentrations of the metals in the core sediments were compared with the average elemental concentration in estuarine sediments from different parts of India as well as guideline values. Even though Cr content is recorded higher in the present study seems to be lower compared to Dhamara, Adyar and Cochin estuaries (Table.1). Co content in all the cores are

Table 1. Comparison of metals in Ashtamudi estuary sediments with other estuaries of India and their guideline values.

Location/Metals	Fe	Mn	Cr	Co	Ni	Cu	Zn	Pb
[a] Core 1 (AS 05):Range	194570-270510	139-240	146-164	9-12	66-91	16-48	ND	41-72
Mean	227310	191.6	155.9	10.6	74.3	26.9		52.9
[a] Core 2 (AS 16):Range	173710-183140	496-898	160-190	11-12	89-102	33-144	37-138	ND
Mean	177045	694.4	177.8	11.6	95.1	67.8	66.5	
[a] Core 3 (AS 17):Range	185190-192550	248-403	182-193	11-14	77-83	13-32	2-18	ND
Mean	188208	326	186.2	12.5	80.3	22.8	9.4	
[a] Ashtamudi: Range	173710-270510	139-898	146-193	9-14	66-102	13-144	2-138	41-72
Mean	192812	446.1	175.6	11.7	85.0	42.3	47.5	52.9
[b] Dhamara estuary	3.21%	652	347	67	65	29	71	32
[c] Cauvery	1.76%	319	ND	64	ND	12	26	10
[d] Ganges	3.1%	553	67	36	32	26	71	29
[e] Krishna	4.23%	1040	ND	47	ND	49	31	9
[f] Narmada	3.14	514	ND	29	ND	46	50	5
[g] Adyar estuary	-	345	318	10	426	-	168	2
[h] Godavari estuary	-	1059	2.2	28.8	25.7	47.8	-	55.8
[i] Hugli estuary	-	502.61	49.89	14.34	27.52	19.19	80.02	29.31
[j] Cochin estuary	52760	11420	ND	ND	67.17	1488	964.4	66.57
[k] Coleroon estuary	2744	32.1					51.4	7.02
[l] Sundarban Mangrove region	-	495-862	28.8–49.3	10.4–15.9	26.5–44.5	21.5–64.1	26–162	13.7–24.9
[m] Cochin estuary, Vembanad lake	41756	308.0	250.4	ND	ND	152.4	541.3	45.6
SQG's non-polluted	-	-	<25	-	-	<40	<90	-
SQG's moderately polluted	-	-	25-75	-	-	40-60	90-200	-
SQG's heavily polluted	-	-	>75	-	-	>60	>200	-
TEL	-	-	52.3	-	22.7	18.7	124	-
PEL	-	-	160	-	47.6	110	270	-
ERL	-	-	81	-	-	34	150	-
ERM	-	-	370	-	-	270	410	-

TEL threshold effect level, PEL probable effect level (adverse effect likely to occur), ERL effect range low, ERM effect range medium (adverse effect infrequent).

[a] Present study, [b] Asa et al., 2013; [c] Biksham and Subramanian 1988; [d,f] Subramanian et al., 1988; [e] Ramesh et al., 1990, [g] Hema Achyuthan et al., (2002); [h] Ray et al., 2006; [i] Chatterjee et al., 2007; [j] Harikumar and Nasir (2010); [k] Anithamary et al 2012; [l] Sarkar et al., 2004; [m] Dipu et al., (2013).

recorded less compared to many estuaries in India and comparable with Adyar estuary. Likewise, Ni content in studied cores are two to three fold higher compared to many estuaries, and the same time 4-5 fold lower than those values from Adyar estuary. Cu values are comparable with Sundarban mangrove region, Narmada, Krishna, Ganges, Dhamara etc. but 3-5 folds lower than the Cochin estuary sediments. Zn content in core 3 is low compared to core 2 as well as estuarine sediments from different parts of India. But core-2 shows Zn content (66.5ppm), which is higher than the Zn content recorded in Cauvery, Krishna, Narmada and Coleroon estuaries. The Pb content was measured in core 1 and their concentration is comparable with Godavari and Cochin estuary (Vembanad Lake). The enrichment of Cr, Ni, Cu, Zn and Pb infers the influence of anthropogenic activity in addition to the natural estuarine processes and lithology.

Statistical Analysis

In order to study the characteristics of the sediments of the Ashtamudi estuary the trace metal content of the individual core sediments was used for Pearson correlation and principal component analysis (PCA) were carried out using Statistica (Version 8). The trace metals derived from anthropogenic activities are often associated with organic matter, adsorbed on Fe-Mn oxides, and/or precipitated as hydroxides, sulfides and carbonates (Forstner and Wittman,1983). Multivariate statistical analysis, PCA is used to identify the sources of the contaminants and employed to understand the linear combination of original variables of trace metals. It can account the largest part (~80%) of the total variance. The negative relationship of Mn with Ni and the poor association of Mn with other trace metals in core 1 (Table 2) and core 3 (Table 3) suggested that Mn-oxide may be only a minor host phase for trace metals in these sediments. Similar relationship is observed in Mondovi estuary, west coast of India (Alagarsamy, 2006). Individual correlations reveal that Fe has significant relationship with Co, Mn, and lesser extent to Cr in core 1; significant relationship with Mn, Co and Zn in core 2 and strong relationship with Mn, Zn and Co indicating the probable adsorption of these elements on to the oxyhydroxides of Fe. Non-significant correlations of Mn (except with Co in core 1) with all the elements may be possibly due to the different processes like biological effects and external inputs operating in estuarine sediments (Ray et al., 2006). No strong correlations are observed among the metals in the sediments of core 1 (Table.4), whereas Zn and Cu have significant relationship with Co in sediments of core 2, which indicates that these elements are partly derived from anthropogenic input. The results of the principal component analysis (PCA) are reported in Table.5 and Figure.2. The factor loadings are classified as strong, moderate and weak based on the loading values of >0.70, 0.70-0.50 and 0.50-0.40 respectively (Liu et al., 2003). According to the eigenvalues (>1), five components are extracted for cores 1 and 2 and four components are extracted for the core 3, which explains about 98%, 87% and 93% of the total variance of the cores 1, 2 and 3 respectively.

Core 1 (AS 05)

Five significant components accounting 98% of the variance were distinguished for the analysed data of core-1 sediments. PC 1 describes the general loading of the core sediments with trace metals. It accounts for 22.6% of the total variance and is characterized by strong loadings of Al, Ti, Fe, Na, P, Mn and Co and Si and Ni along with negatively loading of Si and Ni. All the metals except Si and Ni shows positive correlation with Al and Fe indicates that these metals are primarily controlled by clay and Fe-Mn oxyhydroxides. Pb, Cr and Cu are

Table 2. Correlation matrix (R) of total trace elements in core 1 sediments of the Ashtamudi estuary (n=8).

	Si	Al	Ti	Fe	Ca	Mg	Na	K	P	Mn	Cr	Co	Ni	Cu	Pb
Si	1														
Al	-0.94	1													
Ti	-0.69	0.75	1												
Fe	-0.96	0.99	0.79	1											
Ca	-0.11	-0.12	-0.23	-0.08	1										
Mg	-0.41	0.49	-0.04	0.43	0.26	1									
Na	-0.71	0.86	0.67	0.80	-0.42	0.26	1								
K	0.20	-0.20	-0.19	-0.16	0.32	-0.19	-0.15	1							
P	-0.89	0.73	0.45	0.73	0.29	0.31	0.49	-0.35	1						
Mn	-0.72	0.88	0.66	0.83	-0.36	0.36	0.99	-0.07	0.46	1					
Cr	-0.49	0.37	0.61	0.46	-0.27	-0.46	0.23	-0.23	0.48	0.15	1				
Co	-0.93	0.95	0.79	0.95	0.09	0.51	0.72	-0.27	0.76	0.75	0.33	1			
Ni	0.86	-0.93	-0.57	-0.91	-0.10	-0.71	-0.71	-0.01	-0.61	-0.79	-0.09	-0.89	1		
Cu	-0.04	0.13	0.64	0.18	-0.13	-0.12	-0.01	-0.27	-0.13	0.01	0.26	0.32	-0.05	1	
Pb	-0.01	0.24	0.10	0.22	-0.15	0.31	0.34	0.65	-0.37	0.46	-0.40	0.10	-0.45	-0.04	1

Table 3. Correlation matrix (R) of total trace elements in core 2 sediments of the Ashtamudi estuary (n=12).

	Si	Al	Ti	Fe	Ca	Mg	Na	K	P	Mn	Cr	Co	Ni	Cu	Zn
Si	1														
Al	0.23	1													
Ti	-0.15	0.58	1												
Fe	0.14	-0.51	0.18	1											
Ca	-0.14	-0.86	-0.86	0.16	1										
Mg	0.63	-0.54	-0.69	0.27	0.61	1									
Na	0.02	0.11	0.66	0.54	-0.41	-0.33	1								
K	0.28	-0.27	0.30	0.66	-0.18	0.32	0.37	1							
P	-0.38	-0.53	-0.41	-0.01	0.43	-0.02	0.03	-0.03	1						
Mn	0.55	0.22	-0.01	0.07	-0.12	0.42	-0.40	0.16	-0.84	1					
Cr	-0.20	-0.46	0.38	0.86	0.01	-0.07	0.75	0.66	0.27	-0.36	1				
Co	0.50	-0.62	-0.36	0.78	0.48	0.72	0.26	0.48	0.15	0.10	0.52	1			
Ni	-0.66	0.32	0.41	-0.32	-0.27	-0.85	0.40	-0.54	0.27	-0.70	0.06	-0.57	1		
Cu	0.57	-0.13	-0.62	0.03	0.35	0.47	-0.16	-0.24	0.29	-0.01	-0.23	0.54	-0.28	1	
Zn	0.42	-0.09	0.22	0.81	-0.12	0.16	0.42	0.44	-0.21	0.29	0.53	0.67	-0.34	0.35	1

Table 4. Correlation matrix (R) of total trace elements in core 3 sediments of the Ashtamudi estuary (n=14).

	Si	Al	Ti	Fe	Ca	Mg	Na	K	P	Mn	Cr	Co	Ni	Cu	Zn
Si	1.00														
Al	0.07	1.00													
Ti	0.45	-0.14	1.00												
Fe	0.30	0.41	0.76	1.00											
Ca	0.03	-0.73	0.00	-0.42	1.00										
Mg	0.26	-0.47	0.33	0.04	0.26	1.00									
Na	-0.12	-0.79	-0.35	-0.77	0.58	0.25	1.00								
K	-0.11	0.29	-0.70	-0.54	-0.22	-0.27	0.17	1.00							
P	0.40	-0.49	-0.11	-0.38	0.81	0.22	0.50	0.11	1.00						
Mn	0.17	-0.10	0.64	0.66	0.24	0.25	-0.31	-0.70	0.16	1.00					
Cr	0.03	-0.65	0.66	0.26	0.41	0.25	0.24	-0.43	0.22	0.49	1.00				
Co	0.22	0.45	0.27	0.51	-0.25	0.04	-0.58	0.04	-0.03	0.34	0.05	1.00			
Ni	-0.03	0.32	-0.01	0.13	-0.28	-0.29	-0.24	0.54	-0.04	-0.11	0.20	0.47	1.00		
Cu	0.09	0.00	-0.01	0.26	0.28	-0.10	-0.11	-0.08	0.48	0.48	0.18	0.28	0.17	1.00	
Zn	0.47	0.19	0.35	0.62	-0.08	0.20	-0.36	-0.22	0.25	0.56	0.16	0.46	0.19	0.78	1.00

Table 5. Principal component loadings of variables as per varimax rotation method for core 1 sediments.

Elements	PC1	PC2	PC3	PC4	PC5
Si	-0.97	0.13	-0.11	0.14	0.02
Al	0.99	-0.02	-0.04	0.12	0.08
Ti	0.71	0.02	0.34	0.17	0.58
Fe	0.98	0.01	0.05	0.06	0.14
Ca	0.01	0.07	-0.16	-0.96	-0.08
Mg	0.48	-0.08	-0.84	-0.16	-0.06
Na	0.82	0.09	0.00	0.51	-0.06
K	-0.13	0.93	0.12	-0.27	-0.18
P	0.80	-0.42	0.18	-0.31	-0.22
Mn	0.85	0.19	-0.10	0.45	-0.02
Cr	0.37	-0.26	0.83	0.06	0.16
Co	0.94	-0.12	-0.08	-0.09	0.27
Ni	-0.93	-0.17	0.30	0.06	-0.06
Cu	0.04	-0.09	0.09	0.04	0.99
Pb	0.20	0.86	-0.37	0.26	0.06
Variance (in %)	51	13	12	12	10

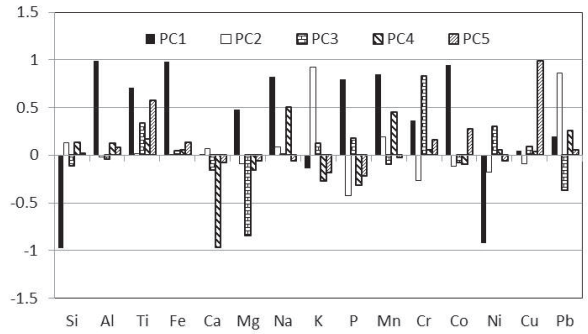

Fig 2. Results of factor analysis in core 1 sediments of the Ashtamudi estuary.

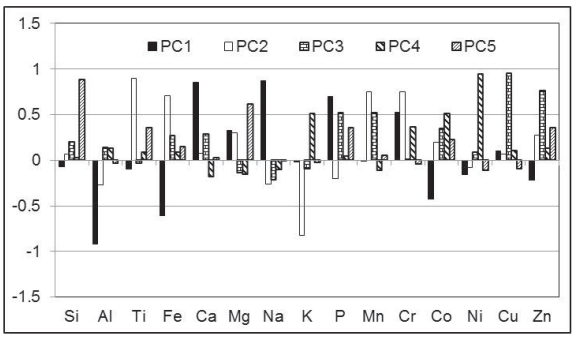

Fig 3. Results of factor analysis in core 2 sediments of the Ashtamudi estuary.

positively loaded in component 2, 3 and 5 respectively, which reflects the influence of different sources of anthropogenic input over the natural geologic processes. Close association of Pb with K (r=0.65) and their positive loading in PC 2 may be related to anthropogenic input from the agricultural areas, which is common phenomenon in the surroundings of the study area. Pb has affinity to attach with clay minerals since it has similar ionic radii (Modak et al., 1992). The Cr is not involved with the ferromagnesian minerals which are confirmed by the negative correlation between Mg and Cr content in these sediments. The Cr and Cu concentration in the sediments may indicate the influence of industrial and domestic wastes, iron and steel industries and sewage. Also Cr is highly loaded in PC 3, which may be related to the environmental conditions of the estuary. Under suboxic to anoxic conditions Cr concentration used to be enriched and accumulated in sediments. Ca and Na is loaded in component 4 and accounted for 12% of the total variance which can be related to carbonated debris present in the sediments.

Core 2 (AS 16)

The original variables of core 2 are accounted into five factors which account for 87% of the total variances. The PC1 explains about 26% of the total variance and it is strongly related to Ca, Na, P as a positive loadings and Al and Fe as strong to moderate negative loadings whereas Cr and Co are least related to PC1. This factor is described as natural pattern distribution. Fe and Co are generally highly interrelated and linked to a geological origin, which is shown by the negative loadings of these in PC1 and also by the significant positive correlation between them (r=0.51). PC2 comprises about 23% of the variance and it is defined by Ti, Fe, Mn, Cr and K, where all the trace metals except K are positively loaded. Those metals revealed the influence of lithology. Particularly Ti minerals are resistant to weathering and often do not decompose in soils. The Ti can be used as an index of soil genesis (Kebata Pendias and Mukherjee, 2007). Strong loading of Ti with these metals should be related to natural geological processes and bound to clay and Fe-Mn oxyhydroxides. PC 3 is loaded by Cu, Zn, Mn and P and explains about 16%. P and Mn are loaded doubly in PC 1 and PC 2 respectively, which clearly indicates that these metals in PC 3 are clearly related to anthropogenic activities. Zn and Cu are more water soluble metals and can be transported with highway runoff to the channels and the estuary. The similarity of the source for these metals are confirmed in sediments of core 2 (AS16) with higher correlation (r=0.78) compared to other cores. PC 4 is also confirmed as influence of anthropogenic by the significant positive loadings of Ni, Co and K which account 11% of the total variance. This also indicates that these metals are scavenged in clay minerals, which is confirmed by close relationship between Ni and K (r=0.54). PC 5 is loaded positively with Si and Mg and accounts 11% of the total variance. This factor may be related to lithology however, these elements are derived from different lithology compared to the other natural elements. Particularly these elements might be derived from laterite and residual soils which are commonly distributed in the source region (Table.6 and Fig.3).

Core 3 (AS 17)

Overall four components were extracted for core 3 and have the total variance of 93%. The first component explains 29% of the total variance, the second component 27% the third component 22 %, and the fourth component 15%. PC 1 includes Fe, Na, K, Cr, Co and Zn. This result coincides with the correlation analysis and these metals should be derived from a common source. All the metals are strongly loaded except Co in this component. PC 2 accounts 27% of the total variance and this component is strong positively loaded with Ca and Mg and negatively loaded with Al, Ti. P and Co are loaded weakly in PC 2. This suggests that adsorption on finer particles (clay) and precipitation with carbonates are responsible for their enrichment. PC 3 accounts 22% of the total variance and are strongly

Table 6. Principal component loadings of variables as per varimax rotation method for core 2 sediments.

Elements	PC1	PC2	PC3	PC4	PC5
Si	-0.08	0.07	0.20	0.03	0.89
Al	-0.92	-0.27	0.14	0.13	-0.03
Ti	-0.10	0.90	-0.03	0.09	0.36
Fe	-0.61	0.71	0.27	0.09	0.15
Ca	0.85	0.07	0.29	-0.17	0.03
Mg	0.33	0.30	-0.13	-0.15	0.61
Na	0.87	-0.26	-0.21	-0.10	-0.01
K	-0.02	-0.82	-0.10	0.51	-0.02
P	0.70	-0.20	0.52	0.05	0.36
Mn	-0.01	0.75	0.53	-0.11	0.05
Cr	0.52	0.75	0.01	0.37	-0.04
Co	-0.43	0.19	0.35	0.52	0.23
Ni	-0.16	-0.08	0.09	0.95	-0.11
Cu	0.10	0.07	0.95	0.10	-0.09
Zn	-0.22	0.28	0.77	0.13	0.36
Variance (in %)	26	23	16	11	11

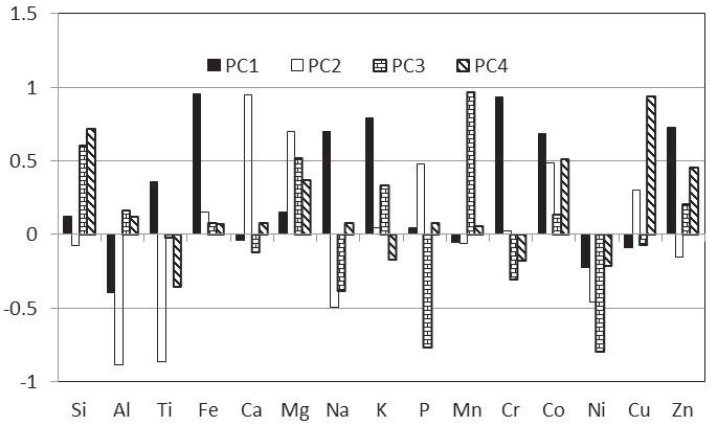

Fig.4. Results of factor analysis in core 3 sediments the Ashtamudi estuary.

loaded positively by Mn and moderately loaded with Si. P and Ni are strongly and negatively loaded in the same component. This may be related to lateritic soils derived from different parent rocks. Particularly Si shows positive correlation with Mg (r=0.63), which could be expected as both oxides from serpentine minerals. Often, lateritic soils are enriched with Fe, Al, Ti, Mn, Ni and Ca. Ni and Co used to be enriched in laterite by variety of hydrometallurgical processes. During the leaching process, Mg and Si are removed due to weathering and on the other hand Fe is enriched in laterite. Since the source area consists of significant amount of laterite and might have gone through different leaching, weathering and hydrometallurgical processes. PC 4 accounts 15% of the total variance. It shows strong positive loading of Si, Cu and moderate loading of Co and Zn (Table.7 and Fig.4). The positive relationship between these metals indicates that these metals may be derived from both natural and anthropogenic processes.

The contamination level of a metal in sediment can be expressed by the contamination factor (Pekay et al., 2004), *i.e.* the ratio between the sediment metal content at a given station and normal concentration levels (NCLs). Contamination factors (CF) greater than and less than 1 indicate the presence and absence of contamination in sediments by the metals. For NCLs we have used average upper crust values reported by Wedepohl (1995) since there is no Indian soil standard. The CF was classified into four groups as 1<CF (low), 1<CF < 3 (moderate), 3< CF<6 (considerable) and 6> CF

Table 7. Principal component loadings of variables as per varimax rotation method for core 3 sediments.

Element	PC1	PC2	PC3	PC4
Si	0.13	-0.08	0.60	0.72
Al	-0.40	-0.89	0.16	0.12
Ti	0.35	-0.87	-0.02	-0.35
Fe	0.95	0.15	0.08	0.07
Ca	-0.04	0.95	-0.12	0.08
Mg	0.15	0.70	0.52	0.37
Na	0.70	-0.50	-0.39	0.08
K	0.79	0.04	0.34	-0.17
P	0.04	0.48	-0.77	0.08
Mn	-0.06	-0.06	0.96	0.06
Cr	0.93	0.02	-0.31	-0.18
Co	0.69	0.48	0.14	0.51
Ni	-0.23	-0.46	-0.80	-0.22
Cu	-0.09	0.30	-0.07	0.94
Zn	0.73	-0.15	0.21	0.45
Variance (in %)	29	27	22	15

(Very high) (Pekay et al., 2004). The average values of CF for the core sediments of the Ashtamudi estuary are shown in Figure 5. The average level of contamination by the metals is as follows:

Cr>Ni>Pb>Cu>Fe>Co>Mn [Core 1]
Ni>Cr>Cu>Fe>Mn>Zn>Co [Core 2]
Cr>Ni>Fe>Cu>Co>Mn>Zn [Core 3]

Core sediments of the Ashtamudi estuary are considerably contaminated (3< CF<6) by Cr, Ni, Pb and moderately contaminated by Fe, Cu, Co (core 2 and 3), and Zn (core 2), which clearly indicates that the sources for these metals are from domestic and industrial effluents, traffic density, vehicular emission and by atmospheric deposition. This is also well supported by the enrichment factor and I_{geo} Indexes of these sediments (Fig. 7 and table 9, respectively).

Pollution Load Index

The extent of pollution by trace metals has been assessed by employing the method based on Pollution Load Index (PLI) developed by Tomilson et al., (1980) and is presented below;

$$PLI=(CF_{Fe}\times CF_{Mn}\times CF_{Cr}\times CF_{Co}\times CF_{Ni}\times CF_{Cu}\times CF_{Pb})^{1/7}$$

Where CF = contamination factor, the metal base values represents its average concentration in UCC (Wedepohl, 1995). PLI provides a simple, comparative means for assessing a site or estuarine quality: a value of 0, 1 and >1 indicates absence, presence of them and progressive deterioration of sediment quality respectively (Tomlinson et.al., 1980). Figure 6 depicts that the PLI values on core 1 ranging from 1.56 to 1.95 with an average value of 1.72 and in core 3 the PLI values ranging from 1.62 to 2.07; avg. 1.92; whereas core 2 is recorded higher as 1.91 to 3.07; average 2.33 which indicates that core 2 sediments are highly contaminated than the core 1 and 3 sediments (Fig.6).

Enrichment Factor

The estimation of anthropogenic inputs, non-dimensional enrichment factor (EF) (Balachandran et. al., 2005; Covelli and Fontolan, 1997) was calculated by normalizing with a conservative element such as Al, based on the assumption that Al represents proxies for the clay mineral concentration (Kersten and Smedes, 2002). For a given metal, EF is calculated as follows;

$$EF = (Me/Al)_{sample} / (Me/Al)_{baseline}$$

Where Me and Al are the concentrations of potentially enriched element and proxy element, respectively. The baseline value was calculated from the average Me/Al value of UCC (Wedepohl, 1995). This method has been used effectively to assess the enrichment or depletion of specific elements in riverine, estuarine and coastal environments (Selvaraj et al., 2004; Jayaprakash et al., 2012; Rajmohan et. al., 2014). The EF values <2 and >2 indicates the natural and anthropogenic sources respectively (Grousset et al.,

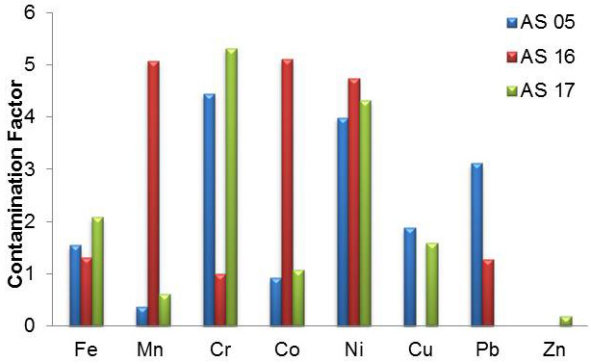

Fig 5. Contamination factor for the trace metal in core sediments (cores 1, 2 and 3) of the Ashtamudi estuary.

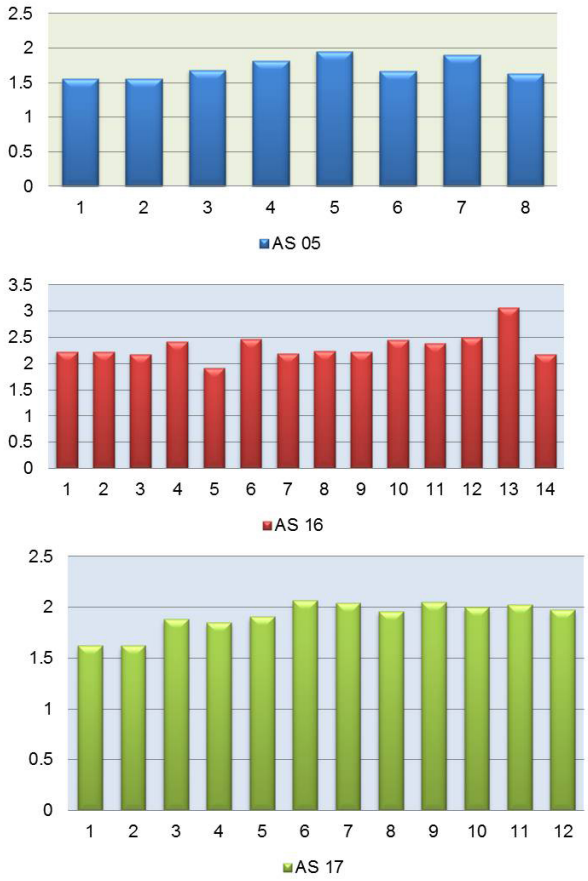

Fig.6. Pollution load index for the core 1,2 and 3 sediments of the Ashtamudi estuary.

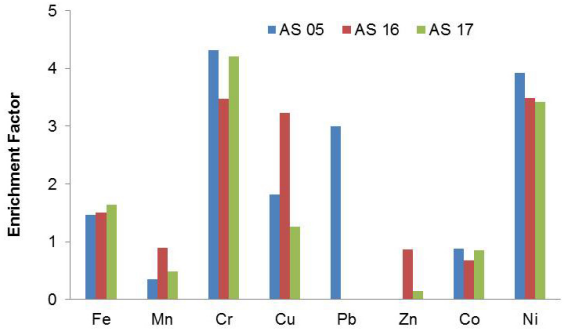

Fig 7. Enrichment factor for the trace metal in core sediments [cores 1(AS 05), 2 (AS 16 and 3(AS 17)] of the Ashtamudi estuary.

Table 8. Geoaccumulation index (Igeo) for core 1 (AS 05), core 2 (AS 16) and core 3 (AS 17) sediments of the Ashtamudi estuary.

Sample Number	Igeo Value (Class)						
	<0 (0)	0-1 (1)	1-2 (2)	2-3 (3)	3-4 (4)	4-5 (5)	>5 (6)
AS 05 – 01	Fe, Mn	Cu, Pb, Co	Cr, Ni				
AS 05 – 02	Fe, Mn	Cu, Pb, Co	Cr, Ni				
AS 05 – 03	Mn, Cu	Fe, Pb, Co	Cr, Ni				
AS 05 – 04	Mn	Fe, Cu, Co	Cr, Pb, Ni				
AS 05 – 05	Mn	Fe, Cu, Co	Cr, Pb, Ni				
AS 05 – 06	Mn, Cu	Fe, Co	Cr, Pb, Ni				
AS 05 – 07	Mn	Fe, Pb, Co	Cr, Cu, Ni				
AS 05 – 08	Mn, Cu	Fe, Pb, Co	Cr, Ni				
AS 16 – 01	Mn, Zn	Fe, Co	Cr, Cu, Ni				
AS 16 – 02	Mn, Zn	Fe, Co	Cr, Cu, Ni				
AS 16 – 03	Mn, Zn	Fe, Co	Cr, Cu, Ni				
AS 16 – 04	Mn, Zn	Fe, Co	Cr, Ni	Cu			
AS 16 – 05	Mn, Zn	Fe, Cu, Co	Cr, Ni				
AS 16 – 06	Zn	Fe, Mn, Co	Cr, Cu, Ni				
AS 16 – 06	Mn, Zn	Fe, Co	Cr, Cu, Ni				
AS 16 – 07	Mn, Zn	Fe, Co	Cr, Cu, Ni				
AS 16 – 08	Mn, Zn	Fe, Co	Cr, Cu, Ni				
AS 16 – 09	Mn	Fe, Zn, Co	Cr, Cu, Ni				
AS 16 – 10	Mn	Fe, Zn, Co	Cr, Cu, Ni				
AS 16 – 11	Mn	Fe, Zn, Co	Cr, Cu, Ni				
AS 16 – 12		Fe, Mn, Zn, Co	Cr, Ni	Cu			
AS 16 – 13	Mn, Zn	Fe, Co	Cr, Cu, Ni				
AS 17 – 01	Mn, Cu,	Fe, Co	Cr, Ni				
AS 17 – 02	Mn, Cu	Fe, Co	Cr, Ni				
AS 17 – 03	Mn, Cu, Zn	Fe, Co	Cr, Ni				
AS 17 – 04	Mn, Cu, Zn	Fe, Co	Cr, Ni				
AS 17 – 05	Mn	Fe, Cu, Co	Cr, Ni				
AS 17 – 06	Mn, Zn	Fe, Cu, Co	Cr, Ni				
AS 17 – 07	Mn, Zn	Fe, Cu, Co	Cr, Ni				
AS 17 – 08	Mn, Cu, Zn	Fe, Co	Cr, Ni				
AS 17 – 09	Mn, Zn	Fe, Cu, Co	Cr, Ni				
AS 17 – 10	Mn, Zn	Fe, Cu, Co	Cr, Ni				
AS 17 – 11	Mn	Fe, Cu, Co	Cr, Ni				
AS 17 – 12	Mn, Cu	Fe, Co	Cr, Ni				
OP	25.75% (60)	38.63% (90)	35.62% (83)	0.86% (02)			

ɡeo value <0(0) unpolluted; 0-1(1) from unpolluted to moderately polluted; 1-2(2); moderately polluted; 2
om moderately to strongly polluted; 3-4(4) strongly polluted;
-5(5) from strongly to extremely polluted; >5 (6) extremely polluted.

Table 9. Guideline values and biological effects of the trace metals in cores 1, 2 and 3 sediments of the Ashtamudi estuary.

Guideline (mg/kg)			Adverse effects (%) Core 1			Adverse effects (%) Core 2			Adverse effects (%) Core 3		
Element	ERL	ERM	<ERL	ERL~ ERM	>ERM	<ERL	ERL~ ERM	>ERM	<ERL	ERL~ ERM	>ERM
Cu	34	270	100	0	0	7	93	0	100	0	0
Ni	20.9	51.6	0	0	100	0	0	100	0	0	100
Pb	46.7	218	13	87	0	ND	ND	ND	ND	ND	ND
Cr	81	370	0	100	0	0	100	0	0	83	17
Zn	150	410	ND	ND	ND	100	0	0	100	0	0

1995). The calculated average EF values for the core sediments of Ashtamudi estuary inferred as;

Cr>Ni>Pb>Cu>Fe>Co>Mn [Core 1]
Ni>Cr>Cu>Fe>Mn>Zn>Co [Core 2]
Cr>Ni>Fe>Cu>Co>Mn>Zn [Core 3]

The variation in EF values between the cores is presented in Figure 7. As a whole, the average enrichment factors of Cr (4.31; 3.47; 4.21 in core 1; 2 and 3 respectively), Ni (3.92; 3.49; 3.42 in core 1, 2 and 3 respectively) and Cu (3.23 in core 2) are found to be >2, suggesting contamination of these metals in the Ashtamudi estuary sediments.

Geoaccumulation Index (Igeo)

The geoaccumulation index (Igeo), (Muller,1981), was used to quantitatively measure the metal pollution in the core sediments based on a pollution intensity classification (Igeo class), which consists of seven classes (0-6; Table 8). The geoaccumulation index (Igeo) values were calculated for the surface sediments of study area using the equation after (Muller, 1981).

$$I_{geo} = \log [Me]_{studied\ area} / 1.5[Me]_{baseline\ values}$$

in which, [Me] baseline value which represents the metal concentration in the average crust values taken from Wedepohl (1995) since the standard background values for Indian soils are not available. The 1.5 factor is included because of possible variations in the background data due to lithogenic effects (Salomons and Forstner, 1984). The highest class indicates 100-fold enrichment of metal pollution over the baseline values. The calculated Igeo values from the core 1 sediments are as follows; -0.27 to -0.53 for Fe; -2.51 to 1.72 for Mn; 1.48 to 1.64 for Cr; -0.42 to 1.16 for Cu; 0.69 to 1.50 for Pb; 1.24 to 1.71 for Ni; and 0.84 to 0.92 for Co respectively. The calculated Igeo values for cores 2 and 3 are ranges as follows; 0.46 to 0.68 and 0.36 to 0.61 for Fe; -0.67 to 0.18 and -1.67 to 1.88 for Mn; 1.61 to 1.86 and -0.03 to 1.86 for Cr; 0.62 to 2.75 and -0.72 to 0.22 for Cu; -1.08 to 0.82 and -5.29 to -2.12 for Zn; 1.67 to 1.87 and 1.46 to 1.57 for Ni; and 0.63 to 0.75 and 0.77 to 0.97 for Co in the sediments of core 2 and core 3 respectively. The average geoaccumulation indexes are less than zero for Mn in core 1; Mn and Zn in core 2; and Cu and Zn in core 3 suggesting that the sediments have not been polluted by these metals. Based on the individual trace metals Igeo values, core 1 and core 3 sediments are categorized as unpolluted to moderately polluted (Igeo class 0-2) whereas core 2 sediments are categorized as unpolluted to strongly polluted (Igeo class 0-3). 26% of the elements belong to Igeo class 0; 39% of the elements belong to Igeo class 1(unpolluted to moderately polluted) and 36% of the elements belong to Igeo class 2 (moderately polluted). The remaining 0.86% of the elements (Cu) in sediments of core 2 belongs to Igeo class 3 (moderate-extremely polluted). Overall, results from this study indicated that core -1sediments are moderately polluted by Cr, Pb and Ni; core 2 sediments are moderate to strongly polluted with Cr, Cu and Ni and core 3 sediments are moderate to strongly polluted with Cr and Ni (Table.8).

Biological Effects

At elevated concentrations, many metals become highly toxic and have chronic effects on living organisms in aquatic ecosystem. In the present study, various metals in the core sediments of the Ashtamudi estuary have been compared to the Effects-Range Low (ERL) and Effects-Range Median (ERM) guidelines derived from Long et al., (1995) to evaluate the degree of contamination connected with biological effects. Sediment chemical concentrations below ERL are interpreted as rarely being associated with adverse health effect. Exceedances of ERM values and maximum baseline values were used to identify metals of ecological concern. The percentage of adverse effect of the metals in the core sediments of Ashtamudi estuary is presented in Table 9. This study indicates that Ni concentration is recorded higher than the ERM values in all the core sediments suggesting more ecological concern. Cu concentrations in core-2 (AS 16); Pb concentrations in core-1 (AS 05); Cr concentrations in core 3 (AS 17) potentially of greatest concern, as the value are between ERL and ERM with an effect of 93%, 87% and 83% respectively. Cu (in core 1 and 3), Cr (in 1 and 3), and Zn (in core 2 and 3), concentration in all the sediments are recorded lower than the ERL value, whereas Pb concentration in core 1 shows that 13% of samples are recorded lower than the ERL value.

CONCLUSIONS

- The PLI values on core 1 ranging from 1.56 to 1.95 with as average value of 1.72 and in core-3 the PLI values ranging from 1.62 to 2.07; average 1.92 whereas core 2 is recorded higher as 1.91 to 3.07; average 2.33, which indicate that core 2 sediments are highly polluted compare to that of the core 1 and 3.
- The overall, the average enrichment factors of Cr (4.31; 3.47; 4.21 in core 1; 2 and 3 respectively), Ni (3.92; 3.49; 3.42 in Core 1, 2 and 3 respectively) and Cu (3.23 in core 2) are >2, suggesting contamination of these metals in the Ashtamudi estuary sediments.
- The adverse effect of the metals in the core sediments of the Ashtamudi estuary indicates that Ni concentration is recorded higher than the ERM values in all the core sediments.
- Cu concentration in core 2; Pb concentration in core 1; Cr concentration in core 3 potentially of greatest

concern, as their concentrations are between ERL and ERM with an effect of 93%, 87% and 83% respectively.

- Cu in core 1 and 3, Cr in core 1and 3 and Zn in core 2 and 3 recorded lower than the ERL value, however, in core 1 only 13% of samples recorded lower than the ERL value for Pb.

Acknowledgements: The authors are thankful to the Director, National Centre for Earth Science Studies Thiruvananthapuram for grant of permission to use the XRF facility to carry out the geochemical analysis. RN is thankful to UGC–DRS Phase III grant for laboratory facilities in the Department of Geology. This work forms the part of the DST sponsored project (SR/S4/ES-310/2007).

References

Alagarsamy, R (2006). Distribution and Seasonal Variation of Trace Metals in Surface Sediments of the Mandovi Estuary, West Coast of India. *Estuarine, Coastal and Shelf Science, 67, 333-339.*

Anandkumar, A., Nagarajan R., Prabakaran, L and Rajaram R (2017). Trace metal dynamics and risk assessment in the commercially important marine shrimp species collected from the Miri coast, Sarawak, East Malaysia. Regional Studies in Marine Science. https://doi.org/10.1016/j.rsma.2017.08.007.

Anithamary, I., Ramkumar,T and Venkatramanan,S (2012). Distribution and accumulation of metals in the surface sediments of Coleroon River estuary, East Coast of India. *Bull. Environ. Contam.Toxicol. 188, 413-417.*

Asa, S. C., Rath, P., Panda, U. C., Parhi, P. K and Bramha, S (2013). Application of sequential leaching, risk indices and multivariate statistics to evaluate metal contamination of estuarine sediments: Dhamara Estuary, east Coast of India. *Environmental Monitoring and Assessment. doi:10.1007/s10661-013-3060-3.*

Balachandran, K.K., Laluraj, C.M., Nair, M., Joseph, T., Sheeba, P. and Venugopal, P. (2005). Metal accumulation in a flow restricted, tropical estuary. *Estuarine, Coastal and Shelf Science, 65,361-370.*

Biksham, G and Subramanian, V (1988). Elemental compositions of Godavari sediments (Central and Southern Indian Subcontinent). *Chem. Geol., 70, 275-286.*

Calvert, S.E (1990). *Geochemistry and origin of the Holocene sapropel in the Black Sea*. In: Ittekkot V., Kempe, S., Michaelis, W., Spitzy, A. (Eds.), Facets of Modern Biogeochemistry. Springer, 326-352.

Casper, S. T., Mehra, A., Farago, M.E and Gill, R.A (2004). Contamination of Surface Soils, River Water and Sediments by Trace Metals from Copper Processing Industry in the Churnet River Valley, Staffordshire, UK. *Environmental Geochemistry and Health, 26, 59–67.*

Chatterjee, M., Silva Filho, E.V., Sarkar, S.K., Sella, S.M., Bhattacharya, A, Satpathy, K.K., Prasad, M.V.R., Chakraborty, S., and Bhattacharya, B.D (2007). Distribution and possible source of trace elements in the sediment cores of a tropical macro-tidal estuary and their ecotoxicological significance. *Environ. Int., 33, 346-356.*

Ciszewski, D (1997). Source of pollution as a factor controlling distribution of metals in river Chech³o bottom sediments. *Environ Geol, 28, 50-57.*

Covelli,S and Fontolan, G (1997). Application of a normalization procedure in determining regional geochemical baselines. *Environ Geol., 30, 34–45.*

Dipu, S., Anju and Kumar, A. (2012). Distribution of mercury and other trace metals in the sediments of Cochin estuary (a Ramsar site), Kerala, India. *Environ Monit Assess., DOI 10.1007/s10661-012-3028-8.*

Forstner, U. and Wittmann, G.T.W (1983). *Metal pollution in aquatic environment*. New York, Springer-Verlag.

Govil, P.K (1985). X-ray fluorescence analysis of major, minor and selected trace elements in new IWG reference rock samples. *Jour. Geol Soc India, 26, 38–42.*

Grousset, F.E., Quetel, C.R., Thomas, B., Donard, O.F.X., Lambert, C.E., Guillard, F. and Monaco, A (1995). Anthropogenic vs. lithogenic origins of elements (As, Cd, Pb, Rb, Sb, Sc, Sn, Zn) in water column particles north-western Mediterranean Sea. *Marine Chemistry, 48, 291-310.*

Harikumar, P.S and Nasir, U.P (2010). Ecotoxicological impact assessment of metals in core sediments of a tropical estuary. *Ecotoxicology and Environmental Safety, 73(7), 1742-1747.*

Hema Achyuthan., Richard Mohan, D., Srinivasalu, S and Selavaraj, K (2002). Trace metals concentrations in the sediment cores of estuary and tidal zones between Chennai and Pondicherry, along the east coast of India. *Indian Journal of Marine Science, 21, 141-149.*

Jayaprakash, M., Nagarajan, R., Velmurugan, P.M., Giridharan, L., Neetha, V and Urban, B 2014. Geochemical Assessment of Sediment Quality Using Multivariate Statistical Analysis of Ennore Creek, North of Chennai, SE Coast of India. Pertanika J. Sci. & Technol., 22 (1), 315 – 328.

Jayaprakash, M., Nagarajan, R., Velmurugan, P.M., Sathiyamoorthy, J. Krishnamurthy, R.R. and Urban, B. (2012). Assessment of metal contamination in a

historical freshwater canal Buckingham Canal, Chennai. India. *Environ Monit Assess. doi:10.1007/ s10661-011-2509-5.*

Kabata-Pendias, A and Mukherjee, A.B (2007). *Trace Elements from soil to human*. Berlin Springer Verlag.

Kersten, M and Smedes, F (2002). Normalization procedures for sediments contaminants in spatial and temporal monitoring. J. *Environ. Monit, 4, 109-115.*

Liu,C.W., Lin,K.H., and Kuo,Y.M (2003).Applications of factor analysis in the assessment of groundwater quality in a Blackfoot disease area in Taiwan. *The science of Total Environment, 313, 77-89.*

Long, E., MacDonald, D., Smith, S and Calder, F (1995). Incidence of adverse biological effects within ranges of chemical concentrations in marine and estuarine sediments. *Environmental Management, 19, 81-97.*

Modak, D.P., Singh,K.P., Chandra, H and Ray,P.K (1992) Mobile and bound forms of trace elements in sediments of the lower Ganges. *Water Res 26(11), 1541-1548*.

Muller, G (1981). The metal pollution of the sediments of Neckars and its tributary: A stock taking. *Chem. Zei., 105, 157-164*.

Nabi Bidhendi, G. R., Karbassi, A. R., Nasrabadi, T and Hoveidi,H (2007). Influence of copper mine on surface water quality. *International Journal of Science and Technology, 4*(1), *85–91*.

Nagarajan, R ., Jonathan, M.P., Roy, P.D., Prasanna, M.V and Elayaraja, A 2014. Enrichment pattern of leachable trace metals in roadside soils of Miri City, Eastern Malaysia. Environmental Earth Sciences. 72: 1765-1773. DOI:10.1007/s12665-014-3080-5.

Pekay, H., Karakas, D., Ayberk, S., Tolun, L and Bakoglu, M (2004). Ecological risk assessment using trace elements from surface sediments of Izmit Bay North-eastern Marmara Sea Turkey. *Marine Pollution Bulletin, 48, 946-953.*

Rajan,T.N., and AnilKumar, P. S. (2005). *Geology and mineral resources of the states of India, Part IX-Kerala*, Geological Survey of India, Misc.publ.30, 91p.

Rajmohan, N., Prathapar, S.A., Jayaprakash, M and Nagarajan R (2014). Vertical distribution of heavy metals in soil profile in seasonally waterlogging agriculture field in Eastern Ganges Basin. Environmental Monitoring and Assessment. 186 (9), 5411-5427.

Ramesh, R., Subramanian, V and Van Grieken, R (1990). Metal distribution in sediments of Krishna river basin, India. *Environmental Geology Water Science 15, 207-216.*

Ray, A. K., Tripathy, S. C., Patra, S. and Sarma, V. V (2006). Assessment of Godavari estuarine mangrove ecosystem through trace metal studies. *Environ. Int., 32, 219- 223.*

Sajwan, K.S., Senthil Kumar, K., Parmasivarn, S., Compton, S.S. and Richardson, J.P (2008). Elemental status in sediments and American Oyster collected from Savannah marshy estuarine ecosystem, a preliminary assessment. *Arch. Environ. Cont. Toxicol. 54, 245–258.*

Salomons, W and Forstner, U (1984). *Metals in the hydro cycle*. New York: Springer-Verlag, 63-98.

Sarkar, S. K., Bilinski, S. F., Bhattacharya, A., Saha, M and Bilinski, H (2004). Levels of elements in the surficial estuarine sediments of the Hugli River, northeast India and their environmental implications. *Environment International, 30, 1089–1098*.

Selvaraj, K., RamMohan, V and Szefer, P (2004). Evaluation of metal contamination in coastal sediments of the Bay of Bengal, India: geochemical and statistical approaches. *Mar. Pollut. Bull., 49, 174-185.*

Subramanian, V., Jha, P.K., and Van Grieken, R (1988). Heavy metals in the Ganges estuary. *Marine Pollution Bulletin, 19, 290–293.*

Tomlinson, D.C., Wilson, J.G., Harris, C.R and Jeffery, D.W (1980). Problems in the assessment of metals levels in estuaries and the formation of a pollution index. *Helgol. Wiss. Meeresunters, 33(1-4), 566-575.*

Wedepohl, H. (1995).The continental crust. *Geochim. Cosmochim Acta, 59, 1217-1239.*

Jour. Indian Association of Sedimentologists, Vol. 34, Nos. 1 & 2. (2017), pp. 141-155

Textural Studies a Tool to Decipher the Depositional Environment- A Case Study off Palk Strait, Tamil Nadu, Southeast Coast of India

M. Suresh Gandhi*, K.Kasilingam and N.Suresh
Department of Geology, University of Madras, Guindy Campus, Chennai-600 025, India
Email: msureshgandhi@gmail.com

Abstract: The Palk Strait ecosystem is endangered due to the shallowing of the bay resulted due to continuous siltation. In this paper we attempt to infer the depositional environment using grain size analysis studies. Grain size studies of sediments from Mandapam to Kodiyakarai divided into 9 sectors, indicate that sediments are unimodal to polymodal in nature, fine to very fine grained, well sorted to poorly sorted, and positively-negatively skewed in character. Bivariant plots show that the Attankarai, Kodiyakarai and Mallipattinam sectors can be classified as beach environments, whereas the Devipattinam, Thondi and Kottaipattinam sectors come under the influence of riverine environment. The CM Pattern shows the presence of sediments is found to have a spread within OP segments. The inference to be drawn from these studies is that the variation in sedimentological parameters is governed by fluvial input, wave dynamics, and littoral transport of the sediments highlight depositional processes.

Keywords: Textural Analysis, depositional environment, Mandapam and Kodiyakarai, Palk Strait, Southeast Coast of India, Tamil Nadu.

INTRODUCTION

Granulometric studies of beach sediments provide a wealth of information on the intrinsic properties of sediments and their depositional environment. Further, they help to delve into the nature and energy flux of the multifarious agents transporting the sediments. Systematic granulometric studies of the east and west coasts of India have been carried out by Rajamanickam and Gujar (1984, 1985, 1993), Chaudhri et al., (1981); Rao et al., (2005). Especially along the northern and central Tamil Nadu coast, using textural parameters, Mohan (1990) and Chandrasekar (1992) have made significant contributions in differentiating the environments of beach and river sediments. The distribution of grain size parameters along 11 km stretch of the beach sediments between Karikal and Nagore, reveals that the mean grain size exhibits a marked decreasing trend on either side of the mouth of the Tirumalairajanar River which flow from west to east was studied by Venkatraman et al., (2011). Using grainsize analysis Rajmohan et al., (2012) inferred the depositional environment of coastal sediments at Ponnaiyar and Gadilam estuary, East coast of India. However, information is lacking on the grain size characteristics of such sediments and on the processes operating along the Palk bay coast.

Study area

The study area extends from the coast between Mandapam and Kodiyakarai, Palk Strait, Southeast Coast of India, Tamil Nadu. A base map with the scale 1:10,000 was prepared using the toposheets (Nos.58 K, J, O, N) (Nos. 58 N/3, 4 and 8, 7, 11, 15, 58 K/9 to16, 58 O/9, 1 to 4, 7 and 8, 58 J/16 scale 1:250,000 and 1:50,000) naval hydrographic charts, taluk and village maps of Tamil Nadu land surveys. All the prominent and permanent objects, rivers, tanks, roads and elevation were marked on the base map with co-ordinates (Fig.1).

METHODOLOGY

72 Offshore surface sediment samples were collected between Mandapam and Kodiyakarai using Vanveen grab sampler. The sediment samples were dried in an oven at 60^{O}C. The bulk sample was reduced by coning and quartering, and a 100 gm portion of the sample was selected for laboratory analysis. Organic matter and ferruginous coatings were removed from the samples by treatment with 30% by volume H_2O_2 and $SnCl_2$. After this pre-treatment, the samples were sifted at 0.25 ø intervals through ASTM sieve sets using a Ro-Tap sieve shaker for 20 minutes. The sieved materials were collected and weighed. The carbonates present in

Table 1. Results of grain size analysis of the study area.

		LOGARITHMIC METHOD			FOLK AND WARD METHOD			
SL NO	MEAN ($\bar{\imath}_\phi$):	SORTING (σ_ϕ):	SKEWNESS (Sk_ϕ):	KURTOSIS (K_ϕ):	MEAN (M_Z):	SORTING (σ_I):	SKEWNESS (Sk_I):	KURTOSIS (K_G):
MP 1	3.304	0.625	-0.503	3.290	3.322	0.651	-0.084	1.098
MP 2	2.314	0.607	0.685	5.221	2.296	0.572	0.207	1.201
MP 3	2.299	0.706	0.636	4.197	2.306	0.685	0.320	1.100
MP 4	2.692	0.848	0.140	2.613	2.666	0.847	0.144	0.842
MP 5	2.716	0.877	0.216	2.429	2.699	0.887	0.215	0.810
MP 6	3.266	0.841	-0.492	2.626	3.257	0.877	-0.162	0.804
MP 7	3.288	0.780	-0.557	2.776	3.271	0.821	-0.185	0.861
MP 8	4.255	0.404	-2.926	8.232	4.306	0.313	0.010	0.990
AK 1	2.868	0.472	-0.476	4.915	2.897	0.470	0.070	1.065
AK 2	2.677	0.478	0.148	5.156	2.626	0.467	-0.050	1.584
AK 3	2.738	0.452	-0.428	6.771	2.741	0.433	0.007	1.253
AK 4	2.671	0.511	-0.725	7.303	2.667	0.480	-0.076	1.271
AK 5	2.628	0.431	-0.152	7.011	2.601	0.404	-0.057	1.098
AK 6	2.739	0.528	0.009	4.856	2.733	0.532	0.099	1.720
AK 7	2.532	0.519	-0.155	5.709	2.520	0.491	0.007	1.088
AK 8	2.715	0.551	-0.315	6.016	2.713	0.543	0.091	1.445
DP 1	3.527	1.080	-1.123	3.616	3.565	1.070	-0.510	1.016
DP 2	3.528	1.063	-1.095	3.582	3.568	1.056	-0.476	1.003
DP 3	3.765	0.976	-1.354	4.231	3.838	0.918	-0.527	1.037
DP 4	3.589	1.102	-1.202	3.766	3.615	1.080	-0.550	0.973
DP 5	3.523	1.058	-1.212	3.981	3.561	1.038	-0.466	1.088
DP 6	3.523	1.075	-1.148	3.742	3.570	1.059	-0.489	1.026
DP 7	3.488	1.110	-1.062	3.396	3.504	1.120	-0.474	1.029
DP 8	3.567	1.082	-1.272	4.035	3.611	1.060	-0.539	1.087
TH 1	2.905	0.748	-0.463	4.194	2.883	0.713	-0.206	1.137
TH 2	2.994	0.697	-0.266	2.950	3.001	0.729	-0.151	0.978
TH 3	3.438	0.813	-0.726	3.009	3.433	0.829	-0.251	1.021
TH 4	3.769	0.726	-0.883	3.694	3.860	0.729	-0.293	0.939
TH 5	3.655	0.802	-0.772	3.168	3.735	0.814	-0.251	0.987
TH 6	3.388	0.912	-0.833	3.543	3.362	0.914	-0.232	0.955
TH 7	3.242	0.871	-0.504	3.119	3.242	0.896	-0.092	0.806
TH 8	3.573	0.755	-0.760	3.401	3.592	0.748	-0.227	1.000
KP 1	3.737	0.847	-1.362	5.125	3.864	0.797	-0.386	1.092
KP 2	3.682	0.891	-1.179	4.240	3.777	0.876	-0.414	1.053
KP 3	3.499	0.940	-0.805	3.241	3.527	0.979	-0.246	1.004
KP 4	3.868	0.704	-1.396	5.553	3.939	0.685	-0.355	1.105
KP 5	3.815	0.749	-1.154	4.339	3.904	0.740	-0.344	1.001
KP 6	4.004	0.673	-1.536	5.629	4.050	0.636	-0.357	1.064
KP 7	3.806	0.734	-1.219	4.676	3.896	0.725	-0.359	1.095
KP 8	3.767	0.807	-1.119	4.109	3.866	0.787	-0.386	0.967
MMK 1	3.729	0.894	-1.197	4.236	3.859	0.837	-0.408	0.951
MMK 2	3.620	0.944	-0.872	3.217	3.671	0.950	-0.381	0.832
MMK 3	3.728	0.877	-1.062	3.696	3.812	0.862	-0.430	0.909
MMK 4	3.729	0.854	-1.262	4.849	3.852	0.800	-0.383	0.962
MMK 5	3.948	0.795	-1.589	5.758	4.001	0.740	-0.448	1.056
MMK 6	3.725	0.912	-1.207	4.261	3.809	0.879	-0.455	0.918
MMK 7	3.880	0.775	-1.344	4.922	3.947	0.744	-0.409	0.950
MMK 8	4.003	0.409	-1.663	9.584	4.011	0.393	-0.310	1.534
SBC 1	3.534	0.948	-0.917	3.393	3.570	0.978	-0.359	1.040
SBC 2	3.364	1.038	-0.852	3.333	3.371	1.028	-0.238	0.831
SBC 3	3.068	0.819	-0.395	3.429	3.109	0.855	-0.062	1.028
SBC 4	3.669	0.716	-0.830	3.970	3.744	0.705	-0.176	1.024
SBC 5	3.556	0.903	-0.849	3.324	3.576	0.948	-0.281	1.024
SBC 6	3.901	0.641	-1.207	5.436	3.950	0.635	-0.308	0.921
SBC 7	3.776	0.766	-1.233	4.847	3.882	0.747	-0.354	1.068
SBC 8	3.713	0.827	-1.202	4.936	3.833	0.780	-0.345	0.955
MPT 1	3.013	0.831	-0.283	2.776	3.056	0.850	-0.109	0.833
MPT 2	3.921	0.817	-1.729	6.639	3.985	0.742	-0.439	0.039
MPT 3	3.929	0.723	-1.768	7.683	3.995	0.661	-0.338	0.983
MPT 4	4.008	0.586	-1.498	7.124	4.051	0.549	-0.242	0.912
MPT 5	3.818	0.586	-1.237	6.362	3.854	0.565	-0.299	1.118
MPT 6	3.834	0.658	-1.374	6.618	3.906	0.640	-0.305	1.069
MPT 7	3.869	0.597	-1.131	5.109	3.914	0.600	-0.323	1.135
MPT 8	3.890	0.579	-1.423	7.023	3.930	0.558	-0.315	1.166
KK 1	2.984	0.563	-1.508	9.145	3.012	0.500	-0.034	1.086
KK 2	2.606	0.477	-1.214	10.49	2.597	0.411	-0.062	1.025
KK 3	2.909	0.509	-0.639	6.665	2.398	0.496	0.146	1.193
KK 4	2.862	0.491	-1.153	8.591	2.898	0.459	0.067	1.070
KK 5	2.519	0.549	0.271	3.206	2.511	0.564	0.138	1.010
KK 6	3.088	0.400	-0.148	4.484	3.069	0.409	0.025	0.920
KK 7	2.988	0.586	-1.288	7.374	3.029	0.539	-0.087	1.097
KK 8	2.998	0.546	-1.250	7.734	3.022	0.504	-0.075	1.098

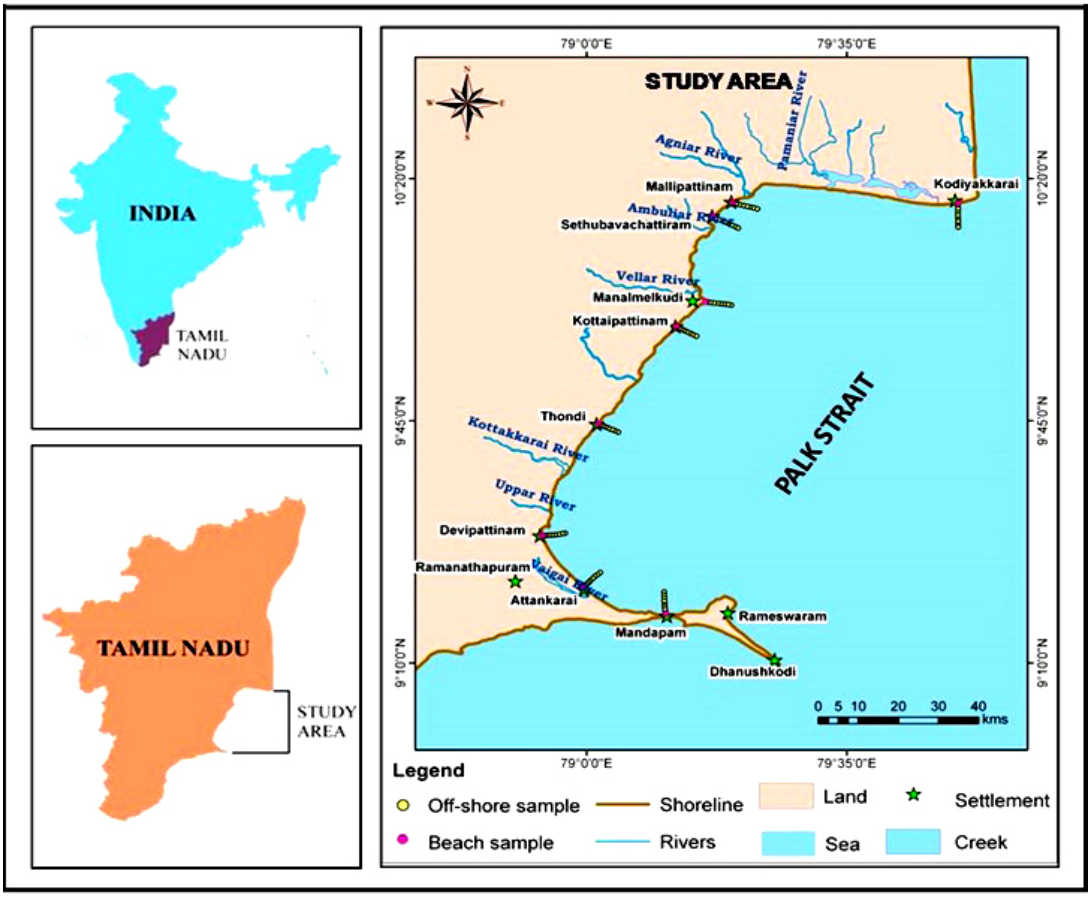

Fig. 1. Location map of the study area.

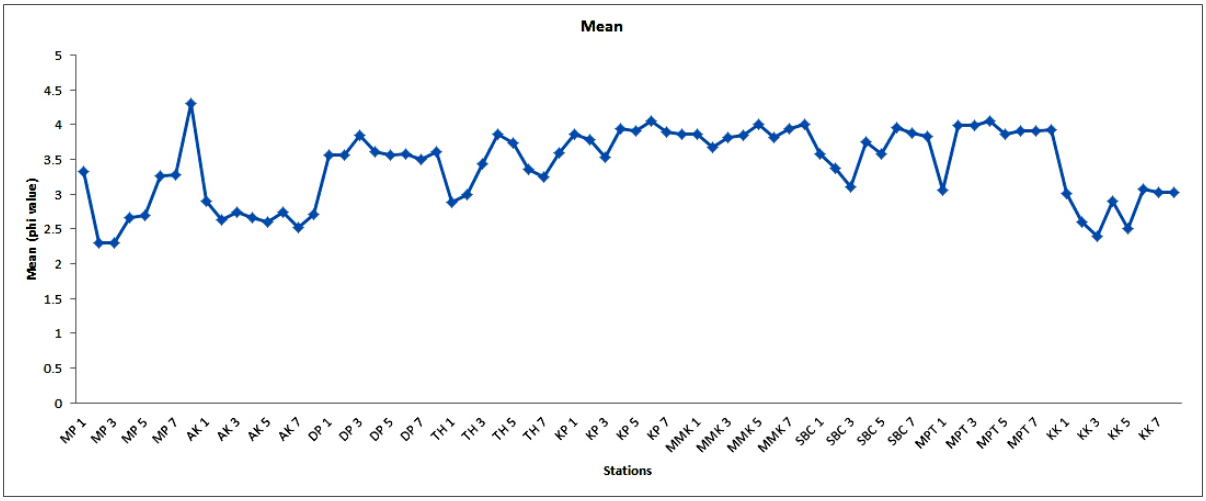

Fig. 2. Mean values for the study area.

the sediments were estimated after sieving by treatment with 1:10 HCl. In order to comprehend the mode of transportation and depositional environments of sediments, granulometric study was carried out using the graphic (Folk and Ward, 1957) and moment methods (Friedman, 1961, 1967). For the present study, Gradistat – Version -4.0 Programme developed by Simon Blatt and Kenneth Pye (2001) is utilized.

RESULTS AND DISCUSSION

Mean (Mz)

The moment mean values are identical to the graphic mean data of the analysed samples, so, after Folk and Ward (1957), who observed that 'the graphic mean values are twice as accurate an approximation as the

moment mean data', we discuss only graphic mean values. In the study area, mean value ranges from 2.296 ö to 4.306 ö for Mandapam; 2.296 ö to 4.306 ö, for Attankarai; 2.520 ö to 2.897 ö, for Devipattinam; 3.504 ö to 3.838 ö, for Thondi; 2.883 ö to 3.860 ö, for Kottaipattinam; 3.527 to 4.050 ö, for Manalmelkudi; 3.671 ö to 4.011 ö, for Sethubavachattram; 3.109 ö to 3.950 ö, for Mallipattinam; 3.056 ö to 4.051 ö, for Kodiyakarai; 2.398 ö to 3.069 ö. (Fig.2). The study region shows unimodal to polymodal in nature (Fig. 3a to c). The Mandapam region shows fine sand to very fine sand in nature except last station. It shows very coarse silt in nature. The distribution of fine sediments in this region might have occurred from the dislodging of coarser lighter sediments by the panning action of high velocity waves.

The Attankarai and Kodiyakarai region shows unimodal nature reflects the deposition of sediments primarily by waves and currents and the Devipattinam region shows bimodal to polymodal nature with poorly sorted to moderately sort. It clearly indicates that whatever sediment transport from the river settles in the estuary and not reach to the coastal region. Similar observations are also found by Angusamy and Rajamacikam (2006).

Standard Deviation (óI)

In the study region sorting values shows range from 0.313 ö to 1.120 ö, for Mandapam; 0.313 ö to 0.887 ö, for Attankarai; 0.404 ö to 543 ö, for Devipattinam; 0.918 ö to 1.120 ö, for Thondi; 0.713 ö to 0.914 ö, for Kottaipattinam 0.636 ö to 979 ö, for Manalmelkudi; 0.393 ö to 0.950 ö, for Sethubavachattram; 0.635 ö to 1.028 ö, for Mallipattinam; 0.549 ö to 0.850 ö, for Kodiyakarai; 0.409 ö to 0.564 ö is noticed (Fig.4). The sorting value indicates well sorted to poorly sort in nature. Mandapam region shows moderately well sorted to very well sorted in nature whereas Attankarai region shows almost well sorted in nature prevailing low wave energy condition. Devipattinam region shows poorly sorted in nature may be due to the high energy condition. Thondi and Kottaipattinam region shows moderately sorting nature may be due to the addition of sediments of different grain size from the reworking of beach ridges or by alluvial action and the prevalence of strong wave convergence throughout the year and similar sorting nature may be due to the prevalence of strong northerly drift. The currents moving from down south region carry the sediments to the northern regions. In this process the sediments are imparted with moderate to well sorting nature. Similar observations are found in the East Coast of India (Vijayam, et al., 1961). Chakrabarti (1977) and Chaudhri et al., (1981) have observed that moderately sorted sands are predominant on the beaches of the east and west coasts of India, respectively. Kodiyakarai shows a well sorting with an alternate moderately well sorting. It may be inferred in such a way that a tongue like movement of currents in a particular minor channel paths are disturbing only a portion of a seabed at a particular depth. In other words, the long shore currents are probably returning from the spit in a channel like pattern observed in the bathymetric disposition, through 3 m and 5 m depth zones.

Skewness (SKI)

The skewness values for Mandapam ranging from -0.185 ö to 0.320 ö, for Attankarai; -0.076 ö to 0.099 ö, for Devipattinam; -0.550 ö to -0.466 ö, for Thondi; -0.293 ö to -0.092 ö, for Kottaipattinam; -0.414 ö to -0.246 ö, for Manalmelkudi; -0.455 ö to -0.310 ö, for Sethubavachattram; -0.359 ö to -0.062 ö, for Mallipattinam; -0.439 ö to -0.109 ö, for Kodiyakarai; -0.087 ö to 0.146 ö (Fig.5). In general, based on the classification of Folk and Ward (1957) the skewness values of the study region vary from negatively skewed to positively skew in nature. The Mandapam, Attankarai and Kodiyakarai region show almost positively skewed in nature. The positively skewed distribution (a greater quantity of ûne sediments) indicates a depositional tendency (Duane, 1964). Devipattinam, Thondi, Kottaipattinam, Manalmelkudi, Sethubavachattram and Mallipattinam region shows negatively skewed in nature. Negatively skewed distribution illustrates the depletion of ûne-grained sands and suggests the dominance of erosion processes. Attankarai and Kodiyakarai display positive skewness. It suggests the possibility of taking them to non-beach sediments or a deposit, formed under the conditions of low energy. Attankarai being at the mouth of river confluence, one expects a supply of terrestrial material rather than the beach sediments. The Attankarai transect indicates a mixed sorting from well sorted to moderately well sorted. It suggests the prevalence of alternate high and low energy condition in the seabed. As in the case of Sethubavachattram, the current returning back from Devipattinam is expected to enter through Attankarai where the presence of irregular relief must have conducted the currents to take course through those minor channels to the deeper channel. Such channel banks may be providing a better sorting comparatively to the channel bed which undergoes the disturbance of the returning currents enabling to get poor sorting in such zone. The complete positive skewness at Kodiyakarai may be attributable to the low energy condition of deposition or otherwise the dominant influence of dune/ridge sediments noticed around the Vedaranyam ridge.

Kurtosis (KG)

On the basis of Folk's classification, the study area is leptokurtic to platykurtic in nature. The leptokurtic to platykurtic nature indicates multiple environment i.e. one derived from riverine/aeolian environment and the other primarily derived from the marine environment. The

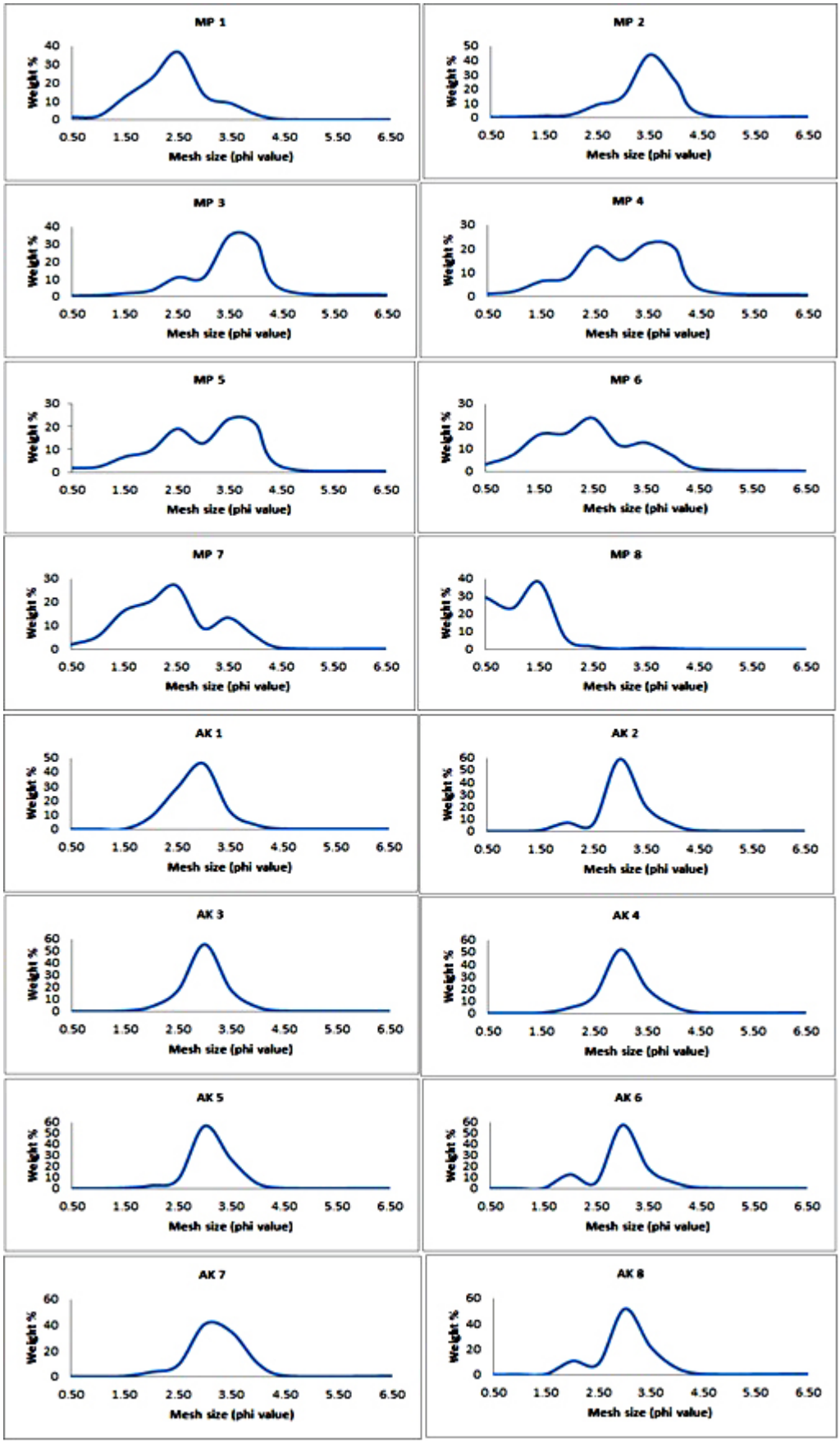

Fig. 3a. Frequency curves for the study area.

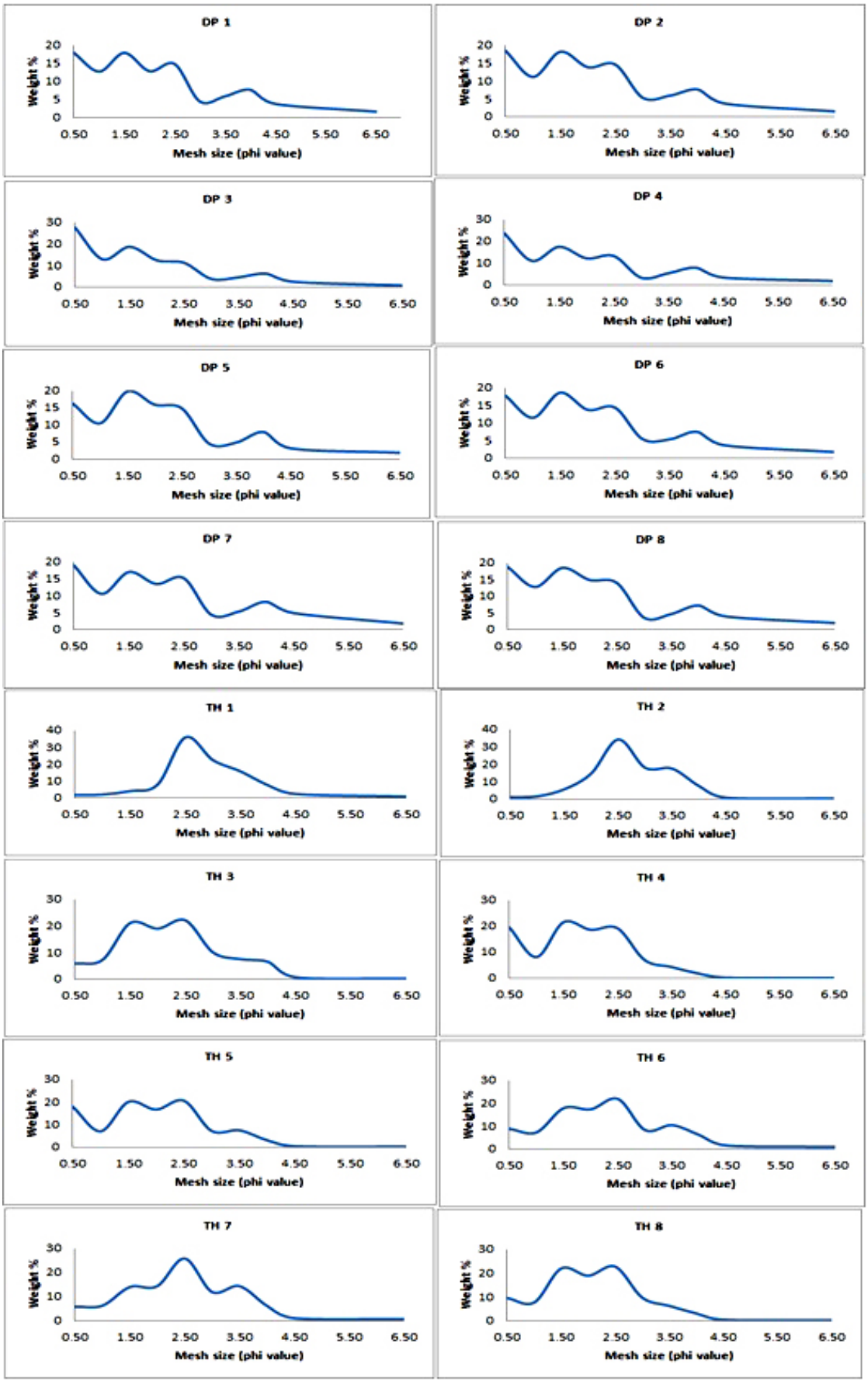

Fig. 3b. Frequency curves for the study area.

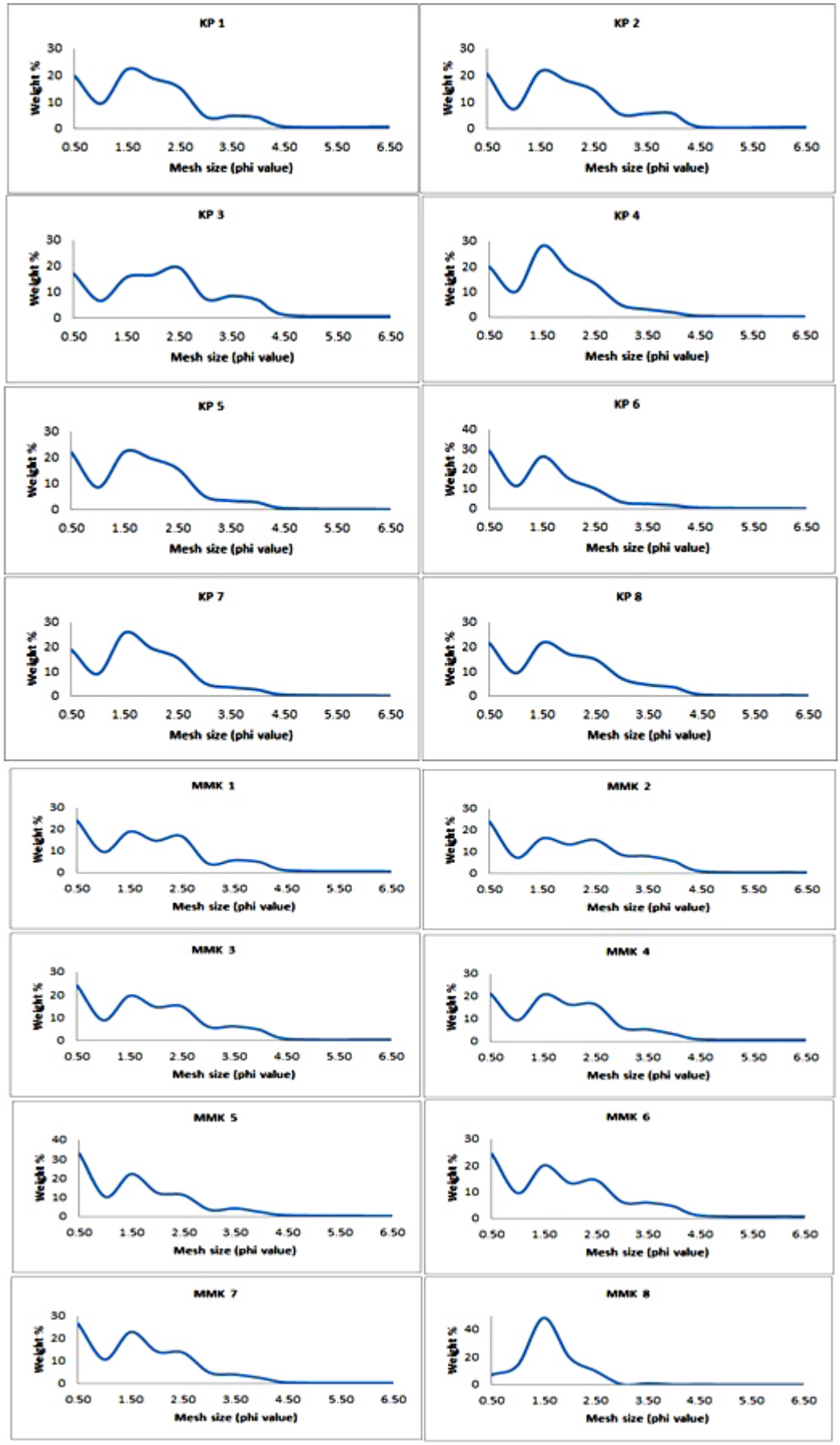

Fig. 3c. Frequency curves for the study area.

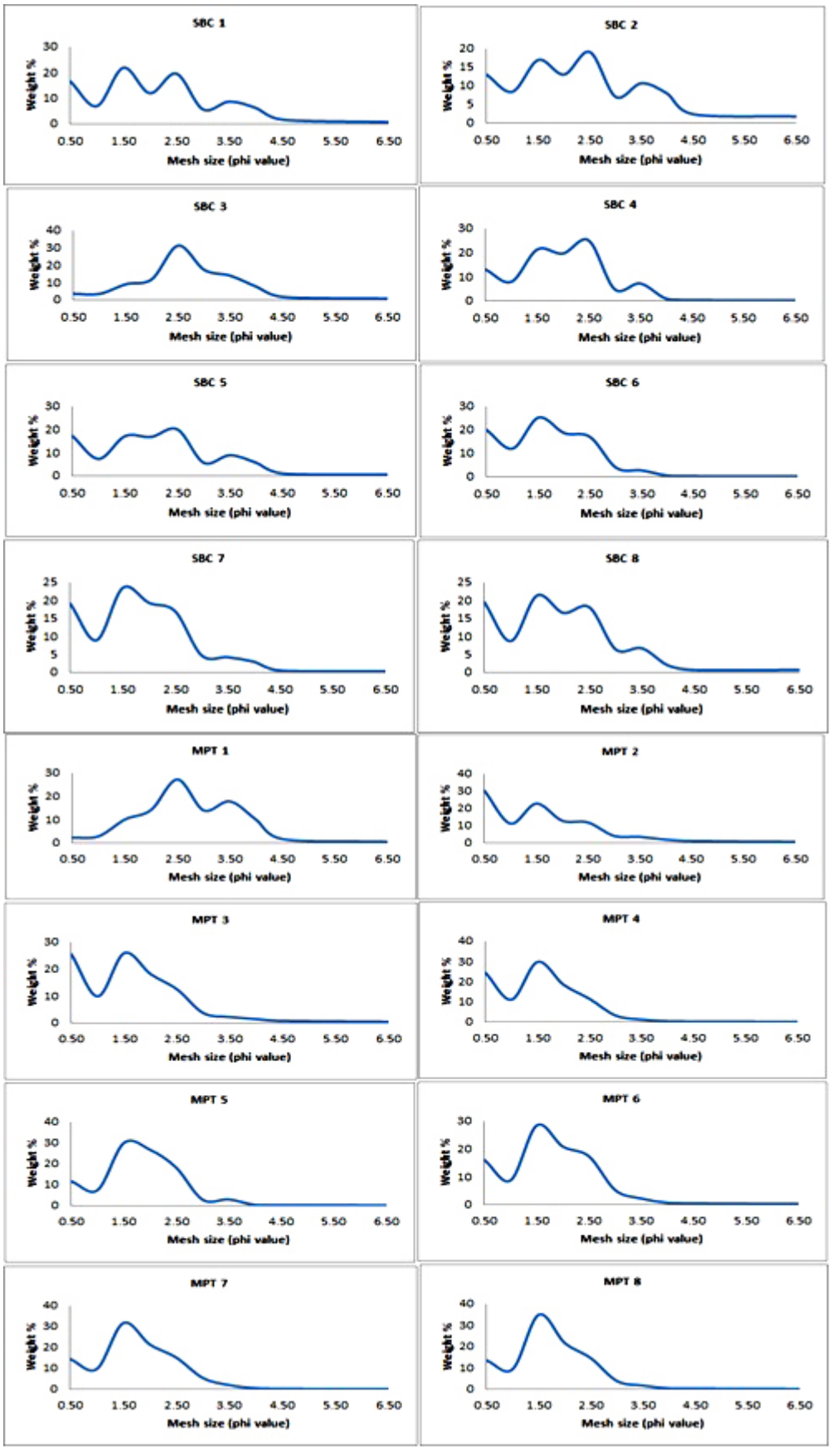

Fig. 3d. Frequency curves for the study area.

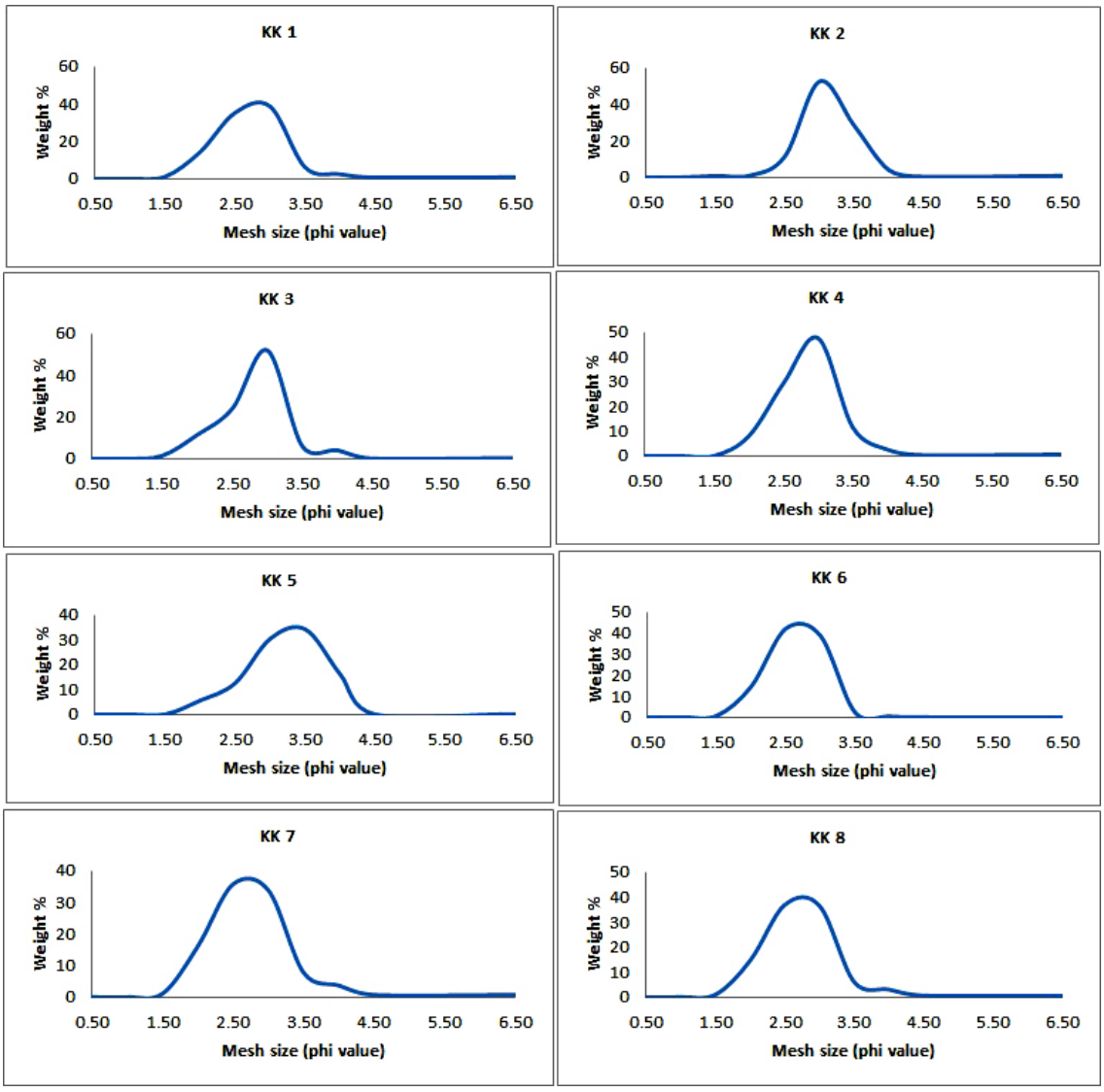

(MP1 – MP8, Mandapam; AK1-AK8, Attankarai; DP1-DP8, Devipattinam; TH1-TH8, Thondi; MMK1 – MMK8, Manalmelkudi; KP1-KP8, Kottaipattinam; SBC1-SBC8, Sethubavachattiram; MPT1-MPT8, Mallipattinam; KK1 – KK6 Kodiyakarai))

Fig.3e. Frequency curves for the study area.

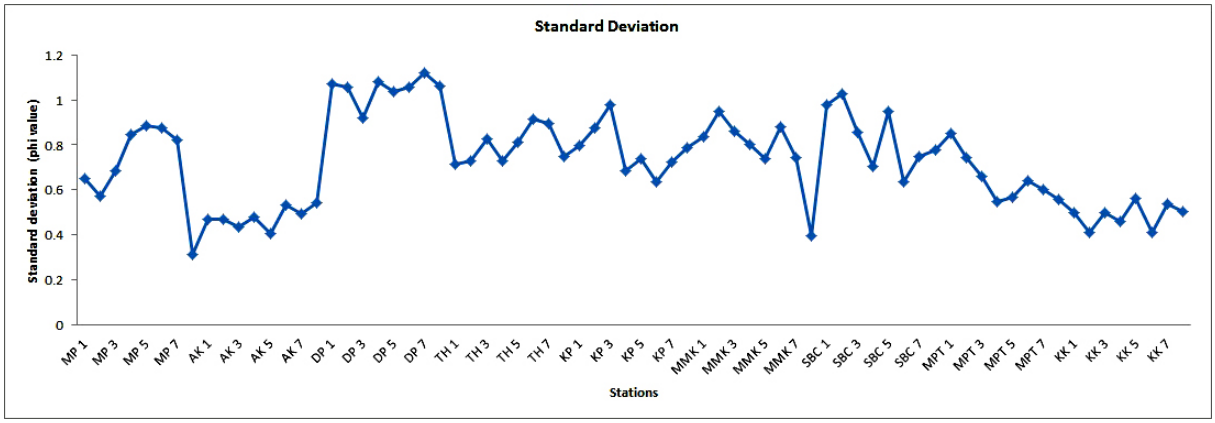

Fig. 4. Sorting values for the study area.

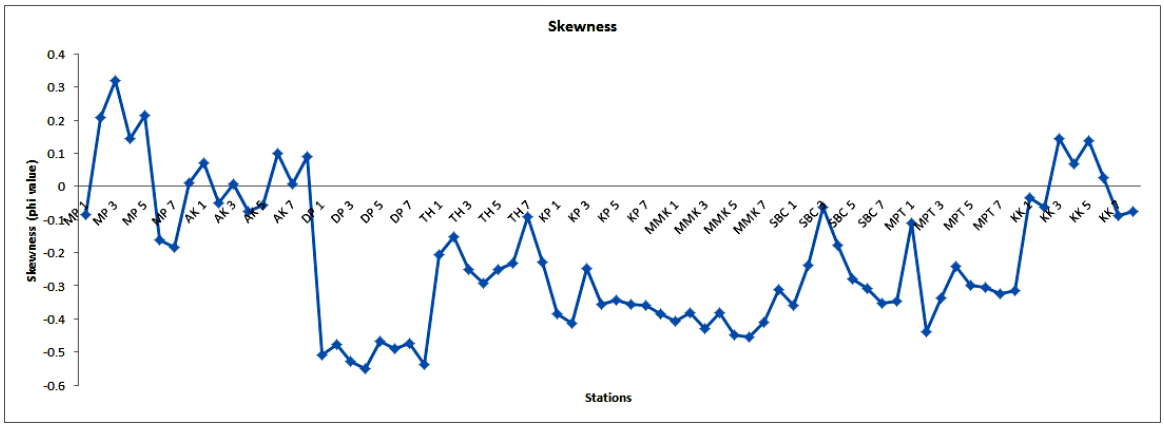

Fig. 5. Skewness values for the study area.

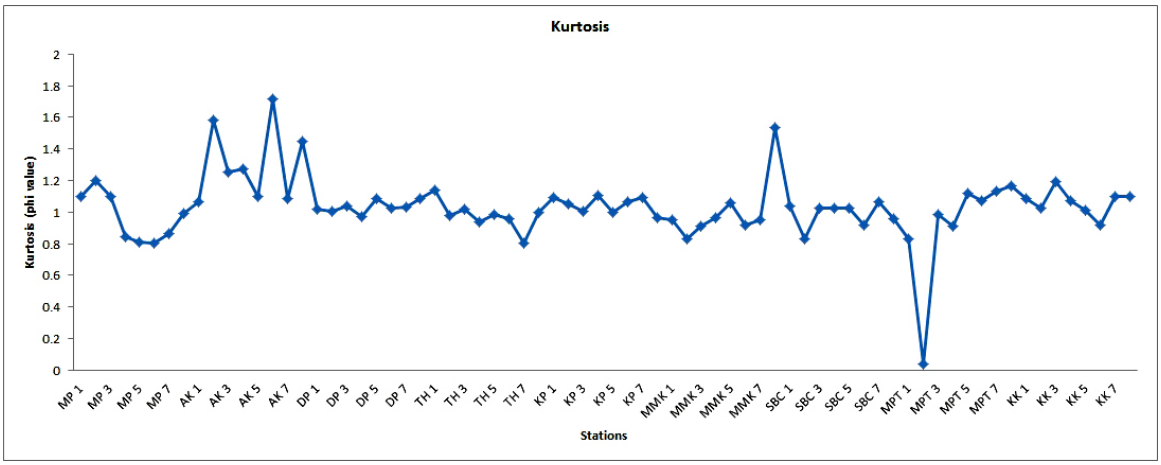

Fig. 6. Kurtosis values for the study area.

moment kurtosis values are found to vary from 2.429 ö to 10.492 ö (Fig. 6). This uneven nature clearly designates the mixing of two-end populations. The movement of longshore currents and the fluvial discharge of sediments have probably brought out these two populations mixing. This is also attributable to the widely varying nature of sediments and change in gradients of the coastline. It displays the presence of sediments having platykurtic nature and supports the presence of more than one population and that too, in sub-equal amounts whereas the leptokurtic nature deals with a type of a population which has one dominant population with other subordinates (Mason and Folk, 1958; Spencer, 1968; Jaquet Vernet, 1976).

DEPOSITIONAL ENVIRONMENT

Bivariant Plots

Many early workers like Folk and Ward (1957), Mason and Folk (1958), Friedman (1961, 1967, 1979) and Moila and Weiser (1968) have exposed that the environment of deposition can be separated by using bivariant plots of one sediment size against another. Friedman (1961) has successfully differentiated beach and dune sands by plotting mean vs. skewness and beach and river sands by plotting inclusive skewness vs. Inclusive standard deviation. Moila and Weiser (1968) have indicated that the scatter plots by graphic methods are effective to discriminate between modern beach, coastal dune and inland dunes and river sands. The plot of mean vs. Standard deviation is considered to be the most valuable. Maison and Folk (1958) fruitfully used the plot of skewness vs. kurtosis for defining limits of the fields of beach, dune and river sands in the west coast of India, Rajamanickam (1983) has established the use of bivariant plots by utilizing both graphic and moment measures and brought out the dune and river zonation from the plot of standard deviation vs. skewness.

In the present study, various textural parameters obtained through both graphic and movement methods have not shown many variations. Several earlier workers like Moila and Weiser (1968), Hails and Hoyt (1969),

Table 2. Results of textural parameters of the study area.

Textural parameters	Mean	Sorting	Skewness	Kurtosis
Mandapam	Fine sand to Very coarse Silt	Moderately sorted to Very well sorted	Symmetrical to Coarse skewed	Platykurtic to Mesokurtic
Attankarai	Fine sand	Well sorted to Moderately well sorted	Symmetrical	Mesokurtic to Leptokurtic
Devipattinam	Very fine sand	Moderately sorted to Poorly sorted	Very coarse skewed	Mesokurtic
Thondi	Fine sand to Very fine sand	Moderately sorted	Symmetrical to Coarse skewed	Platykurtic to Leptokurtic
Kottaipattinam	Very fine sand to Very coarse Silt	Moderately sorted to Moderately well sorted	Coarse skewed to Very Coarse skewed	Mesokurtic
Manalmelkudi	Very fine sand to Very coarse Silt	Moderately sorted to well sorted	Very Coarse skewed	Platykurtic toMesokurtic
Sethubavachattram	Very fine sand	Moderately sorted to Poorly sorted	Symmetrical to Very Coarse skewed	Platykurtic toMesokurtic
Mallipattinam	Very fine sand to Very coarse Silt	Moderately sorted to Moderately well sorted	Coarse skewed to Very Coarse skewed	Platykurtic to Leptokurtic
Kodiyakarai	fine sand to Very fine Sand	Moderately well sorted to well sorted	Symmetrical to fine skewed	Mesokurtic to Leptokurtic

Jaquet and Vernet (1976), Rajamanickam (1983) and Rajamanickam and Gujar (1984, 1993), Angusamy and Rajamanickam (2007), Solai et al., (2013) have also expressed similar views. Mean Vs standard deviation is plotted in Fig. 7. It shows that the stations Attankarai, Kodiyakarai and Mallipattinam comes under the beach environment whereas at Mandapam, four stations comes under beach environment and Devipattinam, Thondi and Kottaipattinam samples are falling in the river environments.

In Figure. 8, standard deviation vs skewness is plotted. The following stations Attankarai, Kodiyakarai, Kottaipattinam and Mallipattinam falls in beach environment. The remaining station falls in riverine environment and beach environment. The abundant fine mode in the sediments results in negative skewness for the majority of samples (Fig.9).

CM Pattern

In the study region, C=290 to 300 µ and M ranges between 150 and 2,300. In the CM pattern shows samples are clusterly distribution close to the line C = M = 2,000 µ indicating their moderately sorted nature. The spread of dividing line to 2,000 µ closer to the normal pattern suggests the distribution of very finer size of the sediments. The presence of sediments is found to have a spread within OP segments. The presence of sediment distribution in OP sectors discounts the deposition of sediments complexity in the hydrodynamic processes within the near shore marine environment. Moreover, the close and dense populations of sediment fraction in the OP sector indicate sediments are found in the high turbulent discriminate. The abundant sediment distribution in the OP sector indicates the transportation of riverine sediments by long-shore drift currents and deposited in the study area. In other words, the long-shore sediment transportation is the leading process for migration of the sediments. The CM plots indicate that the Palk Strait sediments underwent the bottom suspension and rolling under active current.

Log -Normal Distribution

In order to corroborate the inferences drawn from the other methods of grain size statistics, the log normal distribution of sediments is attempted here. Visher (1969) has put forward the effectual usage of log probability using three types of sub-population viz, the traction, saltation and suspension. Many other workers like Inman (1949), Sindowski (1957), Bagnold (1956), Moss (1963), Rajamanickam (1983), Chandrasekar (1992), Rajamanickam and Gujar (1993), Angusamy (1995) and Gujar (1996) utilized the log probability curves for

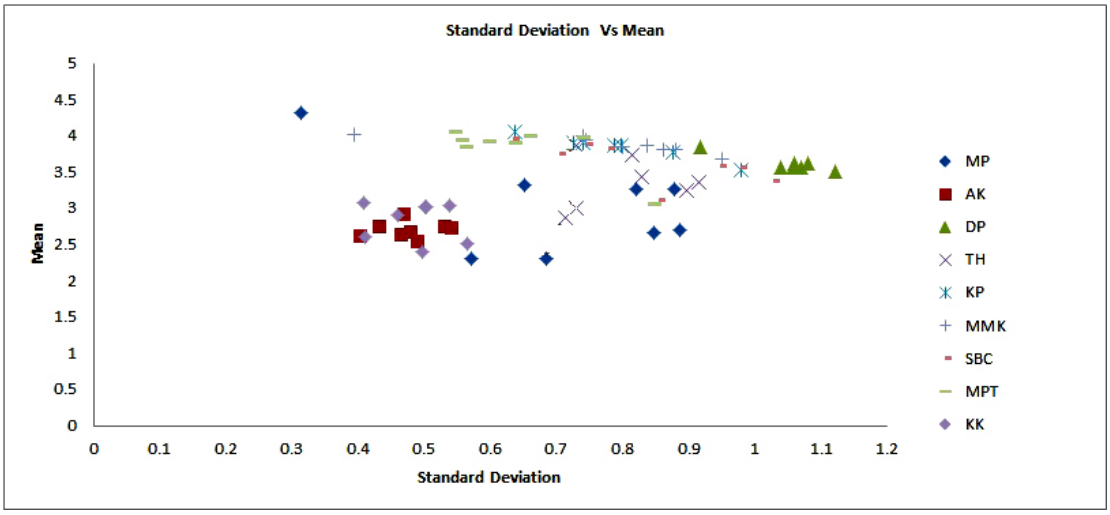

Fig. 7. Mean Vs Standard deviation is plotted.

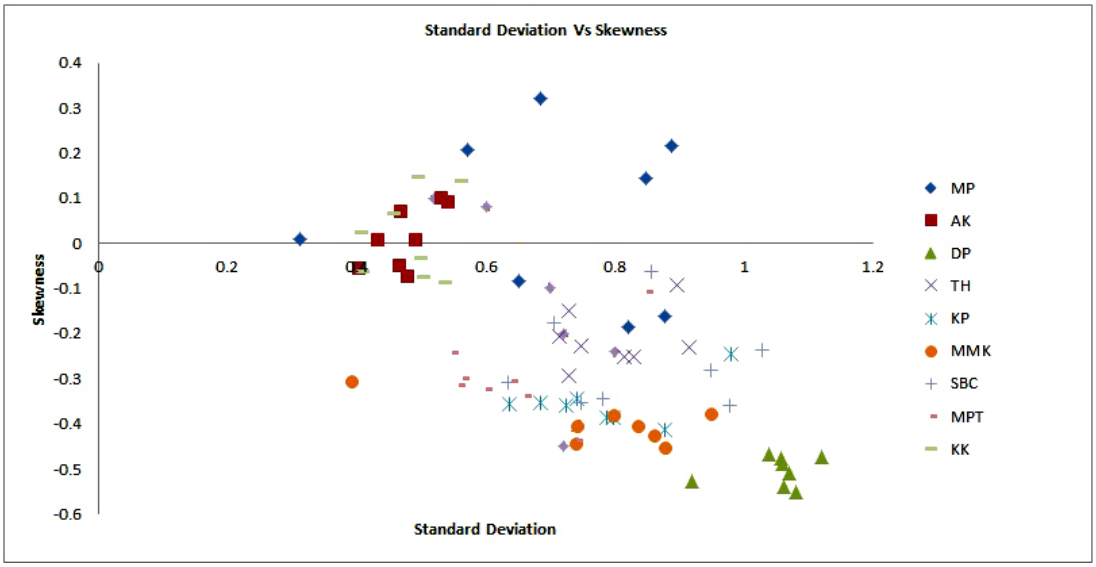

Fig. 8. Standard deviation Vs Skewness is plotted.

recognizing the ancient depositional environment. The binary plots have indicated the prevalence of mixing environments and the marked differences in the respective regions of this sector. The wide variation of surface creep population is explained in the beach and river environment. A strong convergence in the northerly movement of wave direction and other wave directions can be attributed to the difference existed in the surface creep population as well as in beach and river environment and divergence. The presence of clear double saltation with very poor surface creep populations is noticed in the region. Though the influence of the fluvial environment is manifested in frequency curves, sorting and skewness values, the probability curves broadly reflect the influence of the beach and river environment.

CONCLUSIONS

From the analysis of grain size data, different frequency curves have been plotted and they have delineated the erosional and depositional environments. The mean grain size shows the spatial variation along the study area. From the analysis of scatter plots, bivariant plot, CM pattern and log-normal distribution, it is entrenched that characteristic environment of deposition is mainly riverine and marine (beach) in this region. Devipattinam, Thondi, Kottaipattinam, Manalmelkudi, Sethubavachattram and Mallipattinam show negative skeweness may be due to the high energy condition. The Mandapam, Attankarai and Kodiyakarai regions show fine sand to very fine sand and positively skewed in nature may be due to the prevailing low

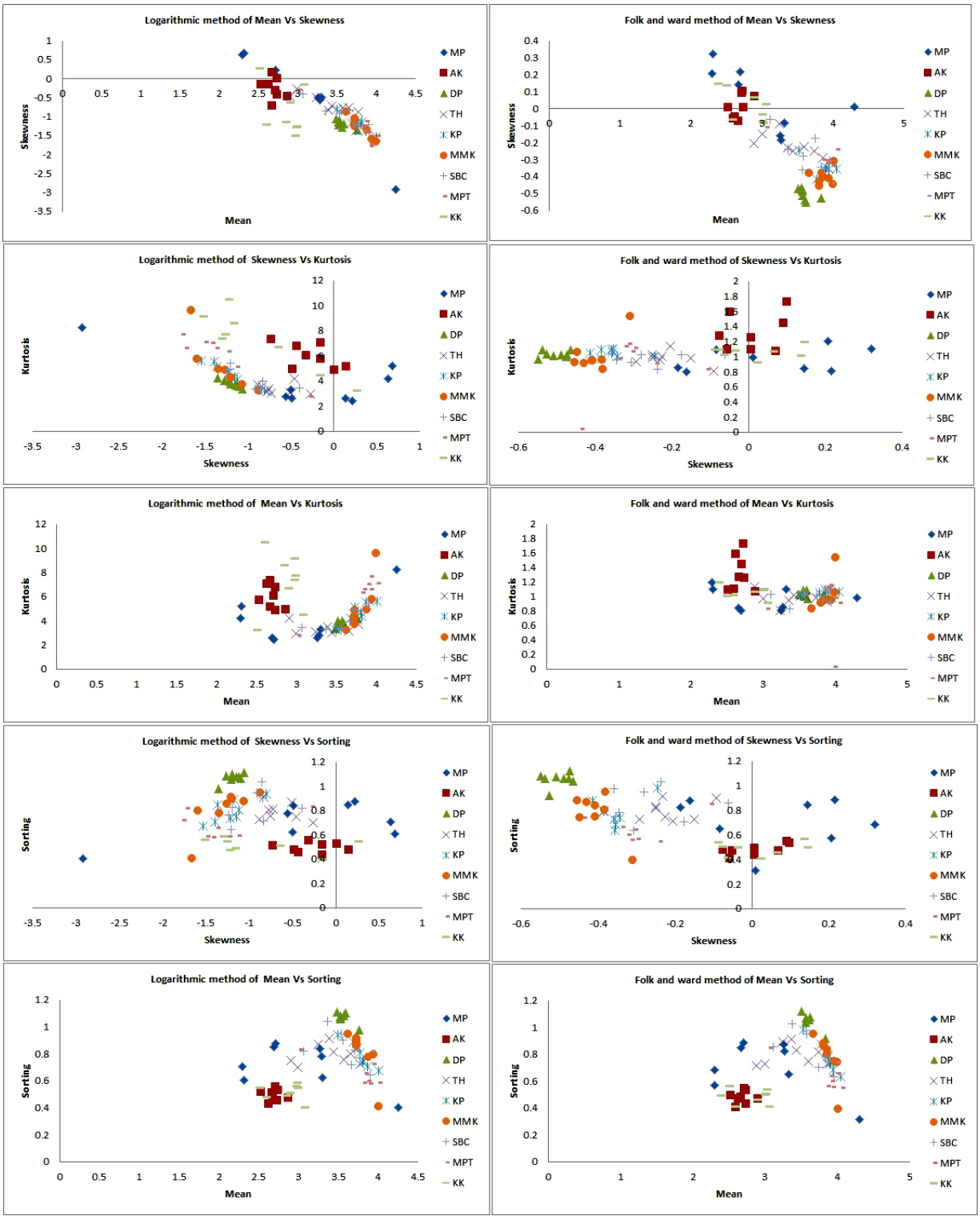

Fig. 9. Folk and Ward and Logarithmic method of scatter plot diagram.

energy condition indicates the depositional environments and its connecting with open sea whatever sediment deposited during the monsoon the sediments altered by tidal influence. The CM pattern indicates the deposition of sediments in graded suspension.

Acknowledgements: The authors are thankful to Prof. G.V.Rajamanickam, Research Director, PRIST University, Thanjavur for his fruitful suggestion and to the Prof.S.P.Mohan, (Retd) Professor and Head, Department of Geology, for proving the lab facilities to carry out this work. The authors also acknowledged the UGC- CPEPA (F.No.8-2/2008(NS/PE) Dt 14.12.2011) for providing financial assistance to carryout fieldwork at Palk Strait.

References

Angusamy N. (1995). A study of beach placers between Mandapam and Kanyakumari, Tamilnadu, India. Published Ph.D. Thesis submitted to Barathidasan University, Tiruchirapalli, p.155.

Angusamy, N. and Rajamanickam, G.V. (2006). Depositional environment of sediments along the southern coast of Tamil Nadu, India, Oceanologia, 48, 87–102.

Angusamy N. and Rajamancikam G.V. (2007). Coastal processes of Central Tamil Nadu, India: clues from grain size studies, Oceanologia, 49, 41–57.

Chakrabarti A. (1977). Polymodal composition of beach sands from the East coast of India, J. Sediment. Petrol., 47, 634–641.

Chandrasekar N. (1992). Beach placer mineral exploration along the central Tamilnadu coast. Unpublished Ph.D. Thesis, Madurai Kamaraj University, Madurai, p.293.

Chaudhri R.S., Khan H.M.M. and Kaur S. (1981). Sedimentology of beach sediments of the west coast of India. Sedimentary Geology, 30, 79-94.

Duane D.B. (1964). Significance of skewness in recent sediments, Western Pamlico Sound, North Carolina. Jour. Sediment. Petrol, 34, 864–874.

Folk R.L. and Ward M.C. (1957). Brazos river bars: A study in the significance of grain size parameters. Jour. Sediment. Petrol, 27, 3-27.

Friedman G.M. (1961). Distinction between dune, beach and river sands from their textural characteristics. Jour. Sediment. Petrol, 28, 151-153.

Friedman G.M. (1967). Dynamic Processes and Statistical parameters compared for size frequency distribution of beach river sands. Jour. Sediment. Petrol, 37, 327-354.

Friedman G.M. (1979). Differences in size distributions of populations of particles among sands of various origins: Addendum to IAS Presidential Address. Sedimentology, 26, 859–862.

Gujar A.R.(1996). Heavy mineral placers in the near shore areas of south Kongan, Maharastra: their nature, distribution, origin and economic evaluation. Thesis submitted to Tamil University, Thanjavur, p.234.

Hails J.R. and Hoyt J.H. (1969). The significance and limitations of statistical parameters for distinguishing ancient and modern sedimentary environments of the lower Georgia coastal plain. Jour. Sediment. Petrol, 39, 559-580.

Inman D.L. (1949). Sorting of sediments in the light of ûuid mechanics. Jour. Sediment. Petrol, 19, 51–70.

Jaquet J.M. and Vernet J.P. (1976). Moment and graphic size parameters in the sediments of Lake Geneva. Switzerland. Jour. Sediment. Petrol, 46, 305-312.

Maison C.L. and Folk R.L. (1958). Differentiation of beach, dune and Aeolian flat environments by size analysis, Mustang Islands, Texas. Jour. Sediment. Petrol, 28, 211-226.

Mohan P.M. (1990). Studies on the texture, mineralogy and geochemistry of the modern sediments of the Vellar estuary, published Ph.D. Thesis, Cochin University of Science and Technology, Cochin. P.192.

Moila R.J. and Weiser, D. (1968). Textural parameters: An evaluation. Jour. Sediment. Petrol, 38, 45-53.

Moss A.J. (1963). The physical nature of common sandy and pebbly deposits, part II, American Journal of Science, 261, 297-343.

Rajamanickam G.V. (1983). Geological investigations of offshore heavy mineral placers of Konkan coast, Maharashtra, India. Ph.D. Thesis, Indian School of Mines, Dhanbad (published) p.258.

Rajamanickam G.V. and Gujar A.R. (1984). Sediment depositional environment in some bays in central west coast of India. Ind. J. Mar.Sci.14, 13-19.

Rajamanickam G.V. and Gujar A.R. (1985). Indications given by median distribution and CM patterns on clastic sedimentation in Kalbadevi, Mirya and Ratnagiri bays, Maharashtra, India, Giornale di Geologie, Italy, 47, 237-251.

Rajamanickam G.V. and Gujar, A.R. (1993). Depositional processes inferred from the log probability distribution. In: Recent Researches in Sedimentology, ed. Jhingran, 154-164.

Rajmohan S, Singarasubramainian S.R, Suganraj K, Sathya A. and Sundararajan M. (2012). Grain size distribution and depositional environment of coastal sediments at Ponnaiyar and Gadilam estuary, East coast of India. International Jour. of Recent Sci. Res., 3, 919-922.

Rao P.V.N, Suryam R.K. and Rao V.R. (2005). Depositional environment inferred from grain size parameters of the beach sediments between False

Devi Point to Kottapatnam, Andhra Pradesh Coast. Jour. Geol. Soc. India, Vol.65, pp.317–324.

Simon J. Blott and Kenneth Pye. (2001). Gradistat: A Grain Size Distribution and Statistics Package for the analysis of unconsolidated sediments. Earth Surf. Process. Landforms, 26, 1237–1248.

Sindowski K.H. (1957). Die synoptischen Methoden des Kornkurven-Vergleiches zur Aus-deutung fossiler Sedimentationräume. - Geol. Jb., 73, 235-275.

Spencer D.W. (1968). The interpretation of grain size distribution curves of clastic sediments Jour. Sediment. Petrol., 33, 180-190.

Solai A, Suresh Gandhi M, Chandrasekaran K. and Ram Mohan V. (2013). Depositional environment in and around Tamiraparani estuary, and off Tuticorin, Tamil Nadu, India:clues from grain size studies, Arabian Jour of Geosciences, 6, 2419–2446.

Venkatramanan S, Ramkumar T, Anithamary I, and Ramesh G. (2011). Variations in texture of beach sediments in the vicinity of the Tirumalairajanar river mouth of India. International Journal of Sediment Research, 26, 460-470.

Vijayam B.E, Aswathanarayana, U. and Mahadevan C. (1961). Sand movement on the Waltair Beach. Pro.Natl.Inst.Sci.India., 26, 142-150.